NASA CR-730

HANDBOOK OF ORBIT POSITION CONTROL FOR PASSIVE COMMUNICATIONS SATELLITES

Prepared under Contract No. NAS1-5194 by
WESTINGHOUSE DEFENSE AND SPACE CENTER
Baltimore, Md.

for Langley Research Center

NATIONAL AERONAUTICS AND SPACE ADMINISTRATION

For sale by the Clearinghouse for Federal Scientific and Technical Information
Springfield, Virginia 22151 – CFSTI price $3.00

TABLE OF CONTENTS

LIST OF ILLUSTRATIONS

LIST OF TABLES

ABSTRACT

Considerable weight savings may be realized in a system of passive communications satellites if:

- Lenticular reflecting shapes rather than spherical reflectors are used
- Angular positions of the satellites are controlled rather than allowed to drift randomly.

In part 1, an introductory discussion is presented of orbit position control techniques using direct solar pressure and thermal reradiation forces to control the orbit energy and the relative angular position of satellites in orbit; in part 2, complete parametric data are presented related to these techniques; and part 3 presents derivations of scaling factors and other related information.

I. INTRODUCTORY MATERIAL

I. INTRODUCTORY MATERIAL

1.1 INTRODUCTION

The use of satellites to relay communications across large distances on the earth's surface is a reality today. Both passive and active satellites have been launched successfully. Active relay satellites rely on the reception, power amplification, and retransmission of the communication signal; passive satellites consist of large surfaces to return (by reflection) to the earth's surface all signals from the earth that impinge on them.

Presently, the two passive communications satellites which have been successfully installed in orbit fall short of competing with present active satellites by several orders of magnitude. Several recent developments in passive satellite technology show promise for significant change in the position of the two systems in the future.

Major developments are:

- Lighter materials
- The lenticular shape which omits portions of the present spheres that do not reflect signals back to the earth
- Improved manufacturing techniques to reduce scintillation of reflected signals
- Station keeping without mass expulsion to operate for indefinite periods of time.

Satellite systems for communications purposes can be evaluated for comparison by establishing a set of tradeoffs for each system relating to cost. Major elements of cost (in order of significance) are:

- Launch weight and altitude (and certain inclinations which require dog-leg launches)
- Ground hardware
- In-orbit hardware.

The first step in the evaluation procedure is to define the communications system to be achieved, considering its present and future requirements, in terms of bandwidth, earth surface distance to be covered, and schedule.

Next, convert requirements for each system to be compared into the rate of energy expenditure (power loss) in transmission and reception parametrically in terms of the cost elements described above. If existing and/or projected costs are assigned to the significant cost elements and if the parametric variations of each system are kept within feasible limits, minimum or optimum costs for each system can be established. The lower cost generally will decide the best system.

This is a complex task and requires parametric knowledge of each variable or tradeoff in each system.

Typical tradeoffs which will affect cost are as follows:

- The altitude and number of the satellites required
- The lifetime of the orbiting system (i. e., one 10-year satellite equals two 5-year satellites of equivalent launch weight)
- The ground station power versus satellite size (launch weight) for passive reflectors
- The power bandwidth (launch weight) versus ground station power gain for active relays
- The number of random versus spaced satellites (This ratio approaches infinity when 100-percent communications are desired and a low altitude system offers minimum launch weight and ground station power.)

This handbook covers parametrically the means of obtaining the last tradeoff described. The variables used in the aforementioned tradeoff study for a means of station keeping or the adjustment of the orbital period without mass expulsion are derived and explained. The energy source is solar radiation which is exploited in two ways discussed in the following two paragraphs.

The first method makes use of the difference in force received by a totally absorbing surface and that received by a reflecting surface. In this method, the orbital period is changed by presenting one of the above surfaces toward the sun as the satellite moves toward the sun and a surface of the other type

as the satellite recedes from the sun. The resulting difference in the energy received in the two halves of the orbit will change the kinetic energy in the system and hence the period.

The second method makes use of the fact that the emissivity of a surface can be varied, and this method is applied to three dimensional surfaces, wherein the body is made equally absorbent of solar radiation, but emits black body radiation unsymmetrically, determined by the pattern of different emissivities on its surface. By aligning the area of maximum radiation from the body to the velocity vector, the resulting reaction from this radiation adds or subtracts from the momentum of the satellite, thus changing its period.

This handbook also incorporates the results of several years study by Westinghouse Electric Corporation under contract to Langley Research Center of the National Aeronautics and Space Administration (Contracts NAs1-3131 and NAs1-5194), and is intended to provide a summary of the techniques involved and to provide parametric data for satellite systems in the altitude range of 1000 nautical miles to synchronous altitude and at orbital inclinations from 0 to 180 degrees. The handbook is divided into three parts, the first containing a qualitative discussion of the various techniques involved, the second containing necessary parametric data, and the third containing various derivations and other supporting material.

1.2 ORBIT POSITION CONTROL FOR PASSIVE COMMUNICATIONS SATELLITES

The orbit position control techniques described in this section were developed for the purpose of controlling the relative positions of a number of passive, reflective communications satellites. Although the techniques have more general applicability, their description will be framed in terms of this model for the sake of concreteness and simplicity.

Early passive reflective satellite communication studies involved the use of large inflatable balloons on the order of 100 feet in diameter, such as ECHO I. These balloons were placed in orbit in a deflated condition and

allowed to inflate to provide a relatively large surface which, when constructed of suitably RF reflective material, reflected sufficient radio energy toward the ground to permit successful communication (see figure 1-1, part a). A number of such satellites would be used in various orbits, more or less randomly placed, permitting occasional loss of communications capability whenever the satellites drifted apart enough to leave coverage gaps.

1.2.1 Gravity Gradient Lenticular Satellites

Several improvements to this concept were proposed by various individuals. These included the use of lenticular reflective shapes and the use of satellites whose position in orbit was controlled by solar pressure or reradiation forces. The first of these techniques stems from the consideration that only a relatively small portion of a spherical reflective surface reflects radio energy in a useful direction toward the earth. Deleting part of the nonuseful portion of the sphere results in a lenticular shape (as illustrated in figure 1-1, part b), whose surfaces are segments of a sphere. This results in a substantial weight saving, permitting use of much larger satellites for a given launch weight. (The upper surface of the lenticular shape is retained to provide a symmetrical shape for proper inflation.) In order to maintain proper orientation of the lenticular shape, lightweight inflatable booms in a tripod or tetrapod arrangement position the masses of the canister and the attitude control and damping system in such a way that gravity-gradient forces tend to stabilize the satellite in the desired orientation.

The gravity gradient lenticular satellite is shown in more detail in figure 1-2. If a satellite has unequal moments of inertia about its three principal axes, the unbalanced forces resulting from $1/R^2$ variation of gravity with distance tend to cause the satellite to stablize such that the axis associated with the smallest moment of inertia is vertical and the axis associated with the largest moment of inertia is perpendicular to the orbital plane. The tetrapod of inflatable booms is used to position the masses of the canister and control system far enough from the lenticule that the lenticule axis stabilizes

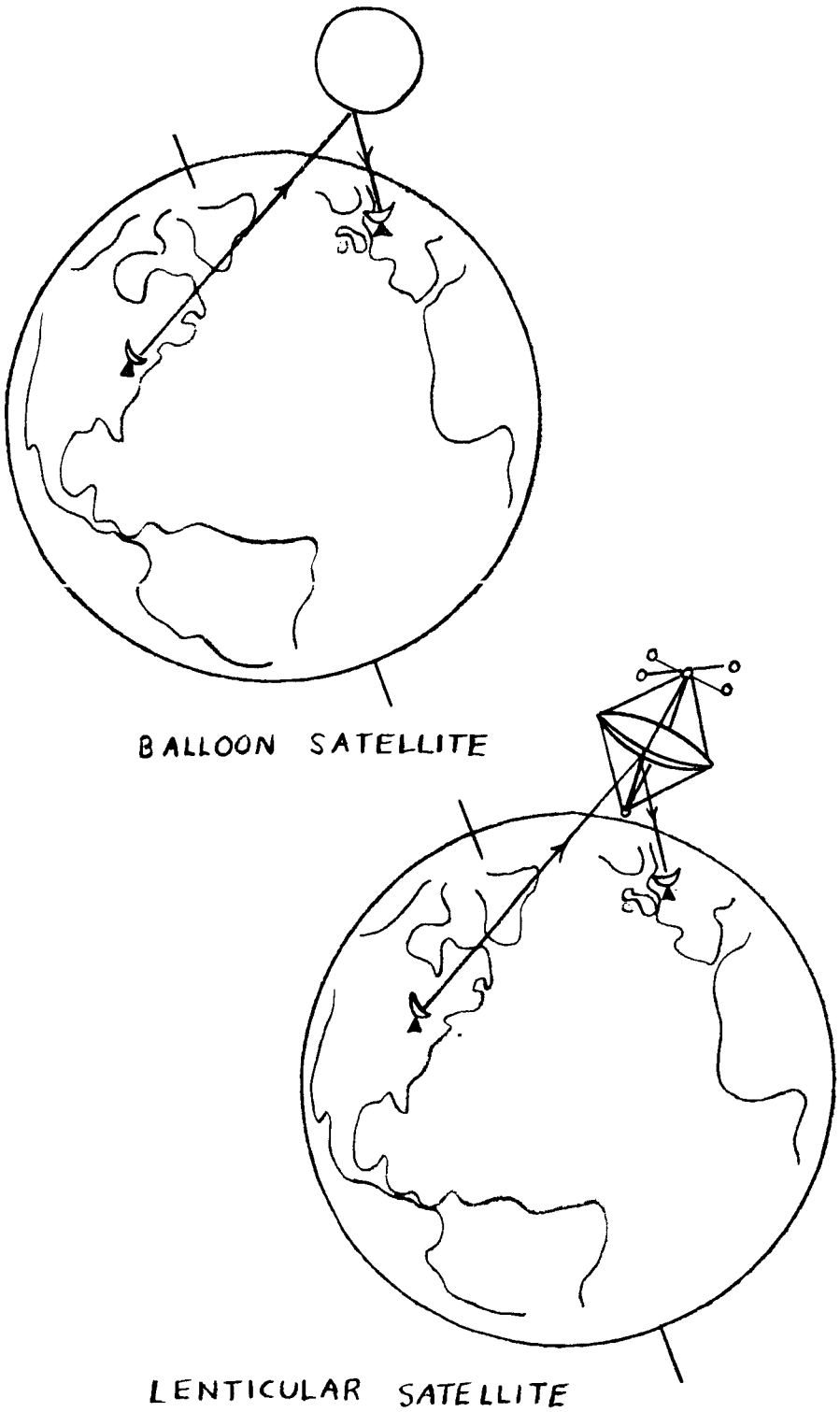

Figure 1-1. Communication By Passive Reflective Satellites

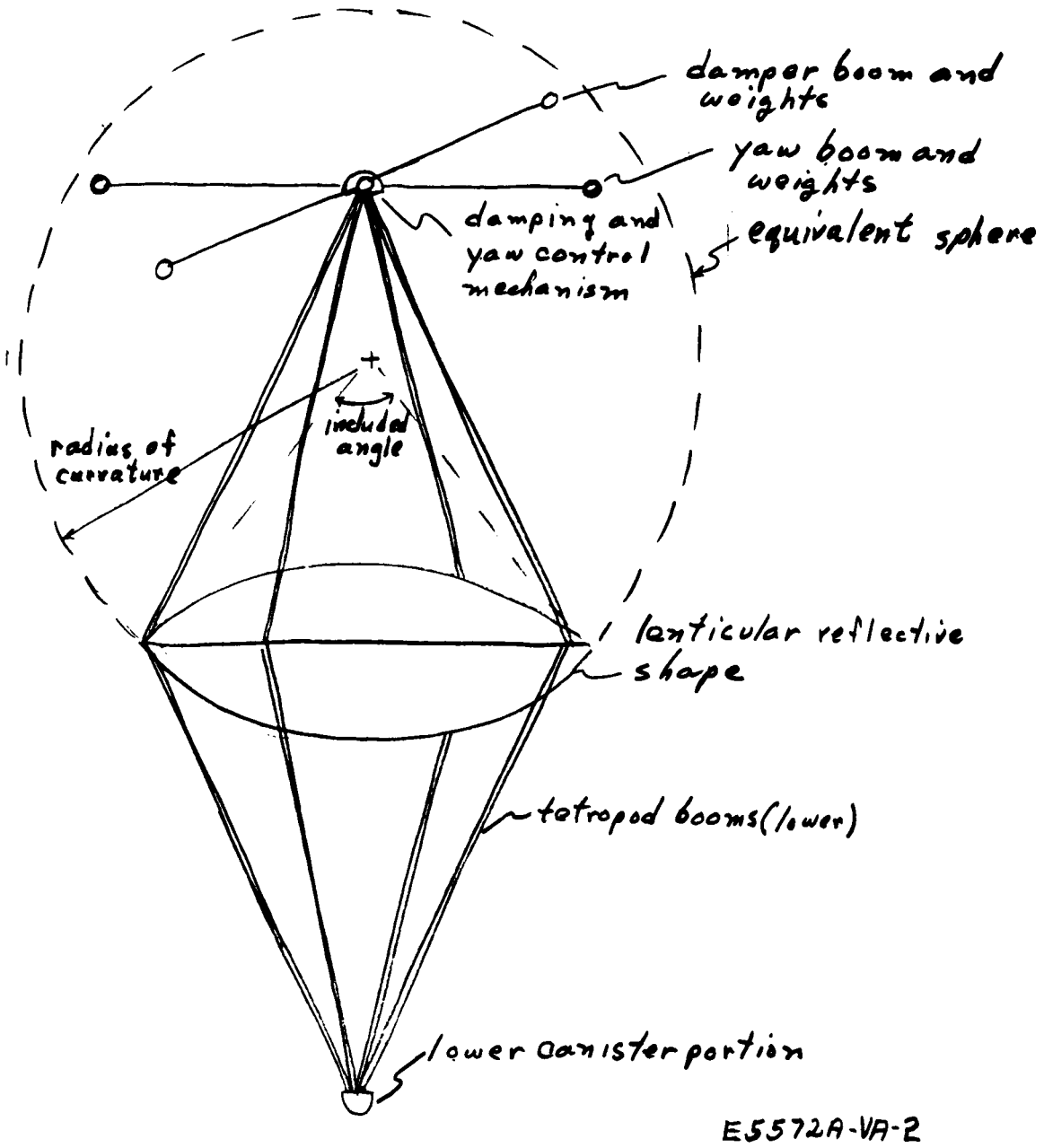

Figure 1-2. Lenticular Reflective Satellite

vertically, while the yaw boom and masses stabilize the satellite in yaw. The lower tetrapod may be constructed of RF transparent materials to minimize interference with the reflection, while the small size of the lower canister portion will minimize its effect. Several damping mechanisms were studied (reference 1, section 2), with selection being made of a rotary damper connected to an Ames-type damping boom as illustrated. Relative motion between the damping boom and the yaw boom during satellite librations is transmitted to the damping mechanism and damped by means of a rotary hysteresis damper. For further information concerning the illustrated satellite structure, the reader shall consult reference 1.

1.2.2 Orbit Position Control

Considerable savings in the number of satellites required for satisfactory communication coverage may be obtained if the relative positions of the satellites in orbit are fixed rather than allowed to drift randomly. Lightweight satellites of this type, if uncontrolled, will drift in position in a complex manner due to the random differences in their periods and unequal results of various perturbing forces. For this reason, one cannot hope to establish the satellites in some fixed pattern that will remain unaltered with the passage of time; rather, orbit position control techniques will be required. Several techniques utilizing solar radiation pressure and reradiation forces were studied (reference 1), with two satellite configurations selected as being most useful. These two configurations are illustrated in figure 1-3 as configurations A and B. (These two configurations are both symmetrical; that is, they have tetrapod booms on both sides of the lenticular shape for gravity-gradient stabilization. Unsymmetrical configurations were also considered as reported in reference 1; however, they were rejected because of the complicated structure and erection procedure.)

Configuration A consists of a lenticular shape constructed of an opaque material having a uniform outside absorptivity (fraction of incident radiant energy absorbed) of 0.35 and a uniform inside emissivity of 0.90. To obtain

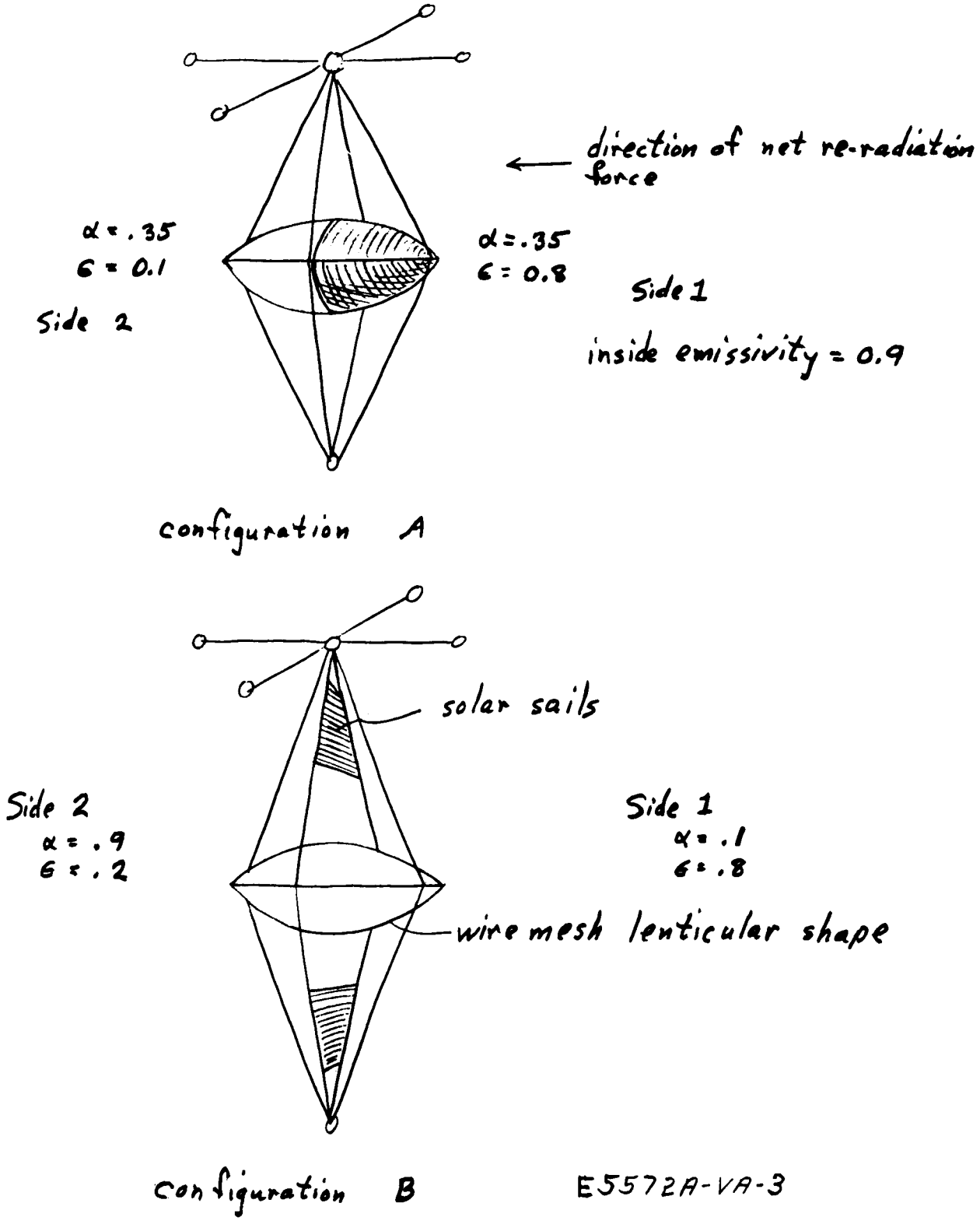

Figure 1-3. Lenticular Satellite Configuration

unbalanced reradiation forces for orbit position control, the outside emissivity was chosen to be 0.80 on one side of the satellite and 0.10 on the other. These values were chosen on the basis of temperature tradeoff studies as discussed later in part 3. Because of the uniform external absorptivity, the component of the solar radiation pressure force tangential to the orbit tends to average out over the orbit, producing no semimajor axis variation. However, the unsymmetrical external emissivity results in a small net force due to unsymmetrical reradiation of infrared energy from the satellite, the force being approximately tangent to the orbit and directed toward the low emissivity side of the satellite. This force increases or decreases the energy of the orbit depending on the orientation of the satellite, thus changing the orbit semimajor axis, its period, and its average angular rate. The effect of the period change is to cause the satellite angular position to drift with respect to the position of a similar satellite of uniform external emissivity, thus achieving a variation in the position of the satellite in its orbit which may be controlled by varying the yaw attitude of the satellite. For example, orienting the satellite with the low-emissivity side in the direction of satellite motion will increase the energy and semimajor axis of the orbit, increasing its period and causing the relative angular position of the satellite to drift backward. The technique for controlling the yaw attitude of the satellite will be discussed in a later paragraph.

The configuration B satellite consists of a lenticular shape constructed of fine wire mesh imbedded in a photolyzable plastic film (reference 2). The film supports the wire mesh structure during inflation and then is broken down into volatile components by the action of sunlight; these volatile components evaporate in the vacuum of space to leave only the ridged wire mesh structure remaining. Because of the open nature of the mesh (each side is about 95-percent transparent), the lenticular shape is much less affected by solar radiation pressure than the configuration A satellite. To obtain orbit position control, sails of lightweight material are added as shown. The sails utilize

both direct solar pressure and thermal reradiation pressure to obtain orbit position control (mobility).

A simple example illustrating this is the case in which the sun lies in the orbital plane of the satellite. If it is desired to increase the semimajor axis and period of the orbit, the satellite should be oriented with side 2 of the satellite in the direction of motion. Then, during the portion of the orbit in which the satellite is moving away from the sun (figure 1-4), the reflective surface (α = . 1) will face the sun and the direct solar radiation force will be relatively large. During the portion of the orbit in which the satellite is moving toward the sun, the reflective surface will face away from the sun and the direct solar radiation force will be relatively small. The average direct solar radiation force over the whole orbit will then be in the direction of satellite motion. Since the sail surface of high emissivity (side 1, ϵ = 0.8) is the side opposite to the direction of motion, the thermal reradiation forces will also be in the direction of satellite motion. Thus, energy is added to the orbit both by direct solar pressure and by thermal reradiation forces, and the semimajor axis and period are increased as desired. The values of absorptivity and emissivity shown in figure 1-3 were chosen on the basis of temperature tradeoff studies as discussed later in part 3. It is appropriate to point out at this time that solar sails may be utilized with any shape satellite, so that the techniques and data presented in this handbook for configuration B lenticular satellites are also applicable to orbit position control of other types of satellites if the necessary sail area is provided.

1.2.3 Mobility

To quantitatively discuss techniques of orbit position control, the concept of mobility was introduced. Mobility may be defined as the time rate of change of orbital semimajor axis, averaged over one orbital period. The basic equations relating the period P and average angular velocity $\dot{\theta}$ of a satellite in an elliptical orbit of semimajor axis a are:

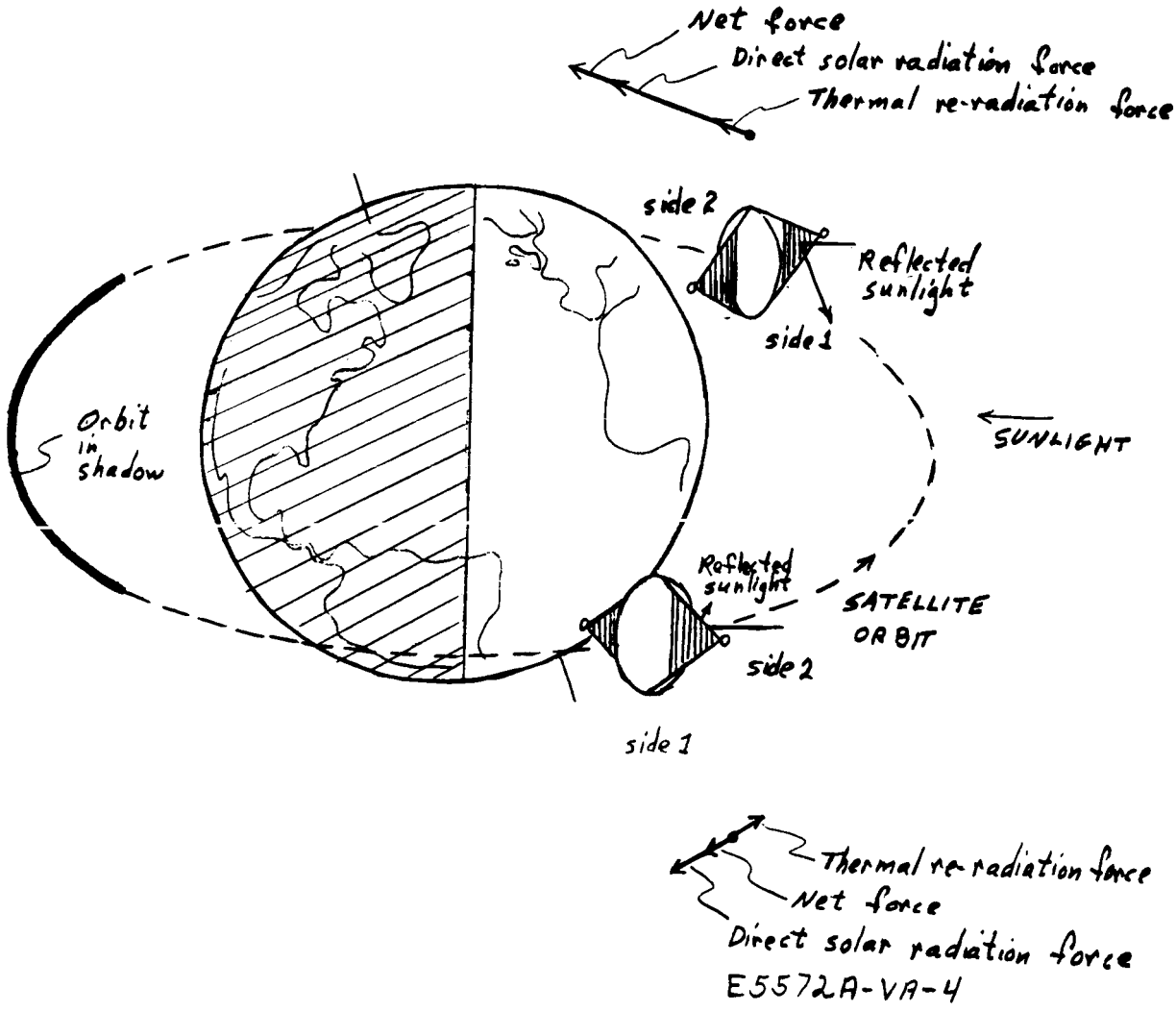

Figure 1-4. Configuration B Orbit Position Control

$$P = K_1 a^{3/2}$$
$$\dot{\Theta} = 2\pi/P$$

where K_1 is a constant equal to $2\pi/k\sqrt{m}$, K being Newton's gravitational constant and m the mass of the earth. Using Taylor's theorem, these equations may be approximated by linear expressions in the neighborhood of any chosen nominal altitude a_o, so that if $\Delta a = a - a_o$, $\Delta P = P - P_o$, $\Delta\dot{\Theta} = \dot{\Theta} - \dot{\Theta}_o$ where $P_o = K_1 a_o^{3/2}$ and $\dot{\Theta}_o = 2\pi/P_o$, then:

$$\Delta P \approx \frac{3}{2} K_1 a_o^{1/2} \Delta a$$
$$\Delta\dot{\Theta} \approx -2\pi \frac{\Delta P}{P_c^2} = -2\pi \frac{\Delta P}{K_1^2 a_c^3}$$
$$\Delta\Theta = \int_{\Delta t} \Delta\dot{\Theta}\, dt \approx -\frac{3\pi}{K_1 a_c^{5/2}} \int_{\Delta t} \Delta a\, dt$$

Thus, for example, an increase in semimajor axis Δa from some nominal value will increase the orbital period, decreasing the average angular velocity and causing the angular position to lag by the amount $\Delta\Theta$ in relation to its hypothetical position had it remained at the nominal semimajor axis value, a_o. With the semimajor axis changing at a rate $\dot{a} = M$, the average angular velocity will change at a corresponding rate:

$$\frac{d}{dt}(\Delta\dot{\Theta}) = -\frac{2\pi}{P_c^2} \frac{d}{dt}(\Delta P) = -\frac{3\pi}{K_1 a_c^{5/2}} M$$

so that mobility can equivalently be expressed as a time rate of change of semimajor axis ($M = \dot{a}$, meters/day) or as a time rate of change of average angular velocity ($M = \frac{d}{dt}(\Delta\dot{\Theta})$, degrees/day^2 or radians/day^2). In either case, if the semimajor axis at the beginning of a time interval Δt is taken as a_o, the angular position control obtained during that time interval is the double integral of the mobility, multiplied by the appropriate dimensional constant:

$$\Delta\Theta = -k \int_o^{\Delta t} \left(\int_o^{t} M\, dt \right) dt \quad \text{degrees}$$

where $k = \frac{3\pi}{K_1 a_o^{5/2}} = \frac{1.485 \times 10^{14}}{a_o^{5/2}}$ when a_o is in meters, M in meters/day, and Δt in days; and where $k = 1$ when M is in degrees/day^2 and Δt in days.

If M is approximately constant in the interval Δt, then $\Delta\Theta \approx -k\ M\ \frac{\Delta t^2}{2}$ degrees.

1.2.4 Yaw Attitude Control

In order to control the satellite mobility, means must be provided to control its yaw attitude. For example, for configuration A satellites, positive mobility (increasing semimajor axis) is obtained with the low emissivity side of the lenticule oriented in the direction of satellite motion; to switch to a decreasing mode, the satellite must be rotated about the yaw (vertical) axis through 180 degrees to orient the high emissivity side in the direction of motion.

A number of techniques for obtaining yaw attitude control were studied (reference 1), including the use of reaction wheels and magnetic torque coils. On the basis of estimated weights and powers, a system was finally chosen whereby the lenticule and tetrapod boom assembly were pivoted with respect to the yaw and damper boom assembly. Since the yaw and damper boom tends to maintain a fixed yaw attitude due to the action of the gravity-gradient forces, the lenticule/sail assembly can be controlled in yaw by rotating it with respect to the yaw/damper boom assembly. This is accomplished by means of a step-servo motor driving through a hermetically sealed harmonic drive, the whole assembly weighing only about 17 pounds including damper and power supply. Further details concerning the design and structure of this system are contained in reference 1.

1.2.5 Uncompensated, Fixed Compensation, and Continuous Compensation Control

For a configuration A satellite (opaque lenticule), the mobility of the satellite does not vary over an extreme range as a function of the sun-line inclination (inclination of sun-line to orbital plane). This is illustrated in figure 1-5, where the satellite orientation is such that the high emissivity side is in the direction of satellite motion (negative mobility). The sun-line inclination i_s is the angle of the vector directed toward the sun from the orbit

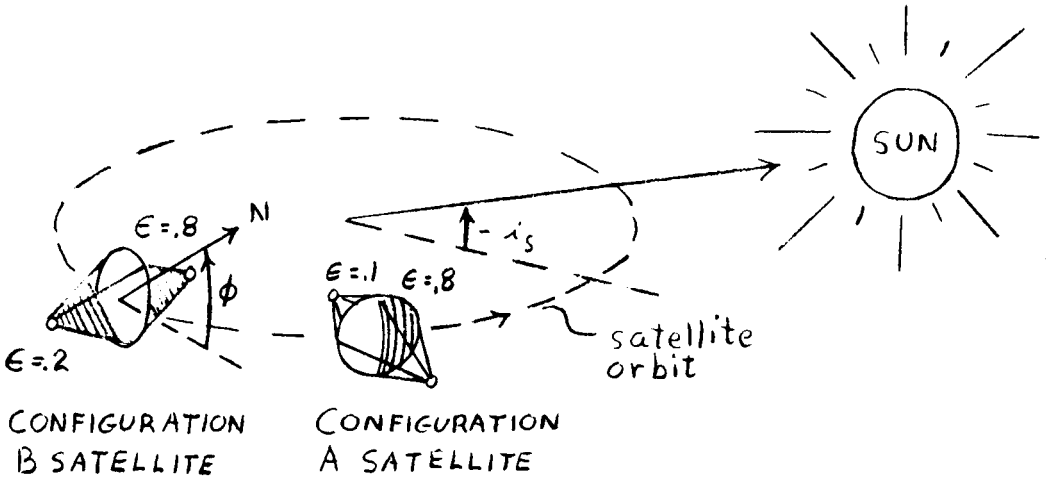

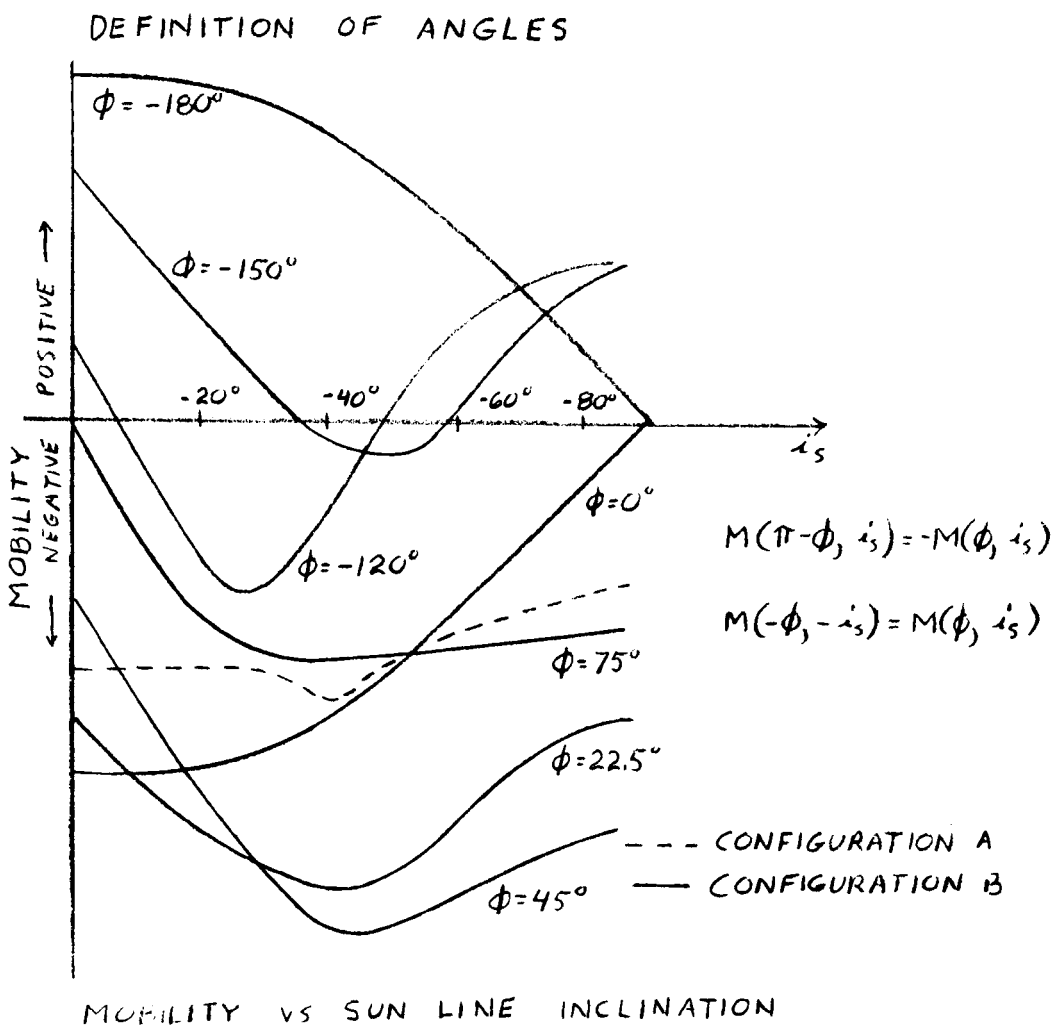

Figure 1-5. Mobility vs Sun-Line Inclination

plane and is taken as negative when the orbital motion as viewed from the sun is counter-clockwise. In part b of figure 1-5, the variation for configuration A is slight.

For the configuration B satellite however, the mobility as a function of sun-line inclination varies significantly with satellite yaw attitude. The satellite yaw attitude is specified by the angle ϕ between the orbit plane and the normal to the sail side 1, the angle being positive when counter-clockwise as viewed from the radius vector as illustrated in figure 1-5, part a. Figure 1-5, part b shows the variation of mobility with sun-line inclination for values of ϕ in the range (0 degree, 90 degrees) and (-90 degrees, -180 degrees); by considering the symmetry of the situation, values of mobility for other values of ϕ and i_s may be obtained from the formulas $M(\pi - \phi, i_s) = -M(\phi, i_s)$ and $M(-\phi, -i_s) = M(\phi, i_s)$. Points of importance are:

- Maximum mobilities are obtained with ϕ in the range (0 degree, 45 degrees) for negative mobilities and ϕ in the range (135 degrees, 180 degrees) for positive mobilities when i_s is negative. For i_s positive, the corresponding ranges are (0 degrees, -45 degrees) and (-135 degrees, -180 degrees).
- ϕ = 0 degree is undesirable at high sun-line inclinations.
- $\phi = \pm 90$ degrees produces no mobility, and may be used to provide a neutral mode.

In view of the variation of mobility with yaw attitude ϕ, three control procedures are defined:

- Uncompensated Control - ϕ = 0 or 180 degrees
- Fixed Compensation Control - ϕ is set to a constant nonzero value representing a reasonable mobility compromise over the range of sun-line inclinations of interest. Generally, the value of ϕ is ± 22.5 or ± 167.5 degrees as appropriate.
- Continuous Compensation Control - ϕ is varied continuously with sun-line inclination to achieve maximum mobility at all times.

In general, the fixed compensation control is believed to represent the best compromise technique. Further details regarding these three procedures may

be found in part 2. A discussion of several other control procedures for configuration B satellites (the Phillips concept and modifications) is presented in reference 1.

1.2.6 No-Neutral-Mode and Neutral-Mode Control Procedures

Two relatively simple control procedures which may be used for orbit position control are the no-neutral-mode and the neutral-mode procedures. In the no-neutral-mode, the satellite is maintained alternately in increasing and decreasing mobility modes $\pm M$ of duration t_b, as illustrated in figure 1-6. This results in a nominally sawtooth variation of period and a variation in angular position which looks sinusoidal but is actually composed of parabolic arcs. The angular position is defined relative to the angular position of a similar satellite in the same orbit but having no orbit position control capability. When the true angular position exceeds some limit Θ_ϵ (which may be the minimum detectable angular error), control is initiated in one of two ways. If the mobility mode at the time the error limit is exceeded is in the direction that would tend to increase the angular error, the mobility is reversed for a time period t_1, as shown. The duration of t_1 is chosen to reduce the angular error to zero in a time interval t_b, after which a second mobility reversal of duration t_2 is applied; t_2 is chosen to reduce to zero the period error resulting from the correction t_1 as well as any other period error existing upon detection of the initial angular position error. In the event that the mobility mode at the time of initial angular position error detection is already in the direction to decrease the angular position error, mobility control is applied by delaying the normal mobility reversal an interval t_1, followed by a similar delay t_b later for an interval t_2. These delays have the same effects that the mobility reversals have in the previous case.

For the neutral-mode procedure, the satellite is normally maintained in a state of zero mobility. For example, this may be accomplished in the case of a configuration B satellite by aligning the sail in the orbit plane. If the angular position error exceeds a limit Θ_ϵ as shown in figure 1-7, a mobility,

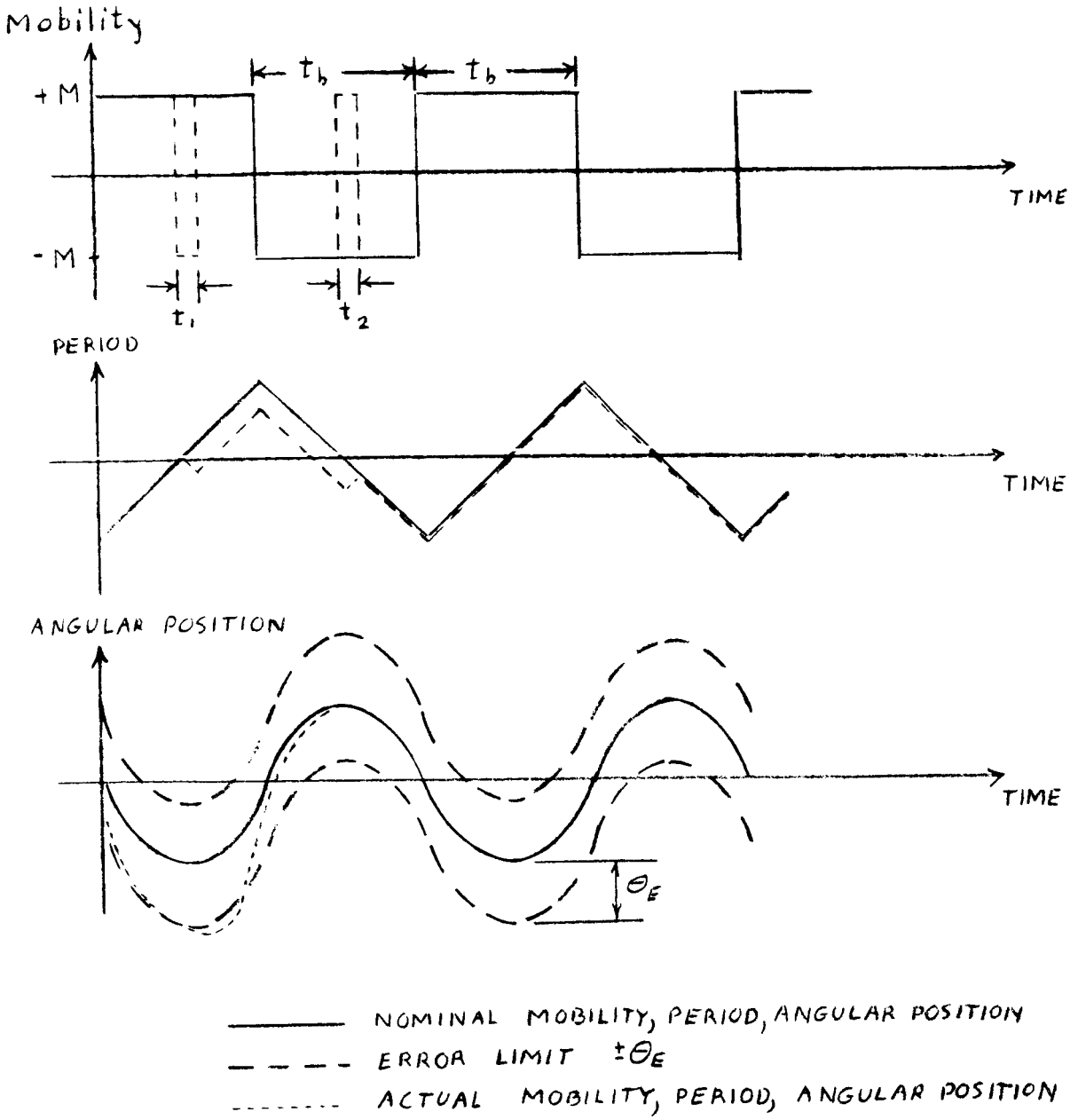

Figure 1-6. No-Neutral Mode Control

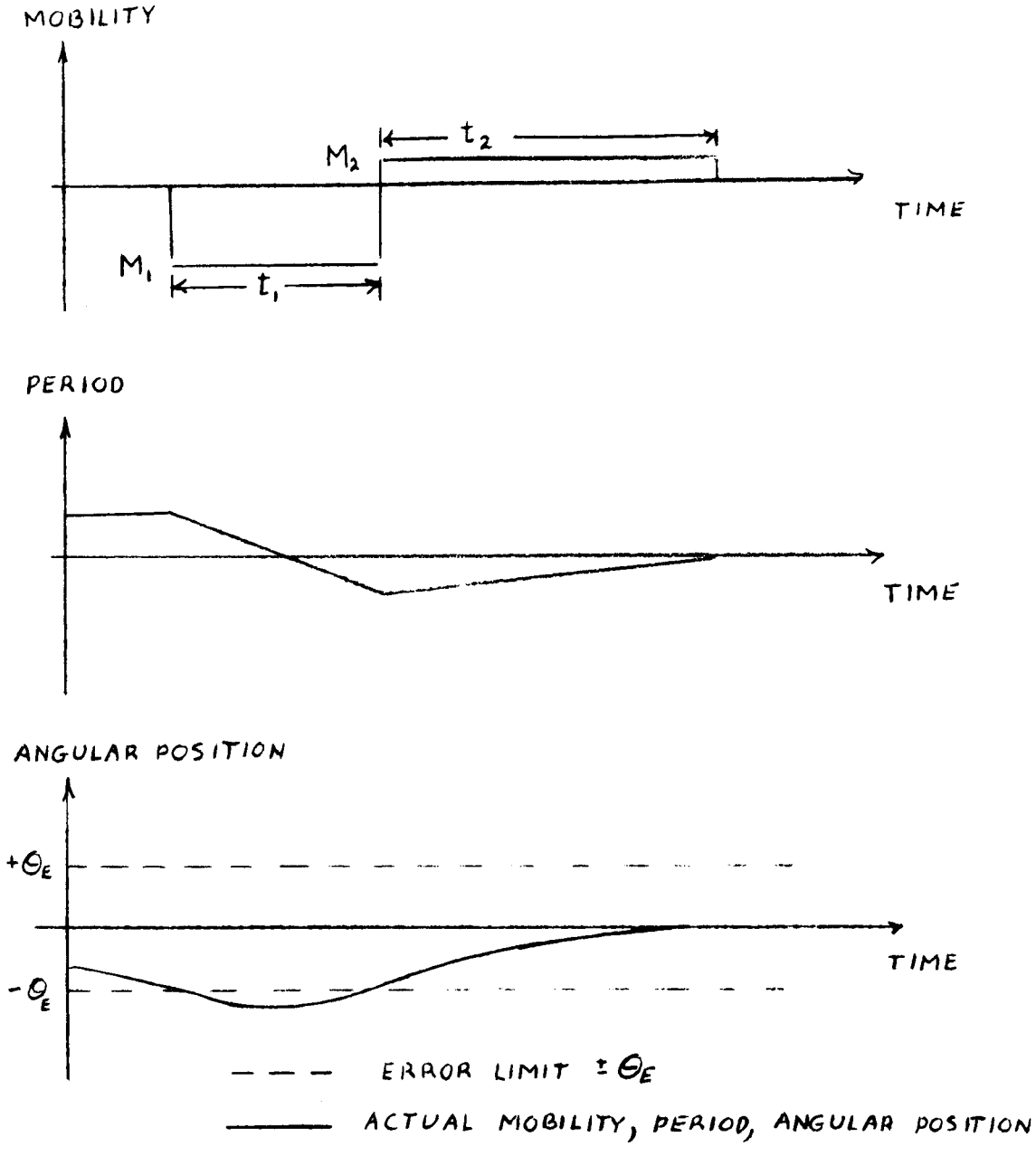

Figure 1-7. Neutral-Mode Control

M_1 is applied for a period t_1 such that at the end of t_1 the angular position error has been returned to θ_ϵ and the period error is in the direction to decrease the angular position error. (This is true on the assumption that the period error at initial angular position error detection is in the direction to increase in magnitude the angular position error. If this is not the case, the initial mobility pulse (M_1, t_1) may be eliminated.) A second mobility pulse of magnitude M_2 and duration t_2 is then applied to reduce both angular position error and period error to zero.

2. PARAMETRIC DATA

2. PARAMETRIC DATA

2.1 USE OF THIS HANDBOOK

Explanations of the various data appearing in this handbook may be found in paragraph 2.2. More detailed derivations and other supporting material appears in part 3. The use of the parametric data is best illustrated by an example.

Suppose that a system of passive communications satellites is to be placed in orbit. Suppose a tentative choice is made to use three orbits of 4000-nmi altitude and 40-degree inclination, spaced 120 degrees in right ascension. If the coverage requirements of paragraph 3.6 are used, five satellites will be required per orbit, and the allowable position error will be ±6.75-degree. Assume two further requirements:

- The five satellites in a given orbit are to be placed in orbit by a single vehicle, the placement to require no more than 2 months
- The diameter required at 4000-nmi altitude is 500 ft.

The required mobility may be found by use of information presented in figures 2-1 or 2-2. If five satellites are to be evenly spaced from a single point, the greatest angular corrections to be made are ±144 degrees. Since they are launched by a single vehicle, they will all have almost exactly the same period; assume therefore that ΔP_o is zero. To move a satellite forward, ϕ_d is negative. Since ΔP_o is zero, table 2-1 indicates the correct initial mobility is altitude decreasing, with the correct sign choice mode (+, +). An initial altitude increasing mode could not be used for negative ϕ_d in this case, since it would imply a (+, -) sign choice mode and for $\Delta P_o = 0$, only the (+, +) sign choice mode exists, as may be seen by examination of the curves of the upper right quadrant of figures 2-1 or 2-2. (The equivalent satellite angle change could be obtained by moving the satellite backward

TABLE 2-1

SIGN CHOICES FOR MANEUVER TIME t_m

Initial Mobility	Sign ΔP_o	Sign ϕ_d	Sign Choice Mode
Altitude increasing	+	+	(-, +)
		-	(-, -)
	- (or zero)	+	(+, +)
		-	(+, -)
Altitude decreasing	+ (or zero)	+	(+, -)
		-	(+, +)
	-	+	(-, -)
		-	(-, +)

360 degrees -144 degrees = 216 degrees rather than forward 144 degrees. In this case, ϕ_d would be positive, the initial mobility mode would be increasing, and again the proper sign choice mode would be (+, +).) Using the (+, +) sign choice mode and figure 2-2, a trail and error procedure leads to the following results:

Mobility	t_m, days
1500	44
1000	53
800	60

Thus, the required mobility to achieve the initial satellite placement is 800 meters/day.

In order to ensure that this placement may be made under all conditions, this value of mobility will be taken as the minimum mobility. Consider now the configuration B satellite using fixed compensation control. Refering to figure 2-3, the minimum mobility for an area-to-mass ratio of 5 ft^2/lb for

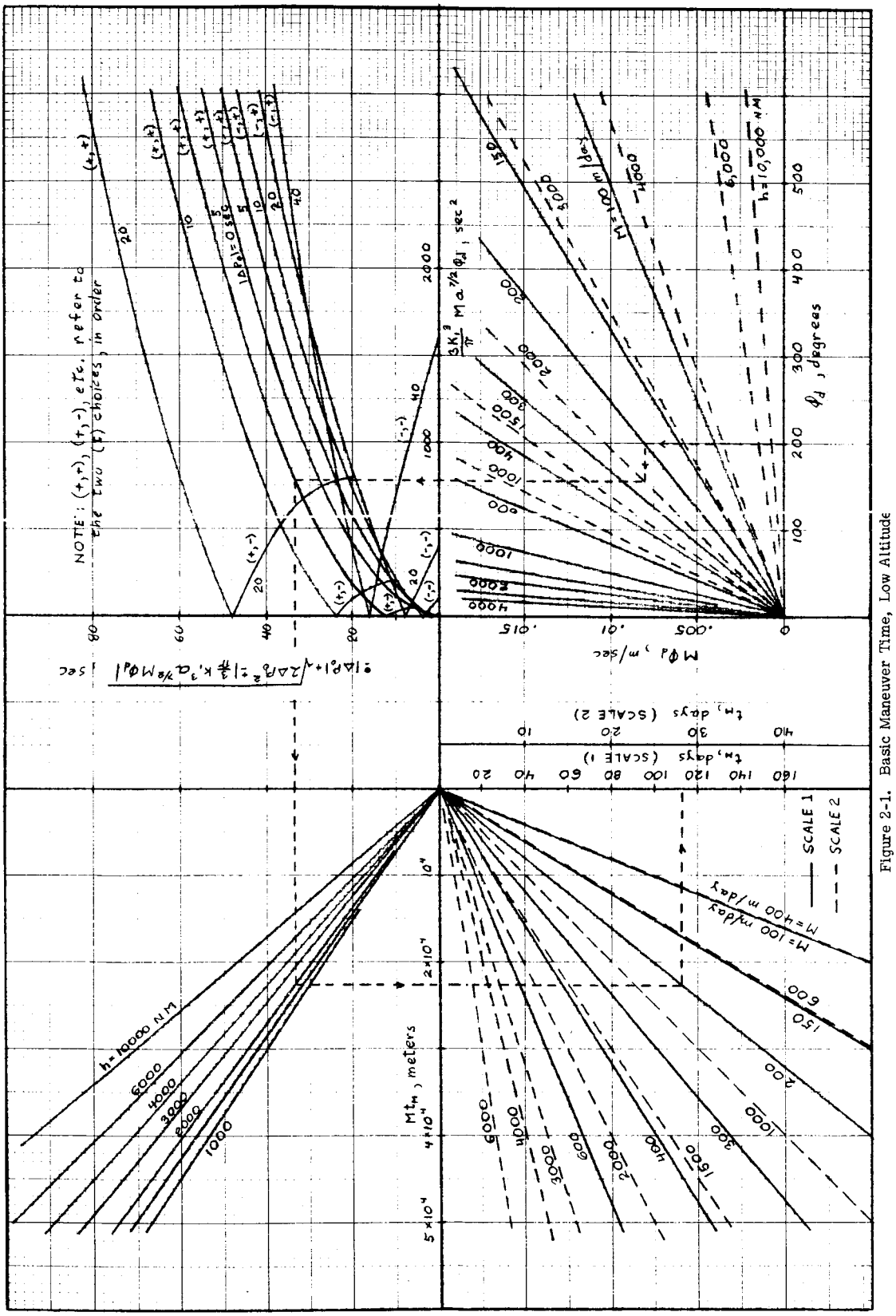

Figure 2-1. Basic Maneuver Time, Low Altitude

Figure 2-2. Basic Maneuver Time, High Altitude

a 4000-nmi 40-degree inclination orbit is 512 meters/day. Thus, the area-to-mass ratio required to achieve a minimum mobility of 800 meters/day is 7.81 ft^2/lb. $\left(\frac{800}{512} \times 5\right)$

Suppose this area-to-mass ratio may be obtained with a satellite weight of 5,000 lb and a sail area of 39,000 sq ft. The required R/D ratio at 4000-nmi altitude, from figure 2-4, is 0.99, so that R=495 ft. Using the equations of paragraph 2.2.4.2, the equivalent area-to-mass ratio for eccentricity scaling is 10.33 ft^2/lb. From figure 2-5 a maximum eccentricity of $^0.064$ is obtained for i = 40 degrees, h = 4000 nmi for an area-to-mass ratio of 20 ft^2/lb. The maximum eccentricity for an area-to-mass ratio of 10.33 is thus $(^{10.33}/_{20})0.064 = 0.0331$.

With this information, the various errors may be found. Assume a NNM type control with t_B = 20 days and an error limit, θ_E, of 4 degrees. The duration of the first correction mobility pulse if θ_E is exceeded will be about 0.7 day, from figure 2-6. If a period error ΔP_o of 0.3 second exists at the time the angular position error exceeds θ_E, and if ΔP_o is such that the angular position error is increasing, t_2 will be less than t_1 by 0.13 day (figure 2-7), so that $t_2 = 0.7 - 0.13 = 0.57$ day. The value of θ_1 obtained from figure 2-8 for a mobility of 80 m/day and a period error ΔP_o of 3 second, at h = 4000 nmi, is about 4.5 degrees. Scaling by $(\frac{1}{10})^2$ and $(\frac{1}{10})$, and dividing by 2 to account for the use of NNM control, an angular error due to the period error ΔP_o of $\theta_1 = 0.0022$ degree for M = 800 meters and $\Delta P_o = 0.3$ second is obtained.

From figure 2-9, for mobility of 80 meters per day and a mode change time of 0.3 day (for example), an error of 0.02 degree is obtained; scaling by 10, and multiplying by 2 to account for the use of NNM control, a value of 0.4 degree is obtained for $|\theta_2|$. From figure 2-10, an overshoot error due to command delay of 0.04 degree for ΔP_o = 3 second, or $|\theta_3| = 0.004$ degree for ΔP_o = 0.3 second, is obtained for a command delay time of 1 day. Finally from figure 2-11, a value of θ_6 of 3.8 degrees is obtained.

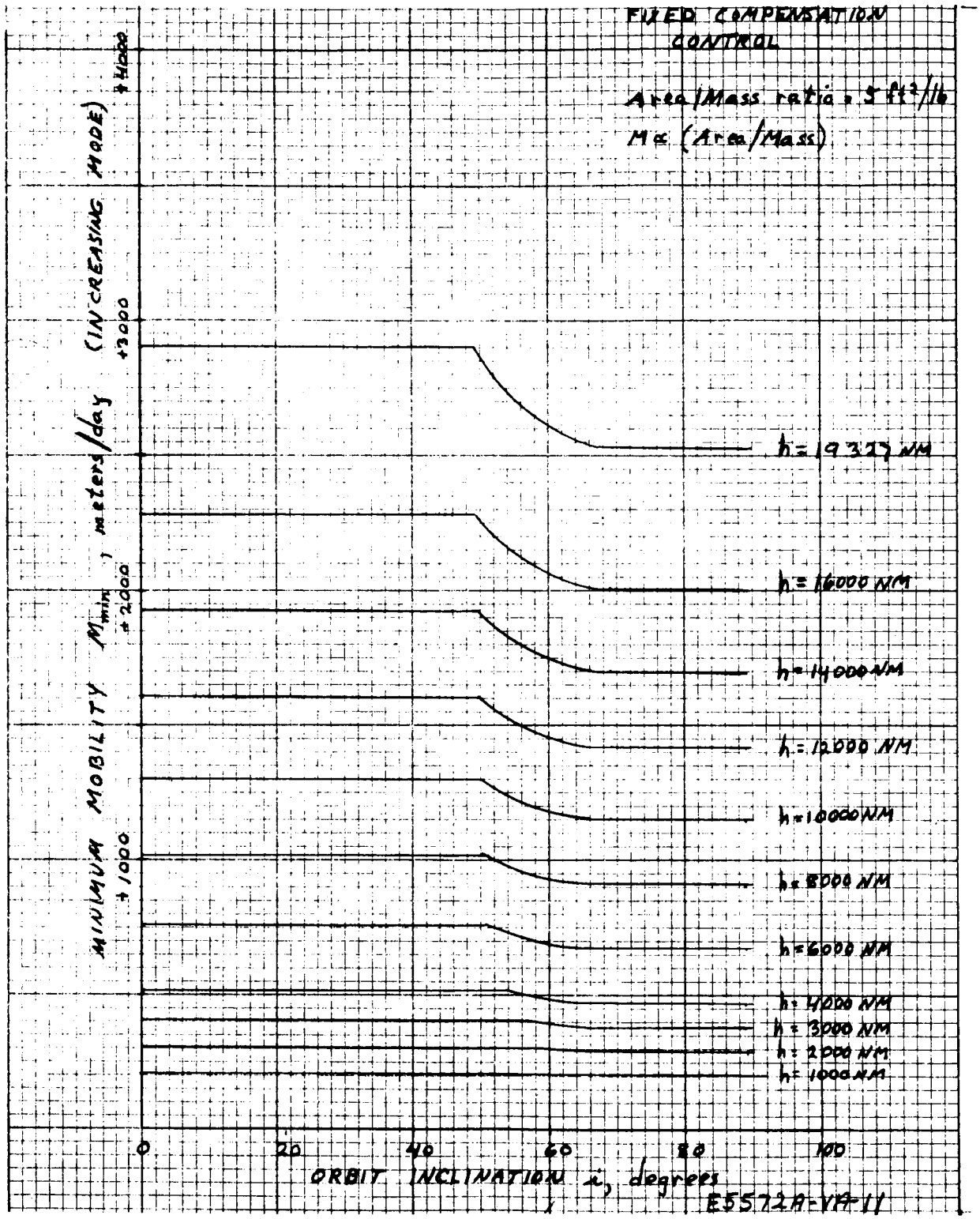

Figure 2-3. Minimum Mobility, M_{MIN}, Vs Orbit Inclination i, Configuration B.

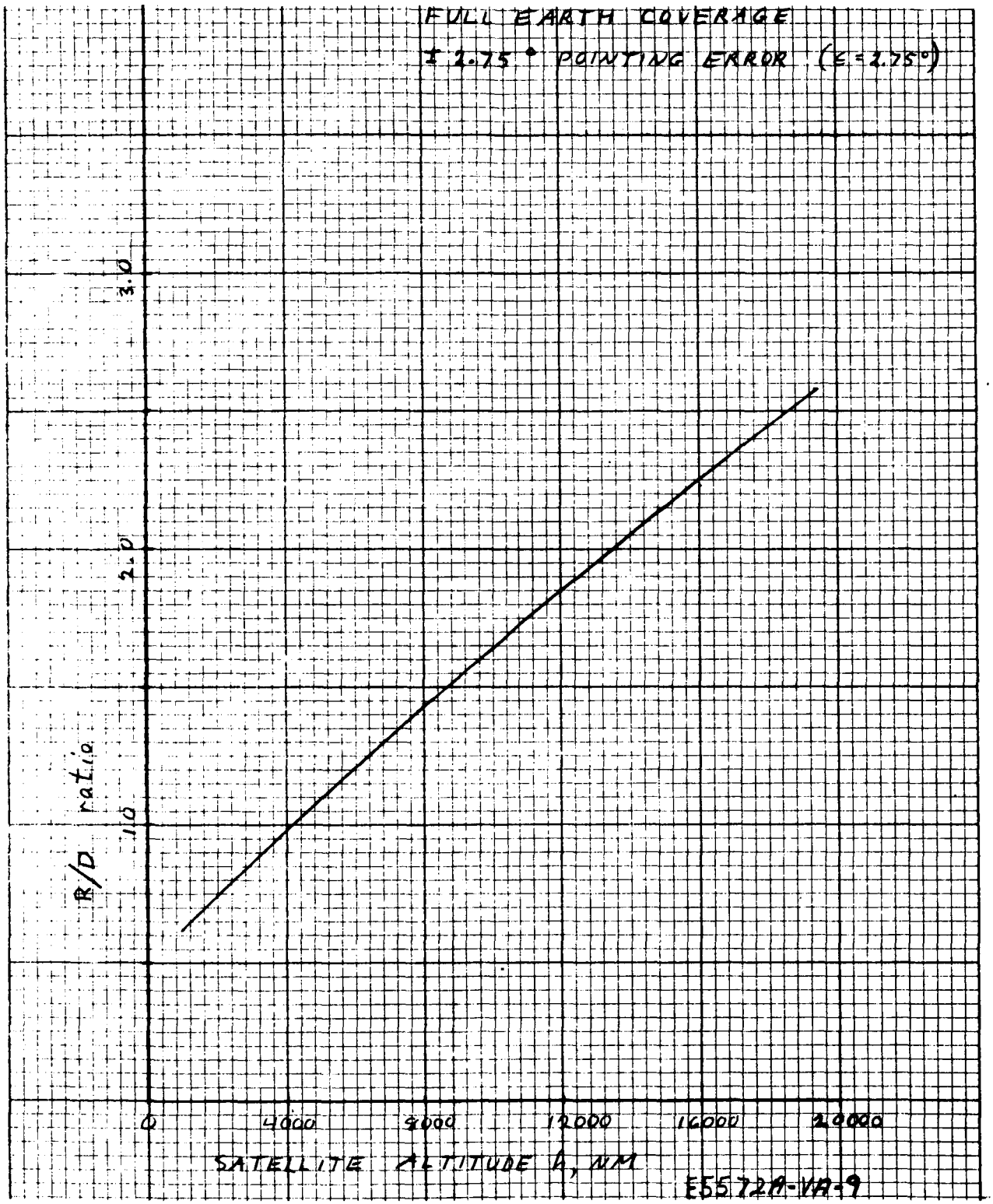

Figure 2-4. R/D Ratio Vs Altitude

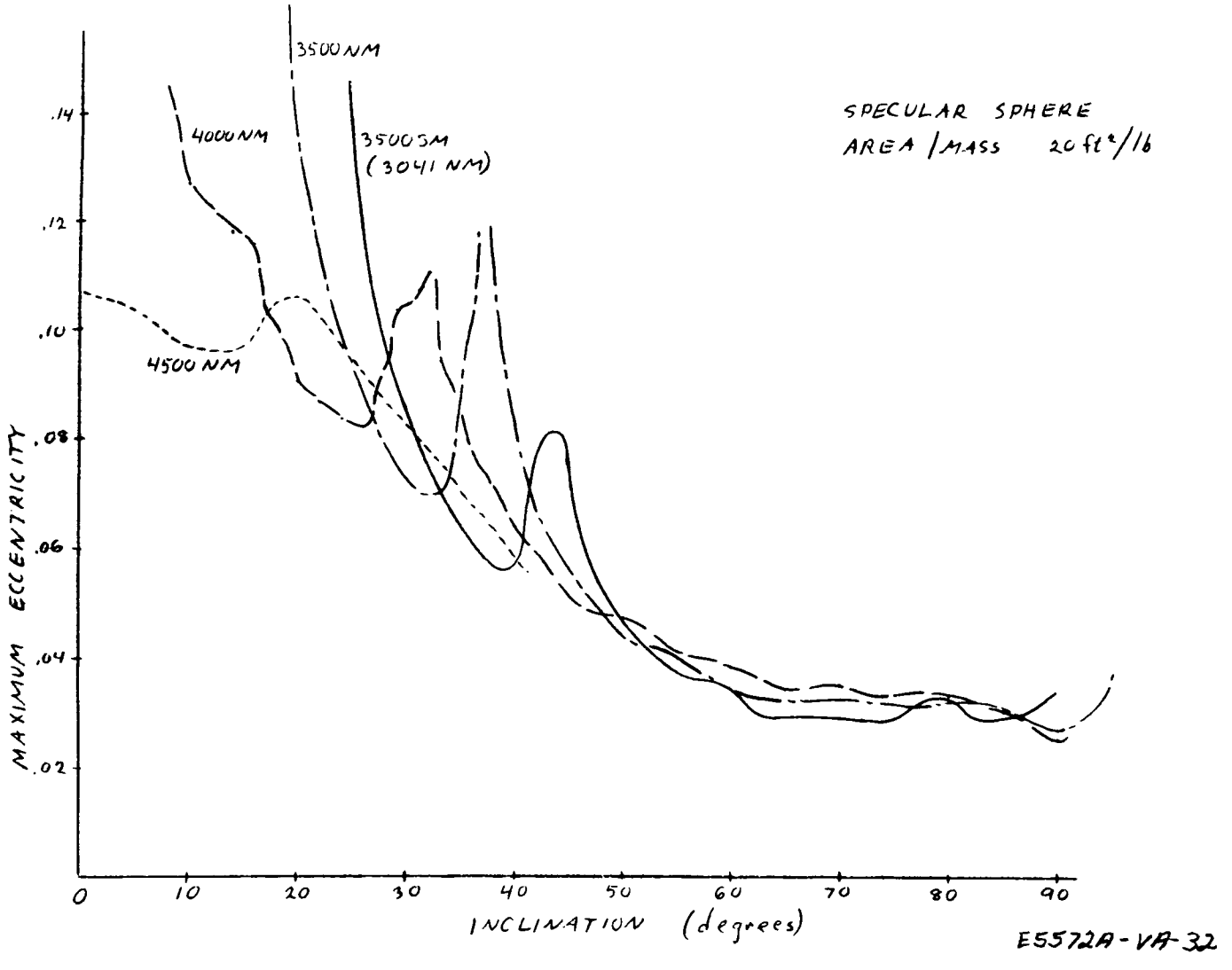

Figure 2-5. Maximum Eccentricity for Posigrade Orbits (3041- To 1500- nmi Altitude)

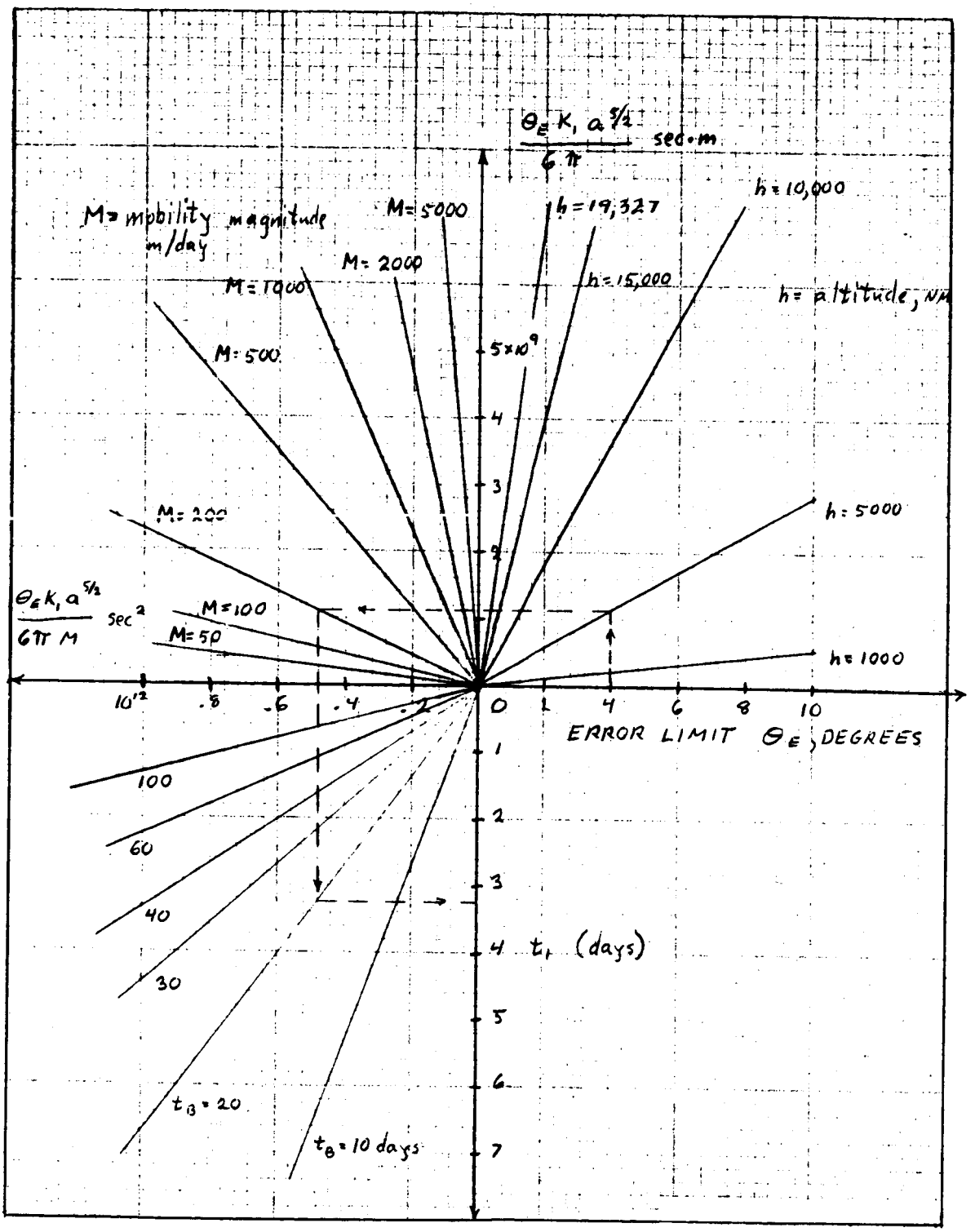

Figure 2-6. t_1 Vs θ_E; No Neutral Mode Control

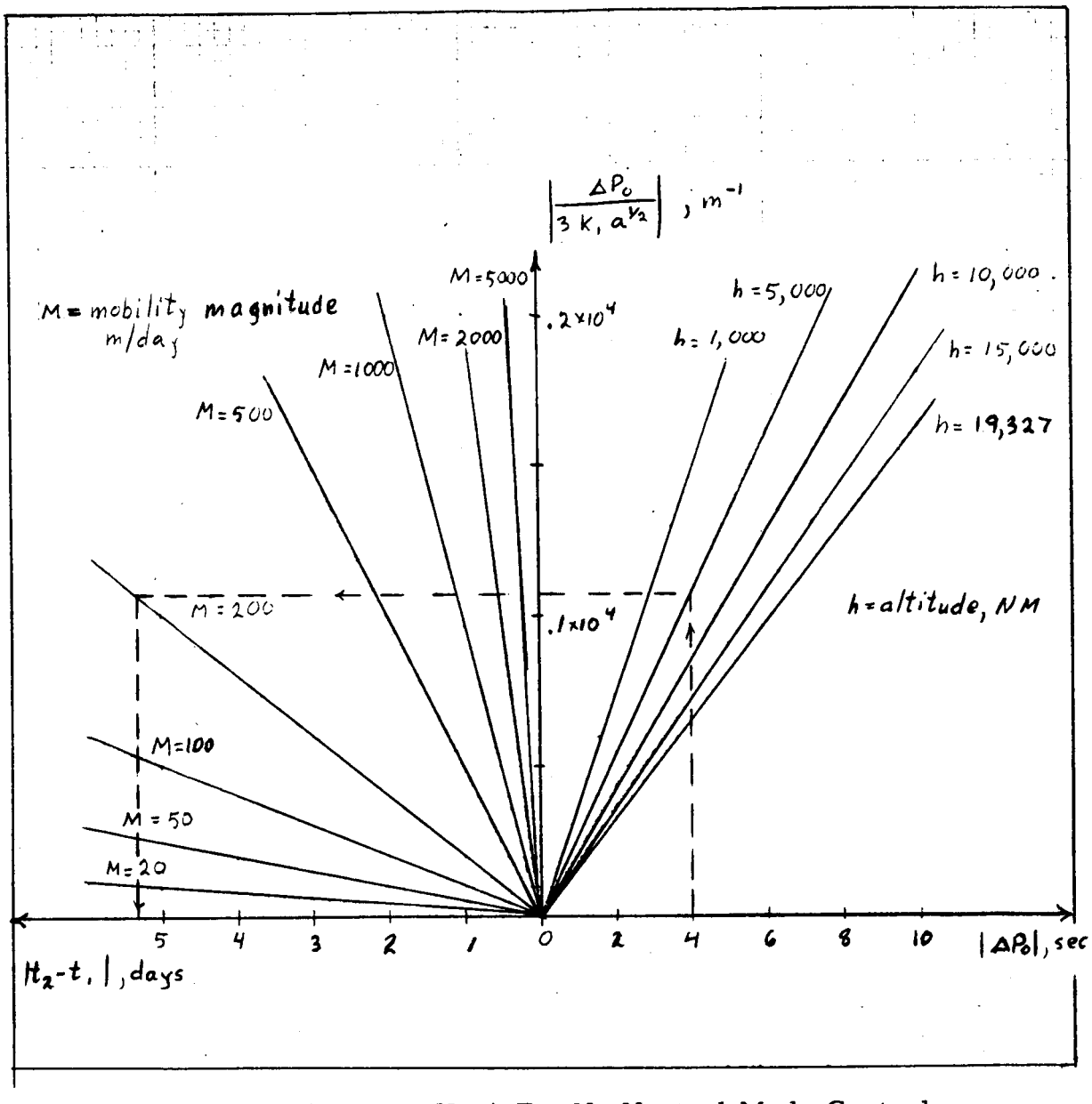

Figure 2-7. t_2-t_1 Vs ΔP_o; No Neutral Mode Control

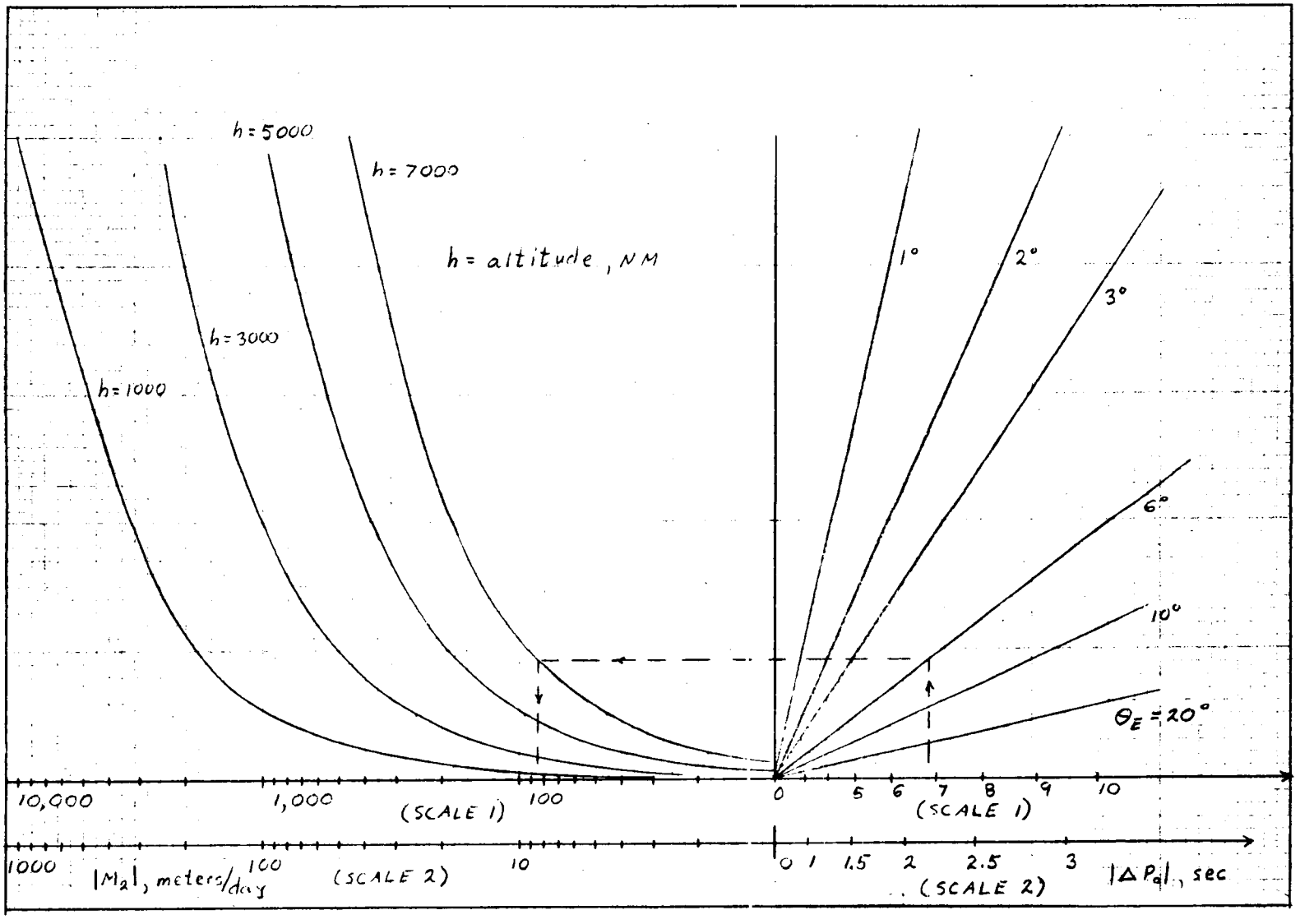

Figure 2-8. M_2 Vs θ_E, ΔP_o ; Neutral Mode Control

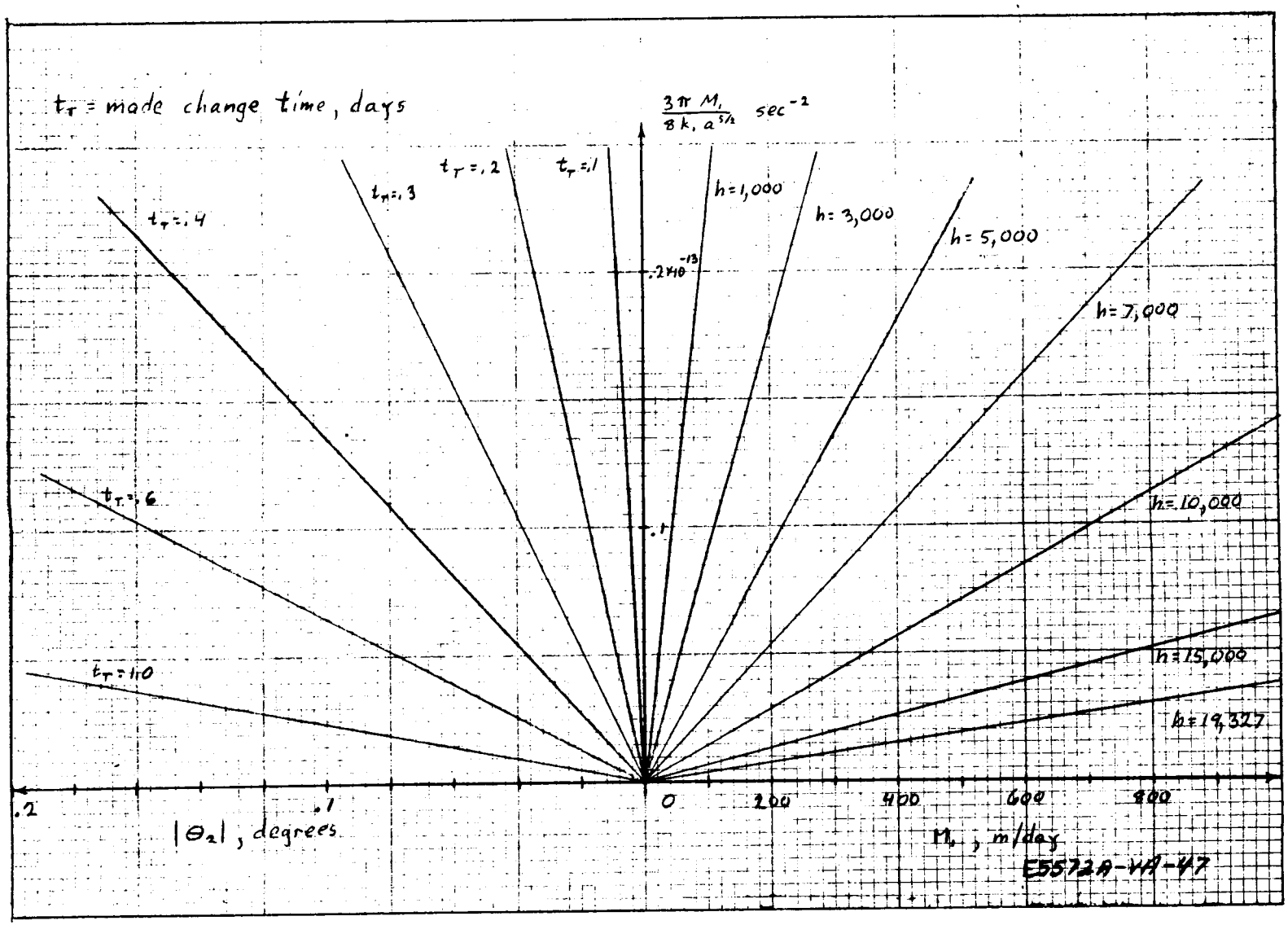

Figure 2-9. Overshoot Error Due To Finite Mobility Mode Change Time (NM Control)

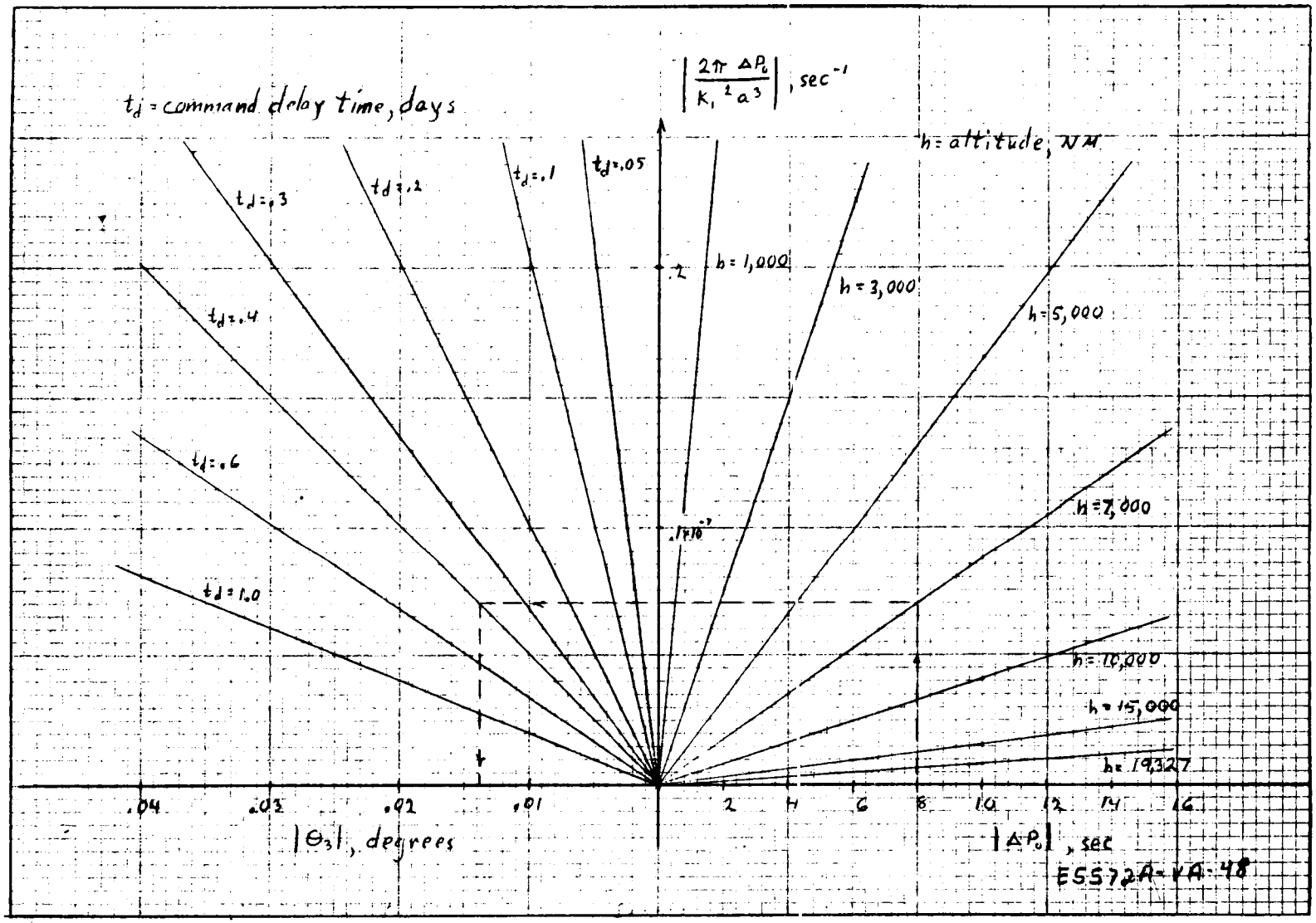

Figure 2-10. Overshoot Error Due To Command Delay

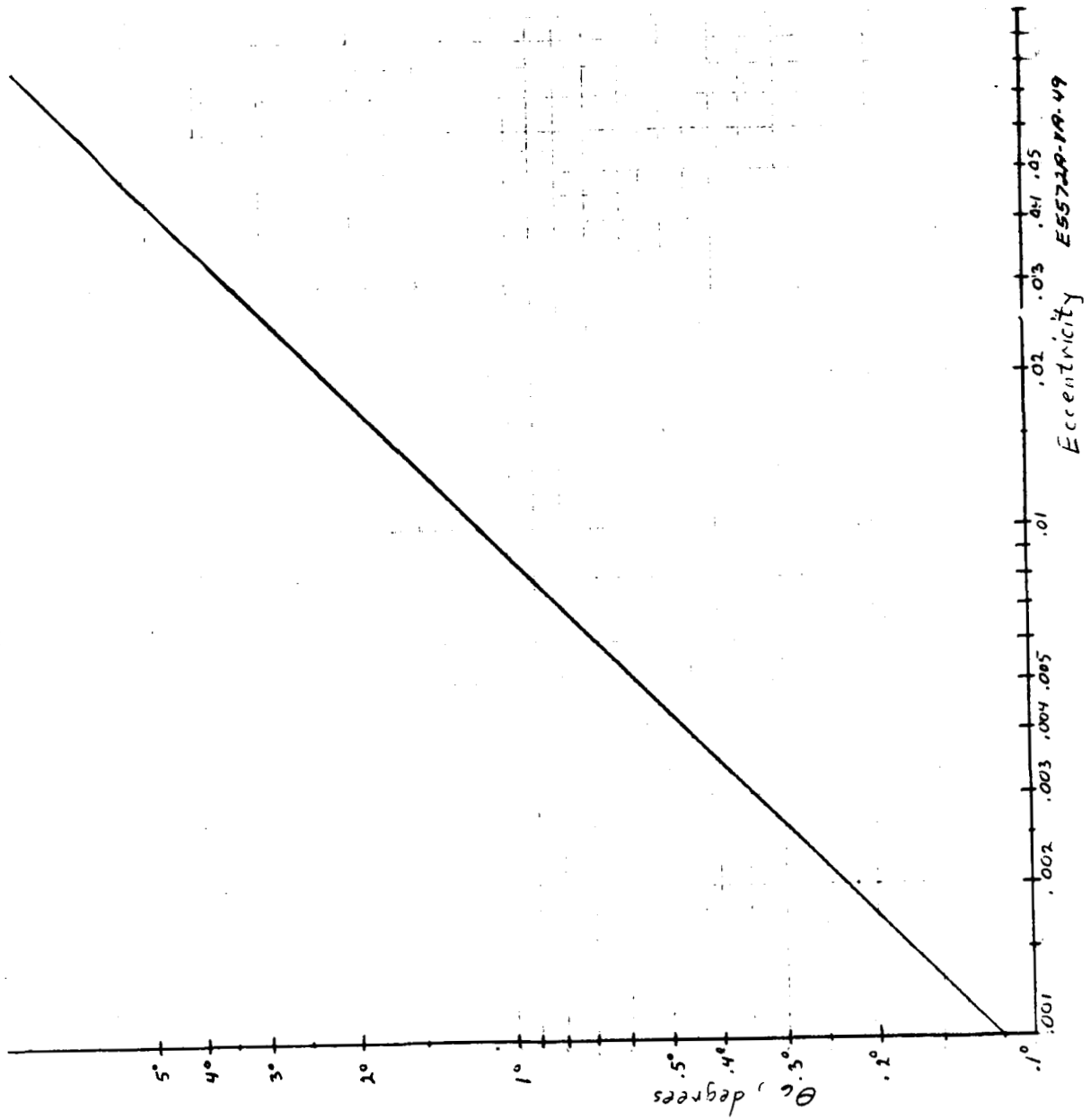

Figure 2-11. Angular Position Error Vs Eccentricity

Assuming these errors to add in a worst case situation, the total worst case error would be $|\theta_E| + |\theta_1| + |\theta_2| + |\theta_3| + |\theta_6| = 4 + 0.0022 + 0.4 + 0.004 + 3.8 \approx 7.2$ degrees. This is greater than the allowed error of 6.75 degrees. Repeating the calculation for θ_E = 3 degrees, t 0.52 day and $t_2 \approx$ 0.37 day, the worst case error is 6.2 degrees which is within the required limits.

Use of the various data graphs for a configuration A satellite is similar to that described above. The major difference is the dependence of mobility on the shape factor, R/D. For a given minimum mobility requirement, figure 2-12 can be used to find the minimum mobility for a satellite having a weight of 1500 lb, a lenticule diameter, D, of 267 ft, and a radius of curvature, R, of 200 ft. This value must first be scaled by the ratio of diameter squared ($500^2/267^2$) and then by the appropriate shape factor (R/D = 0.99; 200/267 = 0.75) as given in figure 2-13 to provide a value of minimum mobility for a 1500-lb satellite having a radius of curvature of R = 495 ft and a diameter D = 500 ft. The maximum mass allowed to achieve the required minimum mobility of 800 meters/day may then be found. Alternatively, given the satellite weight, the resulting minimum mobility may be found and compared with the required value of 800 meters/day to determine if the requirement can be met. Eccentricity and error calculations for the configuration A satellite are similar to those for the configuration B satellite.

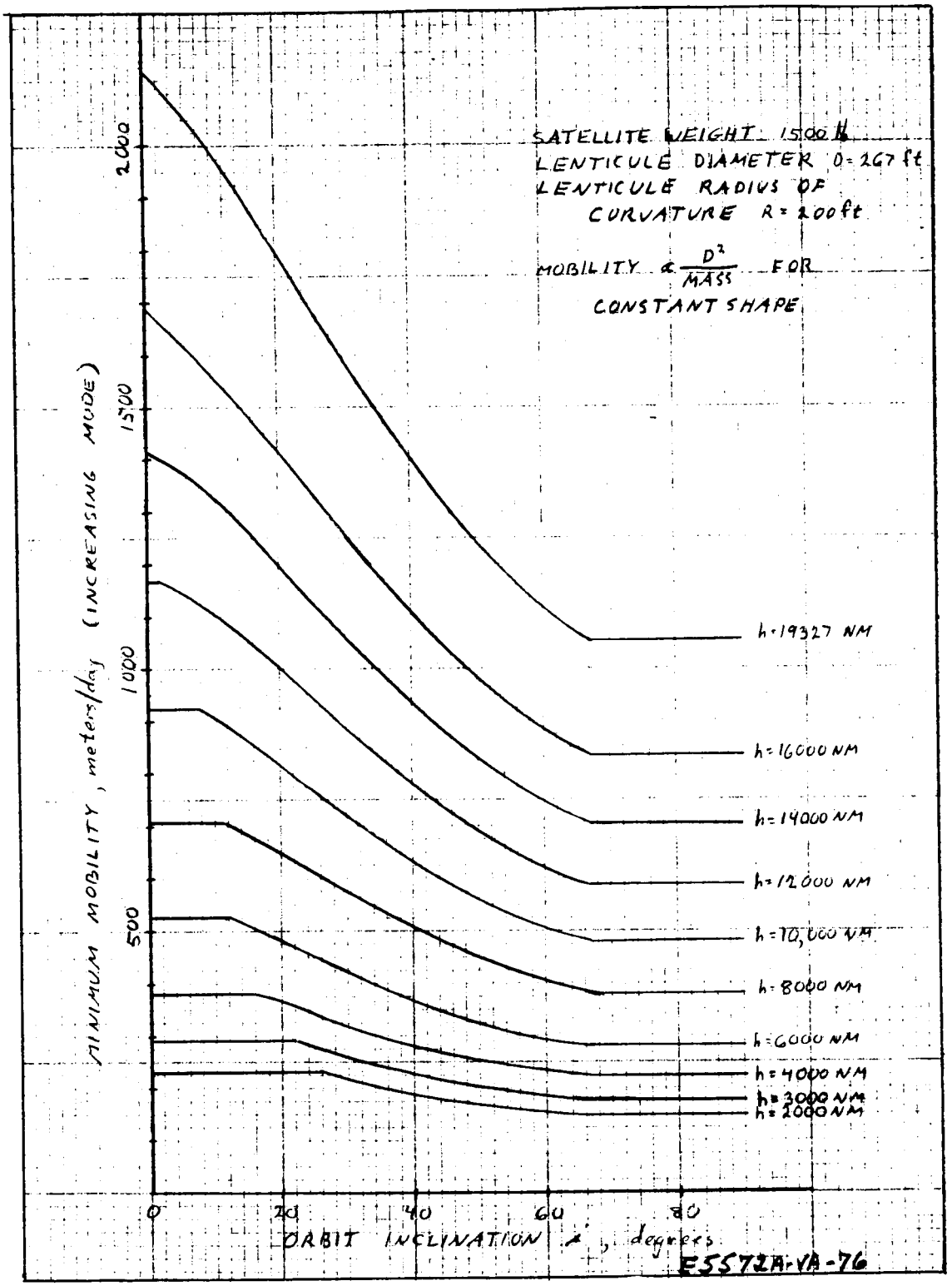

Figure 2-12. Minimum Mobility M_{MIN} Vs Orbit Inclination, i, Configuration A

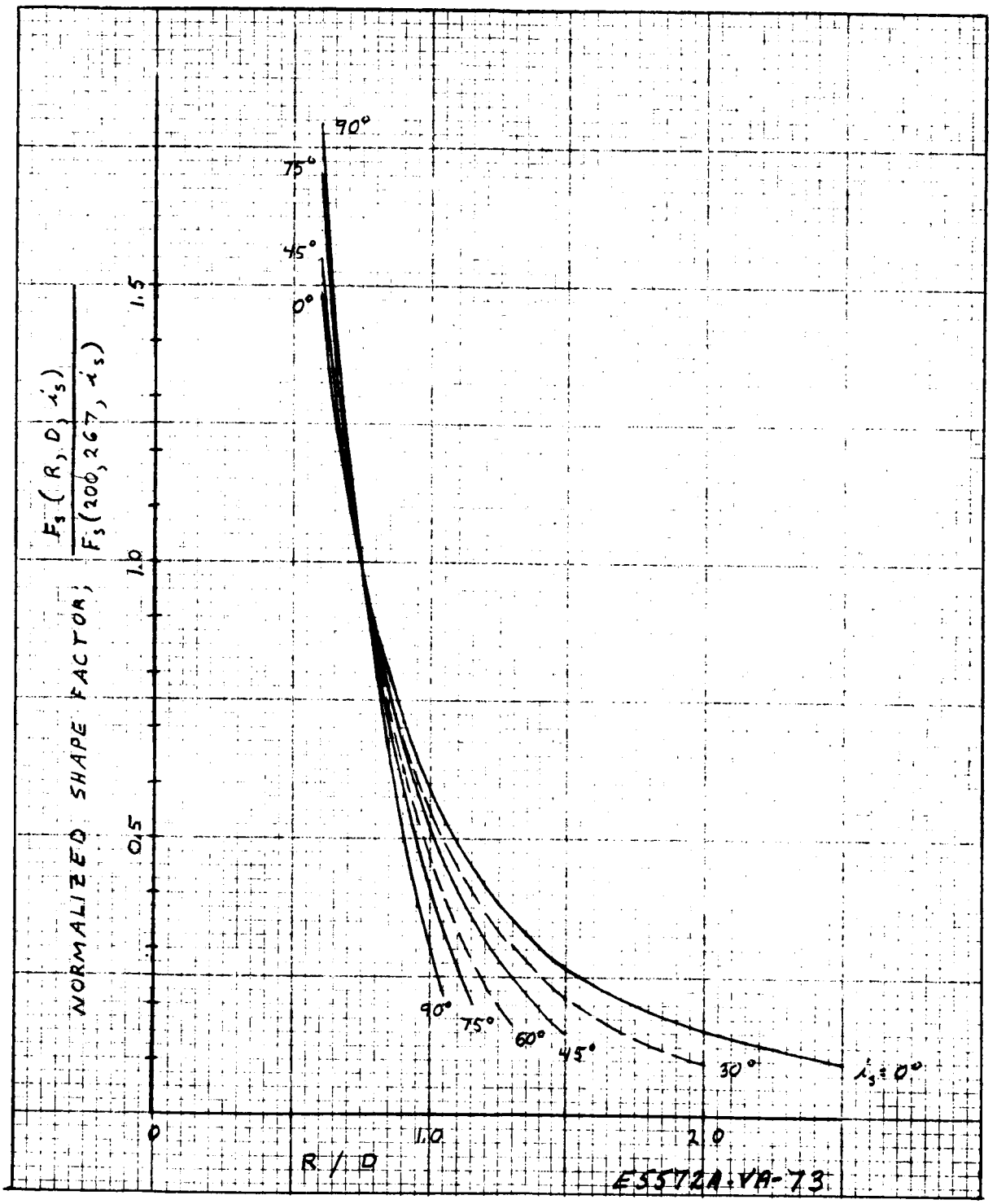

Figure 2-13. Normalized Shape Factor Us R/D Ratio, Configuration A

2.2 DATA

2.2.1 Mobility Versus Altitude and Orbital Inclination

In this paragraph, data are presented relating the mobility of the two satellite configurations to the satellite altitude and orbital inclination. Approximately circular orbits were assumed. For the configuration B satellite, fixed compensated control was assumed with $\phi = \pm 22.5$ or ± 167.5 degrees as appropriate, since continuous compensated control appears to offer only small improvement in return for the additional complexity involved.

The data relating mobility to altitude and orbital inclination was prepared by first separately considering the following relations:

- Mobility versus semimajor axis and sun-line inclination, for a constant size, weight, and shape satellite
- Mobility versus shape factor; i.e., the effect of variation of the ratio of radius of curvature of the lenticule to its diameter (this factor is not applicable to configuration B satellites, since the shape of the satellite has no effect on the mobility in this case).
- Shape factor versus altitude; i.e., the required shape factor for full earth coverage as a function of altitude (this factor is also not applicable to configuration B satellites).
- Distribution of sun-line inclinations as a function of orbital inclination.

Scaling relations were derived for these various effects and checked by digital computer simulation. The separate scaling relations were then combined to yield the final data relating mobility to altitude and orbital inclination. In the following subsections, data relating to these various separate effects and their combined effects are presented. Derivations of the various scaling formulas may be found in paragraph 3.1. In all cases, mobility is constant at any fixed altitude and sun-line inclination for a given satellite shape and area-to-mass ratio, regardless of satellite size. For given shape but variable area-to-mass ratio, mobility is proportional to area-to-mass ratio, so that all mobility data may be scaled with area-to-mass ratio by multiplying by the ratio of (area-to-mass ratio desired) to (area-to-mass ratio for presented data).

2.2.1.1 Mobility Versus Semimajor Axis and Sun-line Inclination

The scaling equations giving mobility as a function of the semimajor axis and of the sun-line inclination may be found in paragraph 3.1 (equations 3-43 to 3-45) for configuration A satellites and in the table found in paragraph 3.1 for configuration B satellites. Derivations may also be found in paragraph 3.1. The equations are plotted parametrically in figure 2-14 for the configuration A satellite (opaque lenticule) and in figure 2-15 for the configuration B satellite (sail). A sail angle of $\phi = 22.5$ degree (fixed compensation control) was assumed for the configuration B satellite, where ϕ is the angle between the normal to the sail and the orbit plane.*

2.2.1.2 Mobility Versus Shape Factor

For the configuration A satellite, the mobility varies as a function of the shape of the lenticule, due to variations of the temperature distribution with shape. A scaling equation for the variation of mobility with R and D is given below, where R is the radius of curvature of the lenticule shape and D is its diameter.

$$M \propto F_s(R, D, i_s) = 1 - \cos\left[\frac{\pi D}{4R}\right]\left(1 + \frac{1}{2}\sin^2\frac{i_s}{2}\right)$$

* The curves for configuration A were prepared using data generated by the mobility digital computer program (paragraph 3.4) for altitudes of 1,000, 2,000, 6,000, and 19,400 nmi. For altitudes of 16,000 and 14,000 nmi, the data were scaled in altitude from 19,400 nmi. For altitudes of 10,000 and 12,000 the average of values scaled from 6,000 and 19,400 were used, while data for 8,000 nmi were sealed from 6,000-nmi altitude. Data for 3000- and 4000-nmi altitudes were obtained by averaging values scaled from 2000 and 6000 nmi. For configuration B, the scaling equations of the table of paragraph 3.1 provided exact mobility values when used with appropriate constants of proportionality.

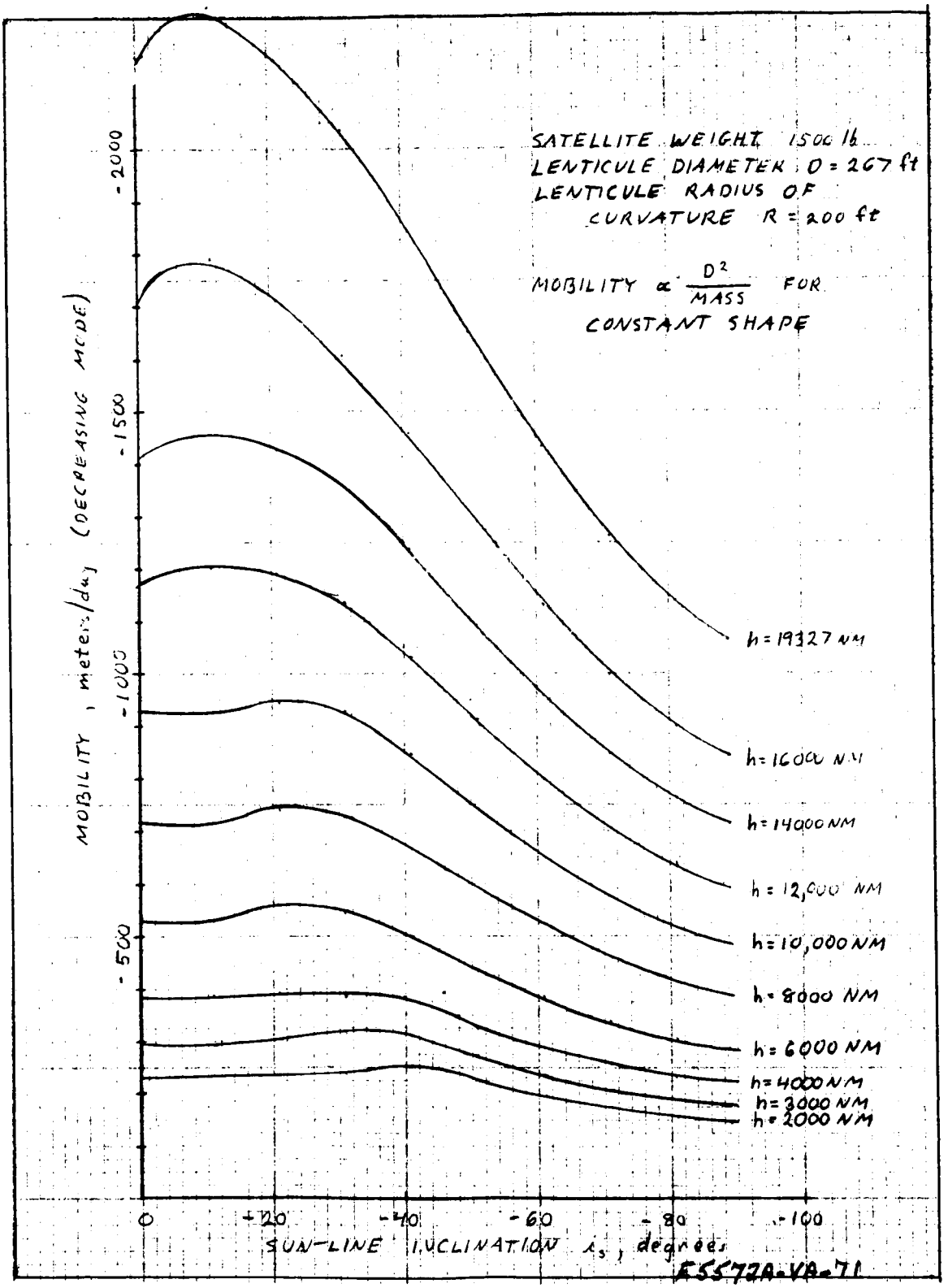

Figure 2-14. Mobility vs Sun-Line Inclination, Configuration A

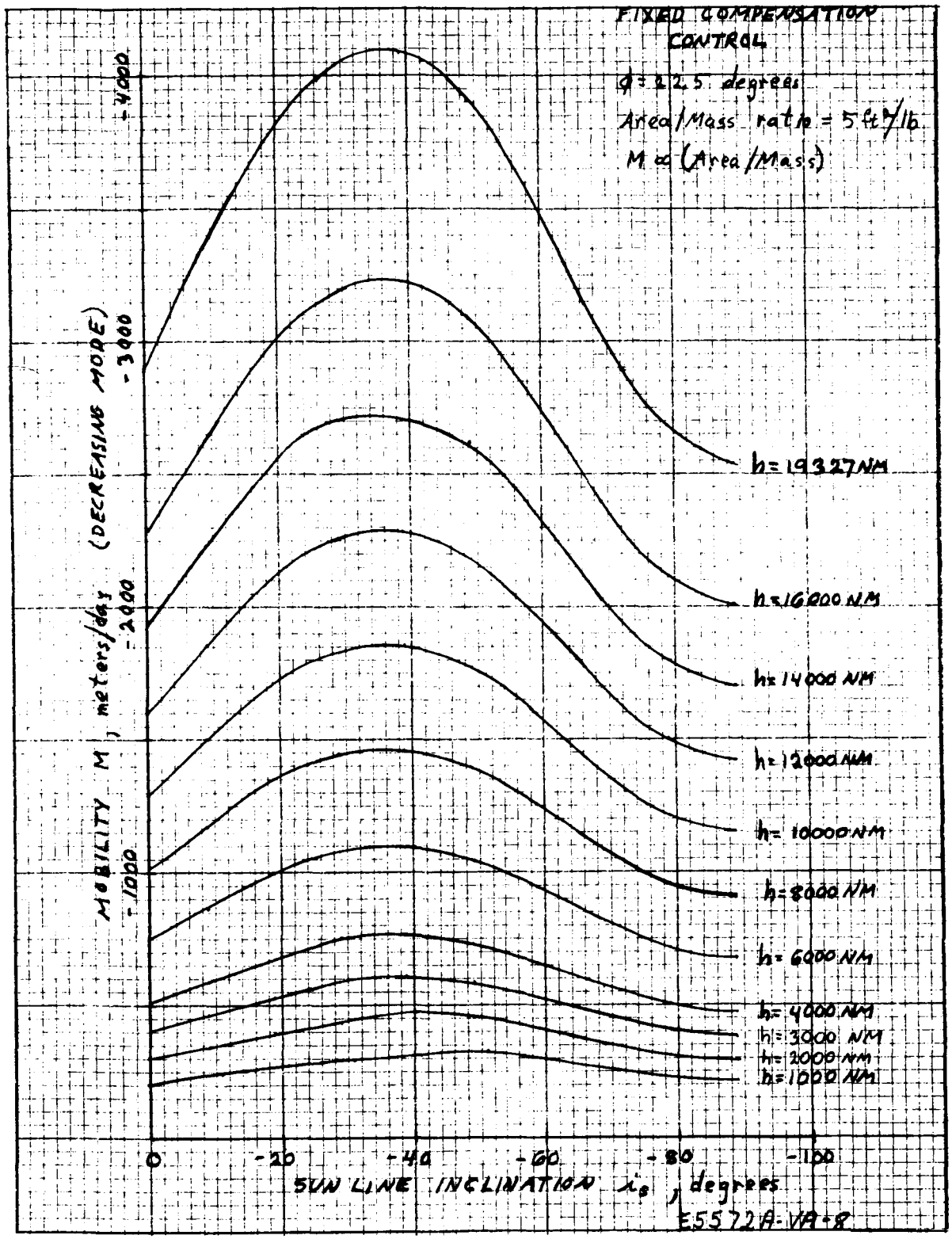

Figure 2-15. Mobility Vs Sun-Line Inclination, Configuration B

The derivation of this equation is given in paragraph 3.1. The shape factor is graphed in figure 2-13, (page 2-17) in normalized form; i.e., $F_s (R, D, i_s) / F_s (R_o, D_o, i_s)$ where R_o = 200 ft, D_o = 267 ft

2.2.1.3 R/D Versus h

A relation between the ratio of lenticule radius of curvature R to its diameter D and altitude h is given by:

$$\frac{R}{D} = \left[2 \sin \left(\sin^{-1} \frac{R_e}{R_e + h} + \epsilon \right) \right]^{-1}$$

where: R_e is the earth radius

h is the satellite altitude

$\pm\epsilon$ is the allowable pointing error

This relation is derived in paragraph 3.1, based on the requirement that the lenticule cover the entire earth at any given altitude and for pointing errors up to $\pm\epsilon$ (i.e., the solid angle subtended by the lenticule at its center of curvature should be greater than the solid angle subtended by the earth by an amount sufficient to accommodate pointing errors as great as $\pm\epsilon$ from the vertical). This relation is shown graphically in figure 2-4 (page 2-7).

2.2.1.4 Sun-line Inclination Distribution

The sun-line inclination, i_s, (angle between the sun-line vector and the orbital plane) varies with the yearly orbital motion of the earth and with the precesion of the right ascension of the satellite orbit. The variation consists primarily of two sinusoidal components, one of 23 degrees amplitude (due to the inclination of the plane of the equator) and the second of amplitude equal to the satellite inclination. The phase of these components is somewhat random. Using the Lifetime-18 computer program (paragraph 3.4), distributions of sun-line inclination angles over a 20-year period were obtained for a number of orbit inclinations, using orbits of 2000-nmi altitude. The resulting distributions are shown in figure 2-16 and are essentially independent of altitude.

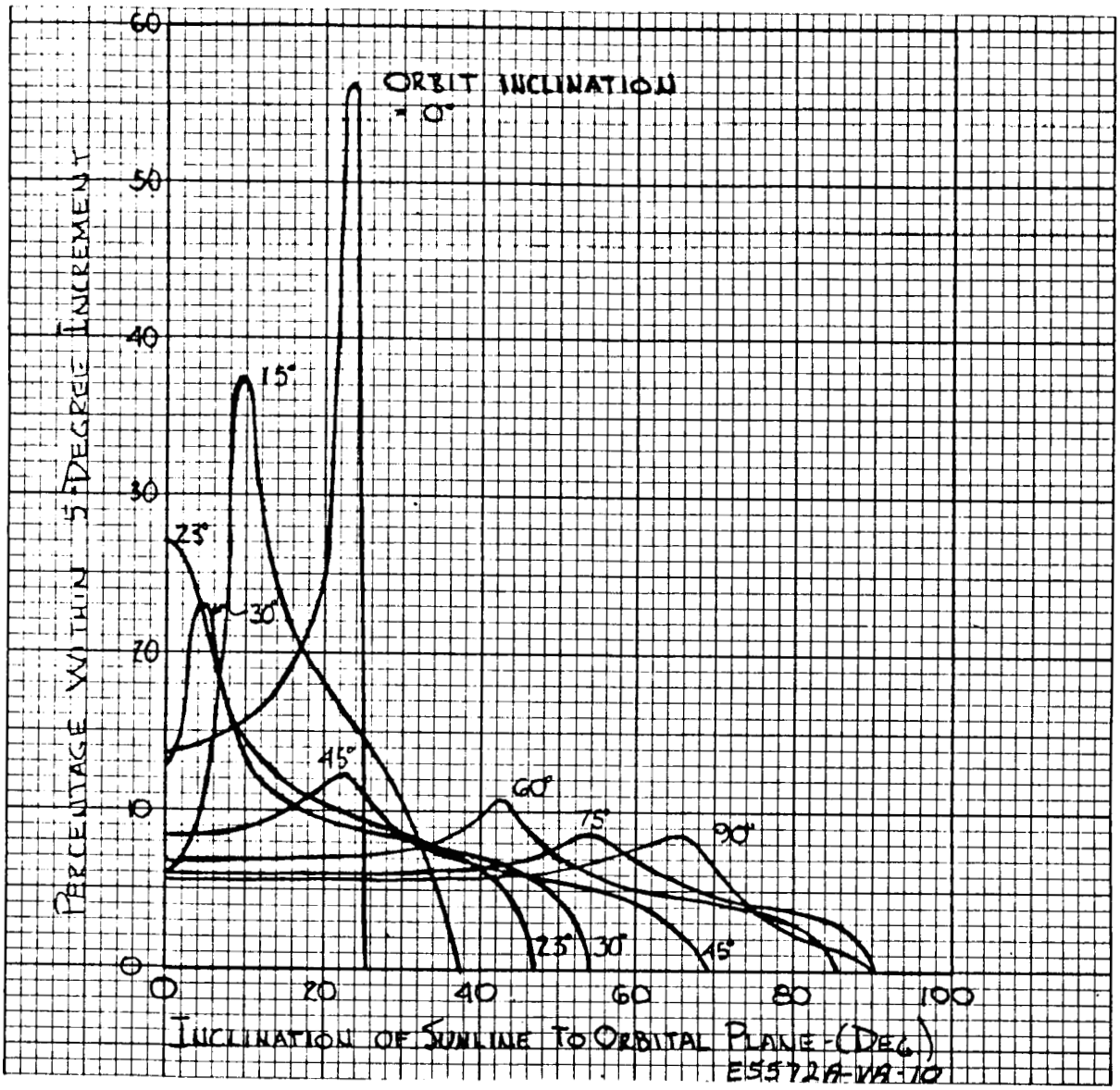

Figure 2-16. Distribution Of Sun-Line Inclinations

2.2.1.5 Mobility Versus Altitude and Orbital Inclination

Using the relations of paragraph 2.2.1.1 through 2.2.1.4, the mobility as a function of altitude, h, and orbital inclination, i, is found as follows:

- Choose h and i
- Determine M versus i_s for the given altitude, h, and nominal shape factor (R = 200 ft, D = 267 ft) or area-to-mass ratio (5 ft/lb)

- Choose the minimum and maximum values of M over the range of the i_s distribution corresponding to the chosen orbital inclination, i. These two values are defined as M_{min} and M_{max}. Average M over the distribution of i_s to yield M_{ave}.
- Correct values of M_{min}, M_{max}, M_{ave} by scaling by the shape factor*, by D^2, and inversely with mass, in the case of configuration A satellites. For configuration B satellites, the corrections are made by scaling according to area-to-mass ratio. R/D as a function of h may be obtained for scaling purposes from figure 2-4 (page 2-7).

The above procedure was followed for a satellite of constant shape, having a diameter of 267 ft, a lenticule radius of curvature of 200 ft, and a satellite weight of 1500 lb (configuration A satellite). The results are presented in figure 2-12 (page 2-16) and figures 2-17 through 2-23. Scaling for other shape factors may be accomplished by use of figure 2-13 (page 2-17). Scaling for other values of satellite diameter and mass may be accomplished by scaling in proportion to the ratio D^2/mass.

For configuration B satellites, similar results are presented in figure 2-3 (page 2-6) and figures 2-24 through 2-30. A constant area/mass ratio of 5 ft^2/lb was used throughout. Scaling for other area-to-mass ratios may be accomplished by scaling in direct proportion to area-to-mass ratio.

* To scale by shape factor, an average value of i_s must be chosen. In most cases, the peak of the i_s distribution curve (figure 2-16) is suitable.

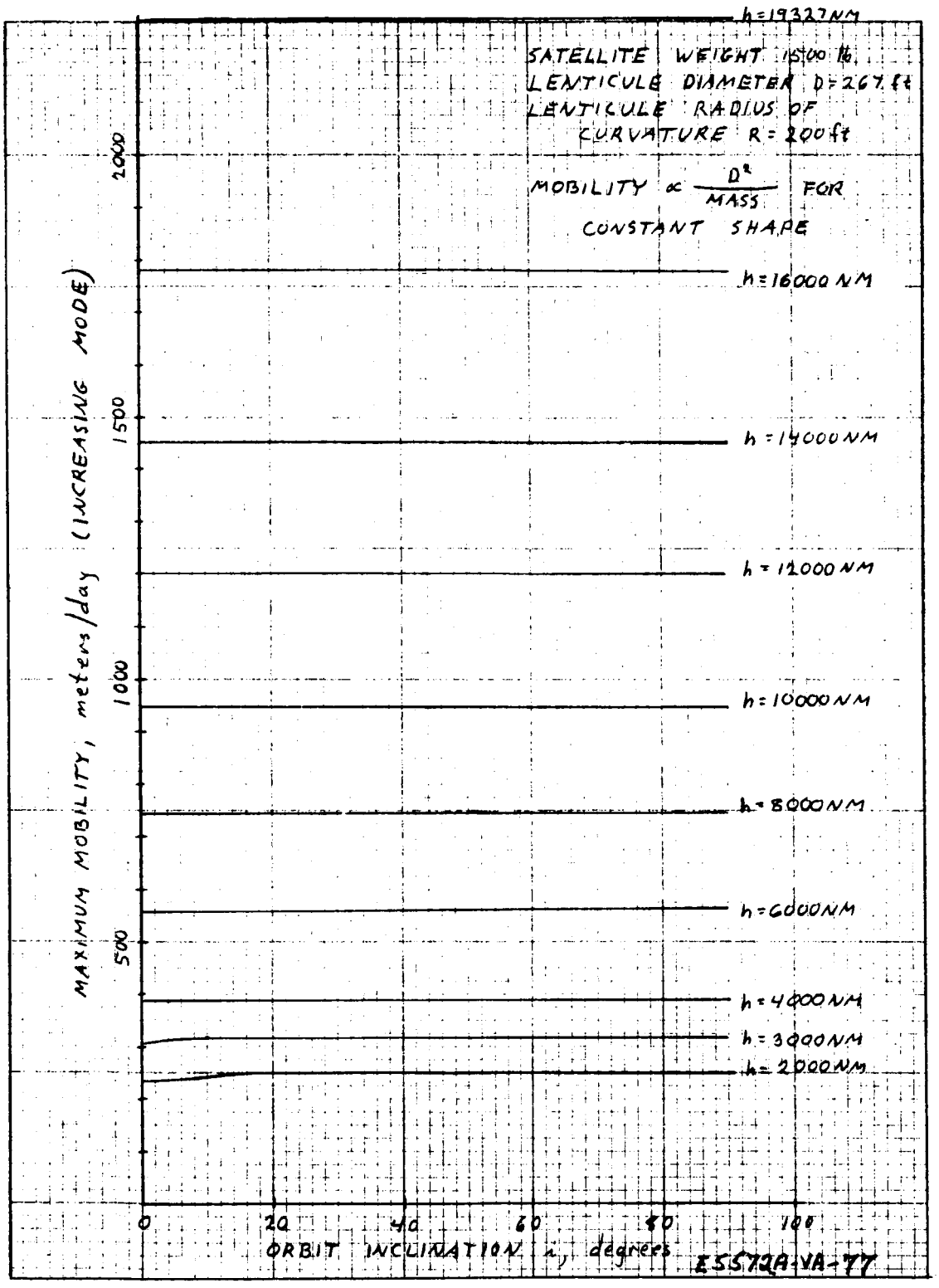

Figure 2-17. Maximum Mobility M_{max} Vs Orbit Inclination i, Configuration A

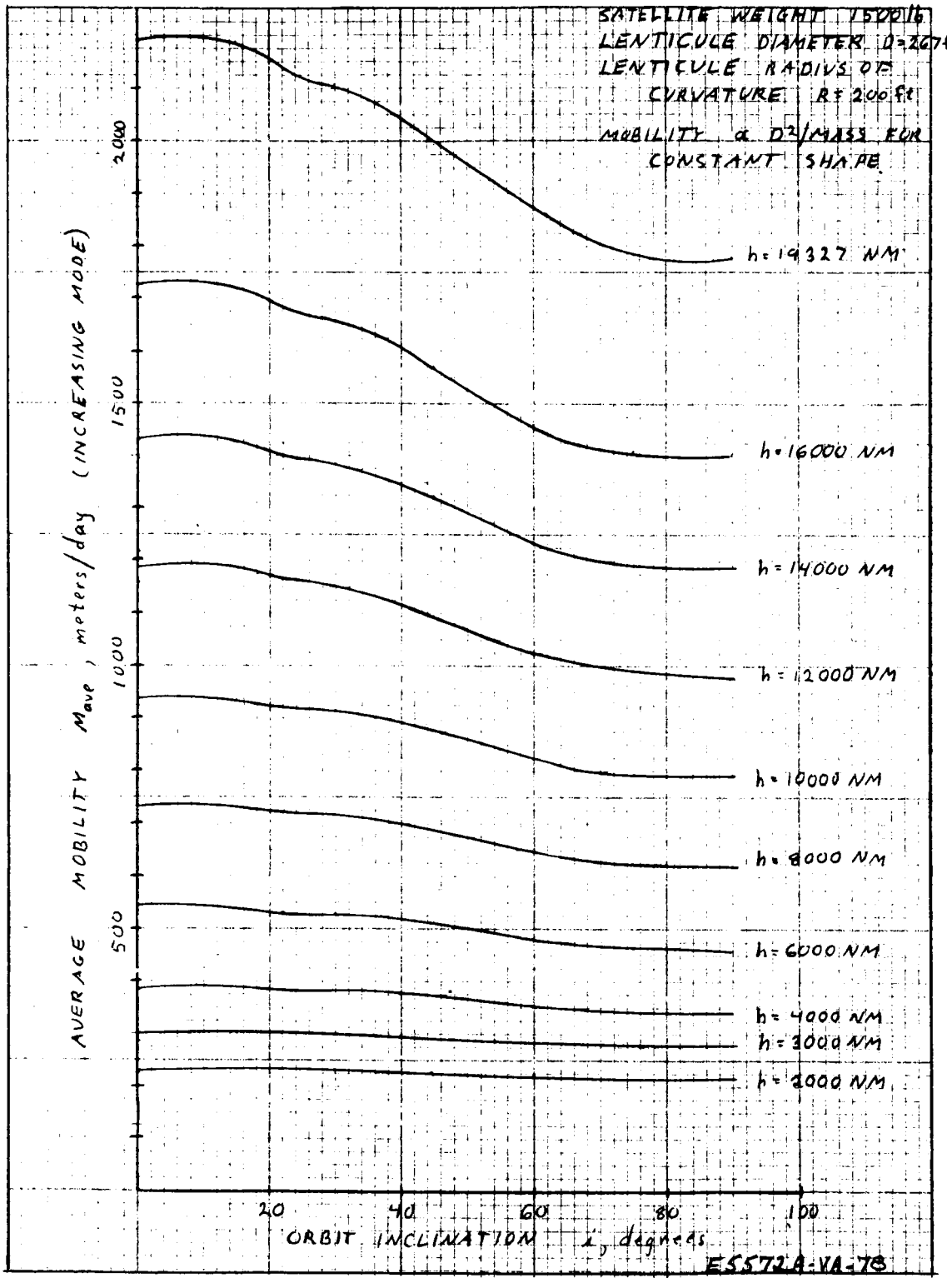

Figure 2-18. Average Mobility M_{ave} Vs Orbit Inclination i, Configuration A

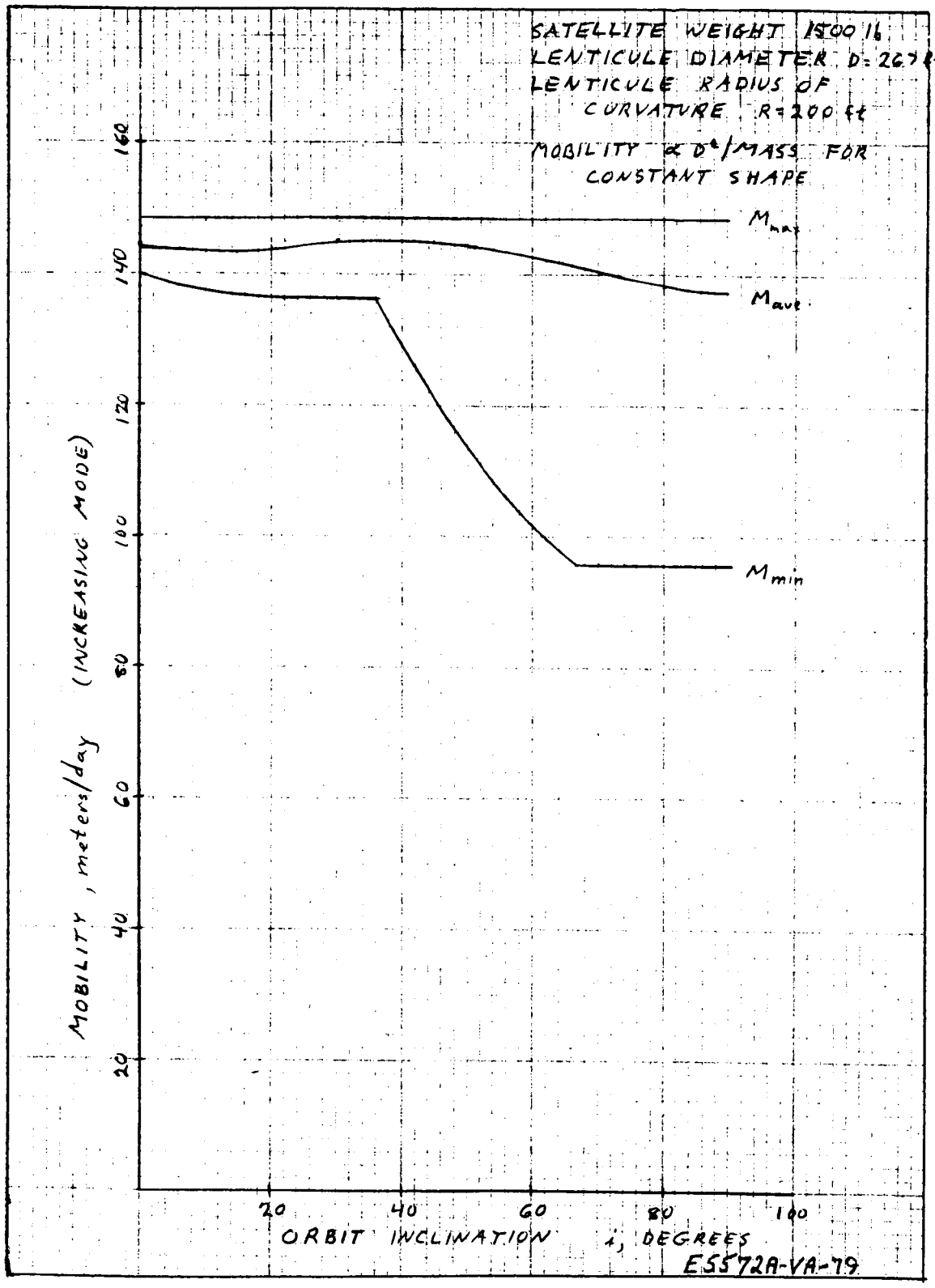

Figure 2-19. 1000-nmi Mobility Vs Orbit Inclination i, Configuration A

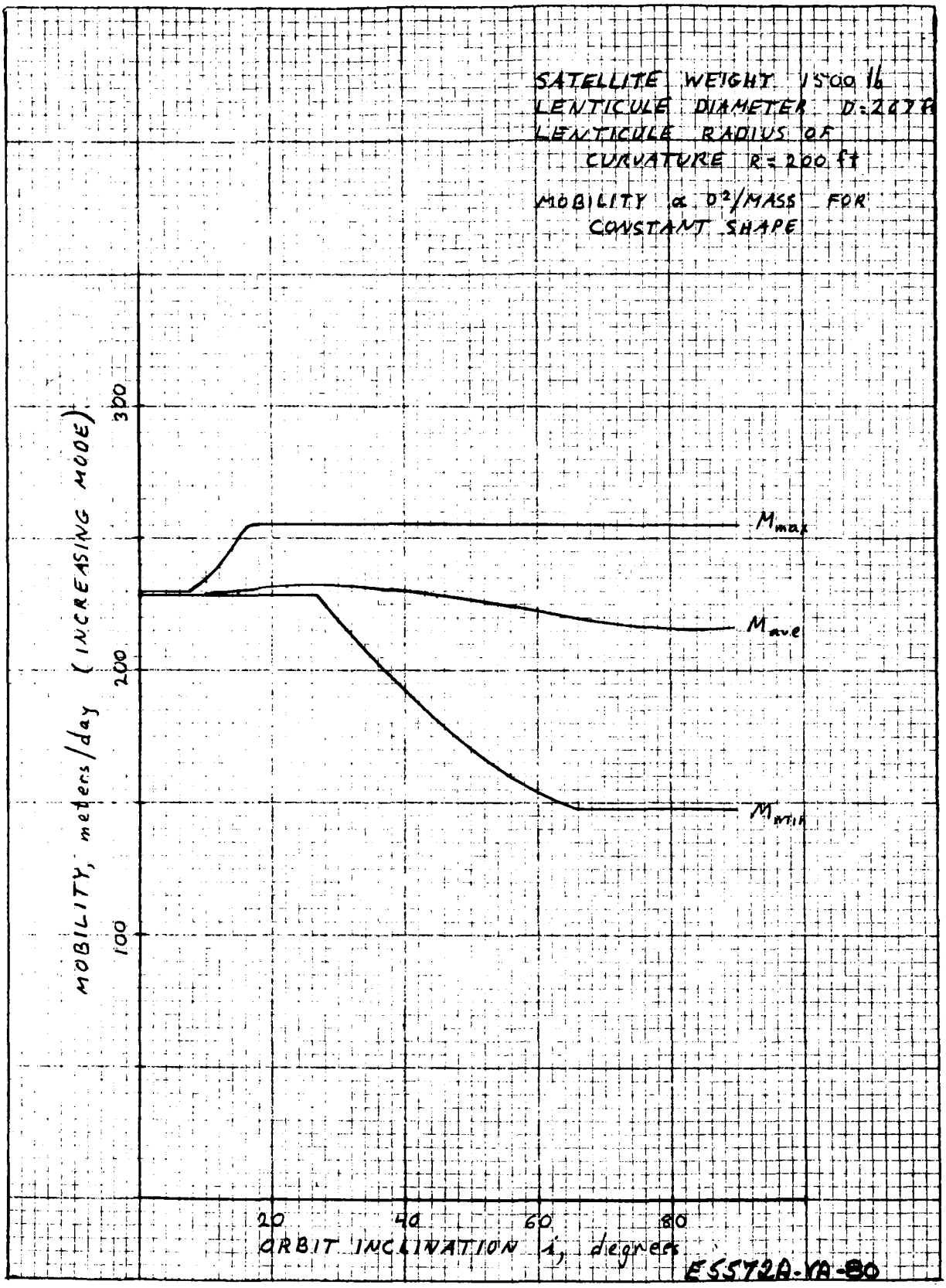

Figure 2-20. 2000-nmi Mobility Vs Orbit Inclination, i, Configuration A

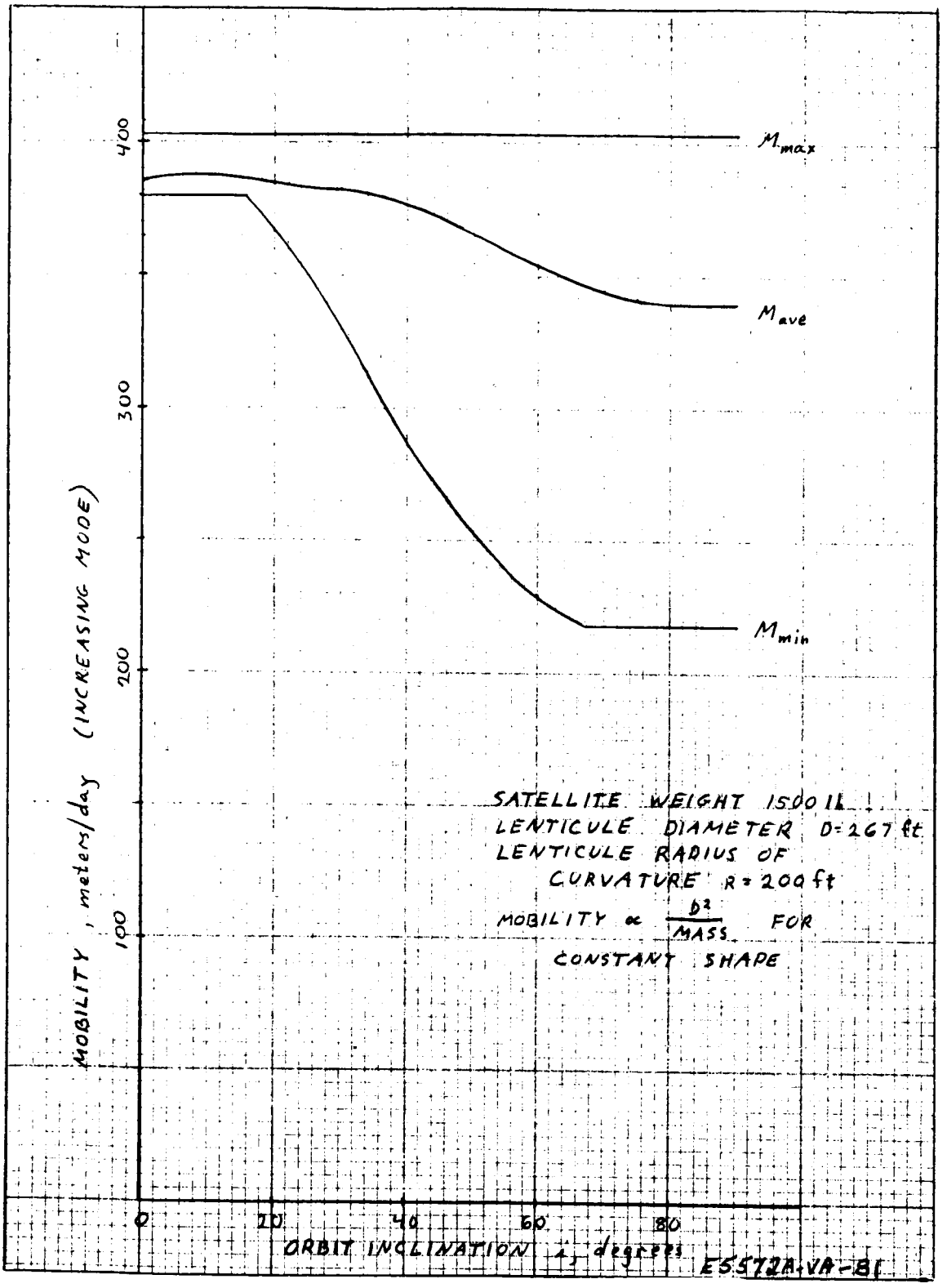

Figure 2-21. 4000-nmi Mobility vs Orbit Inclination, i, Configuration A

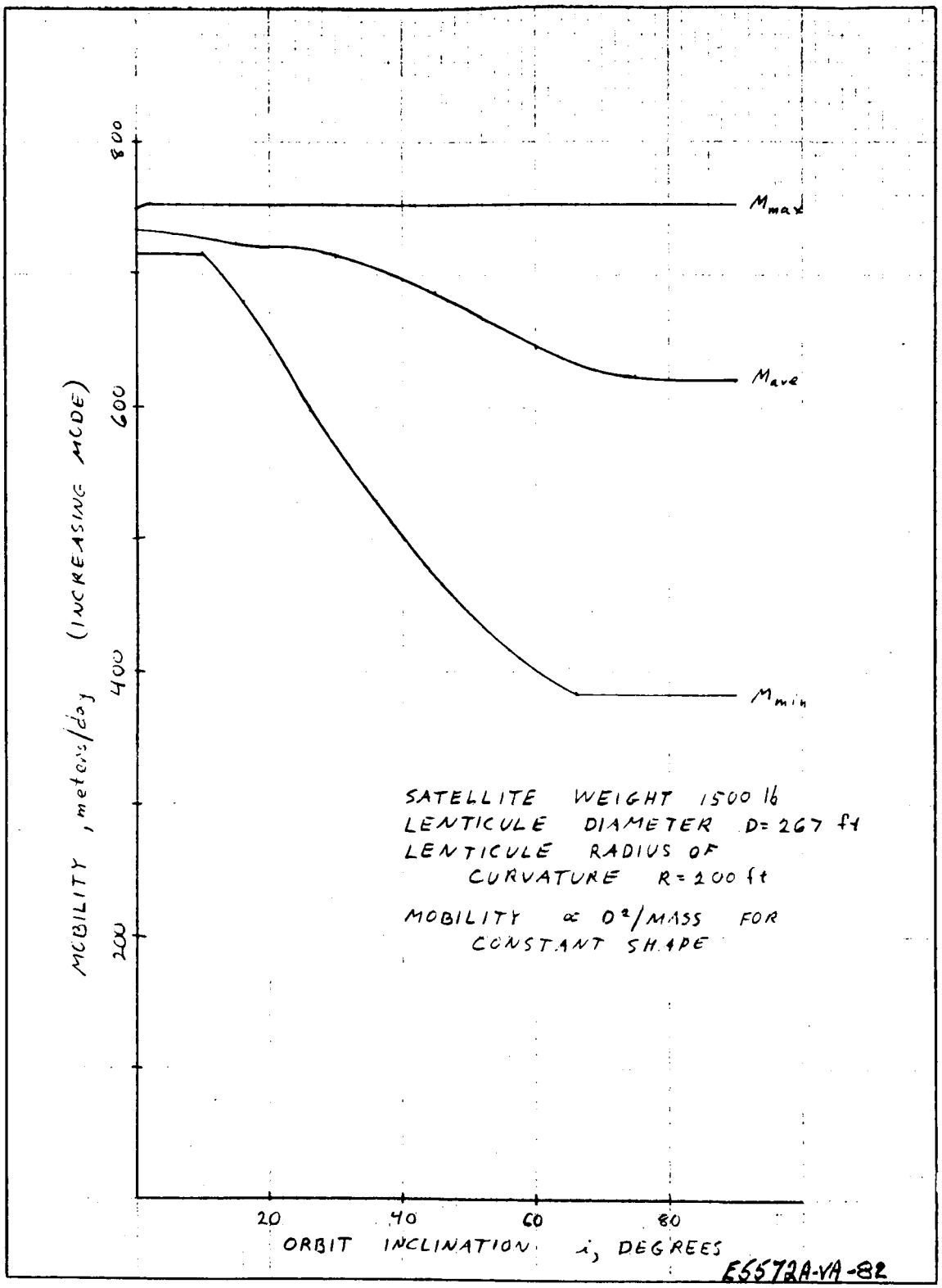

Figure 2-22. 8000-nmi Mobility vs Orbit Inclination, i, Configuration A

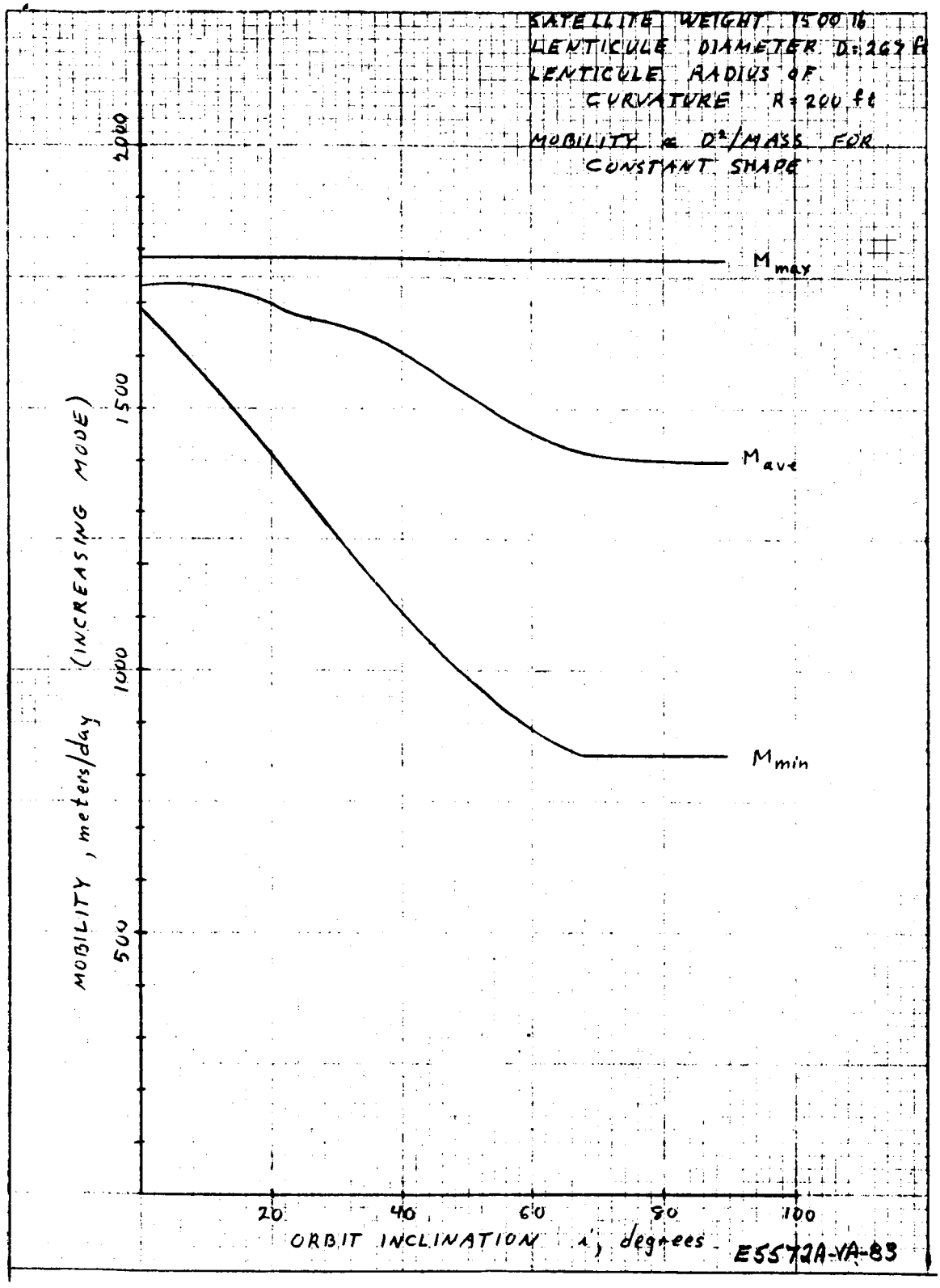

Figure 2-23. 16,000 nmi Mobility Vs Orbit Inclination, i, Configuration A

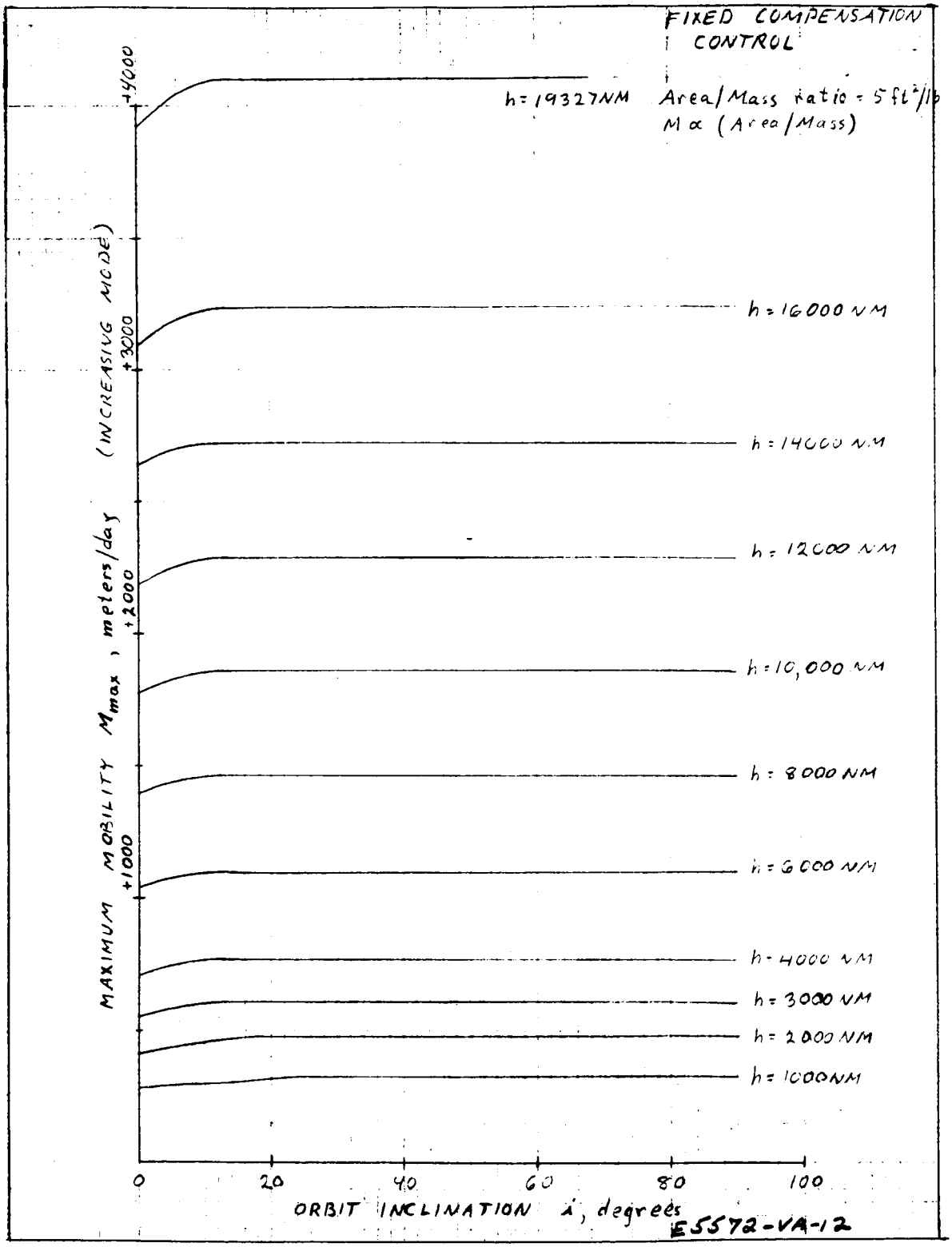

Figure 2-24. Maximum Mobility M_{max} Vs Orbit Inclination, i, Configuration B

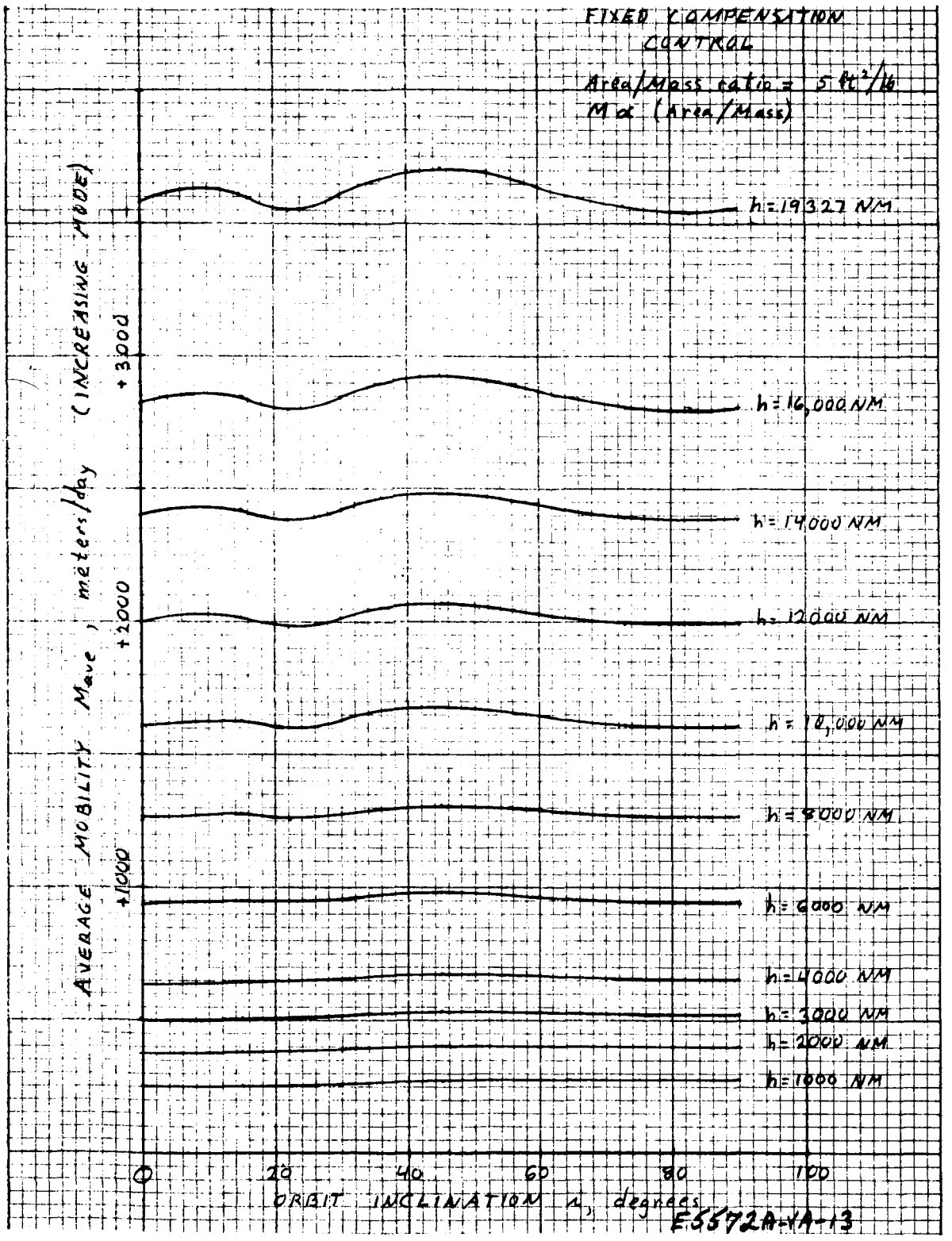

Figure 2-25. Average Mobility, M_{ave}, Vs Orbit Inclination, i, Configuration B

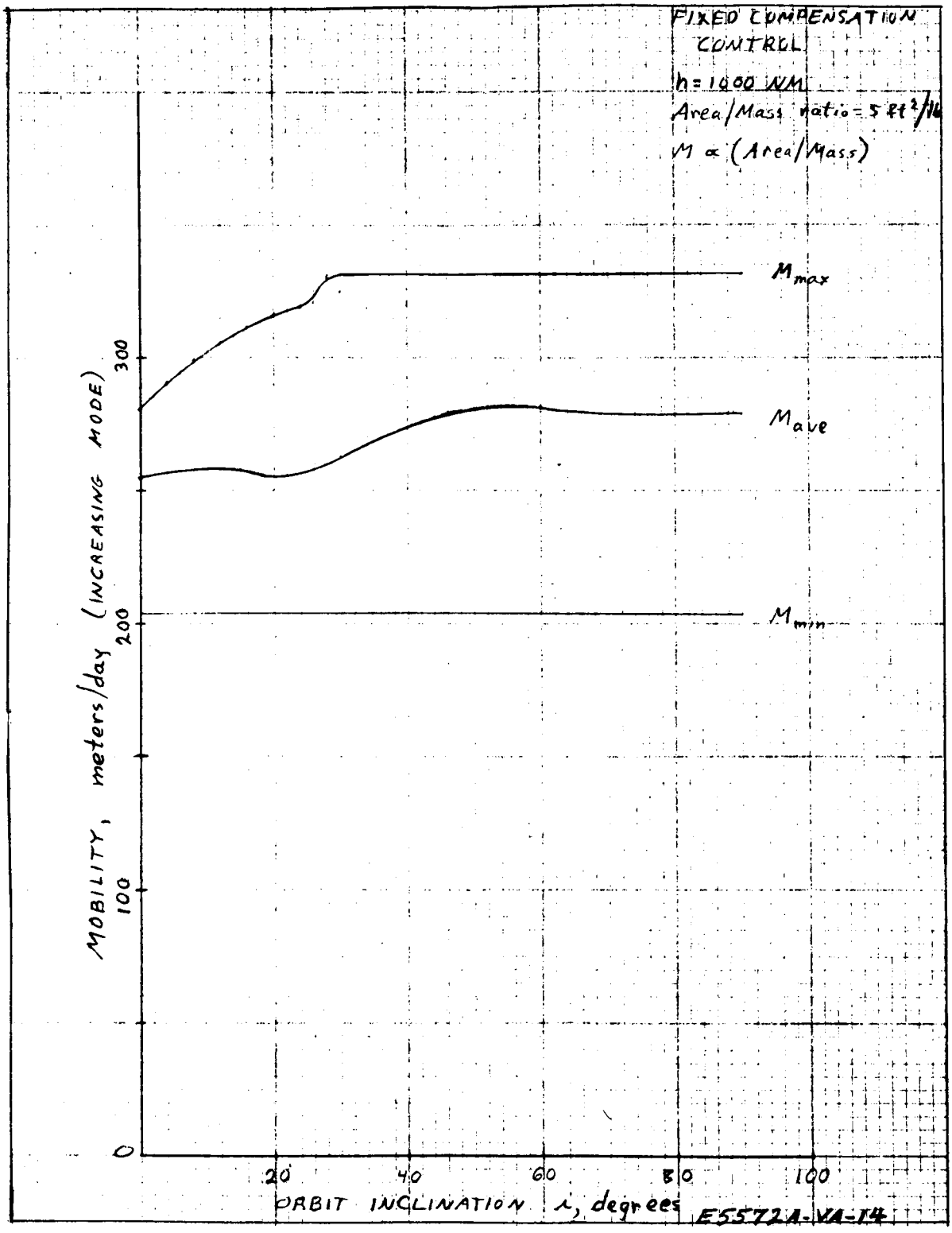

Figure 2-26. 1000-nmi Mobility Vs Orbit Inclination, i, Configuration B

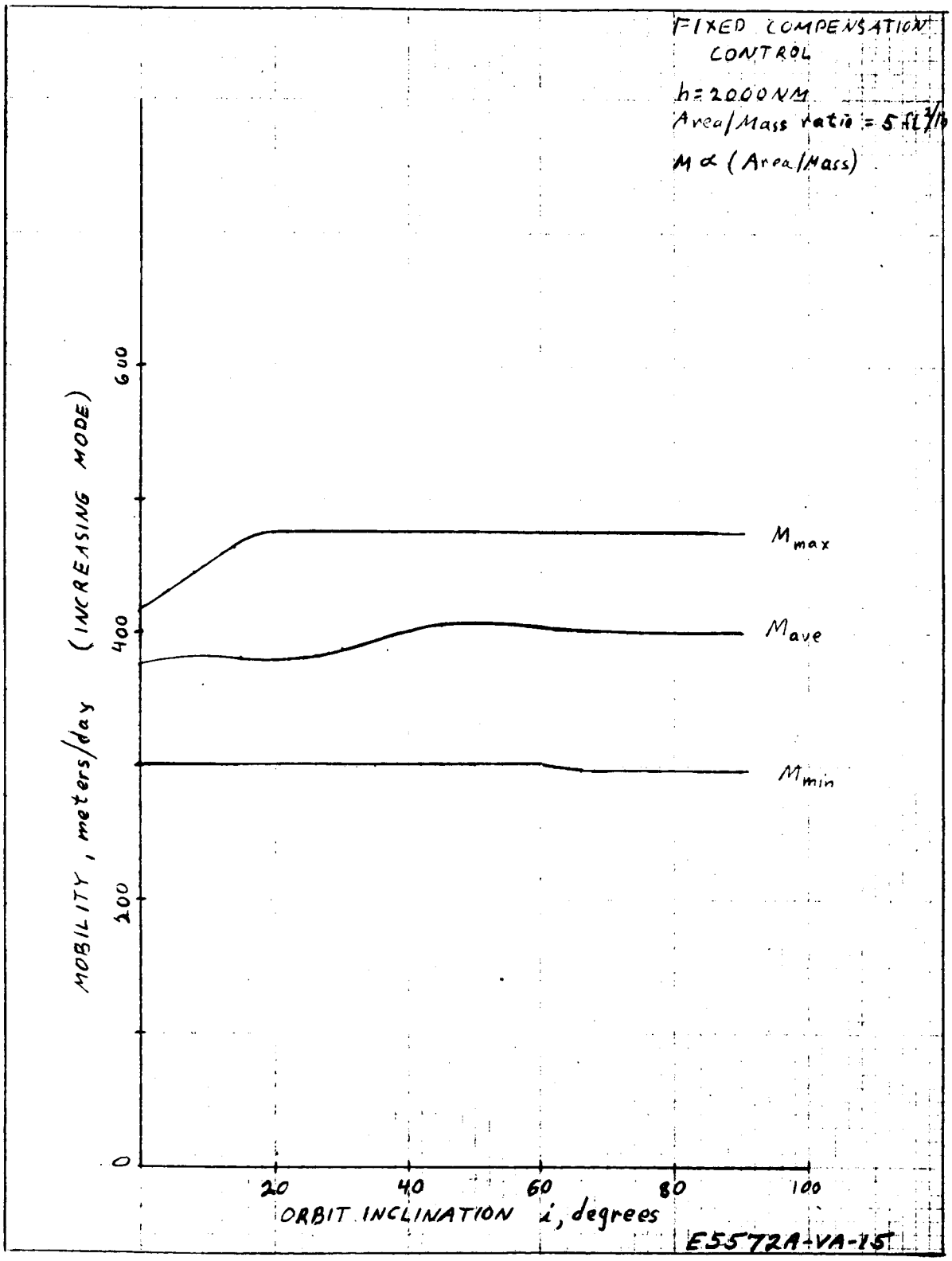

Figure 2-27. 2000-nmi Mobility Vs Orbit Inclination, i, Configuration B

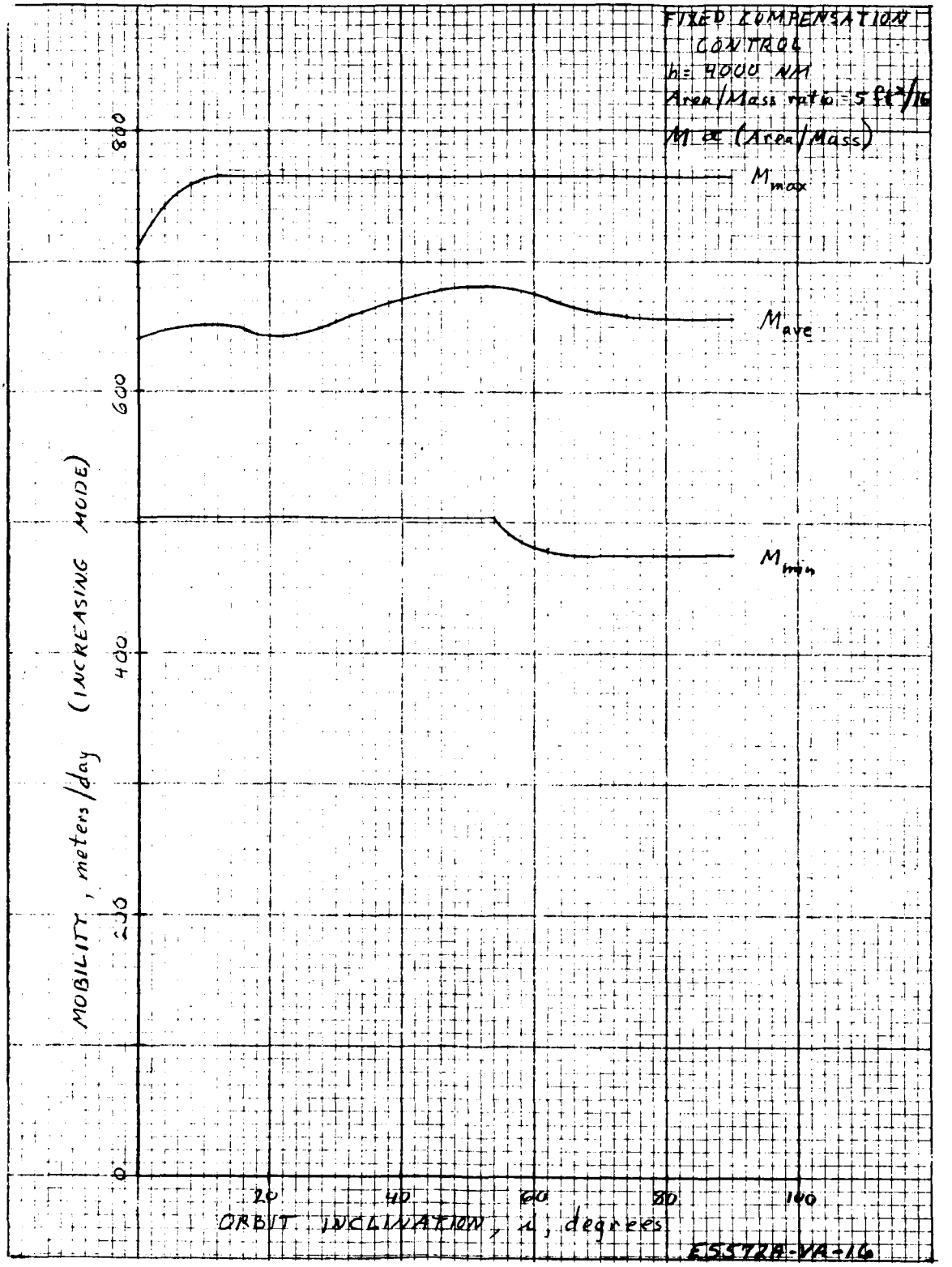

Figure 2-28. 4000-nmi Mobility Vs Orbit Inclination, i, Configuration B

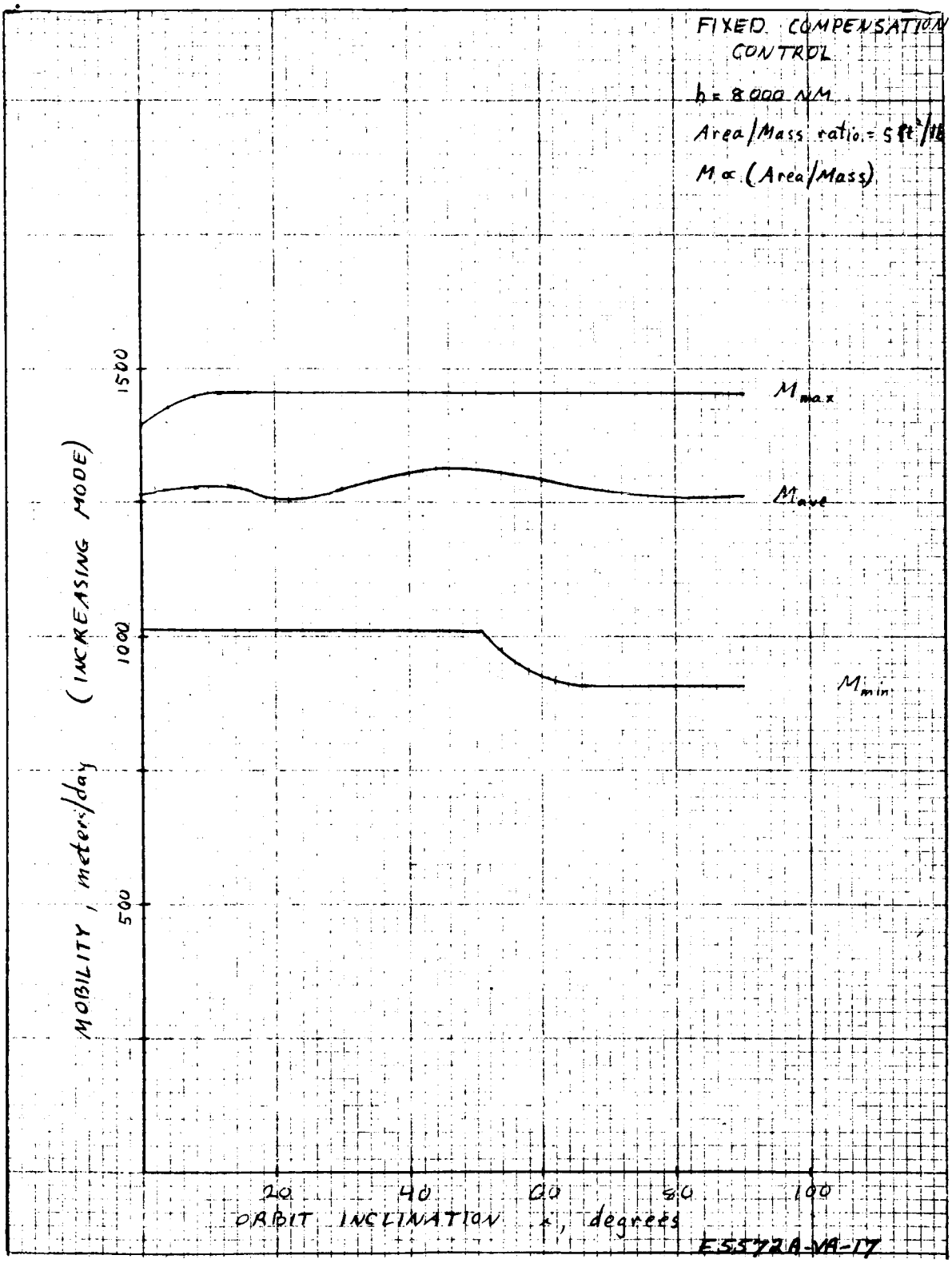

Figure 2-29. 8000-nmi Mobility Vs Orbit Inclination, i, Configuration B

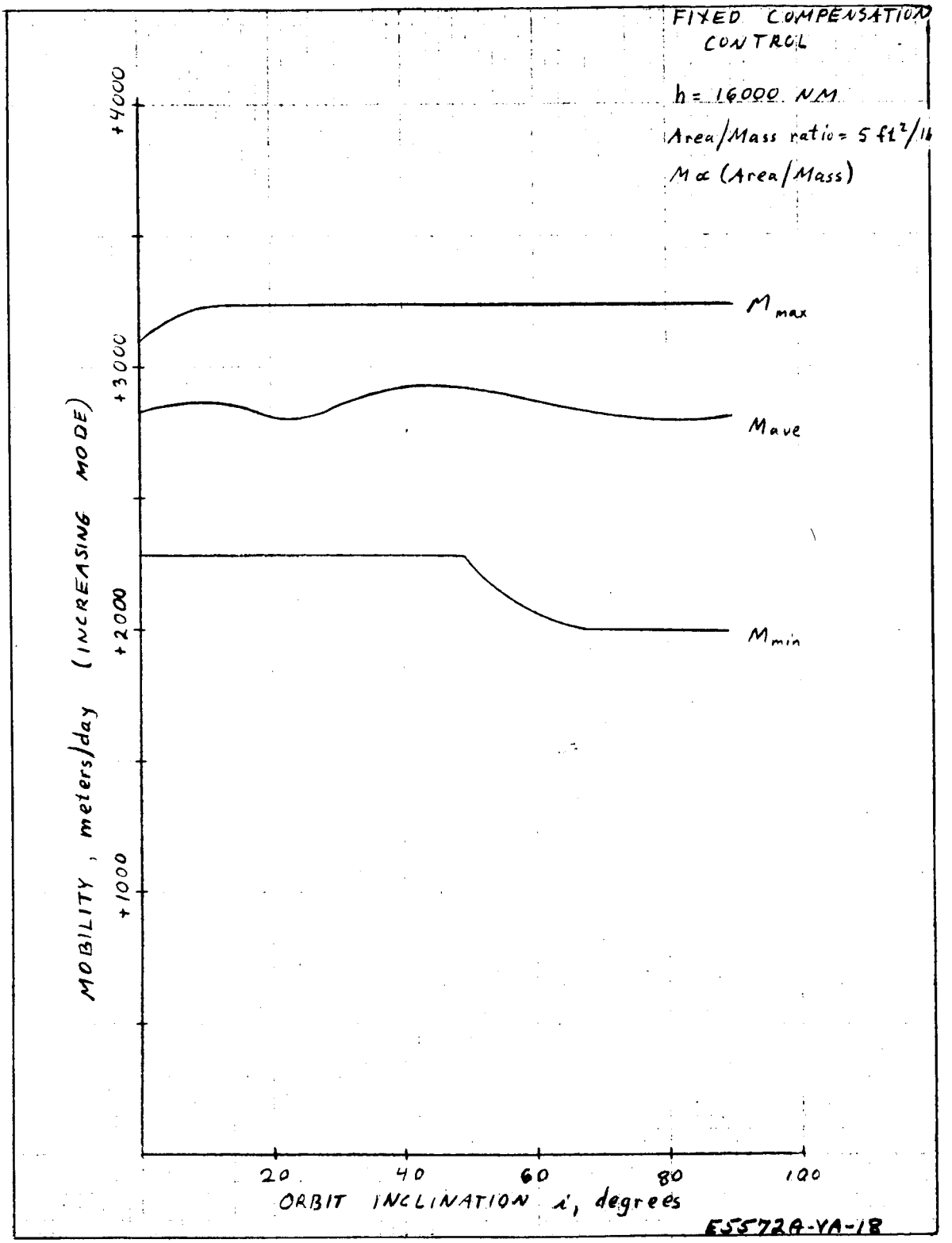

Figure 2-30. 16,000-nmi Mobility Vs Orbit Inclination, i, Configuration B

2.2.2 Mobility Versus Control Technique

2.2.2.1 Configuration B

For the configuration B satellite (solar sail), the mobility obtained for a given area-to-mass ratio depends on the angle of the sail with respect to the orbital plane. Data relating to three control techniques are presented: uncompensated control (sail perpendicular to the orbit plane), fixed compensation control (fixed sail angle), and continuous compensation control (sail angle varied to maximize mobility). The data source was a digital computer simulation using the mobility program described in paragraph 3-4.

Figures 2-31 through 2-35 contain data relating to the mobility of a configuration B satellite as a function of sun-line inclination, i_s, and sail angle, ϕ, where i_s is the angle between the orbital plane and a vector directed toward the sun, and the sail angle, ϕ, is the angle between the normal to the sail (side 1) and the orbital plane. The sign if i_s is such that when i_s is negative, the motion of the satellite in its orbit is counter-clockwise when viewed from the sun. The angle ϕ is positive counter-clockwise when the satellite is viewed from the radius vector, looking toward the orbit center. A constant area-to-mass ratio of 5 ft^2/lb was chosen (actually this figure is the ratio of sail area in square feet to the earth weight of the satellite in pounds). Since the mobility of such a satellite is proportional to its area-to-mass ratio, these curves may be scaled easily for other satellite sizes and weights. Altitudes of 1000, 2000, 4000, and 8000 nmi and synchronous altitudes are considered with the orbits assumed approximately circular. The range of i_s and ϕ plotted are 0 to -90 degrees and 0 to 45 degrees, respectively; values of ϕ between 45 and 135 degrees result in low mobilities for all sun-line inclinations and are thus not shown. Mobilities for other inclinations and sail angles may be obtained from the equations of symmetry:

$$M(-\phi, -i_s) = M(\phi, i_s)$$
$$M(\pi - \phi, i_s) = -M(\phi, i_s)$$

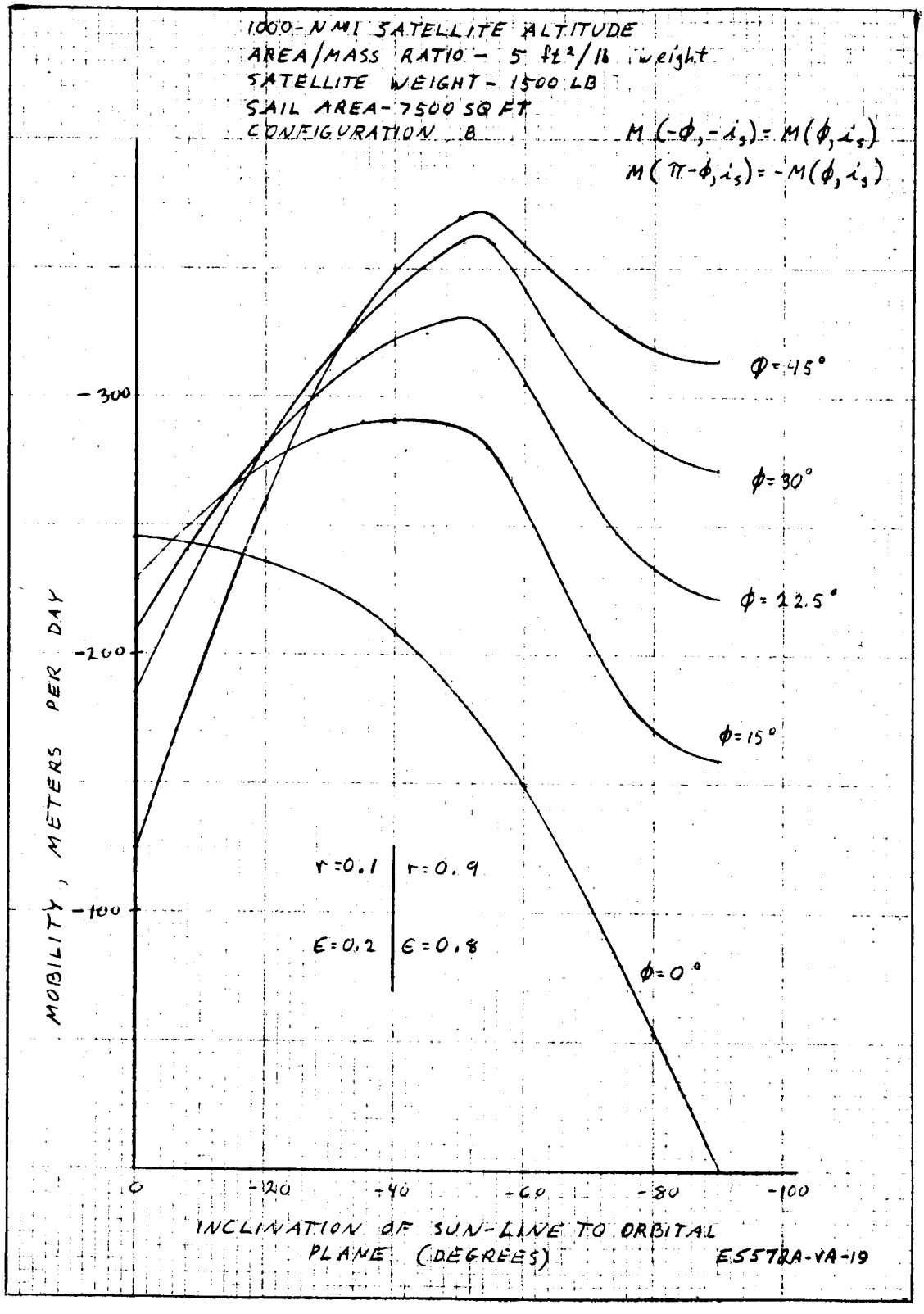

Figure 2-31. Mobility Vs. i_s, Φ, Configuration B (1000 NMI)

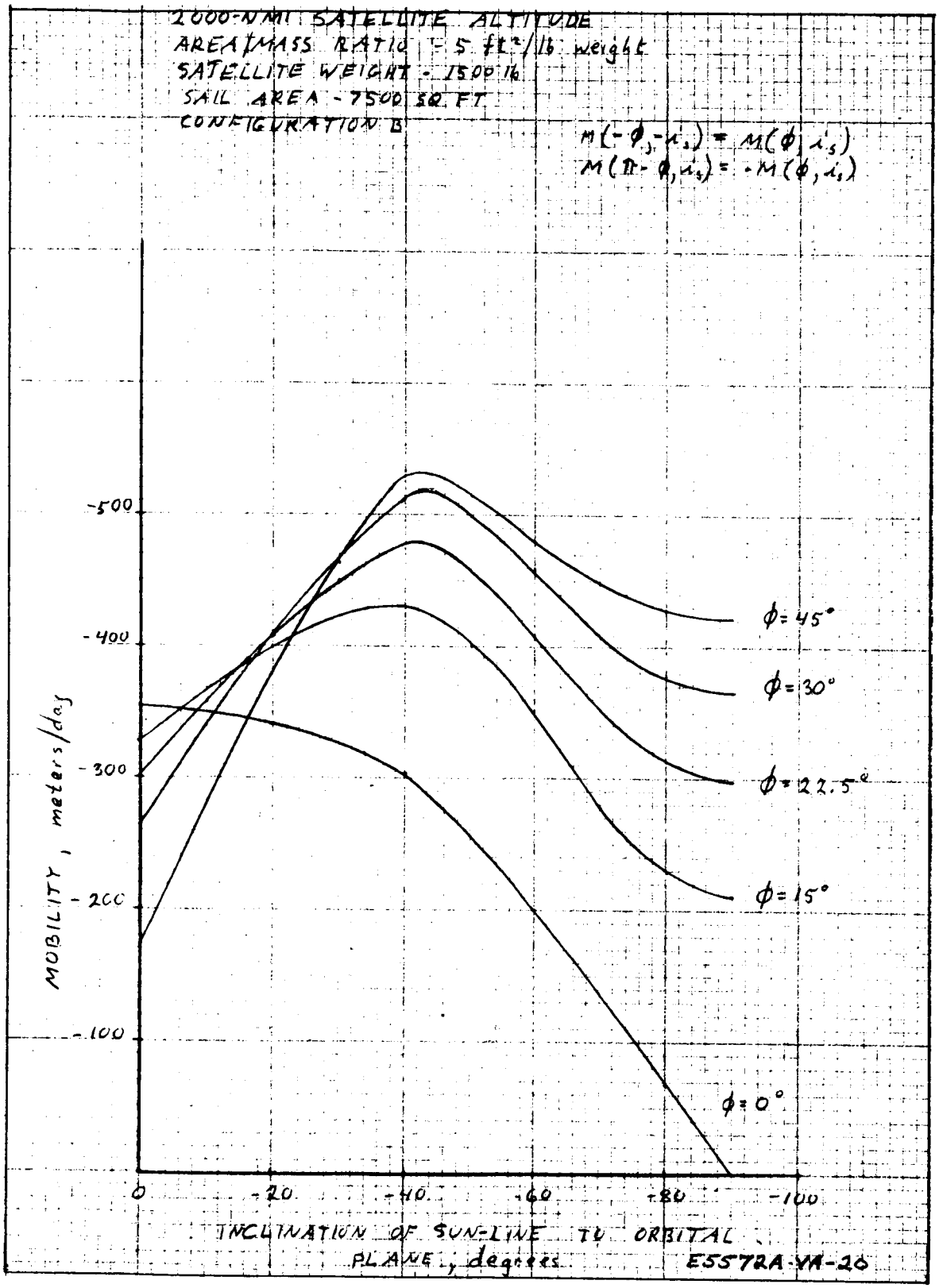

Figure 2-32. Mobility Vs. i_s, Φ, Configuration B (2000 NMI)

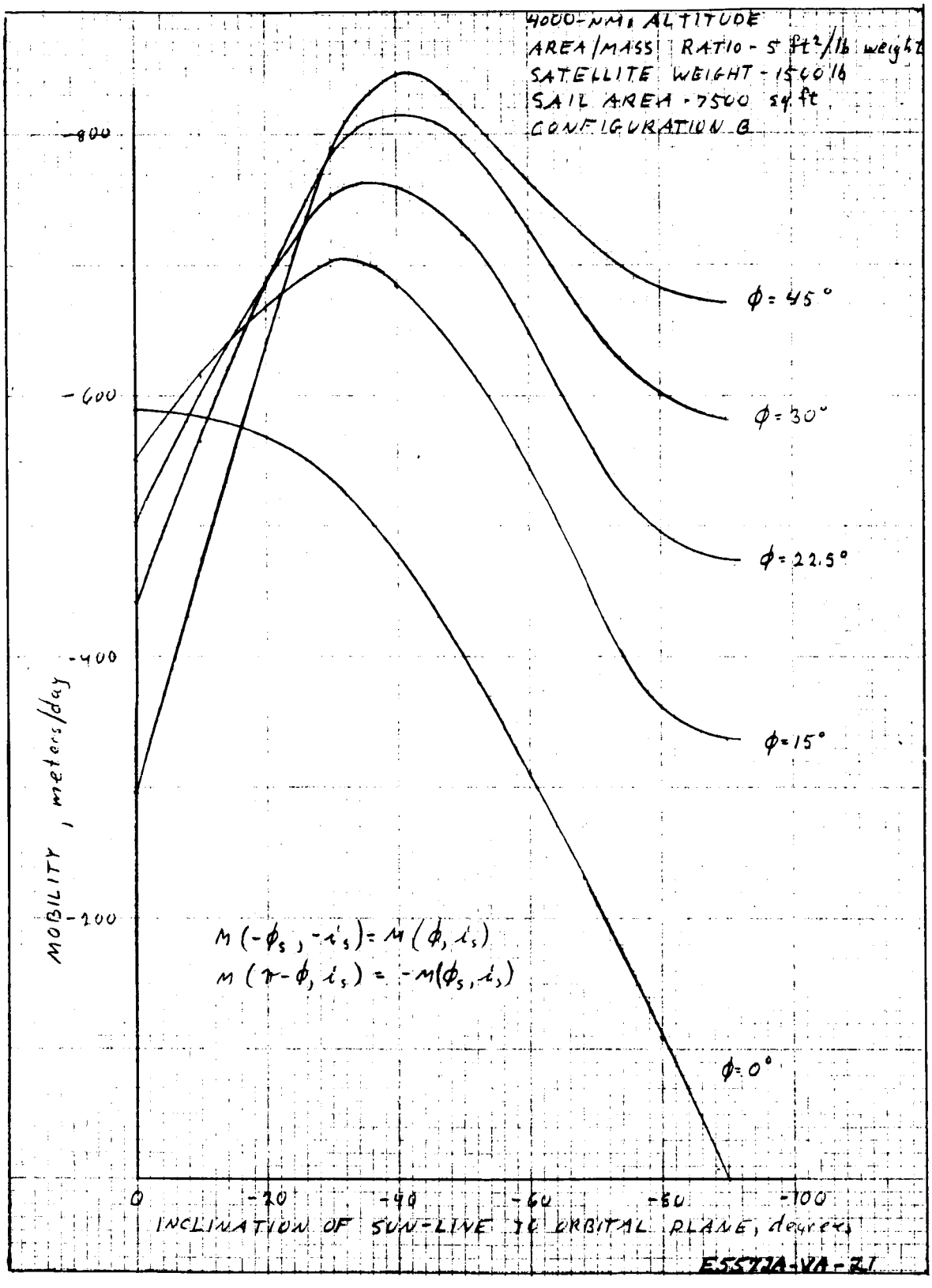

Figure 2-33. Mobility Vs. i_s, ϕ, Configuration B, (4000 NMI)

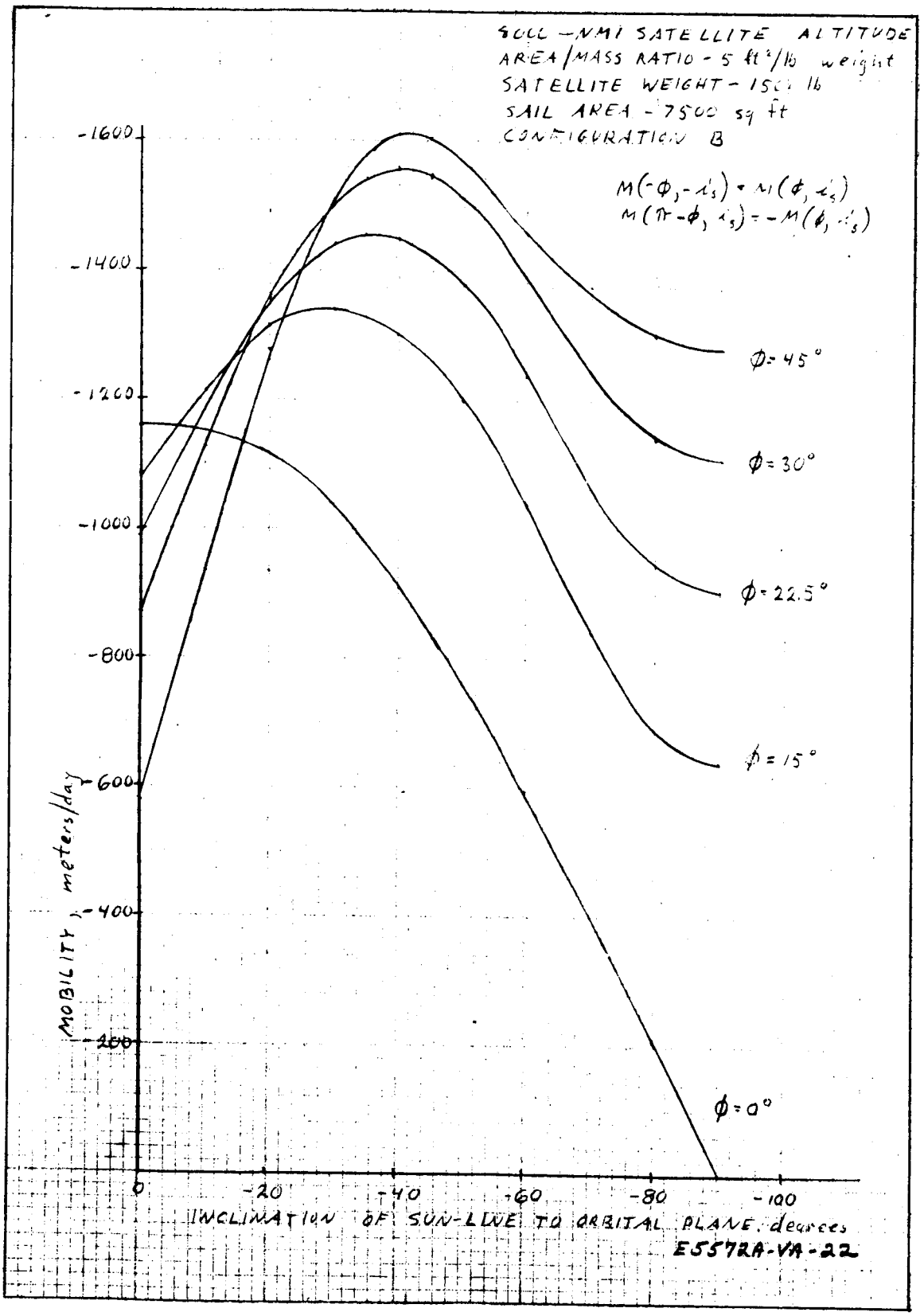

Figure 2-34. Mobility Vs. i_s, Φ, Configuration B (8000 NMI)

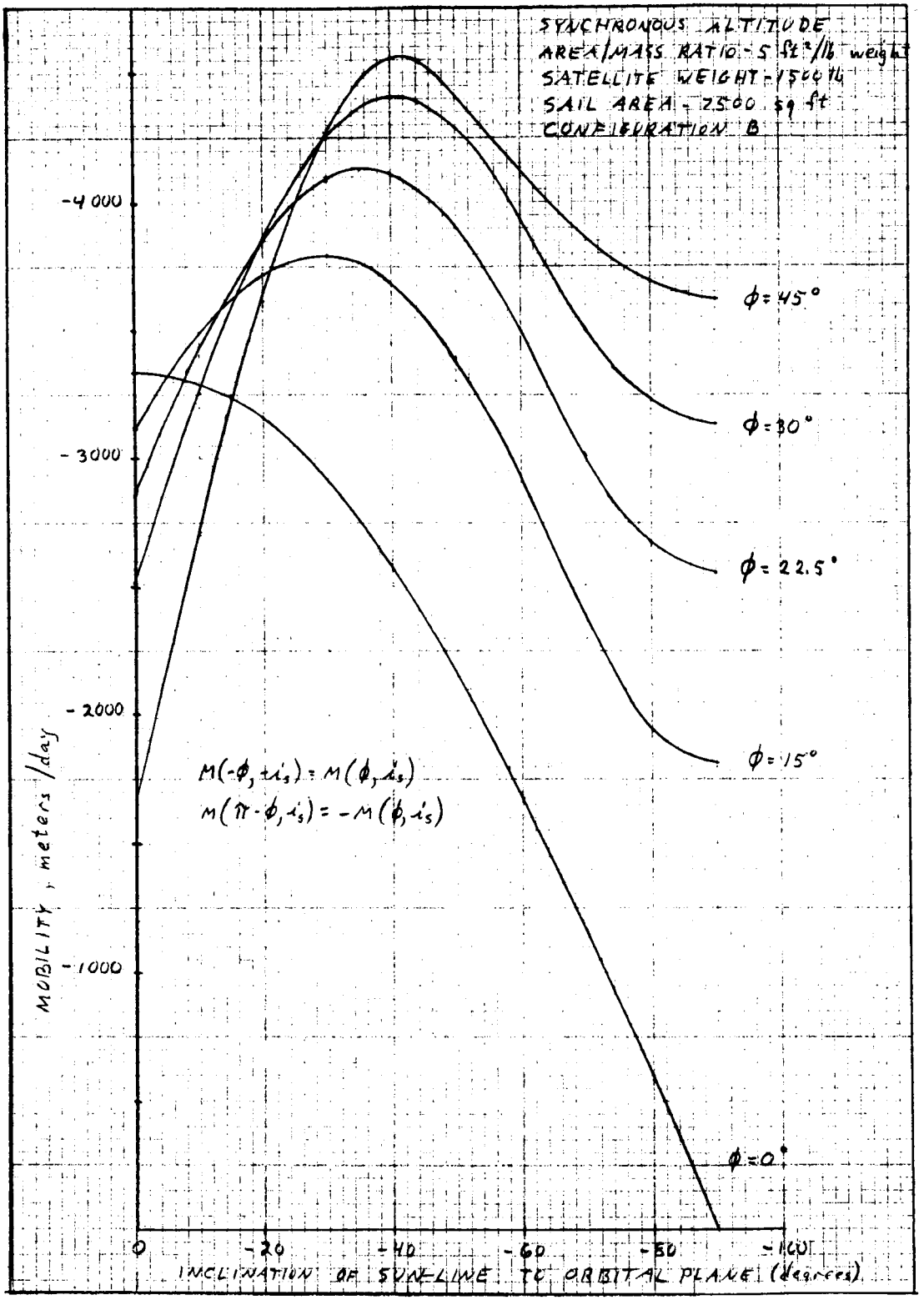

Figure 2-35. Mobility Vs. i_s, ϕ, Configuration B (Synchronous Altitude)

Figures 2-36 through 2-40 present similar data for the three control techniques. It may be noted that the curve for the continuous compensation control is simply the upper envelope of the constant ϕ curves of figures 2-32 through 2-35, while the uncompensated and fixed compensation curves are simply those associated with the values ϕ = 0 degrees and ϕ = 22.5 degrees, respectively. While $\phi = \pm 22.5$ degrees or ± 167.5 degrees is a reasonable compromise over sun-line inclination of -90 to +90 degrees, for a synchronous orbit with an orbital inclination of 0 degree, a fixed compensation angle of ± 15 or ± 175 degrees would be appropriate, since the range of sun-line inclinations is only -23 to 23 degrees in this case. In general, the uncompensated control mobilities are poor over a wide range of sun-line inclinations. The two compensated control techniques give generally better mobility, but the improvement offered by continuous control over fixed compensation is slight.

2.2.2.2 Configuration A

For the configuration A satellite, results of computer simulation indicate that maximum mobility is obtained with the separation plane (the plane separating the high emissivity side of the lenticule from the low emissivity side) perpendicular to the orbit plane. This supports the intuitive concept that with this alignment the reradiation forces will be approximately aligned with or against the satellite velocity vector and will thus be most effective in increasing or decreasing the energy of the orbit. For the configuration A satellite, there is thus only one logical control concept to use that is, ϕ = 0 or 180 degrees, and graphs of mobility versus control technique or versus yaw attitude angle are not applicable.

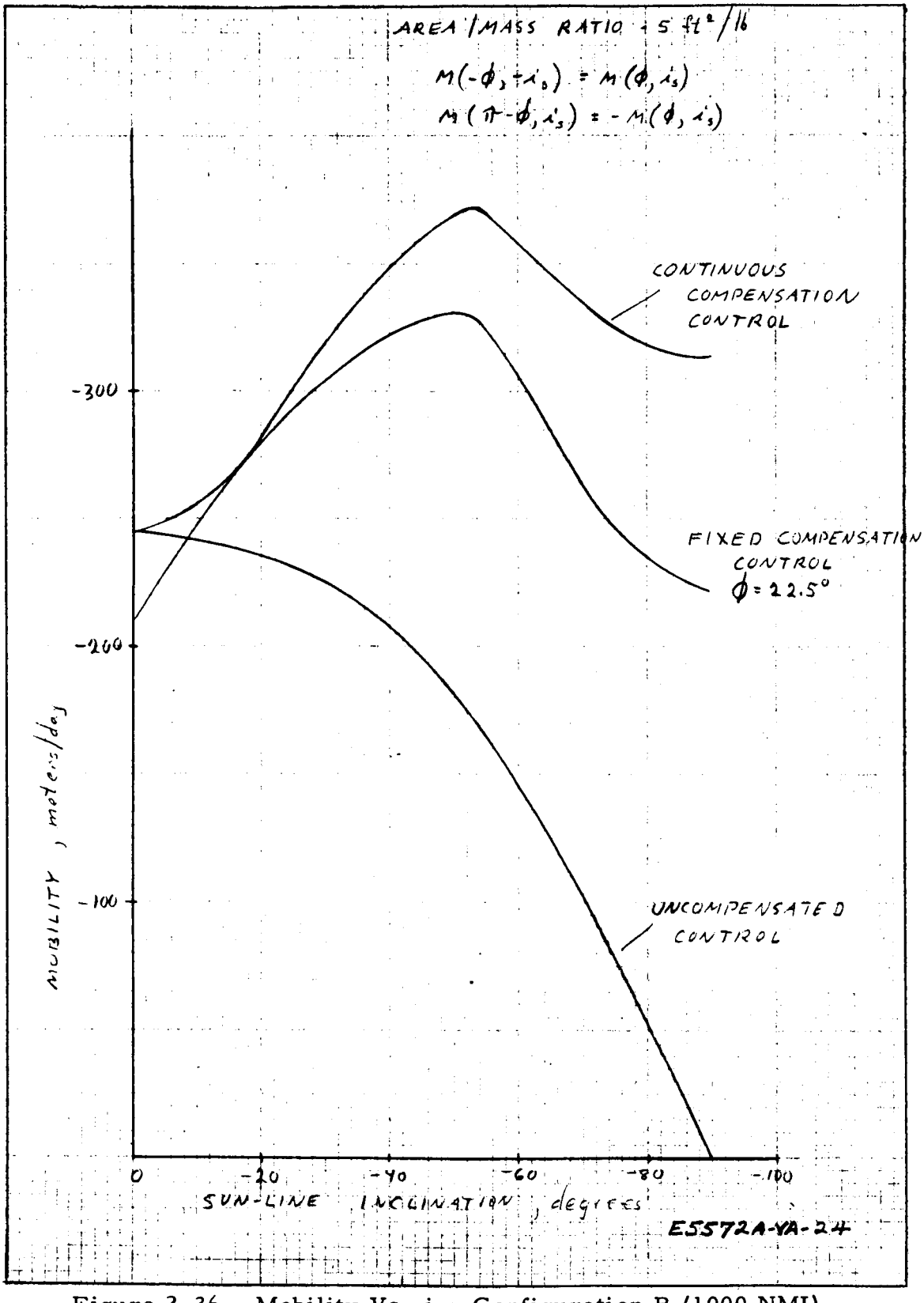

Figure 2-36. Mobility Vs. i_s; Configuration B (1000 NMI)

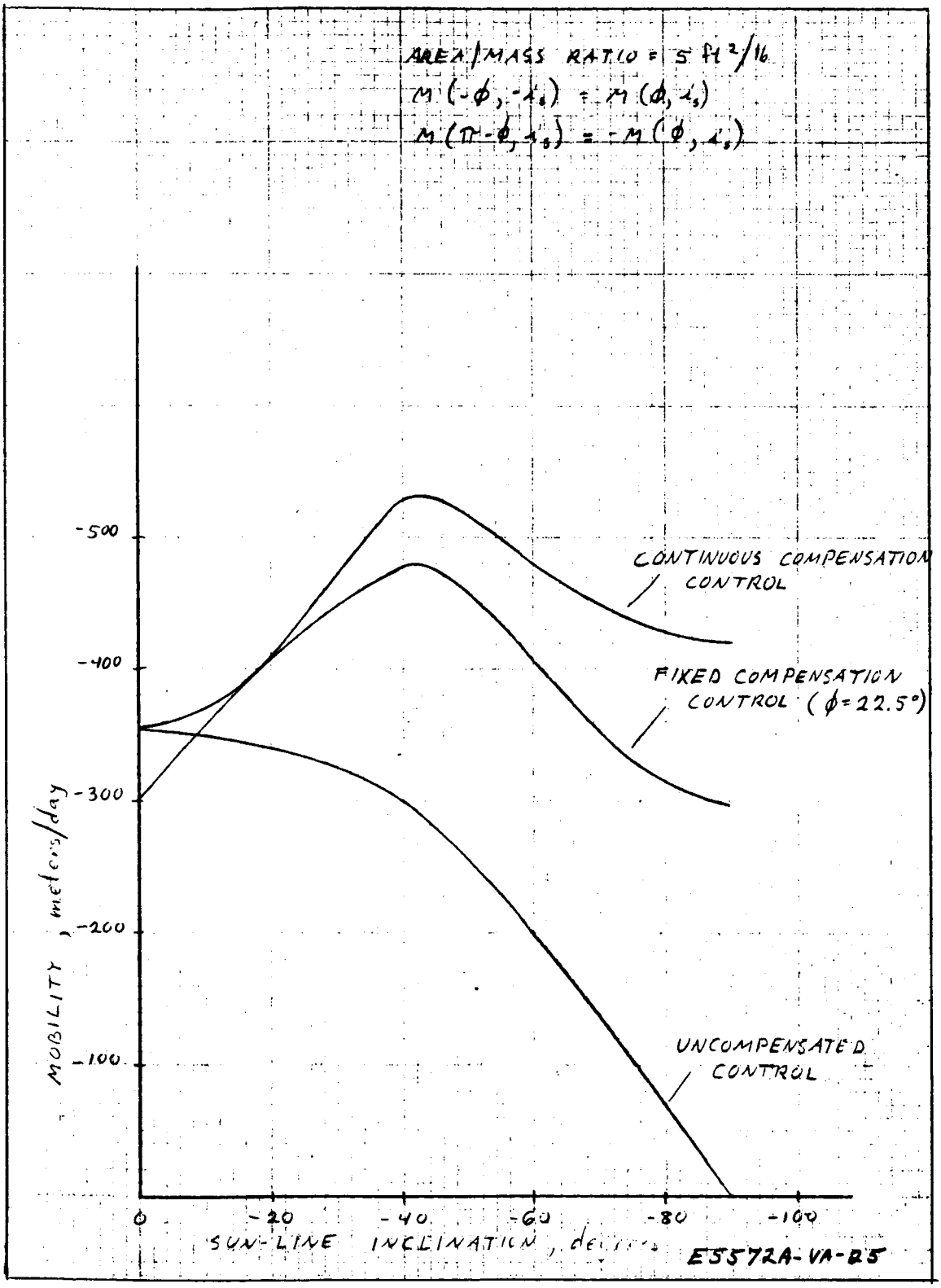

Figure 2-37. Mobility Vs. i_s; Configuration B (2000 NMI)

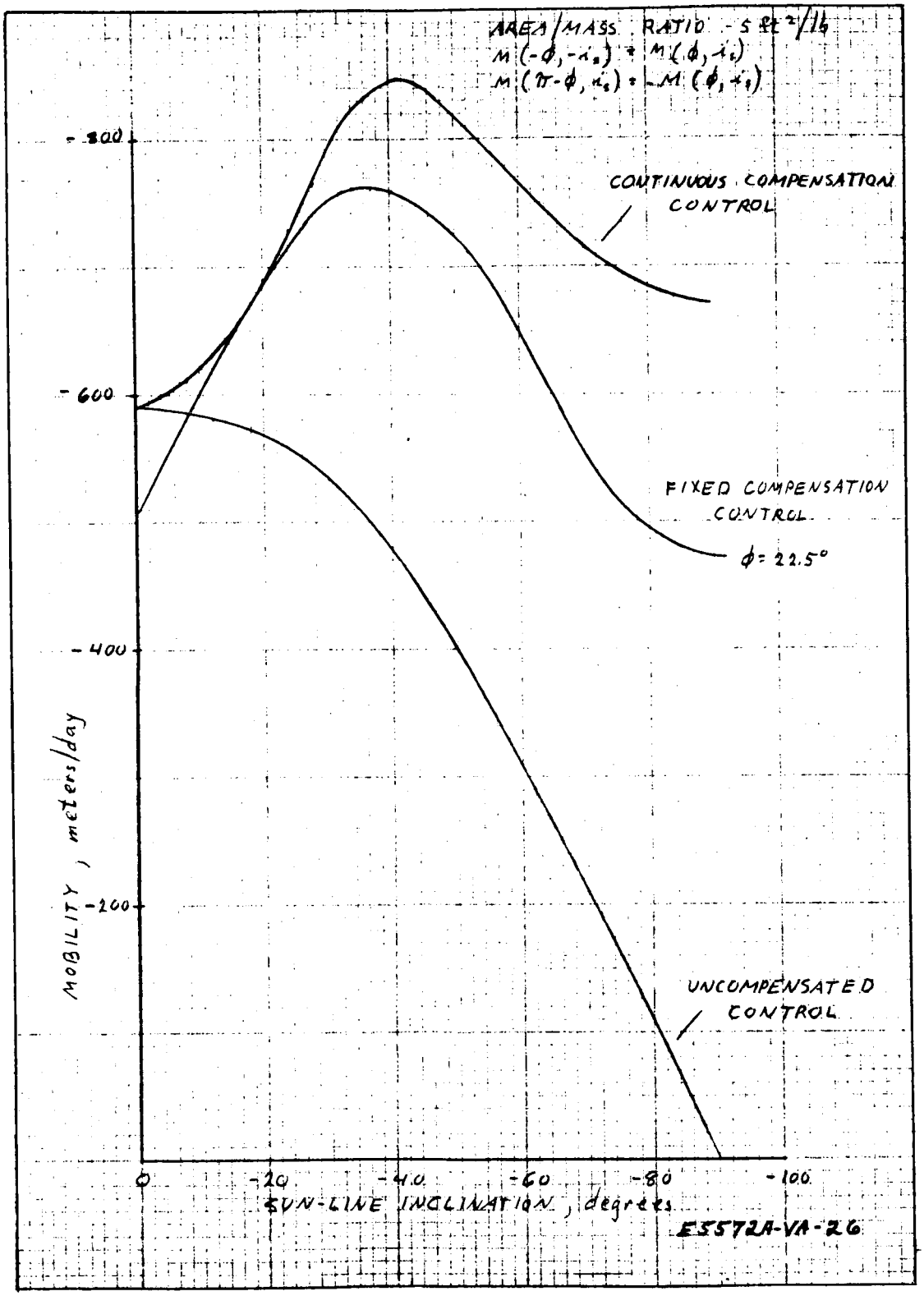

Figure 2-38. Mobility Vs. i_s; Configuration B (4000 NMI)

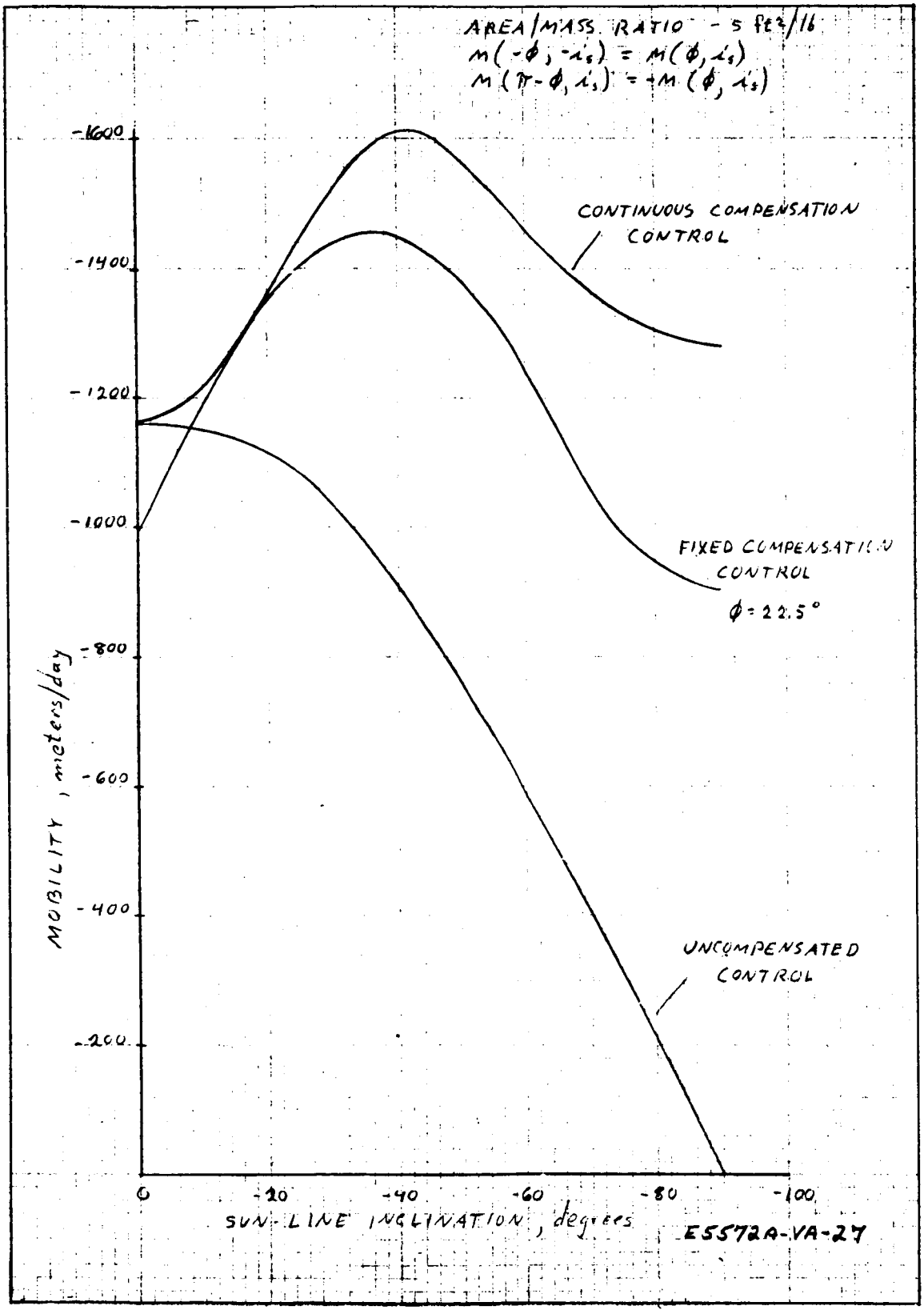

Figure 2-39. Mobility Vs. i_s; Configuration B (8000 NMI)

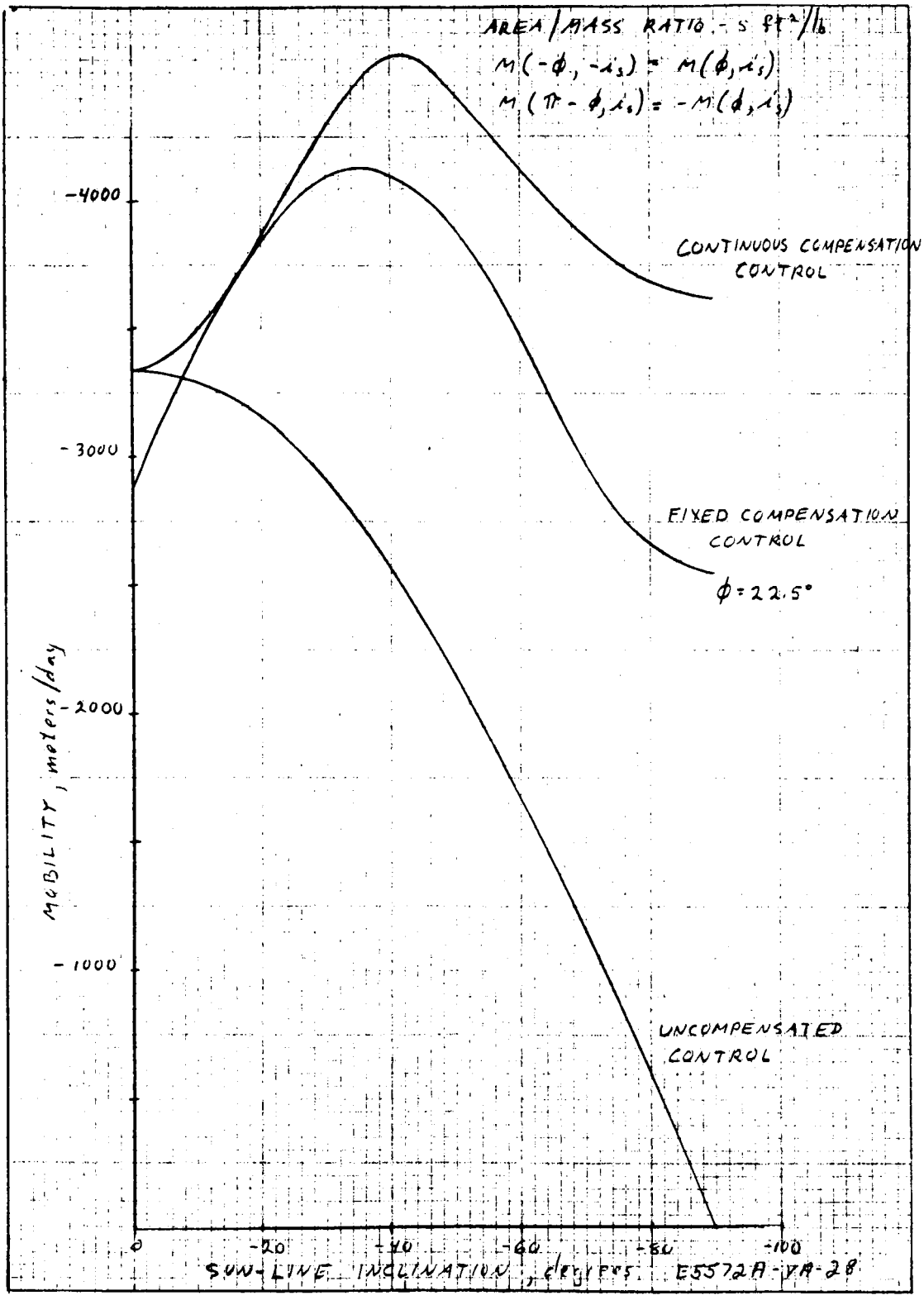

Figure 2-40. Mobility Vs. i_s; Configuration B (Synchronous Altitude)

2.2.3 Determination of Maneuver Times

Both altitude (period) and angular position of the satellite, relative to an uncontrolled satellite, may be changed by a basic maneuver which consists of placing the satellite in opposite modes of operation for specific amounts of time. Such a maneuver may be required, for example, during the initial placement and spacing of the satellite. (For additional control, procedures applicable to correction of small period and angular errors, refer to paragraph 2.3.5)

Assuming a constant mobility magnitude, the proper number of orbits to remain in each mobility mode are given by the following equations (see paragraph 3-2):

$$N_2 = \frac{\mp \Delta P_c + \sqrt{2\Delta P_c^2 + \frac{3K_1^3 a^{7/2} M \phi_d}{\pi}}}{\frac{3}{2} K_1^2 a^2 M}$$

$$N_1 = \frac{N_2\left(\frac{3}{2} K_1^2 a^2 M\right) \pm \Delta P_c}{3 K_1^2 a^2 M}$$

where: N_1 is the number of orbits in the first mobility mode

(N_2-N_1) is the number of orbits in the second mobility mode

ΔP_o is the initial period minus the desired period

ϕ_d is the actual angular position minus the desired angular position

a is the desired semimajor axis

M is the mobility magnitude

$K_1 = 3.147 \times 10^{-7}$ sec/meter$^{3/2}$

The $(\pm)$ and $(\mp)$ sign choices depend on the initial mobility mode. The upper sign represents the case in which a satellite is placed in an increasing energy mode during the initial N_1 orbits and in a decreasing energy mode during the remaining (N_2-N_1) orbits.

The time required for the basic maneuver is given by:

$$t_M = \frac{\mp \Delta P_o + \sqrt{2(\Delta P_o)^2 \pm \frac{3}{\pi} K_1^3 a^{7/2} M \phi_d}}{\frac{3}{2} K_1 M \sqrt{a}}$$

where the same sign conventions are used. In figures 2-1 and 2-2, (pages 2-3, 2-4) parametric curves are shown for the equation

$$t_M = \frac{\pm |\Delta P_o| + \sqrt{2 \Delta P_o^2 \pm \left| \frac{3}{\pi} K_1^3 a^{7/2} M \phi_d \right|}}{\frac{3}{2} K_1 M \sqrt{a}}$$

Table 2-1 (page 2-2) gives the sign choice convention to be used with these curves, where the symbols (+, +), (+, -), (-, +), (-, -) refer to the corresponding segments of the curves of the upper right-hand quadrant. Use of these sign choices will correspond to the sign convention previously explained for the equations for N_1 and N_2. Figure 2-1 covers a range of parameters appropriate to a low altitude satellite, while figure 2-2 covers a range appropriate to high satellites. These curves are read clockwise, as illustrated. That is, starting with an initial value of ϕ_d (e.g., 200 degrees), proceed vertically to the appropriate mobility curves shown in solid lines (e.g., M = 200); then proceed horizontally to an appropriate altitude line (broken lines; e.g., h = 2000 nmi). Next move vertically to the required ΔP_o curve (e.g., ΔP = 5, (+, +) sign choice mode). Move horizontally and then vertically to the appropriate altitude and mobility curves, and finally proceed horizontally to read the maneuver time, t_M. Two scales of t_M are provided, scale 1 corresponding to the solid mobility lines and scale 2 to the broken lines. In this example the solid M = 200 curve is used, and t_M = 112 days may be read from scale 1.

There are generally several ways in which the same ΔP_o and ϕ_d change may be made, since any angular position change of $\phi_d \pm 2n\pi$, n = 0, 1, 2, . . . is equivalent to ϕ_d. The value of $\phi_d \pm 2n\pi$ required to provide minimum maneuver time must be found by trial and error, and generally is less than approximately 3π in magnitude. A computer program was developed to determine optimum values of N_1 and N_2, using the equations listed previously in a trial and error routine.

2.2.4 Eccentricity Perturbations

It is fairly well known that the solar pressure perturbing forces on a high area-to-mass ratio satellite cause significant perturbations of the orbital eccentricity. Furthermore, at certain critical altitudes and inclinations, these perturbations cause an orbital resonance condition (eccentricity continues to increase until satellite falls into dense atmosphere.)

However, in order to attain efficient station keeping of a set of satellites in approximately the same orbit, it becomes necessary to maintain the eccentricity of the orbit within some acceptable limits. Among the reasons for maintaining small eccentricity are the degradation of the lifetime of a satellite at the lower altitudes, a possible loss of mobility due to earth shadowing effects, higher power requirements due to altitude variation, and a variation in the spacing of the satellites. For these reasons, computations have been made to determine the maximum eccentricity which could be expected as a function of altitude and inclination.

2.2.4.1 Spherical Satellite Eccentricity Data

In order to compute the maximum eccentricity reached by a particular orbit, the Lifetime 18 program has been used to calculate the eccentricity oscillation of the orbit over a 5-year period, and the maximum point during that 5-year period has been retained. These data were calculated over the full range of altitude and eccentricity and are shown in figures 2-5 (page 2-8) and 2-41 through 2-45 for various altitudes as a function of orbital inclination. All data shown in these plots have been calculated for a uniformly coated specular spherical satellite having a cross-sectional area-to-mass ratio of 20 square feet per pound. Extrapolation of these data to the configuration A and B satellites can be performed through the use of the extrapolation formulas given in paragraph 2.2.4.2. The derivation of these expressions is presented in paragraph 3-7.

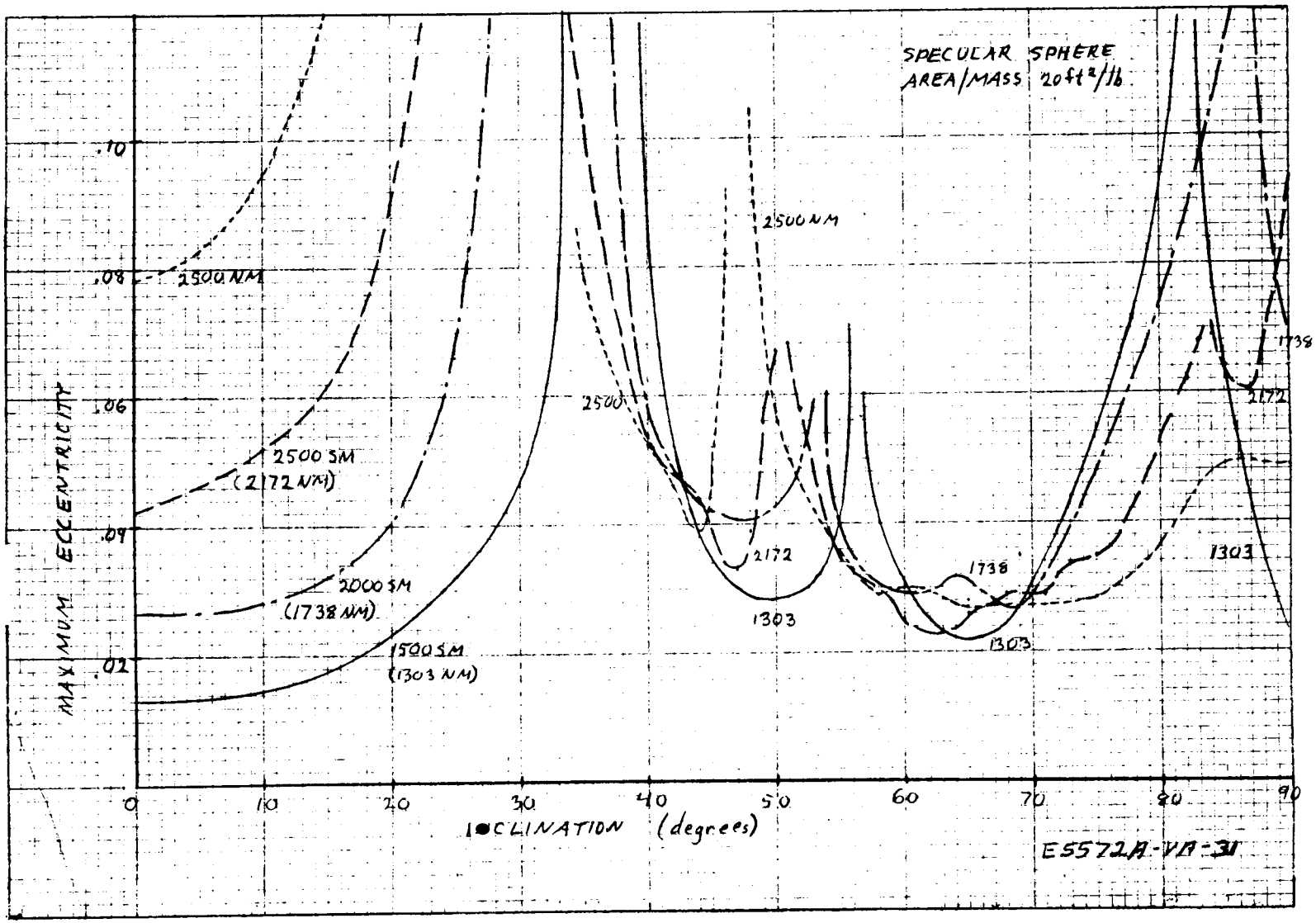

Figure 2-41. Maximum Eccentricity For Posigrade Orbits (1303- to 2500-NMI Altitude)

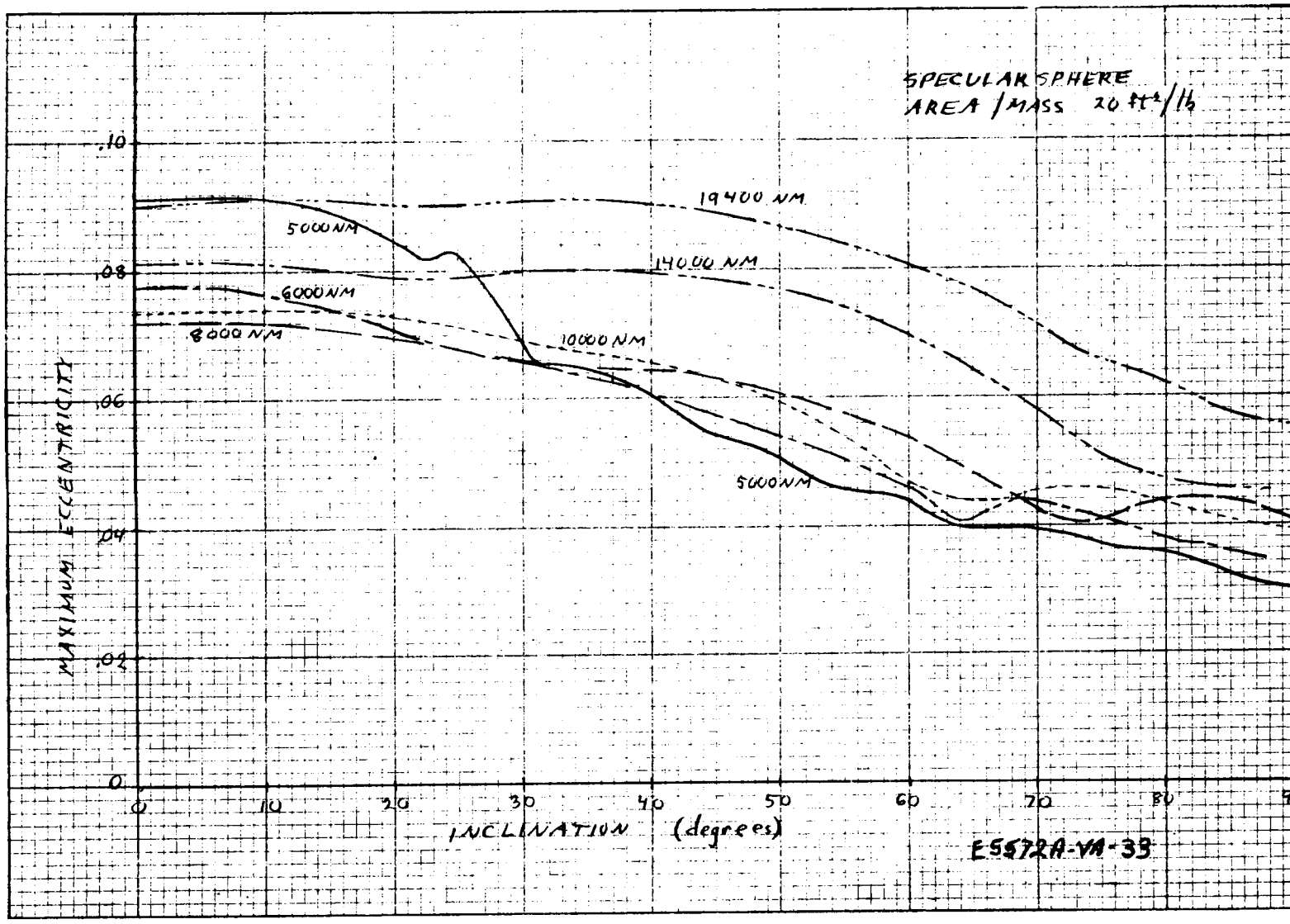

Figure 2-42. Maximum Eccentricity For Posigrade Orbits (5000- to 19,400-NMI Altitude)

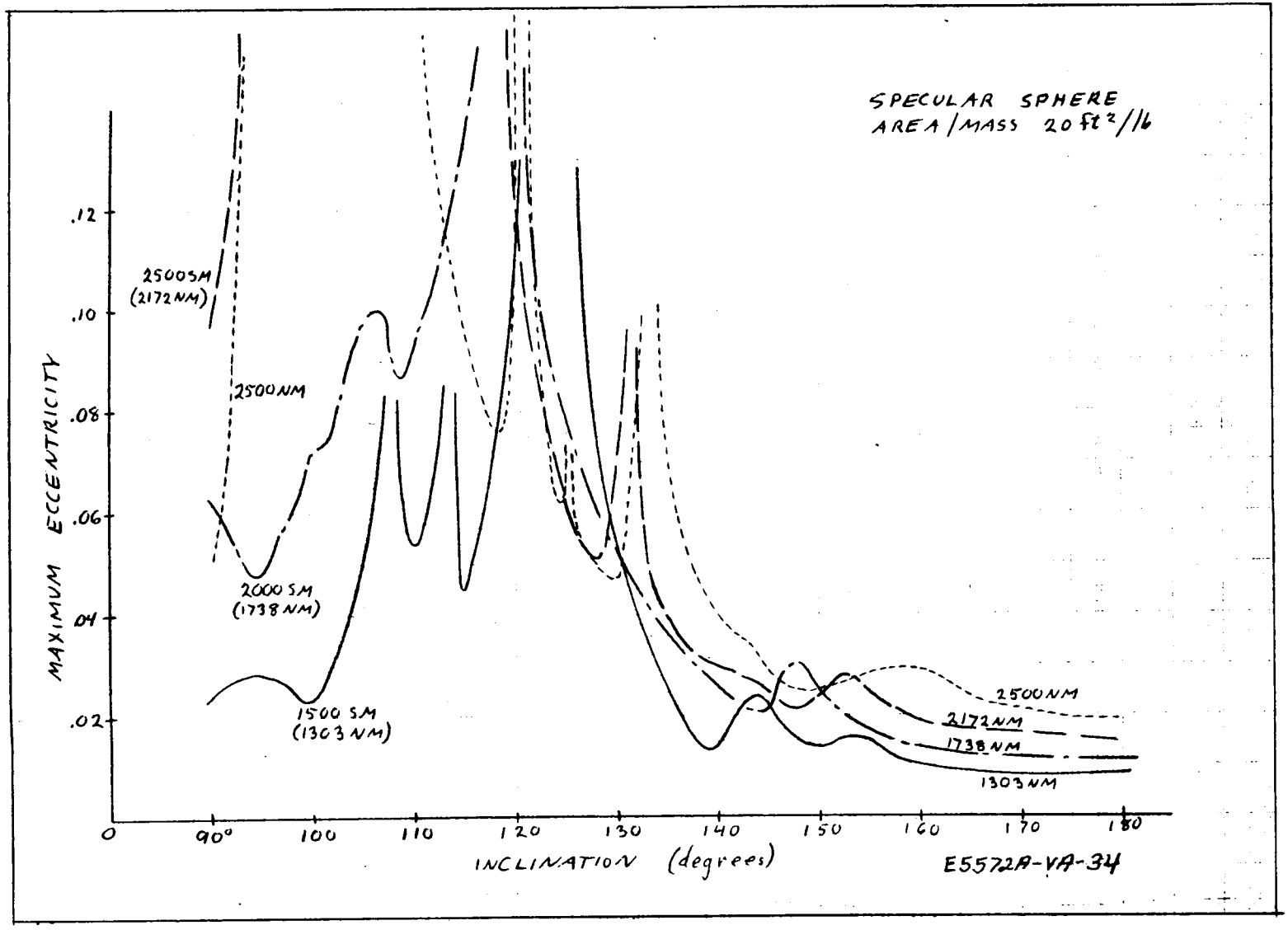

Figure 2-43. Maximum Eccentricity For Retrograde Orbits (1303- to 2500-NMI Altitude)

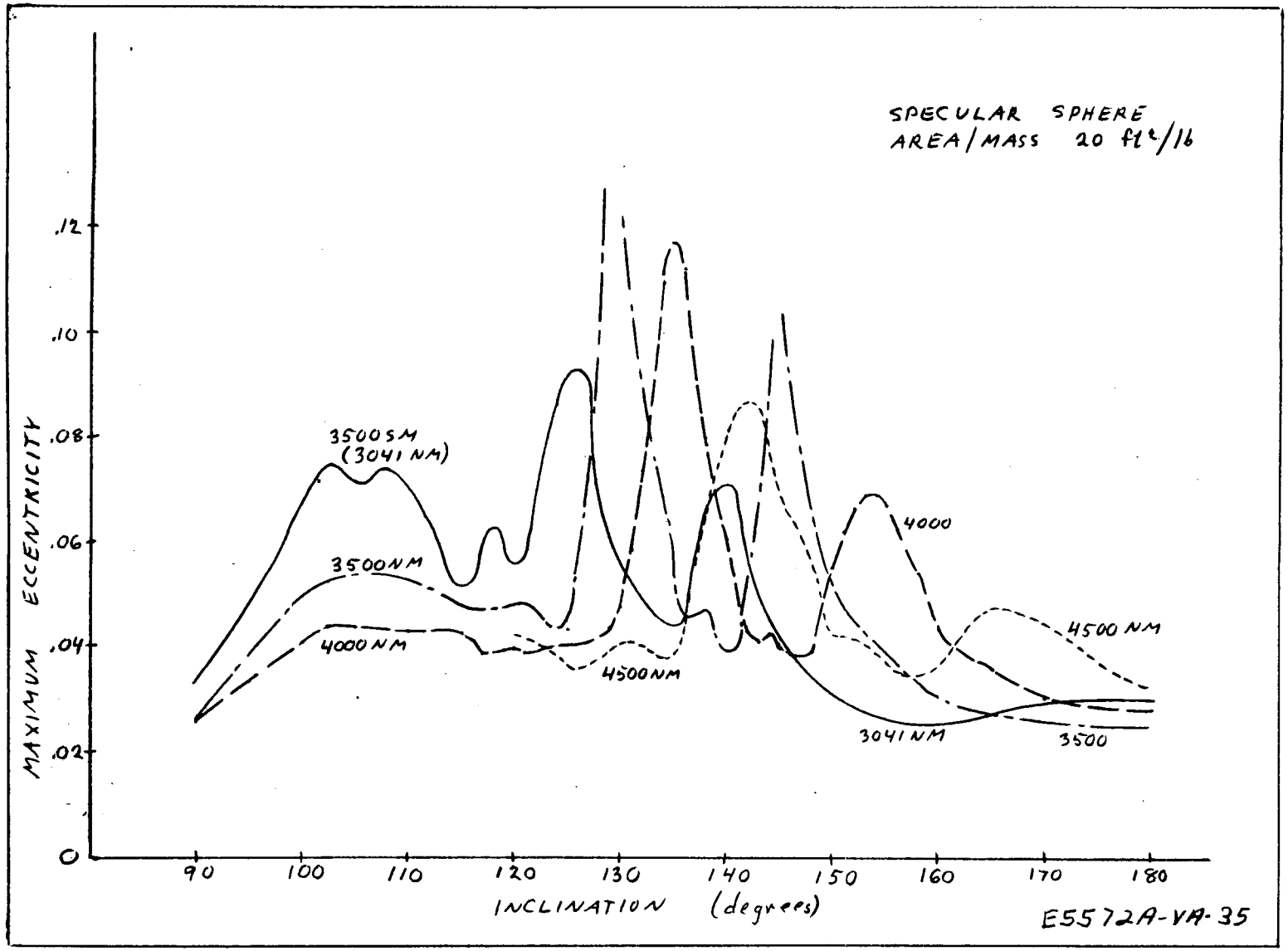

Figure 2-44. Maximum Eccentricity For Retrograde Orbits (3041- to 4500-NMI Altitude)

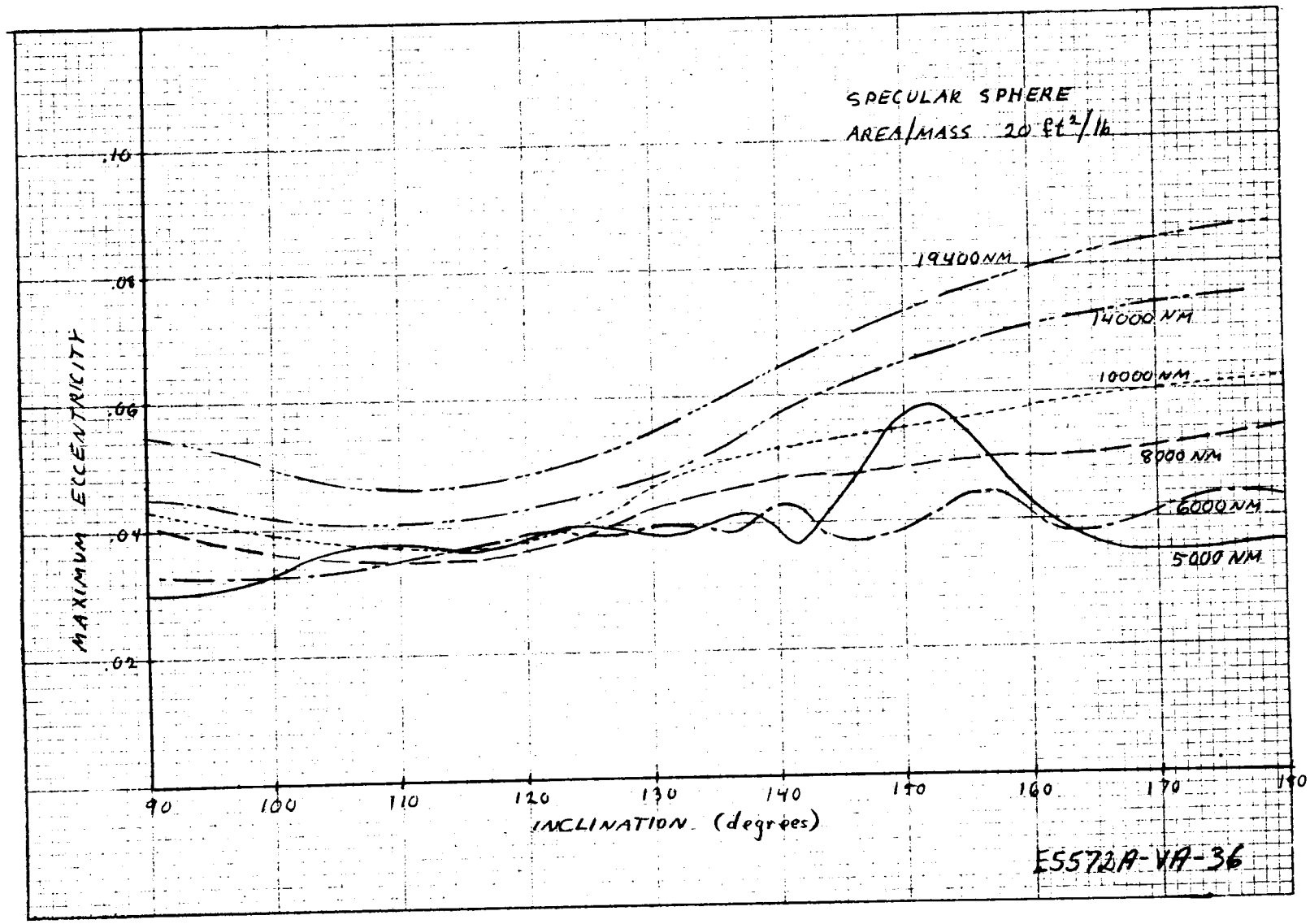

Figure 2-45. Maximum Eccentricity For Retrograde Orbits (5000- to 19,400-NMI Altitude)

As can be seen, there are several distinct resonances at the lower altitudes. The various conditions which can result in orbital resonance can be described by the following relationships;

$\dot{\omega} + \dot{\Omega} - \dot{\Omega}_s = 0$ (stationary perigee)

$\dot{\omega} + \dot{\Omega} + \dot{\Omega}_s = 0$ (equal and opposite motion)

$\dot{\omega} - \dot{\Omega} + \dot{\Omega}_s = 0$ (stairstep effect)

$\dot{\omega} + \dot{\Omega} - \dot{\Omega}_s = 0$ (stairstep effect)

$\dot{\omega} - \dot{\Omega}_s = 0$ (perigee in phase with sun-line)

$\dot{\omega} + \dot{\Omega}_s = 0$ (perigee in phase with sun-line)

where $\dot{\omega}$, $\dot{\Omega}$, and $\dot{\Omega}_s$ are the motion of the argument of perigee, the precession of the right ascension, and the apparent motion of the sun, respectively. For retrograde orbits, the sign of $\dot{\omega}$ should be changed, since by definition positive $\dot{\omega}$ changes from a counterclockwise rotation to a clockwise rotation when looking down from the north pole. A discussion of the physical causes of several of these resonances is given in paragraph 3-8.

Contours of constant maximum eccentricity have been determined from the data shown in figures 2-5 and 2-41 through 2-45 and a contour map of the maximum eccentricity versus altitude and inclination is shown in figures 2-46 and 2-47. Resonance regions and regions of high eccentricity are clearly indicated on these figures. It is interesting to note that the resonant regions are in general not symmetric with respect to the 90-degrees inclination line. This indicates that should any particular desired orbit fall in a region of resonance, the retrograde equivalent of that orbit could be substituted in most cases.

The various peaks shown in the maximum eccentricity data have been categorized with respect to the conditions causing them, and this information is summarized in figure 2-48. The numbers on these lines correspond to the numbered resonance conditions given above. None of the calculated peaks could be attributed to condition number four, although it is a theoretically possible peak.

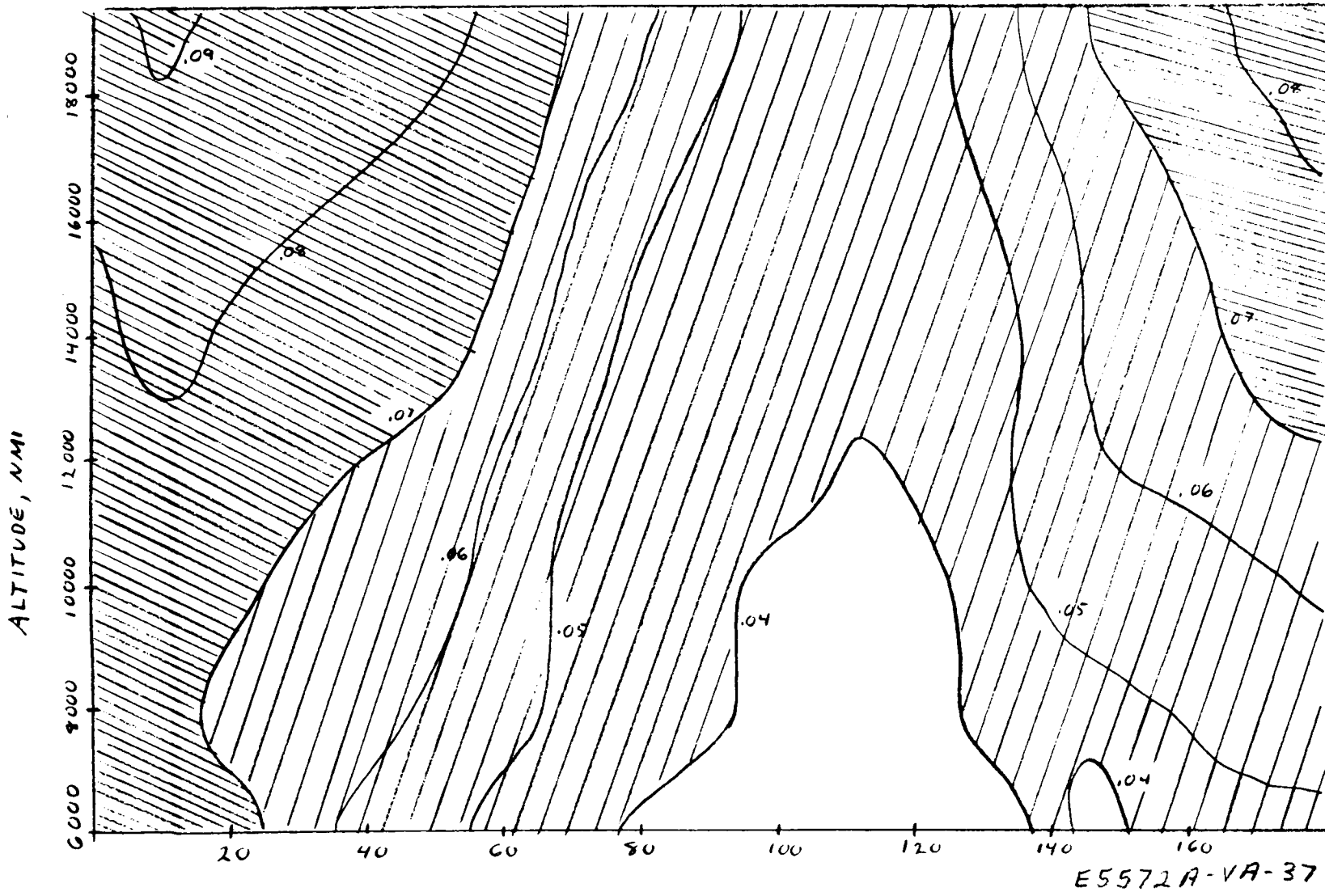

Figure 2-46. Eccentricity Contours

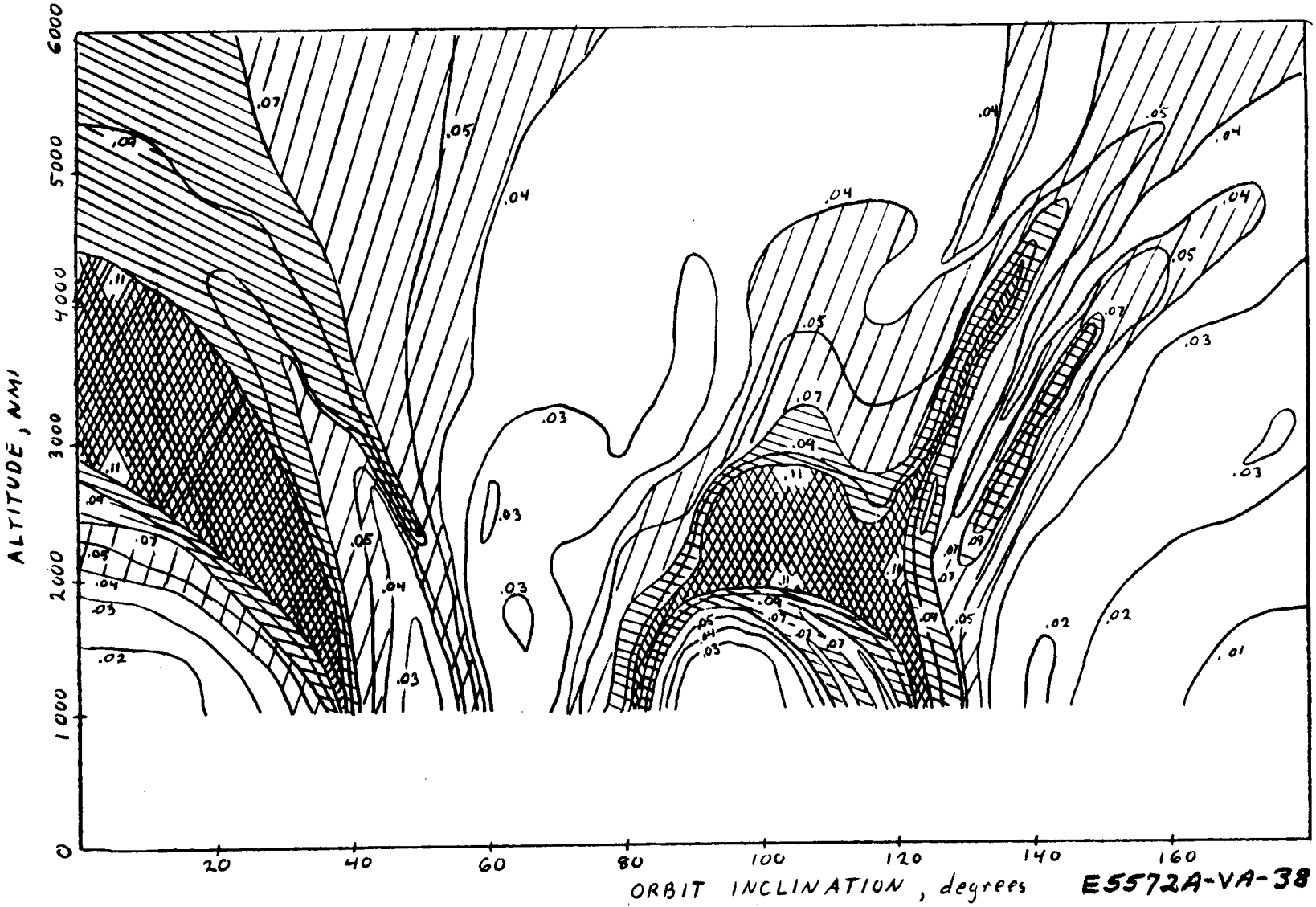

Figure 2-47. Eccentricity Contours

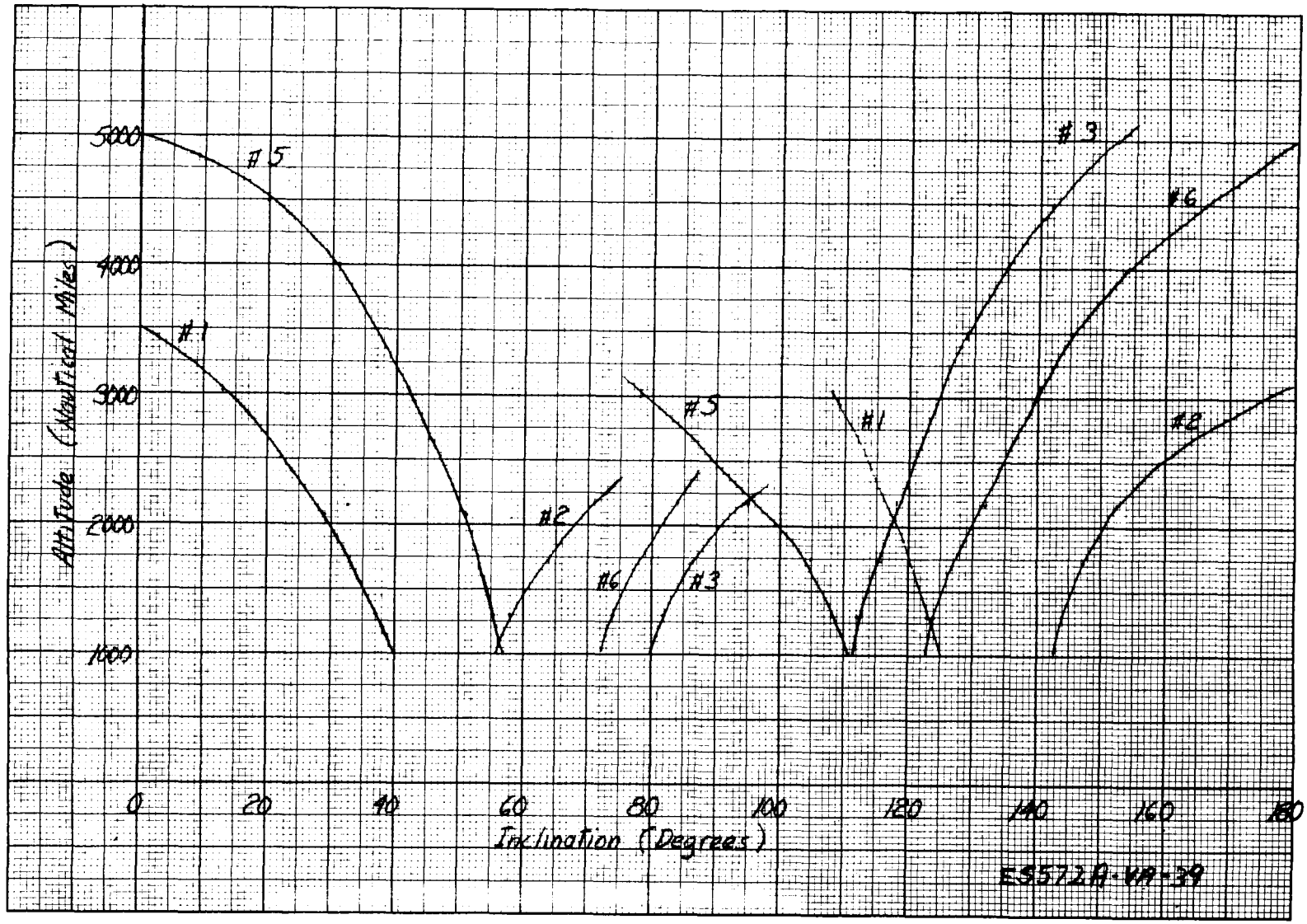

Figure 2-48. Resonant Conditions

The stability of the resonance appears to be a function of both the altitude and the condition causing the resonance. In general, the resonances tend to become wider but weaker with increasing altitude due to the decreasing procession rates of the orbit. For posigrade orbits, conditions Nos. 1 and 5 are seen to cause the most stable resonances while for retrograde orbits, conditions Nos. 3 and 6 cause the most stable resonance. Condition No. 3 for posigrade orbits is also seen to cause a very stable resonance at low altitudes but quickly merges with other conditions and becomes much weaker at higher altitudes. All other conditions are seen to produce a considerably less stable resonance.

In order that the perigee altitude may be readily obtained for any of the orbital conditions, figure 2-49 is included to graphically obtain this figure as a function of both semimajor axis and eccentricity.

It is also known that for high inclination orbits the maximum eccentricity reached by the orbit is a function also of the launch date (time of year) and the launch time of day (right ascension). All data shown in this report were calculated for a launch date of 21 March and a launch right ascension of 0 degrees (launched at vernal equinox with the sun-line in the plane of the orbit). The variation of the maximum eccentricity as a function of launch date is known to be sinusoidal in nature with a period of 1-year and a peak-to-peak amplitude of as much as 25 percent of the nominal values. However, the variation with respect to launch right ascension is somewhat irregular and may change the maximum eccentricity by as much as 50 percent from a nominal average value. The user is cautioned that a more detailed examination of these variables should be made where the maximum eccentricity is critical to a particular application.

2.2.4.2 Eccentricity Scaling

Paragraph 2.2.4.1 presented a discussion of the eccentricity due to solar forces on a spherical satellite and included a quantity of data for this case. In order to use these data, equivalent area-to-mass ratios are defined for

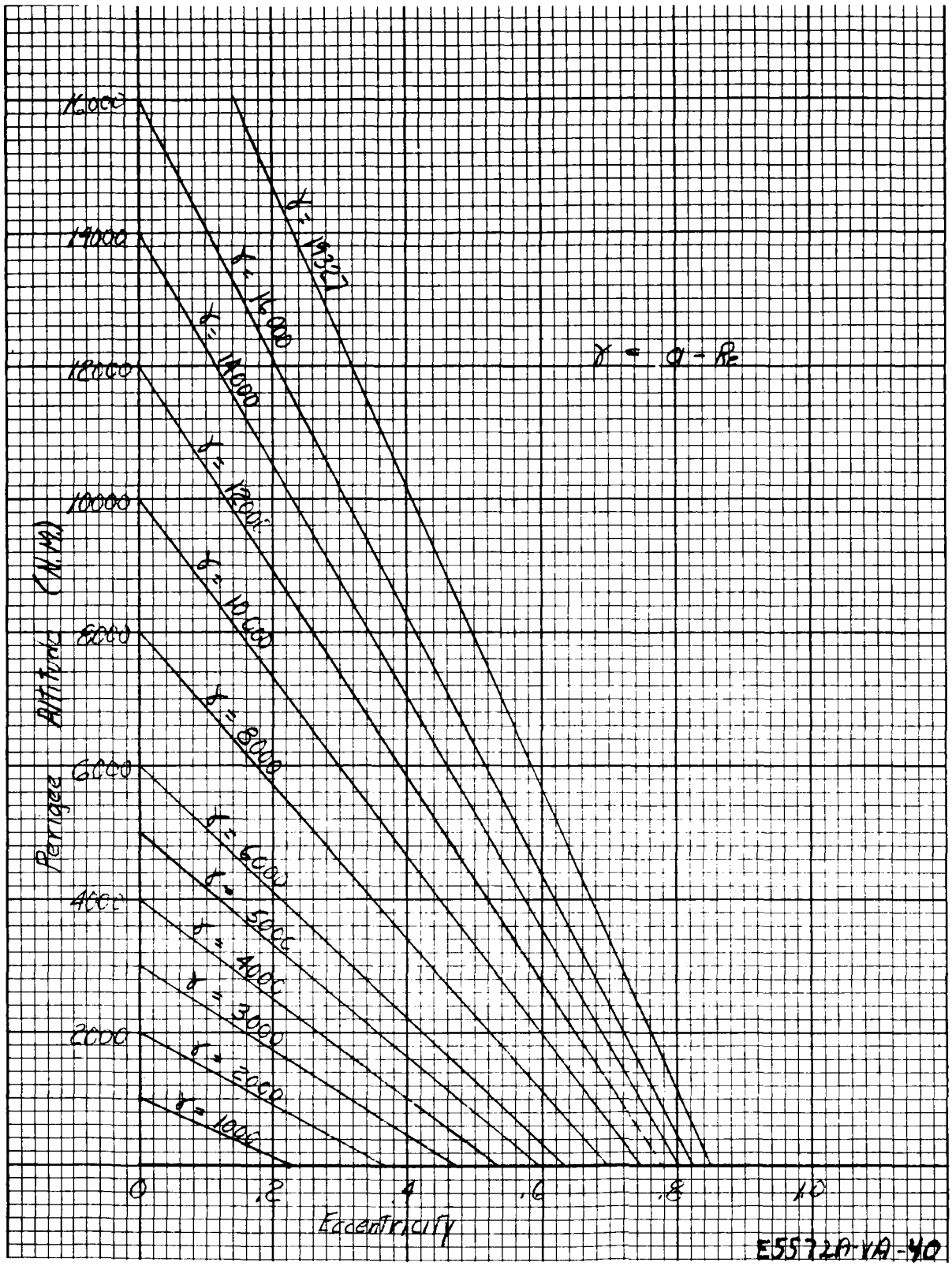

Figure 2-49. Perigee Altitude Vs. Eccentricity

configuration A and B lenticular satellites; the eccentricity data may then be scaled in proportion to the ratio of the equivalent area-to-mass ratio to the area-to-mass ratio assumed for the data plotted (20 ft^2/lb). Derivations of these equivalent area-to-mass ratio formulas may be found in paragraph 3. 7.

2. 2. 4. 2. 1 Configuration A—For a configuration A (opaque lens) satellite, the equivalent area-to-mass ratio for eccentricity scaling is given by:

$$\frac{A_L}{M} = \frac{A_{Lc} + 2A_{L90}}{3M}\left(1 + \frac{4}{9}r\right)$$

$$A_{Lc} = \pi D^2/4$$

$$A_{L90} = 2R^2 \sin^{-1}\frac{D}{2R} - DR\cos\left(\sin^{-1}\frac{D}{2R}\right)$$

where:

D is the lenticule diameter

R is the lenticule radius of curvature

M is the satellite mass

r is the reflectivity of the lenticule

A diffuse reflecting surface was assumed for the lenticule. These scaling relations were checked by computer simulation (paragraph 3. 7) for a range of parameter values about nominal values of R = 200, D = 267' and found to be reasonably accurate. However, caution should be observed in extrapolating beyond a factor of 2 or 3 from these nominal values, since they have not been checked beyond these ranges.

2. 2. 4. 2. 2 Configuration B—For a configuration B (sail) satellite, assuming fixed compensation control, the equivalent area-to-mass ratio for eccentricity scaling is given by:

$$\frac{A_B}{M} = \frac{1}{M}\left(\left[.09917 - .001667\frac{A_{Lc}}{A_{L90}}\right]A_{Lc} + \left[.353 + \frac{.207\sin i}{i}\right]A(1+\hat{r})\right)$$

where i is the orbital inclination, A the sail area, $\hat{r}$ the average reflectivity of the two sail surfaces, and the other terms have been defined previously.

2.2.5 Maximum Angular Position Error and Mobility Control Procedures

The maximum angular position error of a controlled satellite depends on the mobility control procedure used. Data are presented for two control procedures, which are defined below. For a more complete discussion of the two control procedures and for a derivation of the error formula, refer to paragraph 3.3.

2.2.5.1 Control Procedures

2.2.5.1.1 No Neutral Mode (NNM) — The satellite is maintained alternately in increasing and decreasing mobility modes with mobility $\pm M$, the time t_B in each phase being on the order of 15 to 30 days. When the angular position error of the satellite with respect to its desired position exceeds a limit, Θ_E, in either direction, a set of two mobility pulses of opposite sign and separated by the interval t_B is applied to correct this error. The time at which the first pulse is applied depends on the sign of the error and the mobility mode at the time the error exceeds Θ_E. If the mobility at this time is in the direction to increase the angular error, the correction mobility pulse is applied immediately by reversing the mobility for a time period, t_1, followed by a similar reversal, t_B, later for a time period, t_2. If the mobility at the time when the error exceeds Θ_E is in the direction to decrease the error, the correction mobility pulse is applied by delaying the normal mobility reversal which would otherwise occur by a delay of t_1. The reversal of the next mobility phase is likewise delayed an interval, t_2. The time interval, t_1, is chosen to reduce the angular position error from Θ_E to zero in the time interval, t_B; the time interval, t_2, is then chosen to reduce the resulting orbital period error to zero. (If period error is not measured, t_2 is chosen equal to t_1.) These times are given by the formulas:

$$t_1 \approx \frac{\Theta_E K_1 a^{5/2}}{6\pi M t_B} \quad , \quad t_2 \approx t_1 \pm \frac{\Delta P_o}{3 K_1 M a^{1/2}} \quad , \quad t_1, t_2 \ll t_B$$

where Θ_E is the error limit (or minimum detectable error)

ΔP_o is the period error at the time the error first exceeds Θ_E

$K_1 = \frac{2\pi}{K\sqrt{m}}$ where K is the Newton's gravitational constant and m is the mass of the earth; $K_1 = 3.147 \times 10^{-7}$ sec/$m^{3/2}$

a is the orbit semimajor axis

M is the mobility

and the ± sign is to be chosen (-) if the initial angular position error is negative, (+) otherwise.

These equations are graphed parametrically in figures 2-6 and 2-7 (pages 2-9, 2-10). Both figures may be read either counterclockwise (yielding t, vs θ_E and $(t_2 - t_1)$ vs ΔP_o) or clockwise (yielding θ_E vs t_1 and ΔP_o vs $t_2 - t_1$) as indicated by the broken lines. The ranges of Θ_E and ΔP_o included are 0 to 10 degrees and 0 to 10 seconds, respectively; other ranges may be easily obtained by scaling by multiples of ten, since the relations are those of direct proportionality.

2.2.5.1.2 Neutral Mode (NM) — The satellite is normally maintained in a position of zero mobility; for example, by maintaining the sail parallel to the orbital plane in the case of a configuration B satellite. When the angular position error reaches the allowed limit Θ_E, a mobility of magnitude, M_1, is applied for a time, t_1, in the proper direction to reduce the angular position error. The time duration, t_1, is determined such that at its end the angular position error is of magnitude Θ_E and is decreasing in magnitude. (The angular position error has been assumed to be increasing in magnitude due to an associated period error, ΔP_o; if this is not the case, the initial mobility impulse, M_1, of duration, t_1, is not necessary.) Following the first mobility pulse, a second mobility pulse of opposite sense and of magnitude, M_2, and duration, t_2, is applied to reduce both the position error and the period error to zero at the conclusion of the correction. The equations for these quantities are:

$$t_1 \approx \left| \frac{4\Delta P_o}{3K_1 M_1 a^{1/2}} \right|$$

$$|M_2| \approx \frac{2\pi \Delta P_o^2}{3K_1^3 a^{7/2} \Theta_E}$$

$$t_2 \approx \left| \frac{}{3K_1 M_2 a^{1/2}} \right|$$

These equations are graphed parametrically in figures 2-8 (page 2-11) and 2-50 through 2-52; figure 2-8 repeats the information of figure 2-51 for a wider range of M_2. The figures may be read clockwise or counterclockwise. In figures 2-8 and 2-51, two scales are presented for different ranges of ΔP_o and M_2; the scales are to be read together, scale 1 with scale 1 and scale 2 with scale 2.

2.2.5.2 Angular Position Errors

Significant sources of angular position error (relative to the nominal angular position of the satellite) are listed in table 2-2, along with the appropriate formula. The error sources are defined in the following paragraphs; derivations of the formulas may be found in paragraph 3-3.

2.2.5.2.1 Minimum Detectable Error or Error Limit — This error is essentially the error limit, Θ_E, established to initiate the mobility correction procedure. It may be established by the minimum error detection capability of the ground tracking equipment, or it may be set on the basis of a maximum allowable error criteria such as that discussed in paragraph 3.6. Alternatively, it may be calculated on the basis of assumed mobilities in accordance with the equations of table 2-2. The equation listed for the NNM control is presented graphically in figure 2-6, (page 2-9) which should be read clockwise for this purpose. The equation listed for the NM control is graphically presented in figures 2-8 and 2-51 where the value of $|\Theta_e|$ should be read in the parametric coordinates of the first quadrant. For example, corresponding to the values $|\Delta P_o|$ = 8 seconds, $|M_2|$ = 120 meters/deg, and h = 7000 nmi, the corresponding value of $|\Theta_e|$ is approximately 6 degrees.

2.2.5.2.2 Period Error — If, at the time the angular position error exceeds the limits, $\pm\Theta_E$, the period error is such that the angular position error is increasing in magnitude (this will normally be the case); then, an overshoot in the angular position error will occur. This error is given by the equations in table 2-2 for Θ_1. They may be evaluated using the graphs of figures 2-8 and 2-51 in a manner similar to that described above to evaluate $|\Theta_e|$. The

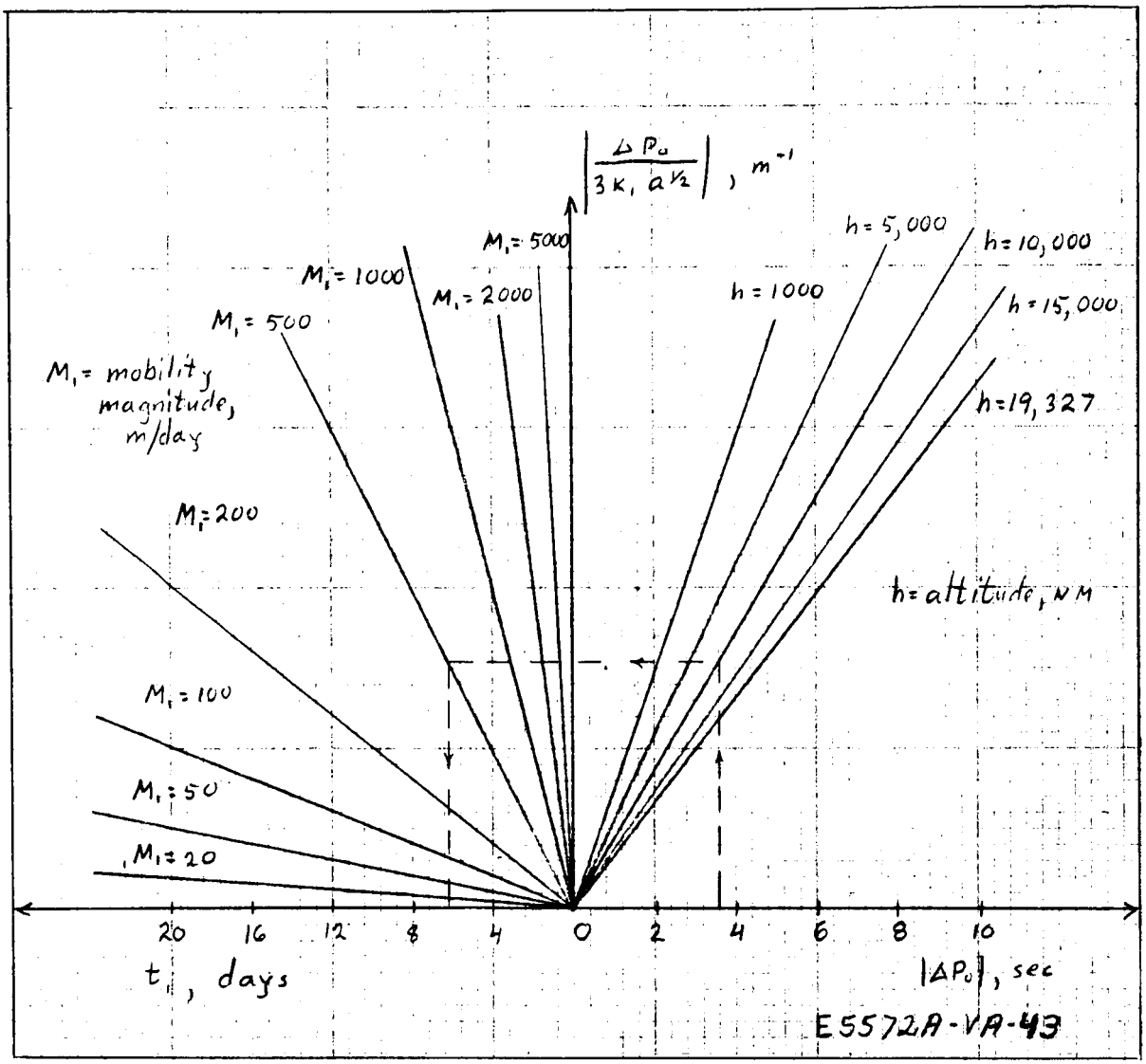

Figure 2-50. t_1 Vs. ΔP_o; Neutral Mode Control

values of mobility for M or M_1 should be used rather than the value for M_2, and the result obtained from the graph should be divided by 2 in the case of NNM control.

2.2.5.2.3 Finite Mode Change Time — If a time interval, t_T, is required to change mobility modes, then an additional angular error component is contributed to the overshoot error, Θ_1. This component is given by Θ_2, and is normally quite small. The equation is graphed parametrically in figure 2-9(p. 2-12)

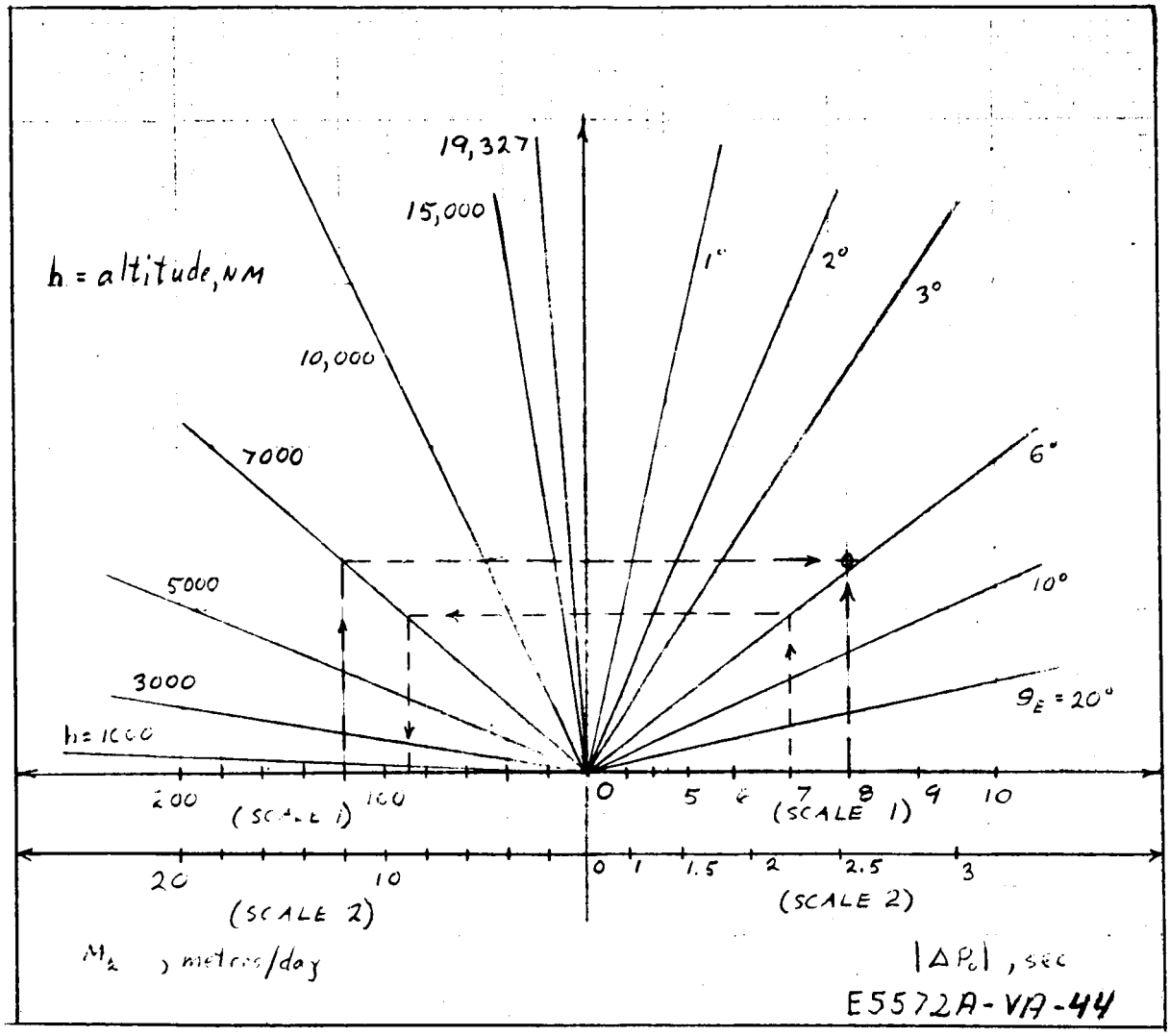

Figure 2-51. M_2 Vs. Θ_E, ΔP_o; Neutral Mode Control

for M_1 range from 0 to 1000 m/day and t_T range from .1 to 1.0 day. Other ranges can easily be obtained by scaling M_1 and t_T by factors of 10, and scaling $|\Theta_2|$ by corresponding factors of 10 or 100, respectively. The chart may also be used for NNM control by multiplying the value of $|\Theta_2|$ obtained by two.

2.2.5.2.4 Command Delay — If the mobility control procedure is delayed an interval, t_d (for example, to wait until the satellite is within range of a

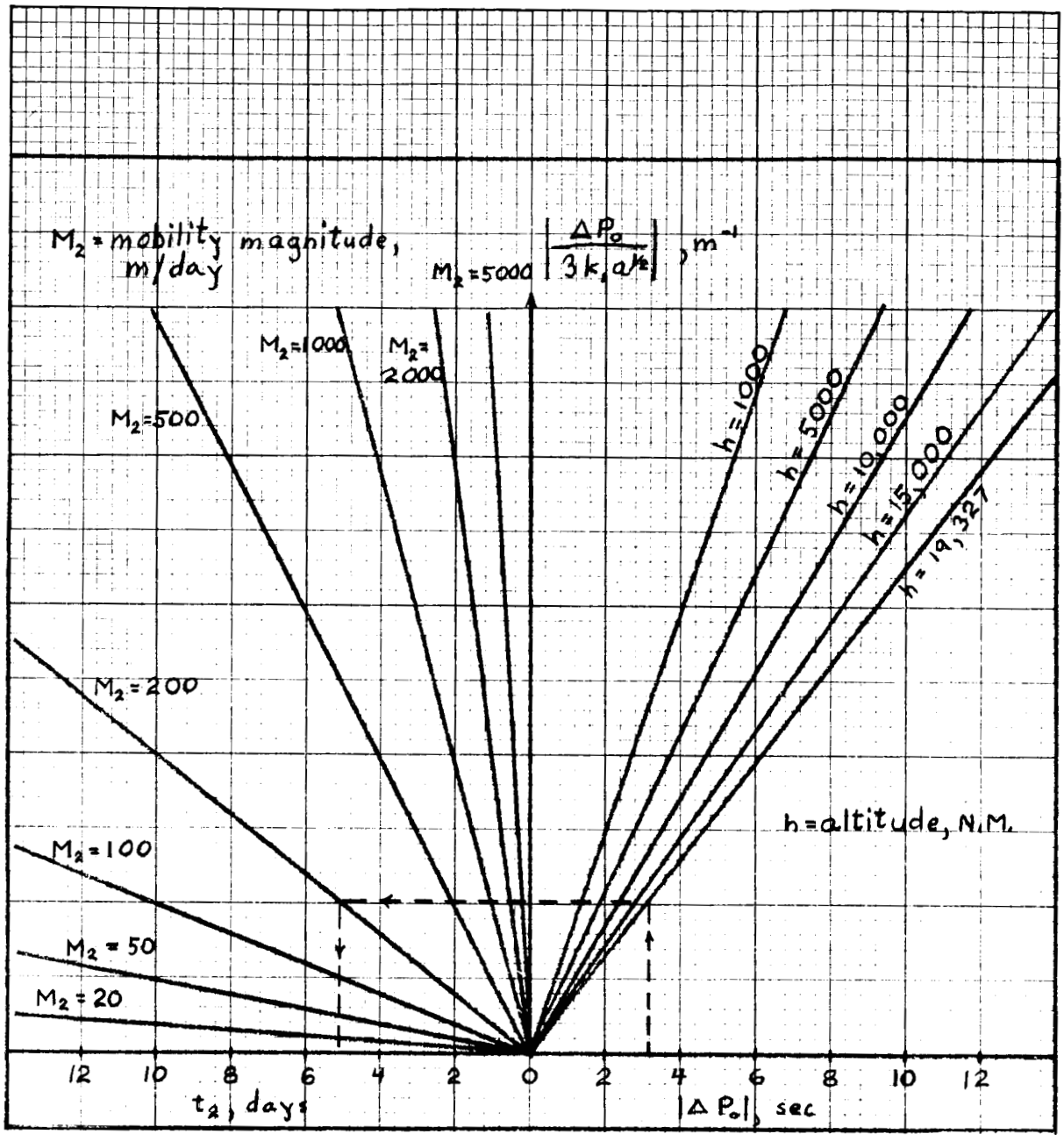

Figure 2-52. t_2 Vs. ΔP_o; Neutral Mode Control

command station), another contribution to the overshoot error results. This term is given by Θ_3 of table 2-2. The equation for Θ_3 is plotted parametrically in figure 2-10, (page 2-13) which should be read counterclockwise as shown. In general, Θ_3 will be small in magnitude.

2.2.5.2.5 Unequal Mobilities — An example of an overshoot error due to a period error is provided by the situation in which, using NNM control, the increasing and decreasing mode mobilities are unequal. Specifically, the

case was considered in which the angular position error and period error were zero at the time an increasing mobility mode was initiated. It was assumed that the increasing mobility was too great by an error, M_E (i. e., the increasing mobility was $M + M_E$ where M is the nominal mobility); M_E was assumed large enough that the angular position error would exceed Θ_E in a time period smaller than t_B. In these circumstances, a period error will exist when the angular position error exceeds Θ_E, and the resulting overshoot angular position error is given by $\Theta_4 \approx \frac{M_E}{M} \Theta_E$. In general, this error will be rather small. Similar results would be obtained in the case of an error in the decreasing mobility mode.

2. 2. 5. 2. 6 Nonzero Neutral Mode Mobility — In the case of NM control, an error similar to Θ_4 will occur if the neutral mode mobility $M_\circ$ is nonzero. The overshoot error in this case is given by $\Theta_5 \approx \frac{M_\circ}{M} \Theta_E$, and again is usually small.

2. 2. 5. 2. 7 Eccentricity — The errors discussed previously have all been derived under the assumption of circular orbits. For noncircular orbits an additional error due to the orbit eccentricity is present. The maximum value of this error for a given eccentricity is given by Θ_6 of table 2-2, and may be one of the most significant errors considered. Θ_6 is plotted against eccentricity in figure 2-11 (page 2-14).

TABLE 2-2

SIGNIFICANT ANGULAR ERROR SOURCES

Error Source	Formula	
	NNM Control	NM Control
Minimum detectable error or error limit	$\lvert\theta_e\rvert \approx \frac{6\pi M t_B t_1}{K_1 a^{5/2}}$	$\lvert\theta_e\rvert \approx \frac{2\pi \Delta P_o^2}{3K_1^3 a^{7/2} M_2}$
Period error	$\lvert\theta_1\rvert \approx \frac{\pi \Delta P_o^2}{3K_1^3 a_o^{7/2} M}$	$\lvert\theta_1\rvert \approx \frac{2\pi \Delta P_o^2}{3K_1^3 a^{7/2} M_1}$
Finite time, t_τ, required for mobility mode change	$\lvert\theta_2\rvert \approx \frac{3\pi M t_\tau^2}{4K_1 a^{5/2}}$	$\lvert\theta_2\rvert \approx \frac{3\pi M_1 t_T^2}{8K_1 a^{5/2}}$
Command delay, t_d.	$\theta_3 \approx -\frac{2\pi \Delta P_o t_d}{K_1^2 a^3}$	
Unequal mobilities	$\theta_4 \approx \frac{M_E}{M} \theta_E$ *	———
Nonzero neutral-mode mobility M	———	$\theta_5 \approx \frac{M_o}{M_1} \theta_E$
Eccentricity e	$\theta_6 = \cos^{-1}(-e) - \frac{\pi}{2} + e \approx 2e$ radians	

* $M_E = \lvert M_I \rvert - \lvert M_D \rvert$, where M_I is the mobility in the increasing mode and M_D is the mobility in the decreasing mode, with M_D assumed equal to M.

3. DERIVATIONS AND SUPPORTING MATERIAL

3. DERIVATIONS AND SUPPORTING MATERIAL

3.1 MOBILITY SCALING RELATIONS

3.1.1 Derivation of Scaling Equations With Respect to Altitude And Solar Inclination

3.1.1.1 Configuration A

The derivation of the mobility of the lenticular satellite is difficult because of its complex shape. A rigorous solution does not result in an expression suitable for scaling calculations. Therefore, the approach adopted here has been to derive an expression based upon a greatly simplified model and modify it so as to provide a useful scaling function. The model assumed was a spherical section oriented with its plane perpendicular to the orbit plane and to the orbit radius as illustrated in figure 3-1. The two outside surfaces of different emissivities e_{IR_1} and e_{IR_2} are symmetrical about a diameter perpendicular to the orbit plane. The outside absorptivity α_o was assumed uniform over the entire outer surface and the inside emissivity e_{IR_i} and absorptivity α_i were assumed constant over the interior surface of the spherical section. The reradiation forces on this section due to direct solar energy were calculated for orbit angles (measured relative to a plane perpendicular to the orbit plane and containing the sunline vector) of $\frac{\pi}{2}$ and $\frac{3\pi}{2}$, and the resultant force used to obtain an approximation of the mobility.

The energy radiated internally due to the incident solar energy can be written for the assumed model as:

$$\int_{-\frac{\pi}{2}+i_s}^{\pi/2} \frac{e_{IR_i}}{e_{IR_1}+e_{IR_i}} RC_s\alpha_s\cos(\psi-i_s)\,d\psi + \int_{\pi/2}^{\frac{\pi}{2}+i_s} \frac{e_{IR_i}}{e_{IR_2}+e_{IR_i}} RC_s\alpha_s\cos(\psi-i_s)\,d\psi$$

$$= RC_s\alpha_s\left[(1+\cos i_s)\left(\frac{e_{IR_i}}{e_{IR_1}+e_{IR_i}}\right) + (1-\cos i_s)\left(\frac{e_{IR_i}}{e_{IR_2}+e_{IR_i}}\right)\right] \quad (3\text{-}1)$$

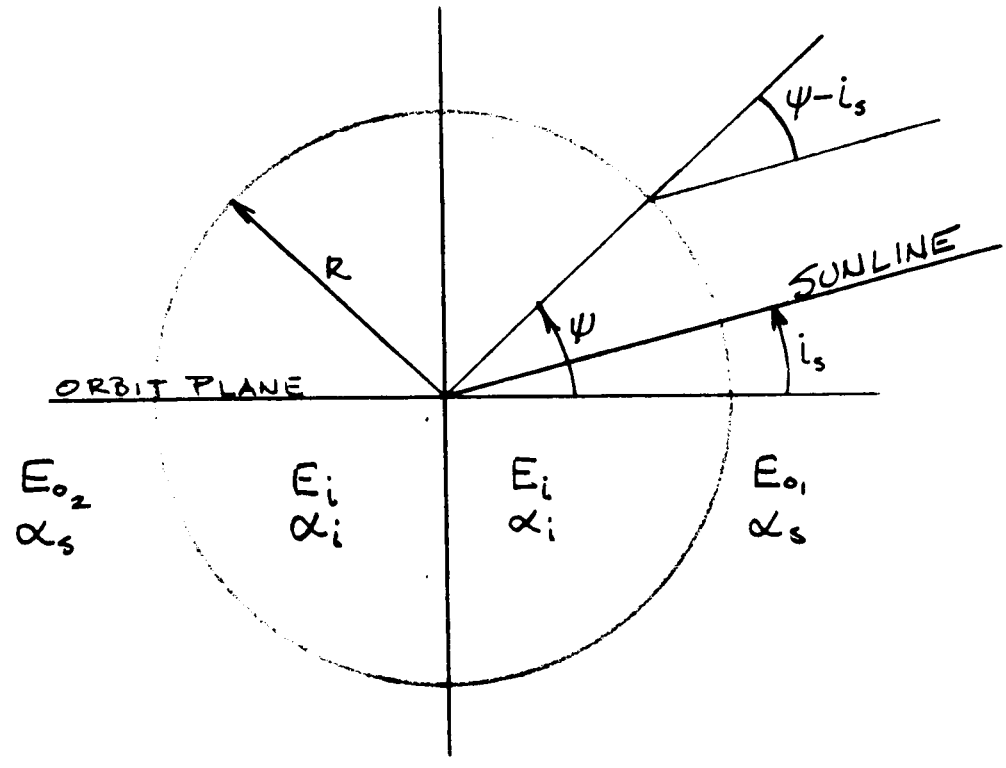

Figure 3-1. Assumed Model

where: e_{IR_i} = internal emissivity

e_{IR_1} = external emissivity of one hemisphere

e_{IR_2} = external emissivity of other hemisphere

R = radius of spherical section

C_s = solar constant

α_s = external absorptivity

The angular quantities are defined in figure 3-1. The fraction of the energy reflected internally can be written as:

$$\int_{-\pi/2}^{\pi/2} \frac{e_{IR_1}}{e_{IR_1} + e_{IR_i}} \alpha_i R\, d\psi + \int_{\pi/2}^{3\pi/2} \frac{e_{IR_2}}{e_{IR_2} + e_{IR_i}} \alpha_i R\, d\psi$$

$$= \pi \alpha_i R \left(\frac{e_{IR_1}}{e_{IR_1} + e_{IR_i}} + \frac{e_{IR_2}}{e_{IR_2} + e_{IR_i}} \right) \qquad (3\text{-}2)$$

The energy, S, incident on the internal surface of the circular section times the absorptivity of the internal surface is given by:

$$\alpha_i S = \frac{C_s \alpha_s}{\pi} \left[\frac{(1+\cos i_s)\left(\frac{e_{IR_1}}{e_{IR_1} + e_{IR_i}}\right) + (1-\cos i_s)\left(\frac{e_{IR_2}}{e_{IR_2} + e_{IR_i}}\right)}{\frac{e_{IR_1}}{e_{IR_1} + e_{IR_i}} + \frac{e_{IR_2}}{e_{IR_2} + e_{IR_i}}} \right] \qquad (3\text{-}3)$$

The resultant force for an orbit angle of $\frac{\pi}{2}$ (side 1 facing the sun) can be written as:

$$F_R = -\frac{2}{3C} \left\{ \int_{-\pi/2 + i_s}^{\pi/2} \frac{e_{IR_1}}{e_{IR_1} + e_{IR_i}} \left[C_s \alpha_s \cos(\psi - i_s) + \alpha_i S \right] R \cos\psi\, d\psi \right.$$

$$+ \int_{-\pi/2}^{-\pi/2 + i_s} \frac{e_{IR_1}}{e_{IR_1} + e_{IR_i}} \alpha_i S R \cos\psi\, d\psi + \int_{\pi/2}^{\pi/2 + i_s} \frac{e_{IR_2}}{e_{IR_2} + e_{IR_i}} \left[C_s \alpha_s \cos(\psi - i_s) + \alpha_i S \right] R \cos\psi\, d\psi$$

$$\left. + \int_{\frac{\pi}{2} + i_s}^{\frac{3\pi}{2}} \frac{e_{IR_2}}{e_{IR_2} + e_{IR_i}} \alpha_i S R \cos\psi\, d\psi \right\} \qquad (3\text{-}4)$$

Equation 3-4 reduces to:

$$F_R = -\frac{2}{3C} R \left\{ \frac{e_{IR_1}}{e_{IR_1} + e_{IR_i}} \left[C_s \alpha_s \left(\frac{\pi}{2} \cos i_s - \frac{i_s}{2} \cos i_s + \frac{1}{2} \sin i_s \right) + 2\alpha_i S \right] \right.$$

$$\left. + \frac{e_{IR_2}}{e_{IR_2} + e_{IR_i}} \left[C_s \alpha_s \left(\frac{i_s \cos i_s}{2} - \frac{1}{2} \sin i_s \right) - 2\alpha_i S \right] \right\} \qquad (3\text{-}5)$$

The force for the orbit angle of $\frac{3\pi}{2}$ is obtained by reversing the subscripts for the two surfaces in equation 3-5. The resultant force obtained by taking the difference of these two expressions is:

$$\Delta F_R = -\frac{2}{3C} R C_s \alpha_s (E_1 - E_2) \left(\frac{\pi}{2} \cos i_s - i_s \cos i_s + \sin i_s + \frac{4G}{\pi} \right) \qquad (3\text{-}6)$$

where

$$E_1 = \frac{e_{IR_1}}{e_{IR_1} + e_{IR_i}} \qquad E_2 = \frac{e_{IR_2}}{e_{IR_2} + e_{IR_i}}$$

$$G = \left(\frac{\frac{e_{IR_i}}{e_{IR_1} + e_{IR_i}} + \frac{e_{IR_i}}{e_{IR_2} + e_{IR_i}}}{E_1 + E_2} \right)$$

Since the mobility, M, has been shown to be given by the expression:

$$M = \frac{a^{3/2}}{\pi m K^{1/2}} \int_{ORBIT} F \, d\theta$$

the mobility is proportional to the terms:

$$M(a, i_s) \propto a^{3/2} \left[\frac{\pi}{2} \cos i_s - i_s \cos i_s + \sin i_s + \frac{4G}{\pi} \right] \qquad (3\text{-}7)$$

Because of the gross approximation used for the lenticular shape and because the determination of the resultant force ΔF_R neglected the effect of the earth's shadow, equation 3-7 must be modified to account for these factors.

The approximation resulting from the shape factor can be improved by the introduction of the multiplying factor $\cos^{1/2} i_s$ and the reduction of the constant term in the brackets of equation 3-7 by a factor of 2. The effect of partial orbit occultation can be accounted for by the introduction of the term $\cos^2 \psi_a (\alpha, i_s)$, where ψ_a is the shadow half angle defined by:

$$\psi_a = \cos^{-1} \left[\frac{a^2 - R_e^2}{a^2 \cos^2 i_s} \right]^{1/2} \qquad (3\text{-}8)$$

When the orbit is no longer occulted, the factor becomes $(1 - \frac{1}{2} \sin^2 \frac{i_s}{2})$.

For the case of orbit occultation, the corrected scaling factor is given by:

$$M(a, i_s) \propto a^{3/2} \left\{ \cos^2 \psi_a \left[\frac{\pi}{2} \cos^{1/2} i_s - i_s \cos^{3/2} i_s + \cos^{1/2} i_s \sin i_s \right] + \frac{2G}{\pi} \right\} \qquad (3\text{-}9)$$

For nonoccultation, the corrected scaling factor is given by:

$$M(a, i_s) \propto a^{3/2} \left\{ \left(1 - \tfrac{1}{2} \sin^2 \tfrac{i_s}{2}\right) \left[\frac{\pi}{2} \cos^{1/2} i_s - i_s \cos^{3/2} i_s + \cos^{1/2} i_s \sin i_s \right] + \frac{2G}{\pi} \right\} \qquad (3\text{-}10)$$

When extrapolating lenticular mobility as a function of altitude or sun-line inclination, equation 3-8 must be applied first to determine if equation 3-9 or 3-10 is used to derive the proportionality constant.

Figure 3-2 illustrates the degree of agreement obtained between scaled values and computer derived values of mobility. The computer derived mobilities for various sun-line inclinations at synchronous altitude were used as the scaling points and the mobility extrapolated down to an altitude of 1000 nmi. The heavy dark data points at these altitudes represent the computer derived values of mobility. The agreement between the extrapolated

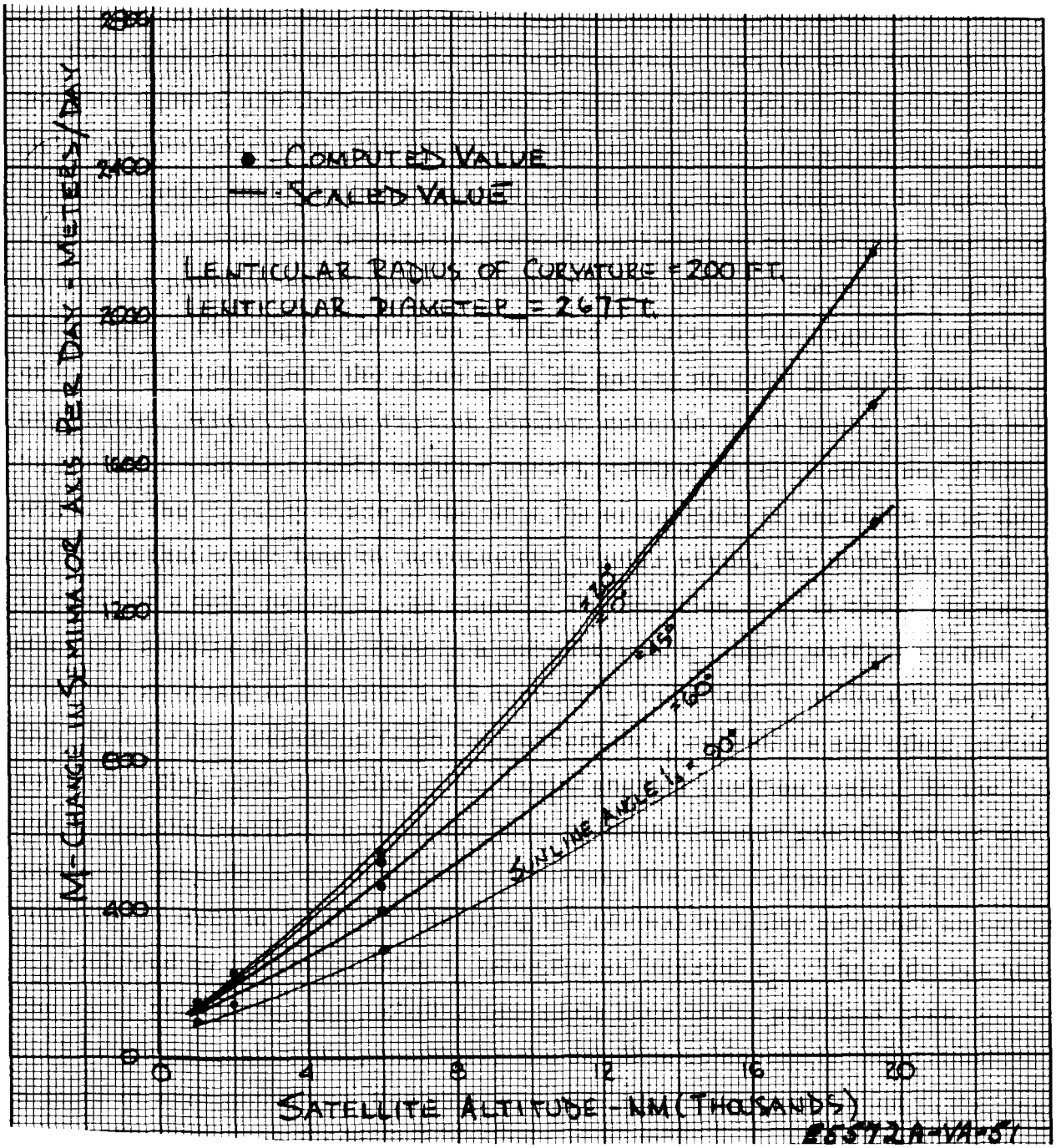

Figure 3-2. Comparison of Computed and Extrapolated Values of Lenticule Mobility

curves and the computer values is good at all altitudes, the difference not exceeding 10 percent in any case. All data points at altitudes of 1000 and 2000 nmi are not shown in the figure because of their close proximity. The slightly increased divergence between the computer points and the extrapolated curves at the lower altitudes is due to the effects of earth radiation, which was not considered in the derivation of the scaling equations.

3.1.1.2 Configuration B

An expression for the mobility of a planar sail satellite can be derived analytically from a consideration of the solar forces on the sail. Let a coordinate system be chosen, as shown in figure 3-3 such that the XY plane coincides with the plane of the orbit and the sun-line vector lies in the XZ plane. The angle γ_a, shown positive in figure 3-3, is the angle between the plane of the sail and the orbit plane. The angle ϕ_a is the angle between the normal to the plane of the sail, $\overline{N}_s$, and the sun-line vector $\overline{r}_s$, while the angle θ_a is the orbit angle measured from the X axis counterclockwise. The vector $\overline{N}_s$ can be written as:

$$\overline{N}_s = \bar{i} \sin\gamma_a \sin\theta_a - \bar{j} \sin\gamma_a \cos\theta_a + \bar{k} \cos\gamma_a \qquad (3\text{-}11)$$

and the vector $\overline{r}_s$ as:

$$\overline{r}_s = \bar{i} \cos i_s + \bar{k} \sin i_s \qquad (3\text{-}12)$$

The angle ϕ_a is thus given by the dot product as:

$$\cos\phi_a = \sin\gamma_a \sin\theta_a \cos i_s + \cos\gamma_a \sin i_s \qquad (3\text{-}13)$$

When the sun-line vector $\overline{r}_s$ is in the plane of the sail, the angle between it and the normal to the plane, ϕ_a, will be 90 degrees. On one side of this point ($0 < \phi_a < 90°$), one side of the sail will be exposed to the sun while the other surface of the sail will face the sun in the remaining quadrant of ϕ_a ($90° < \phi_a \leq 180°$). The angle, α_b, will be defined as the value of θ_a at which this transition takes place. From equation 3-13, α_b is defined as:

$$\sin\alpha_b = \frac{-\cos\gamma_a \sin i_s}{\sin\gamma_a \cos i_s} = -\cot\gamma_a \tan i_s \qquad (3\text{-}14)$$

If the inequality:

$$|\cot\gamma_a \tan\alpha_s| \geq 1 \qquad (3\text{-}15)$$

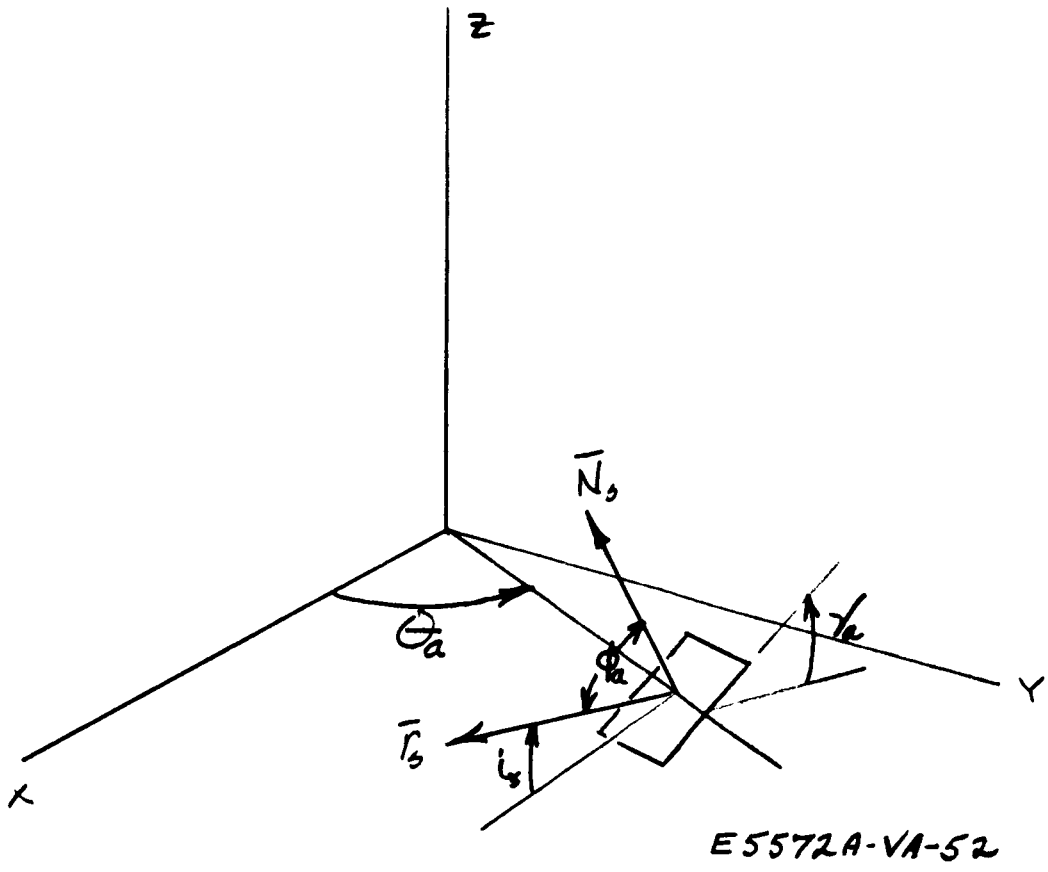

Figure 3-3. Coordinate System

holds, no solution exists for α_b, and the same side of the sail will face the sun for the complete orbit. The above inequality can be reduced to the following form:

$$\begin{aligned} &|\cos\gamma_a \sin i_s| \geq |\sin\gamma_a \cos i_s| \\ &\left|\frac{\sin i_s}{\cos i_s}\right| \geq \left|\frac{\sin\gamma_a}{\cos\gamma_a}\right| \\ &|i_s| \geq |\gamma_a| \end{aligned} \tag{3-16}$$

The inequality of equation 3-16 thus determines whether one or both sides of the sail are visible to the sun during the orbit.

Let the normal to the plane of the sail, $\bar{N}_s$, be defined positive outward from side 1 of the sail. Then, if the inequality of equation 3-16 holds and

the angle, ϕ_a, is less than 90 degrees, side 1 of the sail will face the sun throughout the orbit. For example, if the orbit angle, θ_a, is taken equal to 0, from equation 3-13, $\cos \phi_a = \gamma_a \sin i_s$

If:

$$\cos \gamma_a \sin i_s \geq 0 \tag{3-17}$$

and the inequality of equation 3-16 holds, then side 1 will be toward the sun for the entire orbit. If ϕ_a is greater than 90 degrees, side 2 will be toward the sun for the entire orbit. If the condition of equation 3-16 is not satisfied, both sides will face the sun at some point in the orbit, with the transition occurring at α_b and $\pi - \alpha_b$. To determine within which region of the orbit side 1 faces the sun, the value of the angle ϕ_a can be examined for $\theta_a = 90$ degrees. From equation 3-13 if:

$$\sin \gamma_a \cos i_s \cdot \cos \gamma_a \sin i_s \geq 0 \tag{3-18}$$

the angle ϕ_a will be less than 90 degrees and side 1 will face the sun through the angle:

$$\alpha_b \leq \theta_a \leq (\pi - \alpha_b)$$

and side 2 will face the sun through the remainder of the orbit. If ϕ_a is greater than 90 degrees, then side 2 will face the sun through the angle:

$$\alpha_b \leq \theta_a \leq (\pi - \alpha_b)$$

and side 1 will face the sun for the remainder of the orbit.

The occultation of the solar forces by the earth's shadow during a portion of the orbit introduces another discontinuity. The equation for the ellipse which defines the earth's shadow can be written as:

$$a^2 = \frac{R_e^2 \csc^2 i_s \, R_e^2}{R_e^2 \csc^2 i_s \sin^2 \psi_a + R_e^2 \cos^2 \psi_a}$$

where the various quantities are defined in figure 3-4. This expression can be reduced to:

$$\cos^2 \psi_a = \frac{R_e^2 \csc^2 i_s - a^2 \csc^2 i_s}{a^2 (1 - \csc^2 i_s)}$$

and finally:

$$\psi_a = \cos^{-1} \left[\frac{a^2 - R_e^2}{a^2 \cos^2 i_s} \right]^{1/2}$$

If the condition:

$$\cos \psi_a \geq 1 \qquad (3\text{-}19)$$

is met, the satellite is always in the sunlight and the only discontinuity is that introduced by the transition of the sunlight from one surface of the sail to the other. If condition of (3-19) is not satisfied, then a second discontinuity is introduced.

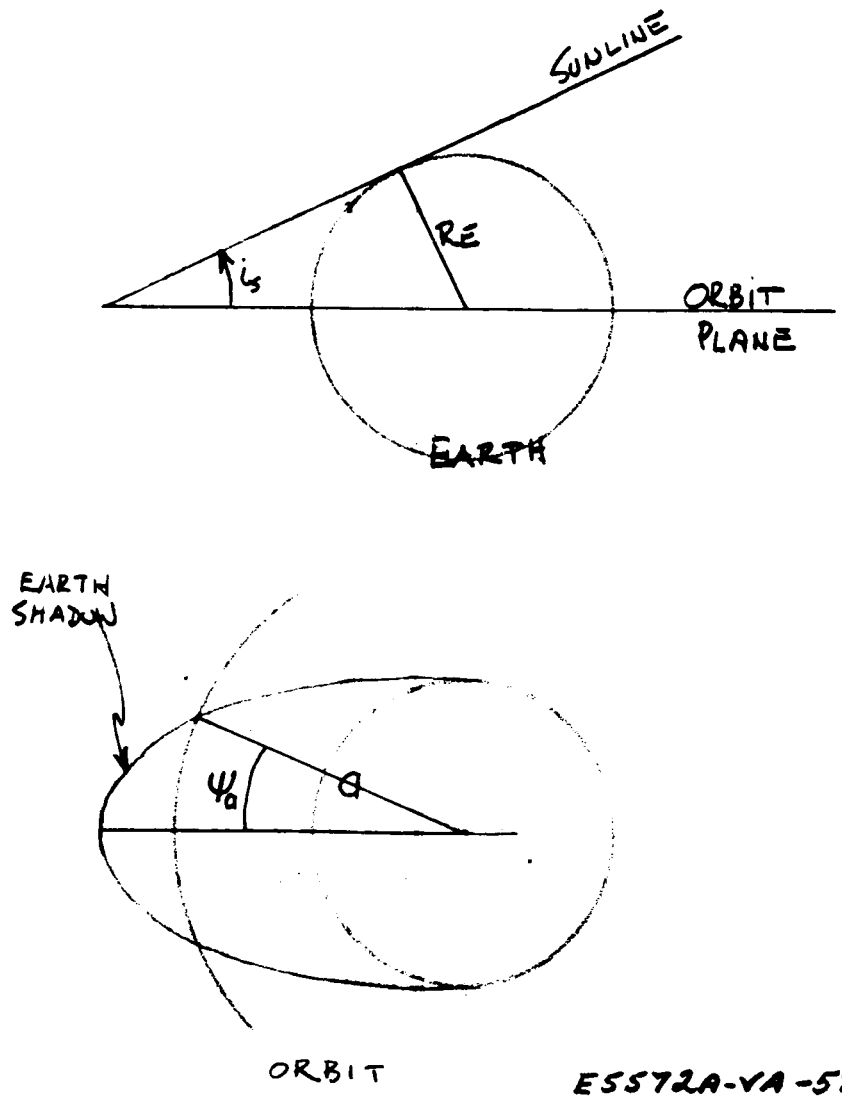

Figure 3-4. Occultation of Orbit by Earth's Shadow

These discontinuities must be compensated for by dividing the integral over the orbit into several subintegrals with limits determined by the points of discontinuity. The flow chart of figure 3-5 illustrates the different possible combinations and the conditions upon which they depend.

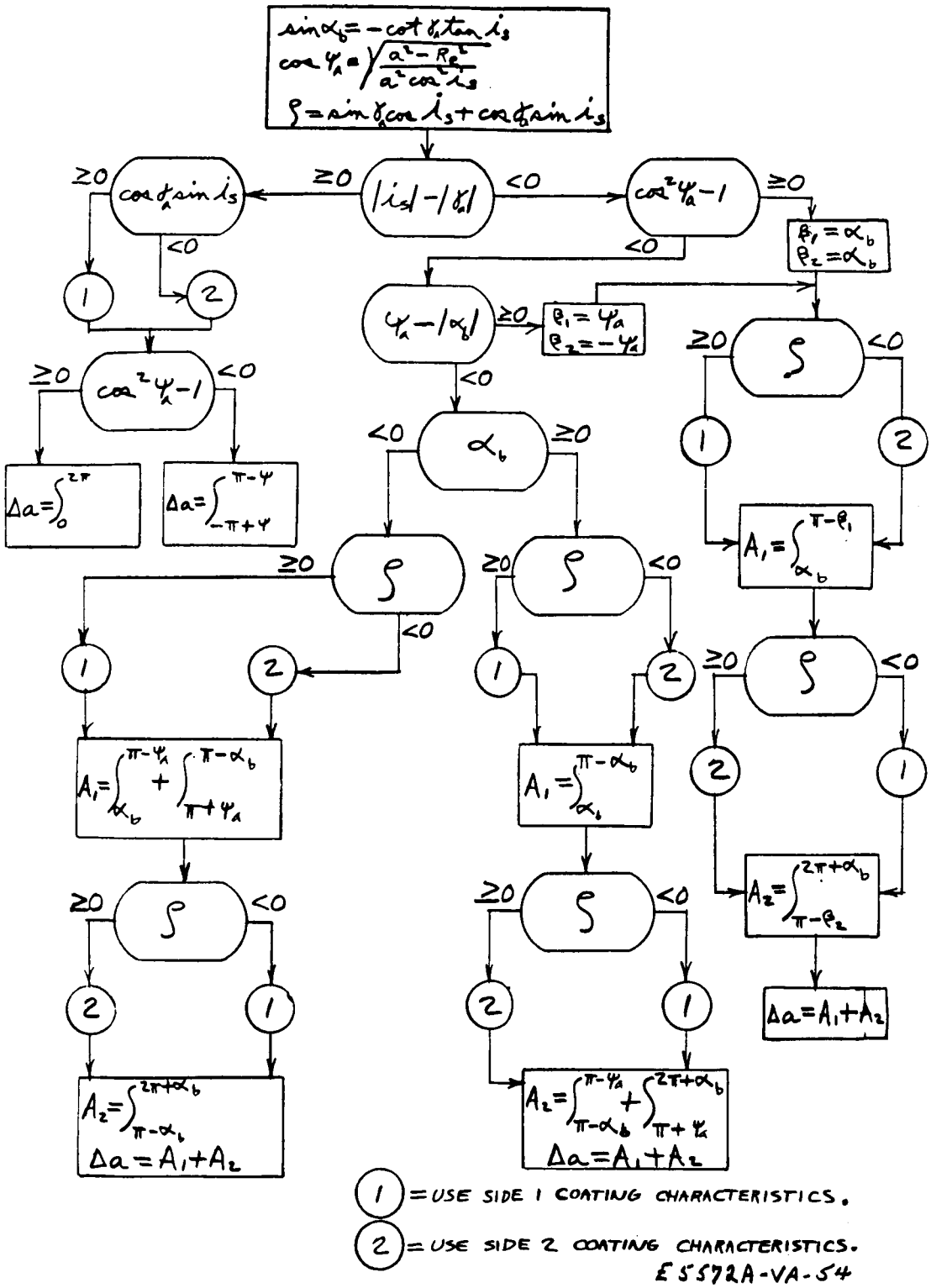

Figure 3-5. Flow Chart

The component of the perturbing solar forces that is of interest is that along the velocity vector of the satellite. The velocity vector can be written as:

$$\bar{V} = -\bar{i} \sin\theta_a + \bar{j} \cos\theta_a \tag{3-20}$$

Taking the dot product of $\bar{V}$ and $\bar{N}_s$, the normal to the plane of the sail, gives the angle β_a between the two vectors as:

$$\cos\beta_a = -\sin\gamma_a \sin^2\theta_a - \sin\gamma_a \cos^2\theta_a = -\sin\gamma_a \tag{3-21}$$

The angle η_a, between $\bar{V}$ and the sunline vector $\bar{r}_s$ can be obtained likewise as:

$$\cos\eta_a = -\cos i_s \sin\theta_a \tag{3-22}$$

Energy is transferred from the incident radiation to the satellite by the vector change in the momentum of the radiation. The components of the incident and reflected direct solar energy along the velocity vector are given by:

$$F_s = -\frac{S_K}{C}\left[\cos\eta_a \pm \frac{2}{3} r_s \cos\beta_a\right] A_s \cos\phi_a \tag{3-23}$$

where S_K is the solar constant, C the speed of light, r_s the reflectivity of the sail surface facing the sun, and A_s is the area of the sail surface. The sail surface is assumed to be a diffuse reflector rather than a specular reflector so that the resultant force of the reflected energy is normal to the sail surface and the component in the direction of the velocity vector is given by the multiplying factor $\cos\beta_a$. Since the angle, β_a, is measured with reference to the vector, $\bar{N}_s$, defined positive outward from side 1 of the sail, the sign of the reflected component must be changed when side 2 is facing the sun; thus the plus or minus sign in equation 3-23.

Another force on the sail to be considered is the force due to the radiation of IR energy from the sail. The reaction force derived from energy radiated out from the surface can be shown by the consideration of energy flow through an element of solid angle to be:

$$F_R = -\frac{2}{3} c E \tag{3-24}$$

where E is the total energy flux emitted, and the force is directed normal to the surface. The total energy flux emitted outward from side 1 of the surface is:

$$E = \frac{e_{IR_1}}{e_{IR_1} + e_{IR_2}} \alpha_s S_k A_s \cos\beta_a \qquad (3\text{-}25)$$

where total reemittance of all energy absorbed is assumed, α_s is the solar absorptivity of the sail surface facing the sun, and e_{IR_1} and e_{IR_2} are the emissivities of sides 1 and 2, respectively, of the sail. Combining equation 3-25 in 3-24, considering forces on both sides of the sail, and taking the tangential component yields for the reradiation force:

$$F_{IR} = -\frac{2}{3} \frac{e_{IR_1} - e_{IR_2}}{e_{IR_1} + e_{IR_2}} \alpha_s S_k A_s \cos\phi_a \cos\beta_a \qquad (3\text{-}26)$$

The effect of the above forces on the satellite can be considered in terms of the perturbation of the semimajor axis of the orbit which occurs; this effect can be derived from orbital energy considerations. The kinetic energy, E_K, of the satellite can be written:

$$\bar{E}_k = \frac{1}{2} m v^2 \qquad (3\text{-}27)$$

where m is the mass of the satellite and v its orbital velocity. The potential energy, E_P, for a central force field at a distance, a, is given by

$$\bar{E}_P = -k \frac{m}{a}$$

where the negative sign indicates the force is inward toward the center of force and k is the gravity constant. Therefore, the total energy per unit mass is given by:

$$\bar{E}_T = \frac{V^2}{2} - \frac{K}{a} \qquad (3\text{-}29)$$

For a circular orbit, the energy change per unit mass for each revolution is given by:

$$\Delta E = E_{T_1} - E_{T_2} = \left(\frac{V_1^2}{2} - \frac{k}{a_1}\right) - \left(\frac{V_2^2}{2} - \frac{k}{a_2}\right) \tag{3-30}$$

Using the equation for circular velocity:

$$V_c = \sqrt{\frac{k}{a}} \tag{3-31}$$

and letting $\Delta a = a_1 - a_2$:

$$\Delta E = \frac{k \Delta a}{2 a_1 a_2} \tag{3-32}$$

The energy change per unit mass due to solar forces is equal to the force per unit mass integrated over a full orbit:

$$\Delta E = \oint \frac{F}{m} ds \tag{3-33}$$

Assuming small altitude changes during each revolution such that the forces acting on the satellite do not change appreciably:

$$\Delta E = \frac{F}{m} \oint ds = \frac{F}{m} 2\pi \left(\frac{a_1 + a_2}{2}\right) \tag{3-34}$$

where $(a_1 + a_2)/2$ is an average radius for the revolution. Using the approximation for the orbital radius, the circular velocity is written as:

$$V_c^2 = \frac{k}{a} = \frac{2k}{a_1 + a_2} \tag{3-35}$$

and

$$\Delta E = 2\pi \frac{k}{m} \frac{F}{V_c^2} \tag{3-36}$$

Now if: $\Delta a / a_1 << 1$ then $a_1 a_2 \approx a_{avg}^2$

and

$$\frac{\Delta a}{rev} = 4\pi \frac{F}{km} a_{avg}^3 \tag{3-37}$$

Written in terms of the mean angular motion, n, which is given by:

$$n = \sqrt{\frac{k}{a^3}} \tag{3-38}$$

equation 3-37 can be written as:

$$\frac{\Delta a}{rev} = 4\pi \frac{S}{n^2} \tag{3-39}$$

where S is the perturbing acceleration in the tangential direction. Equation 3-39 can be written in terms of the change in a per unit time as:

$$\frac{\Delta a}{\Delta t} = \frac{2}{n} S \tag{3-40}$$

and in terms of orbit angle as:

$$\frac{da}{d\theta_a} \frac{d\theta_a}{dt} = \frac{2}{n} S, \tag{3-41}$$

Substituting the expressions for the forces given by equations 3-23 and 3-26 into equation 3-41 yields:

$$\frac{da}{d\theta_a} \frac{d\theta_a}{dt} = -\frac{2}{n} \frac{S_k A_s}{mc} \left[\cos\eta_a \pm \frac{2}{3} r_s \cos\beta_a + \frac{2}{3} \frac{e_{IR_1} - e_{IR_2}}{e_{IR_1} + e_{IR_2}} \alpha_s \cos\beta_a \right] \cos\phi_a \tag{3-42}$$

Expressing this equation as an integral over the orbit to eliminate the secular perturbations gives:

$$\Delta \bar{a} = \frac{2}{n^2} \frac{S_k A_s}{mc} \int_{ORBIT} \left[\cos i_s \sin\theta_a + \frac{2}{3} \left(\pm r_s + \frac{e_{IR_1} - e_{IR_2}}{e_{IR_1} + e_{IR_2}} \alpha_s \right) \sin\gamma_a \right]$$
$$\left[\sin\gamma_a \sin\theta_a \cos i_s + \cos\gamma_a \sin i_s \right] d\theta_a \tag{3-43}$$

Grouping similar terms:

$$\Delta \bar{a} = \frac{2}{n^2} \frac{S_k A_s}{mc} \int_{ORBIT} \left(B \sin^2\theta_a + C \sin\theta_a + D \right) d\theta_a \tag{3-44}$$

where:

$$B = \pm \sin\gamma_a \cos^2 i_s$$

$$C = \left[\frac{2}{3} \left(1 - \frac{2 e_{IR_2} \alpha_s}{e_{IR_1} + e_{IR_2}} \right) \sin^2\gamma_a \pm \cos\gamma_a \sin i_s \right] \cos i_s$$

$$D = \frac{2}{3} \left(1 - \frac{2 e_{IR_2} \alpha_s}{e_{IR_1} + e_{IR_2}} \right) \sin\gamma_a \cos\gamma_a \sin i_s$$

and α_s is the solar absorptivity of the sail surface facing the sun. The term, e_{IR_0}, is the emissivity of the surface facing away from the sun. The plus sign should be used if side 1 of the sail is facing the sun, and the negative sign if side 2 is facing the sun. If the integral of equation 3-43 is evaluated using the limits indicated in the flow diagram of figure 3-5 where a quantity H is defined by:

$$H = \frac{2}{n^2} \frac{S_R A_s}{mc}$$

then

$$H \int_{c}^{2\pi} (\cdots) = 2\pi H (B/2 + D)$$

$$H \int_{\pi+\psi_a}^{2\pi+\alpha_b} (\cdots) = H\left[\left(\frac{B}{2}+D\right)(\pi+\alpha_b-\psi_a) + \frac{B}{2}(\sin\psi_a\cos\psi_a - \sin\alpha_b\cos\alpha_b) - C(\cos\psi_a + \cos\alpha_b)\right]$$

$$H \int_{-\pi+\psi_a}^{\pi-\psi_a} (\cdots) = H\left[2\left(\frac{B}{2}+D\right)(\pi-\psi_a) + B\sin\psi_a\cos\psi_a\right]$$

$$H \int_{\alpha_b}^{\pi-\psi_a} (\cdots) = H\left[\left(\frac{B}{2}+D\right)(\pi-\psi_a-\alpha_b) + \frac{B}{2}(\sin\alpha_b\cos\alpha_b + \sin\psi_a\cos\psi_a) + C(\cos\alpha_b + \cos\psi_a)\right]$$

$$H \int_{\pi+\psi_a}^{\pi-\alpha_b} (\cdots) = H\left[\left(\frac{B}{2}+D\right)(-\alpha_b-\psi_a) + \frac{B}{2}(\sin\alpha_b\cos\alpha_b + \sin\psi_a\cos\psi_a) + C(\cos\alpha_b - \cos\psi_a)\right]$$

$$H \int_{\pi-\alpha_b}^{2\pi+\alpha_b} (\cdots) = H\left[\left(\frac{B}{2}+D\right)(\pi+2\alpha_b) - (B\sin\alpha_b + 2C)\cos\alpha_b\right]$$

$$H \int_{\alpha_b}^{\pi-\alpha_b} (\cdots) = H\left[\left(\frac{B}{2}+D\right)(\pi-2\alpha_b) + (B\sin\alpha_b + 2C)\cos\alpha_b\right]$$

$$H \int_{\pi-\alpha_b}^{\pi-\psi_a} (\cdots) = H\left[\left(\frac{B}{2}+D\right)(\alpha_b-\psi_a) + \frac{B}{2}(\sin\psi_a\cos\psi_a - \sin\alpha_b\cos\alpha_b) + C(\cos\psi_a - \cos\alpha_b)\right]$$

The above expressions are in terms of Δa, the change in the semimajor axis per orbit. They can be given also in terms of M, the average change in the semimajor axis per unit time, which will be defined as the mobility. The mobility is obtained simply by dividing Δa by the period $P = \cdot \frac{2\pi}{n}$. Thus, substitution of the term:

$$H' = \frac{S_k A_s}{\pi n m c}$$

for H in the above expression gives the mobility, M.

Scaling factors for the extrapolation of mobility with respect to altitude and solar inclination can be derived from the set of expressions which were obtained by the evaluation of equation 3-44 for different limits; the limits were determined from the various considerations outlined in figure 3-5. Table 3-1 gives the scaling factors to be used for given conditions and summarizes the equations necessary for their application. Figures 3-6 and 3-7 compare the results obtained by extrapolation, using the factors of table 3-1, with the mobility obtained from the computer program. Figure 3-6 gives mobility, M, as a function of sun-line inclination, i_s, for several satellite altitudes. Figure 3-7 gives the mobility as a function of satellite altitude for several values of sun-line inclination. In each figure, the mobilities derived by extrapolation are represented by the solid curves, and selected values from the computer program are represented by the data points. The agreement in all cases is excellent.

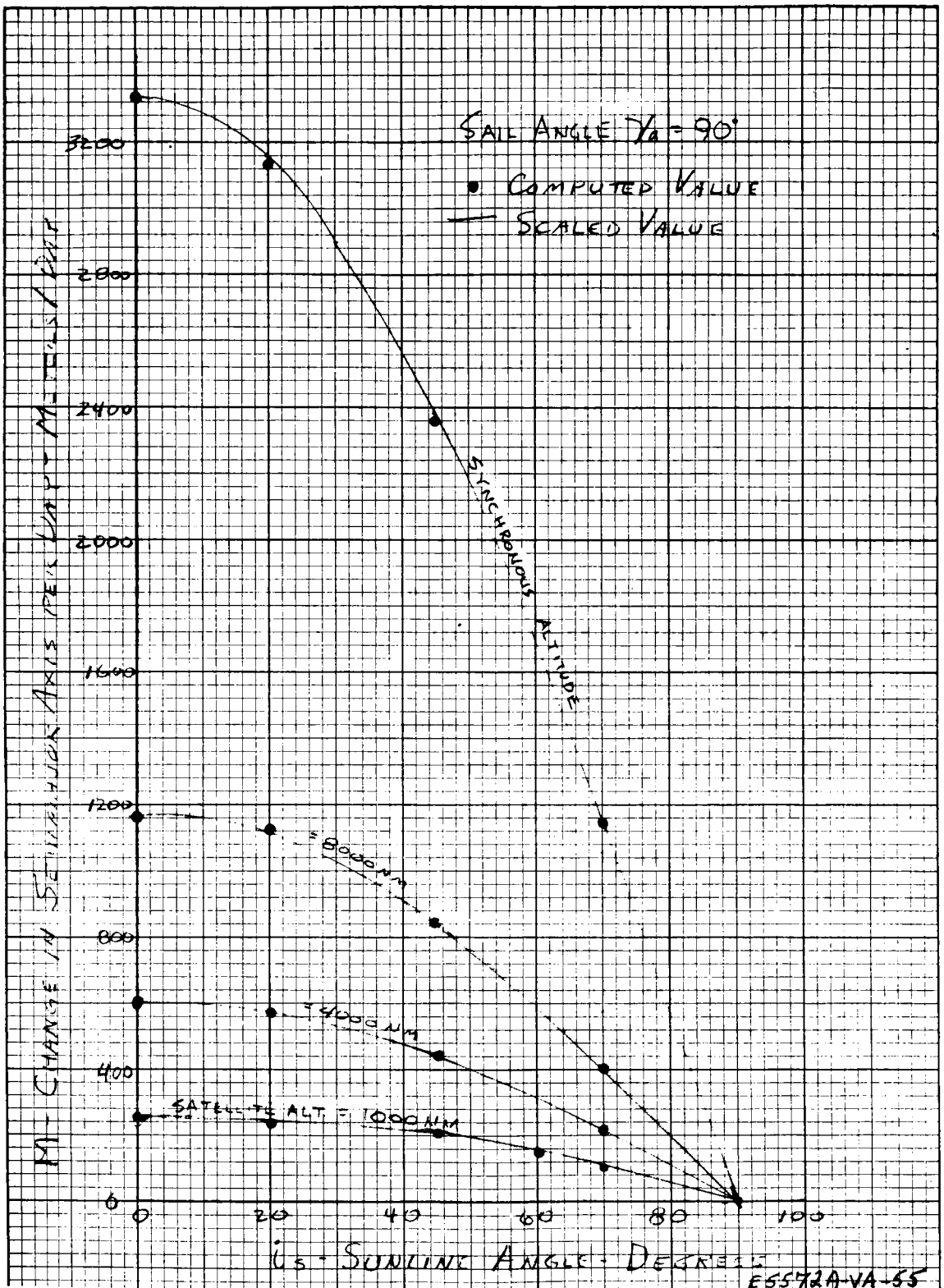

Figure 3-6. Extrapolated Mobility for Planar Sail Satellite

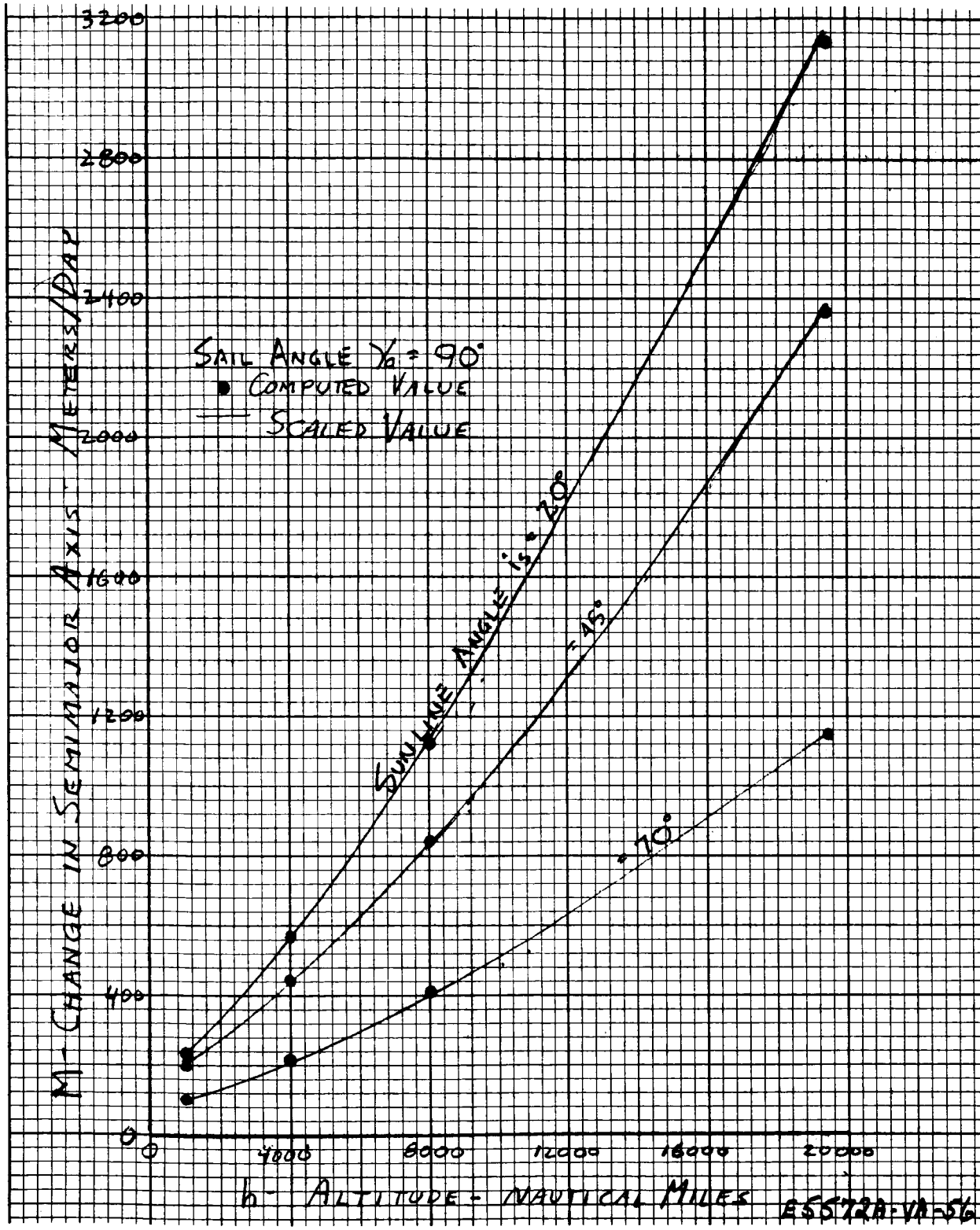

Figure 3-7. Extrapolated Mobility for Planar Sail Satellite

TABLE 3-1

SUMMARY OF SCALING EQUATIONS AND APPLICABLE EQUATIONS FOR PLANAR SAIL SATELLITE

Condition 1	Condition 2	Condition 3	Scaling Equation	Remarks
$\lvert i_s\rvert \geq \lvert \gamma_a\rvert$ (One side of sail always facing sun)	$\cos^2\psi_a - 1 \geq 0$ (Satellite orbit not occulted)		$M(a, i_s) \propto a^{3/2}(B + 2D)$	If $\cos\gamma_a \sin i_s \geq 0$: Use side 1 characteristics If $\cos\gamma_a \sin i_s < 0$: Use side 2 characteristics
	$\cos^2\psi_a - 1 < 0$ (Satellite orbit occulted)		$M(a, i_s) \propto a^{3/2}\left[(B+2D)(\pi - \psi_a) + B\sin\psi_a\cos\psi_a\right]$	
$\lvert i_s\rvert < \lvert \gamma_a\rvert$ (Both sides of sail face sun during orbit.)	$\cos^2\psi_a - 1 \geq 0$ (Satellite orbit not occulted)		$M(a, i_s) \propto a^{3/2}\left[\frac{\pi}{2}(B_1+B_2) + (\sin\alpha_b\cos\alpha_b - \alpha_b)(B_1 - B_2) + 2\cos\alpha_b(C_1 - C_2) + \pi(D_1+D_2) - 2\alpha_b(D_1 - D_2)\right]$	If $\sin\gamma_a\cos i_s + \cos\gamma_a \sin i_s \geq 0$: Use side 1 characteristics for C_1 and D_1 and side 2 characteristics for C_2 and D_2. < 0: Use side 2 characteristics for C_1 and D_1 and side 1 characteristics for C_2 and D_2.
	$\cos^2\psi_s - 1 < 0$ (Satellite orbit occulted)	$\psi_a - \lvert\alpha_b\rvert \geq 0$	$M(a, i_s) \propto a^{3/2}\left[\frac{\pi}{2}(B_1+B_2) + \frac{B_1}{2}(\sin\alpha_b\cos\alpha_b + \sin\psi_a\cos\psi_a - \psi_a - \alpha_b) + B_2(\alpha_b - \sin\alpha_b\cos\alpha_b) + C_1(\cos\alpha_b + \cos\psi_a) - 2C_2\cos\alpha_b + \pi(D_1+D_2) - D_1(\alpha_b + \psi_a) + 2\alpha_b D_2\right]$	
		$\psi_a - \lvert\alpha_b\rvert < 0$, $\alpha_b \geq 0$	$M(a, i_s) \propto a^{3/2}\left[\frac{\pi}{2}(B_1+B_2) + B_1(\sin\alpha_b\cos\alpha_b - \alpha_b) + B_2(\alpha_b - \psi_a + \sin\psi_a\cos\psi_a - \sin\alpha_b\cos\alpha_b) + 2\alpha_b(C_1 - C_2) + D_1(\pi - 2\alpha_b) + 2D_2(\alpha_b - \psi_a) + \pi D_2\right]$	
		$\psi_a - \lvert\alpha_b\rvert < 0$, $\alpha_b < 0$	$M(a, i_s) \propto a^{3/2}\left[\frac{\pi}{2}(B_1+B_2) + \sin\alpha_b\cos\alpha_b(B_1 - B_2) + B_1(\sin\psi_a\cos\psi_a - \alpha_b - \psi_a) + B_2\alpha_b + 2\cos\alpha_b(C_1 - C_2) + \pi(D_1+D_2) - 2D_1(\alpha_b + \psi_a) + 2D_2\alpha_b\right]$	

$B = \pm \sin\gamma_a \cos^2 i_s$

$C = \left[\frac{2}{3}\left(1 - \frac{2\varepsilon_{IR_c}\alpha_s}{\varepsilon_{IR_1} + \varepsilon_{IR_2}}\right)\sin^2\gamma_a \pm \cos\gamma_a \sin i_s\right]\cos i_s$

$D = \frac{2}{3}\left(1 - \frac{2\varepsilon_{IR_c}}{\varepsilon_{IR_1} + \varepsilon_{IR_2}}\right)\sin\gamma_a\cos\gamma_a\sin i_s$

$\sin\alpha_b = -\cot\theta_a \tan i_s$ $\qquad \cos\psi_a = \left[\frac{a^2 - R_e^2}{a^2\cos^2 i_s}\right]^{1/2}$

α_s - solar absorptivity of sail surface facing sun

ε_{IR_c} - emissivity of surface facing away from sun

(+) sign used if side one of sail faces sun, (-) sign if side 2 faces sun

3.1.2 Variation of Lenticular Mobility as a Function of Shape Factors

An approximate expression for the extrapolation of lenticular mobility with respect to shape factors, i.e., lenticule diameter and radius of curvature, can be derived from a consideration of the forces on the satellite. If it is assumed that the force that determines mobility is that component of the reradiation force along the velocity vector, figure 3-8 illustrates that mobility can be expressed as:

$$M \propto F \sin\theta \tag{3-45}$$

Integrating this expression over the surface of the lenticule gives:

$$M \propto 1 - \cos\theta$$

Assuming that θ can be approximated by:

$$\theta \approx \frac{D}{2R}$$

The above expression becomes:

$$M \propto \left(1 - \cos\frac{D}{2R}\right)$$

The addition of an empirical term to account for the effect of sun-line angle gives:

$$M \propto 1 - \left(\cos\frac{D\pi}{4R}\left[1 + \frac{1}{2}\sin^2\frac{\iota_s}{2}\right]\right) \tag{3-46}$$

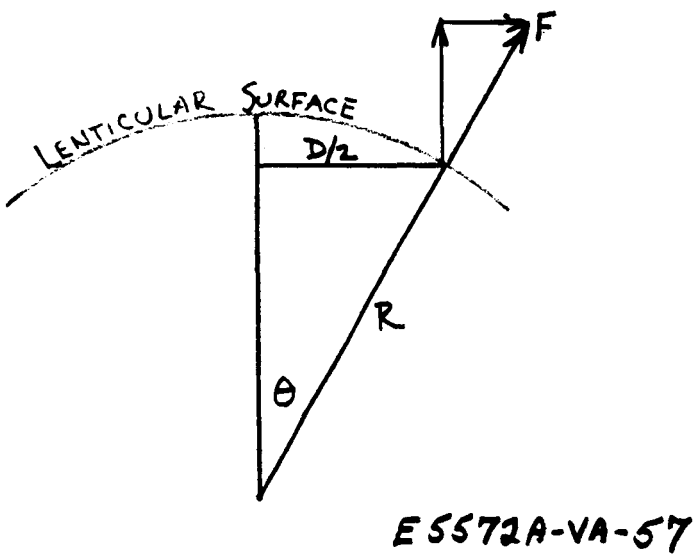

Figure 3-8. Lenticule Geometry

Figure 3-9 illustrates the degree of agreement obtained between computer derived values of mobility and scaled values, using equation 3-46. The agreement between the extrapolated values and the computer derived mobilities is quite good over the range of available data.

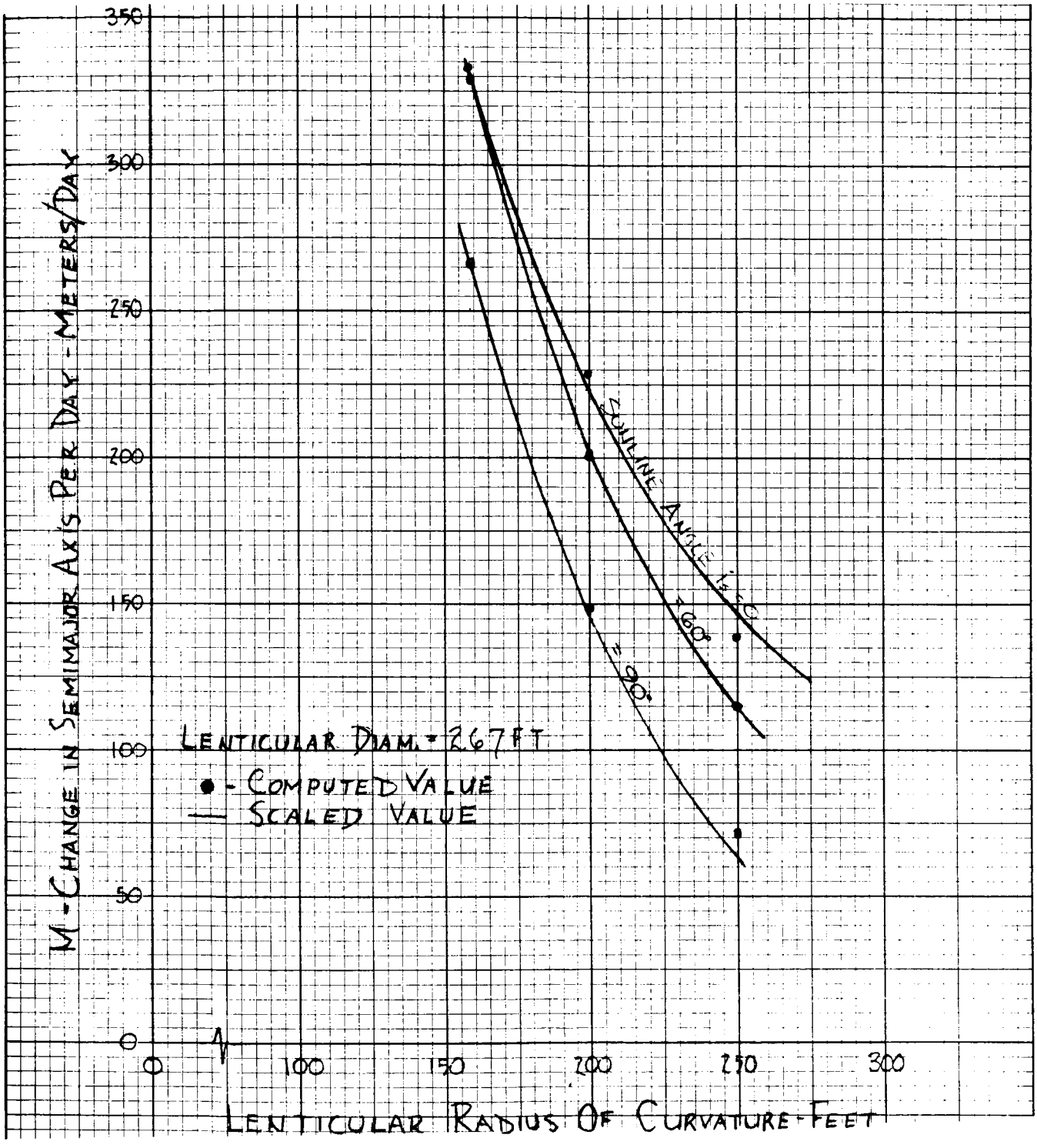

Figure 3-9. Comparison of Computed and Extrapolated Values of Lenticular Mobility as a Function of Radius of Curvature

3. 1. 3 R/D Versus Altitude

The required ratio of lenticule radius of curvature R to diameter D may be derived, provided satellite coverage requirements are defined. In this paragraph, complete earth coverage will be required; that is, the solid angle subtended by the earth at the center of curvature of the lenticule surface must lie completely within the solid angle subtended by the lenticule. This situation is illustrated in figure 3-10. For the angles as defined by this figure:

$$\sin\frac{\alpha}{2} = \frac{R_e}{h + R_e}$$

$$\frac{\phi}{2} = \frac{\alpha}{2} + \epsilon$$

$$\sin\frac{\phi}{2} = \frac{D/2}{R} \quad ; \quad \frac{R}{D} = \frac{1}{2\sin\phi/2}$$

Thus, the R/D ratio required is given finally by:

$$\frac{R}{D} = \frac{1}{2\sin\left[\sin^{-1}\left(\frac{R_e}{R_e + h}\right) + \epsilon\right]}$$

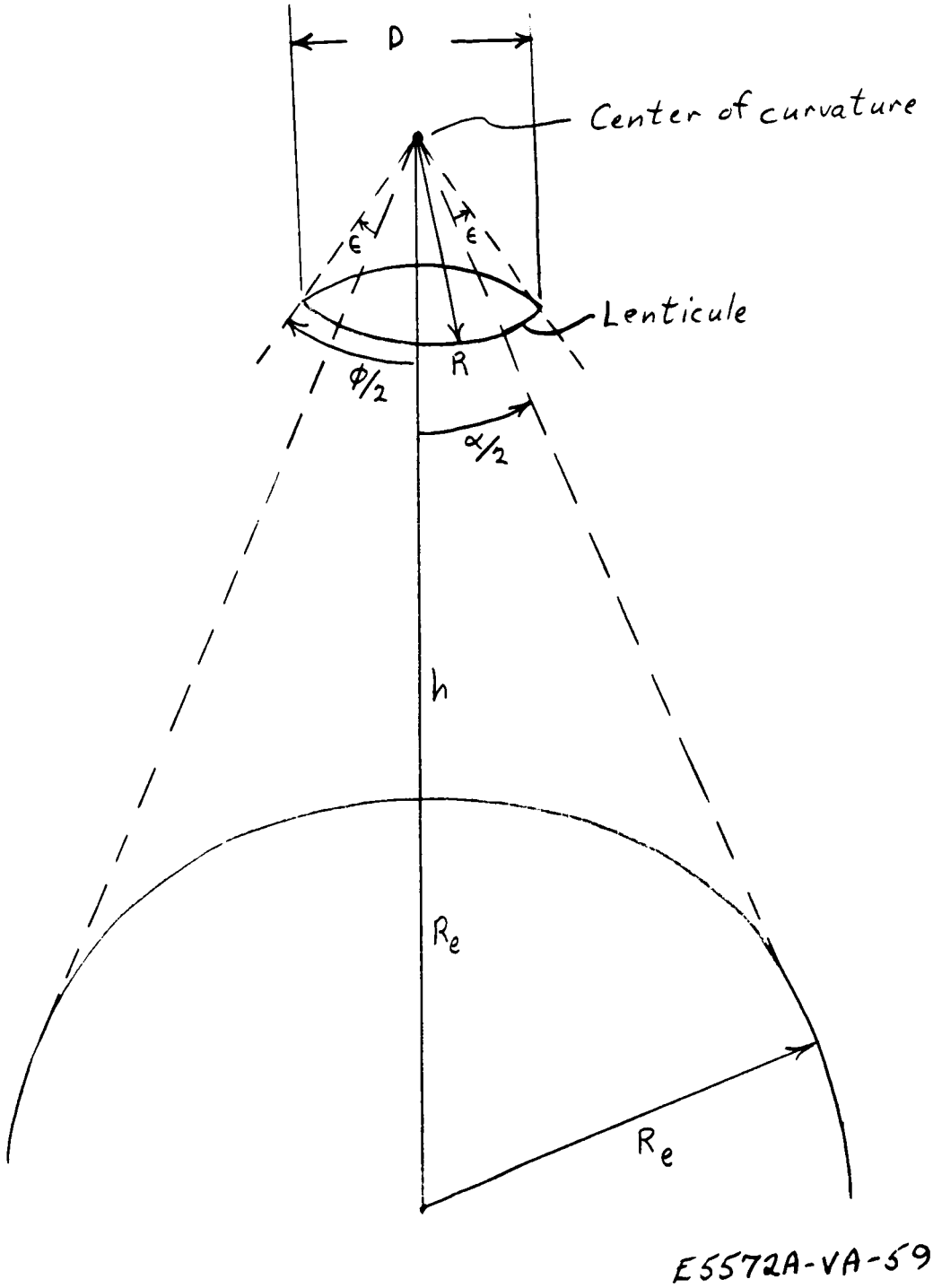

Figure 3-10. Required Satellite Coverage Angle

3.2 DETERMINATION OF MANEUVER TIMES

Both altitude and relative angular position errors of the orbit controlled satellites can be corrected by a basic maneuver which consists of placing the satellite in opposite modes of operation (decreasing and increasing orbital energy) for specified amounts of time. Assuming that the satellite always has a constant amount of mobility available to it (equal to the average mobility for the given altitude and orbital inclination), a closed form solution has been obtained yielding the required amounts of time in each mode for arbitrary altitude and angular position errors.

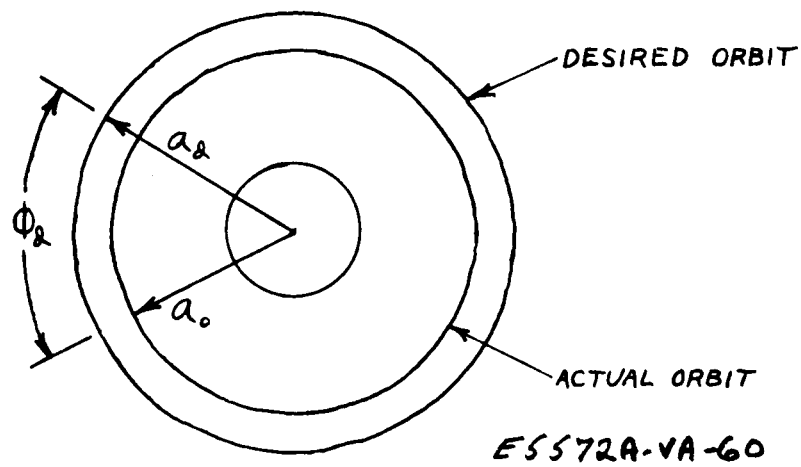

In order to determine a correction procedure for a single satellite, the geometry shown above is defined in the following manner. Assume that the orbit of the satellite has a semimajor axis of a_o and that it is desired to correct the orbit to a semimajor axis of a_d. Furthermore, assume that the angular deviation between the desired position in the desired orbit and the actual position in the actual orbit is φ_d. Thus, φ_d can be thought of as the angular error referenced to the desired position. If it is also assumed that the semimajor axis can be changed at a constant rate, $\overline{\Delta a}$, then (assuming small altitude errors) the orbital period can also be changed at a constant rate equal to:

$$\Delta P_{po} = K_1 \left[a_d^{1/2} - (a_d - \overline{\Delta a})^{3/2} \right] \quad ; \quad K_1 = \frac{2\pi}{k\sqrt{M}}$$

ΔP_{po} is defined on a per orbit basis. K is the Newton's gravitational constant, and M is the mass of the earth. The initial period difference between the actual and desired orbits is:

$$\Delta P_c = P_o - P_d$$
$$= K_1 \left[a_o^{3/2} - a_d^{3/2} \right]$$

Then, the rate of change of both the error angle, ϕ_e, and the period P with respect to the number of orbits N from the start of the maneuver can be expressed by:

$$\frac{d\phi_e}{dN} = -(n - n_d) P = -\frac{2\pi}{P_d}(P_d - P) = -\frac{2\pi}{P_d}(\Delta P_o \mp N \Delta P_{po})$$

$$\frac{dP}{dN} = \pm \Delta P_{po}$$

where n and n_d are the mean angular motions of the actual orbit and the desired orbit, respectively; and the plus or minus sign is chosen depending on whether the satellite is placed in an increasing or decreasing energy mode. Assume now that the correction maneuver will be made as a two-stage process. That is, the satellite will initially be placed in one mode of operation and will be changed to the opposite mode at some precomputed time such that by remaining in the second mode of operation, the correction on both angular position and altitude can be completed. Thus, by integrating the two differential equations over the range of orbits in each mode of operation, N_1 and $N_2 - N_1$, and placing the constraints of $-\phi_d$ and P_d on the integrals of angular deviation and period, respectively, the following relationships are obtained:

$$-\phi_d = -\frac{2\pi}{P_d}\left[\int_o^{N_1} (\Delta P_o \pm N \Delta P_{po}) dN + \int_{N_1}^{N_2} (\Delta P_{N_1} \mp N \Delta P_{po}) dN \right]$$

$$P_d = P_o + \int_o^{N_1} \pm \Delta P_{PO}\, dN + \int_{N_1}^{N_2} \mp \Delta P_{PO}\, dN$$

and where the quantity, ΔP_{N1}, represents the period difference between the actual orbit at time, N_1, and the reference orbit adjusted to account for the use of the total N orbits in the integrand rather than the number of orbits in the second mode and is:

$$\Delta P_{N1} = \Delta P_o \pm 2 N_1 \Delta P_{PO}$$

When integrated, these expressions yield:

$$\phi_d = \frac{2\pi}{P_d}\left[N_2 \Delta P_c \pm 2 N_1 N_2 \Delta P_{PO} \mp N_1^2 \Delta P_{PO} \mp \frac{1}{2} N_2^2 \Delta P_{PO}\right]$$

$$P_d = P_c \pm (2N_1 - N_2)\Delta P_{PO}$$

and a solution of these equations for N_1 and N_2 yields:

$$N_2 = \frac{+\Delta P_c \pm \sqrt{2\Delta P_o^2 \pm \frac{2\Delta P_{PO} P_d \phi_d}{\pi}}}{\Delta P_{PO}}$$

$$N_1 = \frac{N_2 \Delta P_{PO} \pm \Delta P_c}{2\Delta P_{PO}}$$

In the expression for N_2, the plus or minus sign choice results from the solution of a quadratic equation for N_2. This sign can be determined from the following analysis. If the restriction that $N_1 \leqq N_2$ is imposed on the equation for N_1, the following inequality results:

$$N_2 \geq \mp \frac{\Delta P_o}{\Delta P_{PO}}$$

Comparing this restriction with the equation for N_2, it can be seen that the plus sign must always precede the radical since the first term is exactly

equal to the inequality and ΔP_{po} is always positive by definition. Thus, the expressions for N_1 and N_2 become:

$$N_2 = \frac{\mp \Delta P_o + \sqrt{2\Delta P_o^2 \pm \frac{2\Delta P_{pc} P_d \phi_d}{\pi}}}{\Delta P_{po}}$$

$$N_1 = \frac{N_2 \Delta P_{pc} \pm \Delta P_o}{2\Delta P_{pc}}$$

The remaining choices of plus and minus signs are indicative of the sequence of modes used in performing the mancuver. The upper sign represents the case where the satellite is placed in an increasing energy mode during the initial N_1 orbits and in a decreasing energy mode during the remainder of the total N_2 orbits. The opposite case is, of course, represented by the lower sign.

For any arbitrary correction, the choice of signs should be made to give a solution which is the minimum of all possible solutions. In addition, it can be seen that incrementing or decrementing the desired angular correction by multiples of 2π does not change the end conditions in that the same effective correction is made. Thus, a search for an absolute minimum time must include an examination of the above equations not only for the original ϕ_d specified, but for ϕ_d plus or minus all multiples of 2π until a minimum time is found.

It is desired that the time, t_m, required to maneuver a satellite to a new relative angular position and/or period be related to ϕ_d (the change in angular position), ΔP_o (the change in period), a (the semimajor axis), and M (the time rate of change for the semimajor axis), where an average M is assumed.

From the equation for N_2 above, t_m can be expressed in terms of ϕ_d, ΔP_o, a, and M. First:

$$P = K_1 a^{3/2}$$

where $K_1 = 3.147 \times 10^{-7}$ sec/met $^{3/2}$.

$$\frac{dP}{da} = \frac{3K_1\sqrt{a}}{2}$$

$$\Delta P_{PO} = \frac{3K_1\sqrt{a}\,\Delta a}{2}$$

$$\Delta a = K_1 a^{3/2} M$$

$$\Delta P_{PO} = \frac{3K_1^2 a^2 M}{2}$$

Also:

$$t_M = N/2\, K_1\, a^{3/2}$$

Then:

$$t_M = \frac{\mp \Delta P_c + \sqrt{2\Delta P_c^2 t \frac{3}{\pi} K_1^3 a^{7/2} M \phi_d}}{\frac{3}{2} K_1 M \sqrt{a}}$$

3.3 DETERMINATION OF STATION KEEPING PRECISION

3.3.1 Introduction and Requirements

This paragraph deals with the definition of maximum relative angular position-in-orbit error (called "maximum angular error" below) as a function of the mobility, the minimum detectable error, and other effects which will be listed later. Two control procedures are considered:

- Increasing and decreasing energy modes only
- Increasing, decreasing, and neutral modes.

In addition to the tracking or minimum detectable angular position error, θ_E, and minimum detectable period error, P_e, a number of other effects help govern the maximum angular error. In table 3-2 below, all of the error effects are listed for each of the two control approaches:

TABLE 3-2

ERROR EFFECTS

	No Neutral Mode	Neutral Mode
θ_E	X	X
P_e	Negligible	Negligible
ΔP_o	X	X
Neutral Mode Sail Angle	Not Applicable	X
Maneuver Mode Sail Angle	Negligible	Negligible
Nonnominal Mobility	Negligible	Negligible
Computation Errors	Negligible	Negligible
Finite Time for Sail Angle Change	X	X
Command Delay Due to In-sight Requirement	X	X
Quantized Sail Angle Commands	Negligible	Negligible
Unequal Mobilities in Increasing and Decreasing Modes	X	None
Orbit Eccentricity	X	X

The X's in the table indicate items which help govern the maximum angular error in a position sustaining phase. The table is not applicable to an initial placement phase.

The magnitude of P_e would affect the maximum angular error in general, but is negligible here because of the specific mechanizations and logic used.

ΔP_o is the period error when the angular error first exceeds θ_E in magnitude; i. e., ΔP_o = (true period - nominal period).

Before defining the error effects further, the two control methods will be derived.

3. 3. 2 Control Methods

Whether a neutral mode is used or not, there are several possible mechanizations for the control process. The two which are described below were chosen: (1) because they are straightforward and (2) to minimize the maximum angular position error. In both cases, it is assumed as a simplifying step that the mobility is constant over the period of one maneuver. This assumption will cause errors in command which will affect the duty cycle to a certain extent, but has a negligible effect on maximum angular position error.

3. 3. 2. 1 No Neutral Mode Case

For this case, the sail angles or orientations of all satellites in one orbit plane are alternated together between two conditions - one which increases the period and one which decreases the period. When one or more satellites require a relative spacing or period correction, the timing of orientation changes for that satellite(s) must be changed in some appropriate manner.

It is assumed in order to simplify the system that initiation of the routine control procedure (after initial spacing) is based only on the detection of an out-of-limit relative angular position and not on the monitoring of period. The procedure is shown in figure 3-11. When the angular position relative to an orbiting body with low area-to-mass ratio reaches θ_E, a mode reversal of a fixed duration is applied. Exactly one-half cycle later in the decreasing-increasing mode regime, an opposite mode reversal of the same duration is

applied. If the limit were exceeded at a time when the appropriate mode is already in existence, then that mode is prolonged by the same time period, with the opposite mode prolonged equally later.

In figure 3-11, part a, the half-period of the regular orientation changes is t_B, and the durations of the first and second corrective mode reversals are t_{M1} and $t_{M2} - t_B$, respectively. It can be first assumed that the satellite of interest has no appreciable period error when $\theta = \theta_E$; in that case, a time $t_{M1} = t_{M2} - t_B$ can be chosen which will return the relative angular position θ to zero with no net period change. Figure 3-11, part a shows an area, B, which is approximately equal to the product of t_B and the difference between the regular period, P_1, and the special period, P_2. With a_1 the semimajor axis, K the Newton's gravitational constant, m the mass of the earth, and

$$K_1 = 2\pi/K\sqrt{m} = 3.147 \times 10^{-7} \text{ sec/meter}^{3/2}$$

Then

$$B \approx (P_2 - P_1)t_B$$

$$\theta_E \approx \left(\frac{2\pi}{P_2} - \frac{2\pi}{P_1}\right)t_B = \frac{2\pi t_B^2}{P_1 t_B - B} - \frac{2\pi t_B}{P_1} = 2\pi t_B\left(\frac{t_B}{K_1 a^{3/2} t_B - B} - \frac{1}{K_1 a^{3/2}}\right)$$

$$\theta_E \approx -\frac{2\pi B}{\left(K_1 a_1^{3/2} - \frac{B}{t_B}\right)\left(K_1 a_1^{3/2}\right)}$$

Since:

$$K_1 a_1^{3/2} >> \frac{B}{t_B} ,$$

$$\theta_E \approx -\frac{2\pi B}{K_1^2 a^3}$$

Since the period of an orbit is given by $P = K_1 a^{3/2}$, changes in the period are approximately given by $\Delta P \approx \frac{3}{2} K_1 a^{1/2}$. In this case, in the interval,

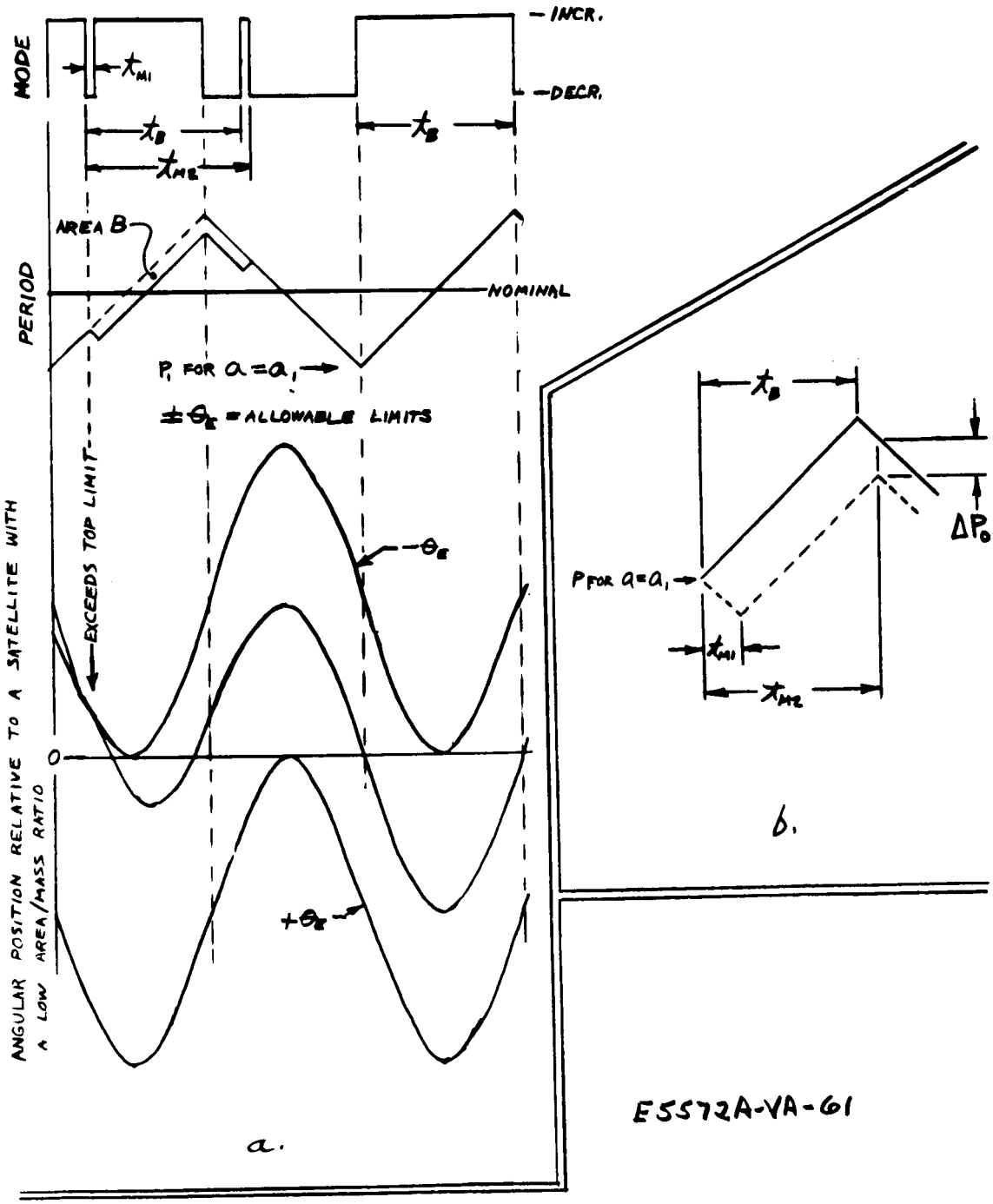

Figure 3-11. Control Method for No Neutral Mode

t_{M1}, the net altitude change between the two orbits is $2Mt_{M1}$ where M is the mobility magnitude. Thus:

$$P_2 - P_1 \approx -3K_1 a^{1/2} t_{M1}$$

$$B \approx -3K_1 a^{1/2} t_{M1} t_B$$

$$\Theta_E \approx \frac{6\pi M t_{M1} t_B}{K_1 a^{5/2}}$$

The duty cycle of the routine control procedure can be reduced by monitoring period as well as relative angular position. A net change to correct a period error, ΔP_o, can be made if $t_{M1} \neq t_{M2} - t_B$ (see part b of figure 3-11)

$$\Delta P_o = K_1 \left[a_1 + Mt_B - M(t_{M2} - t_B)\right]^{3/2} - K_1 \left[a_1 - Mt_{M1} + M(t_{M2} - t_{M1})\right]^{3/2}$$

Let:

$$t_o = t_{M2} - t_B - t_{M1}$$

$$\Delta P_o = K_1 \left\{ \left[a_1 + M(t_B - t_{M1} - t_o)\right]^{3/2} - \left[a_1 + M(t_B - t_{M1} + t_o)\right]^{3/2} \right\}$$

If: $A >> B, C$ then $(A+B)^N - (A+C)^N \approx NA^{N-1}(B-C)$.

Since $(a_1 + Mt_B) >> (-Mt_o - Mt_{M1}), (Mt_o - Mt_{M1})$, then

$$\Delta P_o \approx -3K_1 M t_o \sqrt{a_1 + Mt_B} \approx -3K_1 M t_o \sqrt{a} \qquad (3\text{-}47)$$

Thus: $$(t_{M2} - t_B) \approx t_{M1} - \frac{\Delta P_o}{3K_1 M \sqrt{a}}$$

3.3.2.2 Neutral Mode Case

In the orbit control method of paragraph 3.3.2.1, the satellite's attitude control system is required to maintain either of two orientations or orbit control modes - period increasing and period decreasing. If a neutral mode is added, alternative control methods become possible. The one discussed below is straightforward and minimizes both the maximum angular error and (to an extent limited by the constant mobility approximation) the duty cycle of the orbit controller.

Both angular error, θ, and period error, ΔP_o, are inputs. When θ reaches the allowed limit, θ_E, a mobility, M_1, is applied for a time, t_1, until θ again enters the $\bullet\,\theta_E$ zone. See figure 3-12. M_1 is the maximum available mobility. The period error, ΔP_o, at this time is noted. A mobility, M_2, opposite in sign to M_1, is then applied for a time, t_2, to reduce both the period and angular errors to zero. M_2 will be chosen as a function of ΔP_o, θ_E, and a. At the end of time, t_2, the system is returned to the neutral mode. Considering first the time period t_1,

$$\frac{dP}{da} = \frac{3K_1}{2} a^{1/2} \; ; \; \frac{da}{dt} = M_1$$

$$\frac{dP}{dt} = \frac{3K_1 M_1 a^{1/2}}{2}$$

$$2\Delta t = t_1 = \frac{-4\Delta P_i}{3K_1 M_1 a^{1/2}} \qquad (3\text{-}48)$$

$$\omega = \frac{2\pi}{P} \; ; \; \frac{d\omega}{dP} = -\frac{2\pi}{P^2} = -\frac{2\pi}{K_1^2 a^3}$$

$$\frac{d\omega}{dt} = -\left(\frac{2\pi}{K_1^2 a^3}\right)\left(\frac{3K_1 M_1 a^{1/2}}{2}\right) = -\frac{3\pi M_1}{K_1 a^{5/2}}$$

$$\Delta\omega = -\left(\frac{3\pi M_1}{K_1 a^{5/2}}\right)\left(\frac{t_1}{2}\right)$$

The average relative ω is:

$$\omega_{A,R} \approx \frac{\Delta\omega}{2} = -\frac{3\pi M_1 t_1}{4K_1 a^{5/2}}$$

θ_1, the excursion of θ beyond θ_E, is:

$$\theta_1 = \omega_{A,R}\left(\frac{t_1}{2}\right) = \frac{3\pi M_1 t_1^2}{8K_1 a^{5/2}} = \frac{2\pi \Delta P_c^2}{3K_1^3 a^{7/2} M_1} \qquad (3\text{-}49)$$

Similarly

$$t_2 = \frac{2\Delta P_c}{3K_1 M_2 a^{1/2}} \qquad (3\text{-}50)$$

$$\theta_E = -\frac{2\pi \Delta P_c^2}{3K_1^3 a^{7/2} M_2}$$

$$M_2 = -\frac{2\pi \Delta P_c^2}{3K_1^3 a^{7/2} \theta_E} \qquad (3\text{-}51)$$

From equations 3-51 and 3-50

$$t_2 = \frac{K_1^2 a^3 \theta_E}{\pi \Delta P_c} = -\frac{2\Delta P_c}{3K_1 M_2 \sqrt{a}} \qquad (3\text{-}52)$$

3.3.3 Error Effects

It is worthwhile to begin the design of an orbit control system or control procedure knowing the approximate sizes of the various angular error effects. In this paragraph, these effects will be determined as functions of altitude, mobility, period error, mobility errors, delay times, and orbit eccentricity. Table 3-2 is repeated below, omitting the effects which are negligible and assigning symbols to the various components.

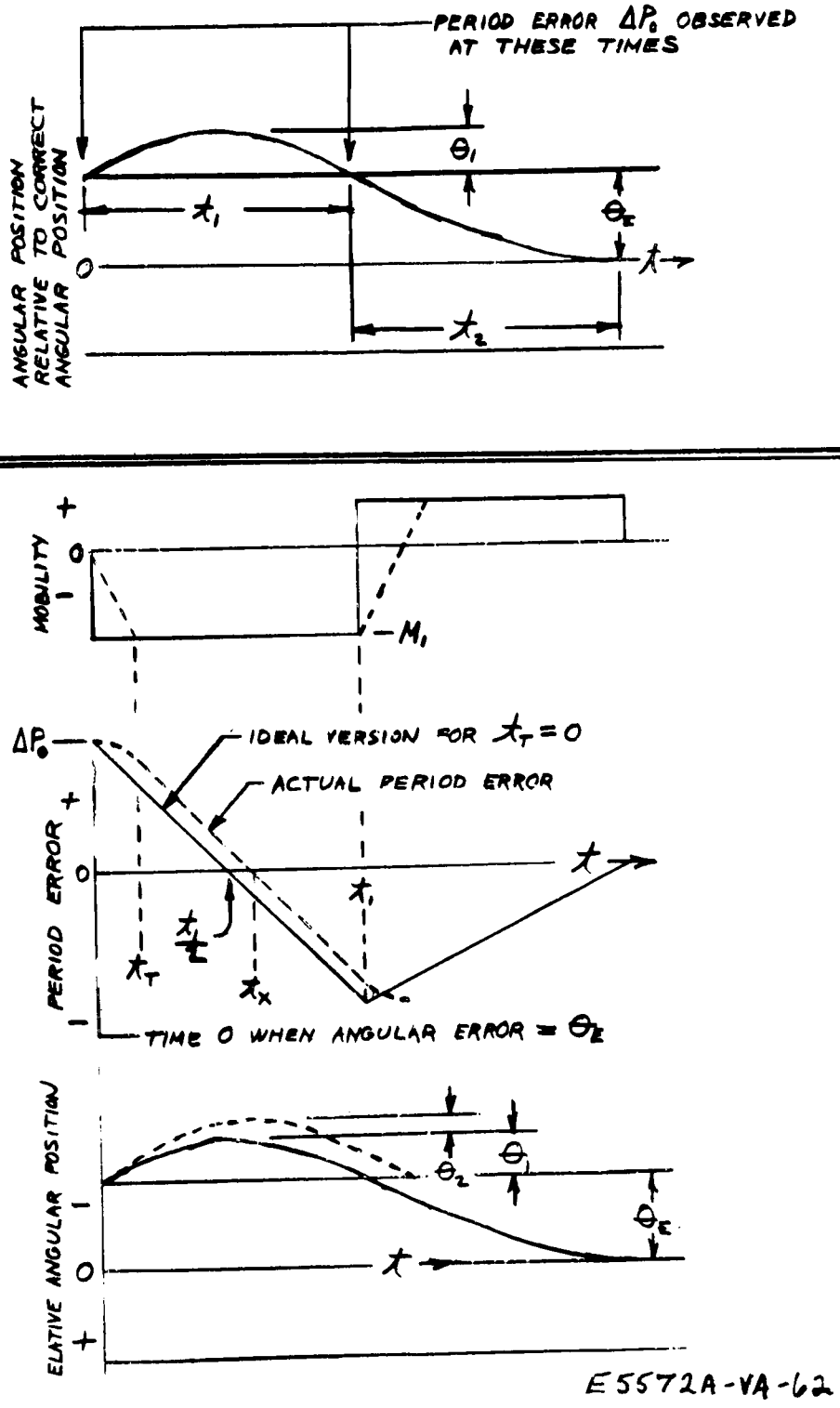

Figure 3-12. a. Time and Angle Definitions
b. Effect of Finite Scil Angle Change Time

	No Neutral Mode	Neutral Mode
Minimum detectable error or set limit	θ_E	θ_E
Period error when $\theta = \theta_E$	θ_1	θ_1
Finite time for sail angle change	θ_2	θ_2
Command delay due to in-sight requirement	θ_3	θ_3
Unequal mobilities in increasing and decreasing modes	θ_4	-
Neutral mode sail angle error	-	θ_5
Orbit eccentricity	θ_6	θ_6

The total maximum angular errors, θ_{MAX}, for the two control cases are:

No neutral mode $$\theta_E + \left\{ \begin{matrix} \theta_1 \\ \text{OR} \\ \theta_4 \end{matrix} \right\} + \theta_2 + \theta_3 + \theta_6$$

Neutral mode $$\theta_E + \left\{ \begin{matrix} \theta_1 \\ \text{OR} \\ \theta_5 \end{matrix} \right\} + \theta_2 + \theta_3 + \theta_6$$

θ_1 is a component caused by a general period error, ΔP_o. θ_4 and θ_5 are components arising from period errors due to specific causes.

For the neutral mode case, θ_1 has already been defined by equation 3-49 as

$$\theta_1 = \frac{2\pi \Delta P_c^2}{3 K_1^3 a^{7/2} M_1}$$

The same equation holds for the no neutral mode case (with M_1 replaced by 2M), which is similar in this respect because the sign of $d\theta/dt$ is changed during time, t_{M1}.

The remaining components θ_2, θ_3, θ_4, θ_5, and θ_6 will be defined.

3.3.3.1 Finite Time for Sail Angle Change

A first order approximation of this effect can be obtained by assuming that the time rate of change of the mobility is constant during the transition period, t_T. This condition is shown in part b of figure 3-12, which is drawn for the neutral mode case. Because the sail angle does not undergo a step change, $d\theta/dt$ does not reach zero at time, $t_{1/2}$, but at time, t_x, where

$$t_x = \frac{t_1 + t_T}{2}$$

Also, θ overshoots θ_E by an amount θ_2 in addition to θ_1.

$$\frac{dP}{da} = \frac{3K_1}{2} a^{1/2}$$

$$\left.\frac{da}{dt}\right|_{t=0}^{t=t_T} = \frac{M_1 t}{t_T} \quad ; \quad \left.\frac{da}{dt}\right|_{t=t_T}^{t=t_x} = M_1$$

$$\left.\frac{dP}{dt}\right|_{t=0}^{t=t_T} = \frac{3K_1 a^{1/2} M_1 t}{2 t_T} \quad ; \quad \left.\frac{dP}{dt}\right|_{t=t_T}^{t=t_x} = \frac{3K_1 a^{1/2} M_1}{2}$$

From: $t = 0$ to $t = t_T$

$$\Delta P_A = \int_0^{t_T} \frac{3K_1 a^{1/2} M_1}{2 t_T} t\, dt \approx \frac{3K_1 a^{1/2} M_1 t_T}{4}$$

The approximation is made because a is nearly constant over t_T.

$$\Delta\omega = \omega_{II} - \omega_I = \frac{2\pi}{P_{II}} - \frac{2\pi}{P_I}$$

Since: $P_{II} \gg \Delta P$,

$$\Delta\omega \approx -\frac{2\pi \Delta P}{P_{II}^2} \approx -\frac{2\pi \Delta P}{K_1^2 a^3} \qquad (3\text{-}53)$$

$$\Delta\omega_A \approx -\frac{3\pi M_1 t_T}{2 K_1 a^{5/2}}$$

From: $t = t_T$ to $t = t_2$,

$$\Delta P_{13} = -\Delta P_c - \Delta P_A = -\Delta P_c - \frac{3K_1 a^{1/2} M_1 t_T}{4}$$

$$\Delta\omega_B \approx \frac{2\pi \Delta P_o^2}{K_1^2 a^3} + \frac{3\pi M_1 t_T}{2K_1 a^{5/2}}$$

$$\theta_1 + \theta_A \approx \left(\frac{\Delta\omega_A}{2}\right) t_T + \left(\frac{\Delta\omega_B}{2}\right)\left(\frac{t_T}{2} - \frac{t_T}{2}\right)$$

and since: $t_1 = -\frac{4\Delta P_o}{3K_1 M_1 a^{1/2}}$,

$$\theta_1 + \theta_2 \approx -\frac{2\pi \Delta P_o^2}{3K_1^3 a^{3/2} M_1} - \frac{3\pi M_1 t_T^2}{8K_1 a^{5/2}}$$

$$\theta_2 \approx -\frac{3\pi M_1 t_T^2}{8K_1 a^{5/2}} \qquad (3\text{-}54)$$

For typical values of M_1 and t_T, θ_2 is quite small. As with the expression for θ_1, the same equation holds for the no neutral mode (with M_1 replaced with 2M) because the sign of $d\theta/dt$ is changed during time, t_{M1}.

3.3.3.2 Command Delay

The command to execute a sail angle change might be delayed for a period, t_D, after $\theta = \theta_E$. One possible reason could be that maneuvers are initiated only when the satellite is within sight of a single ground control station. The delay will cause an additional error, θ_3. From equation 3-53

$$\Delta\omega \approx -\frac{2\pi \Delta P_o}{K_1^2 a^3}$$

$$\theta_3 = \Delta\omega t_D \approx -\frac{2\pi \Delta P_c t_D}{K_1^2 a^3} \qquad (3\text{-}55)$$

θ_3 is typically a small fraction of a degree.

3.3.3.3 Unequal Mobilities

The error component, θ_1, is dependent on ΔP_o. For the no neutral mode case, ΔP_o may arise from a condition of unequal mobilities in the increasing period and decreasing period half cycles, causing error, θ_4, a special case of θ_1. Satellites A and B will be considered, where satellite A has the correct mobility, M, in both increasing and decreasing modes. As in paragraph 3.3.2.2

$$\left.\frac{d\omega}{dt}\right|_{SAT\ A} = -\frac{3\pi M}{K_1 a^{5/2}}$$

Satellite B has correct mobility, M, in the decreasing mode, but has an increasing mode mobility, $M + M_E$, in error by the amount, M_E.

$$\left.\frac{d\omega}{dt}\right|_{SAT\ B} = -\frac{3\pi (M + M_E)}{K_1 a^{5/2}}$$

The angular separation (between satellites A and B) acceleration α is:

$$\alpha = \frac{3\pi M_E}{K_1 a^{5/2}}$$

Time, t_c, is defined as the time in the increasing mode from $\theta = 0$ to $\theta = \theta_E$ for satellite B, and the following derivation holds if $t_c < t_B$. Over the time, t_c, α is essentially constant, and:

$$\theta_E \approx \frac{1}{2}\left(\frac{3\pi M_E}{K_1 a^{5/2}}\right) t_c^2$$

$$t_c \approx \sqrt{\frac{2\theta_E K_1 a^{5/2}}{3\pi M_E}}$$

If $\Delta\omega$ is the difference between the angular rates of satellites A and B at the end of time, t_c:

$$\Delta\omega = \alpha t_c = \sqrt{\frac{6\pi M_E \theta_E}{K_1 a^{5/2}}}$$

From equation 3-53:

$$\Delta P_c = \frac{K_1^2 a^3 \Delta\omega}{2\pi} = \sqrt{\frac{3K_1^3 a^{7/2} M_E \theta_E}{2\pi}}$$

From paragraph 3.3.3:

$$\theta_1 = \frac{2\pi \Delta P_c^2}{3K_1^3 a^{7/2} M} = \theta_4$$

$$\theta_4 = \frac{M_E}{M}\theta_E \qquad (3\text{-}56)$$

3.3.3.4 Neutral Mode Sail Angle Error

For the neutral mode case, ΔP_o, at $\theta = \theta_E$ may arise from a mobility, $M_o \neq 0$, in the neutral mode. The mobility error, M_o, will cause an error, θ_5, a special case of θ_1. Since $da/dt = M_o$,

$$\frac{dP}{dt} = \frac{3K_1 M_o a^{1/2}}{2}$$

Also:

$$\frac{d\omega}{dP} = -\frac{2\pi}{K_1^2 a^3}$$

The average value of the relative angular rate over time, t_N, or the time from $\theta = 0$ to $\theta = \theta_E$ is:

$$\omega_{R,1} \approx \frac{\Delta\omega}{2} = -\frac{\pi \Delta P_c}{K_1^2 a^3}$$

$$t_N = \frac{\theta_E}{\omega_{R,1}} = \frac{K_1^2 a^3 \theta_E}{\pi \Delta P_c}$$

$$\frac{\Delta P_c}{t_N} = \frac{3K_1 M_c a^{1/2}}{2} = \frac{\pi \Delta P_o^2}{K_1^2 a^3 \theta_E}$$

$$\Delta P_c = \sqrt{\frac{3K_1^3 a^{7/2} \theta_E M_c}{2\pi}}$$

Using equation 3-49:

$$\theta_1 = \frac{2\pi \Delta P_c^2}{3 K_1^3 a^{7/2} M_1} = \theta_s$$

$$\theta_s = \frac{M_c}{M_1} \theta_E \qquad (3\text{-}57)$$

3.3.3.5 Eccentricity Error

For the analysis of the effects of the various errors on a system of satellites, a circular orbit was assumed. This allows the assumption of a constant angular motion and the calculation of angular drift rates in terms of altitude differences. However, for an eccentric orbit, the angular motion is not constant with time. Thus, a satellite in a circular orbit and a satellite in an eccentric orbit, whose semimajor axis, a, is equal to the radius of the circular orbit, will not maintain a constant separation between their relative angular positions; the satellite in the eccentric orbit will tend to oscillate about a nominal position corresponding to a circular orbit. Since one of the requirements for a system of satellites is the maintenance of a constant separation of their angular positions, this represents another error source.

The effect of orbit eccentricity on the angular motion can be expressed by means of the equation

$$E - e \sin E = \frac{2\pi}{K_1 a^{3/2}} t_p$$

where t_p is the time from perigee, e is the orbit eccentricity, and E is the eccentric anomaly. Considering two satellites having common orbit planes and equal periods, one in a circular orbit and the other in an elliptical orbit, with their angular positions in orbit, θ, both zero at $t_p = 0$, the angle for the one in the circular orbit is:

$$\theta_c = \frac{2\pi t_p}{K_1 a^{3/2}}$$

The difference in their angular positions in orbit is:

$$\Delta\theta = \eta - \theta_c$$

where η is the true anomaly for the satellite in an elliptical orbit:

$$\eta = \cos^{-1}\left(\frac{\cos E - e}{1 - e\cos E}\right)$$

For small values or e, $\Delta\theta$ is largest at $E \cong \pi/2$:

$$\theta_c = (\Delta\theta)_{max} = \cos^{-1}(-e) - \frac{\pi}{2} + e \qquad (3\text{-}58)$$

$$\theta_c \approx 2e$$

Without a specific orbit, satellite design, tracking ability, and overall control procedure, the various position-in-orbit errors can be considered only approximately. However, it is quite probable that the largest error will be that due to orbit eccentricity. This error may be a fraction of a degree or it may be several degrees. The second largest error will probably be the minimum detectable position error (or set limit, as the case may be), θ_E probably a fraction of a degree. θ_E would be made larger only to lower the control system duty cycle. The component, θ_1, which might be chiefly due to incorrectly detecting period error, could depend on the degree to which tracking facilities are exercised. If ΔP_o is on the order of 1 second at h = 1000 nmi or 100 seconds at synchronous altitude, then θ_1 is approximately as large as θ_E. The mobility error effects (θ_4 and θ_5) are small as causes of period error and probably small compared to the basic error in measuring period. If either M_E or M_o is 10 percent of M, then θ_4 or θ_5 is only approximately 10 percent of θ_E.

The error due to command delay, θ_3, could be on the order of 0.1 or 0.2 degree, especially for a subsynchronous orbit where commands are relayed only when the satellite is within sight of one main station.

Typical delays in changing sail position cause only a very small error (θ_2).

Another quantity of interest is the length of time that the satellite's position-in-orbit error exceeds the set limit, and the values of this time can be summarized as follows:

	Duration of condition $\theta \geq \theta_E$	
Error Cause	Neutral Mode Case	No Neutral Mode Case
θ_E and ΔP_o	t_1	$< 2t_{M1}$
Sail angle turn time (θ_2)	$t_1 + t_T$	$< 2t_{M1}$
Command Delay (θ_3)	$\cong t_1 + 2t_D$	$< 2t_{M1}$
Unequal Mobilities (θ_4)		$< 2t_{M1}$
Neutral Mode Mobility (θ_5)	t_1	
Eccentricity (θ_6)	Depends on relative sizes of θ_E and θ_6.	

3.3.4 Duty Cycle for Neutral Mode Case

There are a number of factors which could influence the duration of the condition $-\theta_E < \theta < +\theta_E$ after a corrective maneuver:

a. θ_E
b. Altitude
c. The position measurement error at $\theta = \theta_E$
d. The period measurement at $\theta = \theta_E$
e. The command delay when changing from M_1 to M_2
f. The command delay when changing from M_2 to $M = 0$
g. An error in the mobility M_2
h. A neutral mode mobility other than zero
i. Eccentricity
j. Times to change sail angle.

It will be assumed that a sail angle change is initiated only when θ rises or falls to θ_E at perigee or apogee, thus eliminating item i as a factor. Also,

item j can be ignored. It has already been seen that item j is usually much smaller than items e and f for practical cases. In addition, item j could be further reduced by starting turns early. Thus, items a through h will be considered.

ΔP_A, t_{2A}, and M_{2A} are defined as the actual period change during time, t_{2A}, the actual time, t_2 and the actual mobility, M_2. ΔP_1 is the period error at the beginning of time, t_2, nominally $-\Delta P_o$. ΔP_{oE} is the residual period error at the end of the maneuver and is $\Delta P_1 + \Delta P_A$. From equation 3-50

$$\Delta P_o = \frac{3K_1 M_2 a^{1/2} t_2}{2} = -\Delta P_1$$

M_{2E} and t_{2ET} are the errors $M_{2A} - M_2$ and $t_{2A} - t_2$.

$$\Delta P_{oE} = \left(\frac{3K_1 a^{1/2}}{2}\right)\left(M_2 t_{2ET} + M_{2E} t_2 + M_{2E} t_{2ET}\right)$$

t_{2ET} has two components: one is a delay t_{2E} in starting the final sail change back to neutral; the other is caused by incorrectly measuring the period error ΔP_1 by an amount P_{ME}.

$$t_{2A} = -\frac{2(\Delta P_1 + P_{ME})}{3K_1 M_2 a^{1/2}} + t_{2E}$$

$$t_{2ET} = -\frac{2P_{ME}}{3K_1 M_2 a^{1/2}} + t_{2E}$$

$$\Delta P_{oE} = -P_{ME}\left(1 + \frac{M_{2E}}{M_2}\right) + \left(\frac{3K_1 a^{1/2} M_2}{2}\right)\left(\frac{M_{2E}}{M_2} t_2 + \frac{M_{2E}}{M_2} t_{2E} + t_{2E}\right)$$

Apply equations 3-51 and 3-52:

$$\Delta P_{oE} = -P_{ME}\left(1 + \frac{M_{2E}}{M_2}\right) - \left(\frac{\pi \Delta P_1^2}{K_1^2 a^3 \theta_E}\right)\left(1 + \frac{M_{2E}}{M_2}\right) t_{2E} - \Delta P_1 \frac{M_{2E}}{M_2} \quad (3\text{-}59)$$

Note that the error due to a delay in executing the change from M_1 to M_2 is essentially avoided by letting θ_E and ΔP_1 above represent the actual angular position and period errors existing when this change is executed, and t_2 represent the time from the actual execution rather than the time from $\theta = \theta_E$. Thus, item e of the list above is also eliminated.

Now it is of interest to find the normalized mobility error, M_{2E}/M_2. Assume that θ is incorrectly measured such that when θ is apparently θ_E, it is actually $\theta_E + \theta_{ME}$. From equation 3-51:

$$M_2 = -\frac{2\pi \Delta P_1^2}{3K_1^3 a^{7/2}(\theta_E + \theta_{ME})}$$

$$M_{2A} = -\frac{2\pi(\Delta P_1 + P_{ME})^2}{3K_1^3 a^{7/2}\theta_E}$$

$$M_{2E} = M_{2A} - M_2 = -\left(\frac{2\pi}{3K_1^3 a^{7/2}}\right)\left(\frac{\Delta P_1^2 \theta_{ME} + (2\Delta P_1 + P_{ME})P_{ME}(\theta_E + \theta_{ME})}{\theta_E(\theta_E + \theta_{ME})}\right)$$

$$\frac{M_{2E}}{M_2} = \frac{\theta_{ME}}{\theta_E + \theta_{ME}} + \frac{P_{ME}(2\Delta P_1 + P_{ME})}{\Delta P_1^2} \qquad (3\text{-}60)$$

A term, F, can be added to the right-hand side to cover the difference between the computed mobility and the mobility actually set. F is the ratio of this difference to M_2.

The time spent in the neutral mode is:

$$t_{NM} \approx \frac{\theta_E}{\Delta\omega_{avg}}$$

where $\Delta\omega$ is the difference between the actual and correct angular velocities. From equation 3-53:

$$\Delta\omega \approx -\frac{2\pi\Delta P}{K_1^2 a^3}$$

$$\Delta P = \Delta P_{oE} + K_1 \left[(a + M_o t_{NM})^{3/2} - a^{3/2} \right]$$

where M_o is the error mobility in the neutral mode. Since $a >> M_o t_{NM}$:

$$\Delta P \approx \Delta P_{oE} + \frac{3 K_1 a^{1/2} M_o t_{NM}}{2}$$

$$\Delta \omega_{avg} \approx - \frac{2\pi \Delta P_{oE}}{K_1^2 a^3} - \frac{3\pi M_o t_{NM}}{2 K_1 a^{5/2}} = \frac{\theta_E}{t_{NM}}$$

$$t_{NM} \approx \left(\frac{1}{3 K_1 a^{1/2} M_o} \right) \left(-2 \Delta P_{oE} \pm \sqrt{4 \Delta P_{oE}^2 - \frac{6}{\pi} K_1^3 a^{7/2} M_o \theta_E} \right)$$

The - sign holds if the ΔP_{oE} and M_o effects tend to cancel; the + sign if they add. M_o and θ_E are always of opposite sign. ΔP_o at the beginning of the next corrective maneuver is the expression for ΔP above. The duty cycle is:

$$\frac{t_1 + t_2}{t_{NM} + t_1 + t_2}$$

where t_1 and t_2 are given in equations 3-48 and 3-52.

The following case will be used as an example of the typical duty cycle:

Satellite and Control Characteristics		Assumed Errors	
h	= 1000 nmi	P_{ME}	= +0.1 second
θ_E	= $+5^o$	F	= 10 percent
M_1	= 10^3 Meters/Day	θ_{ME}	= +0.1 degree
ΔP_1	= +2 second	t_{2E}	= 2 hours
		M_o	= 10 meters/day

For these parameters, the following results are obtained, where N is the ratio of the neutral mode time for a given control period to that whole control period:

	First Control Period	Second Control Period	Third Control Period
P_1	+2 second	+0.794 second	+0.664 second
M_{2E}/M_2	+22.2 percent	+38.8 percent	+44.4 percent
P_{oE}	-0.589 second	-0.451 second	-0.442 second
t_{NM}	102.5 days	82.5 days	81.5 days
t_1	2.95 days	1.2 days	1.0 day
t_2	8.85 days	22.3 days	26.6 days
N	90 percent	78 percent	75 percent
M_2	167 Met/Day	26.3 Met/Day	18.4 Met/Day
$\frac{M_1 t_1 + M_2 t_2 + M_o t_{NM}}{t_1 + t_2 + t_{NM}}$	47.7 Met/Day	24.6 Met/Day	21.1 Met/Day

However, the last row in the table represents the average mobility used over the control period. If minimizing the eccentricity buildup is the prime concern, then this average mobility is more significant than N. The mobility is plotted over the three control periods below in figure 3-13.

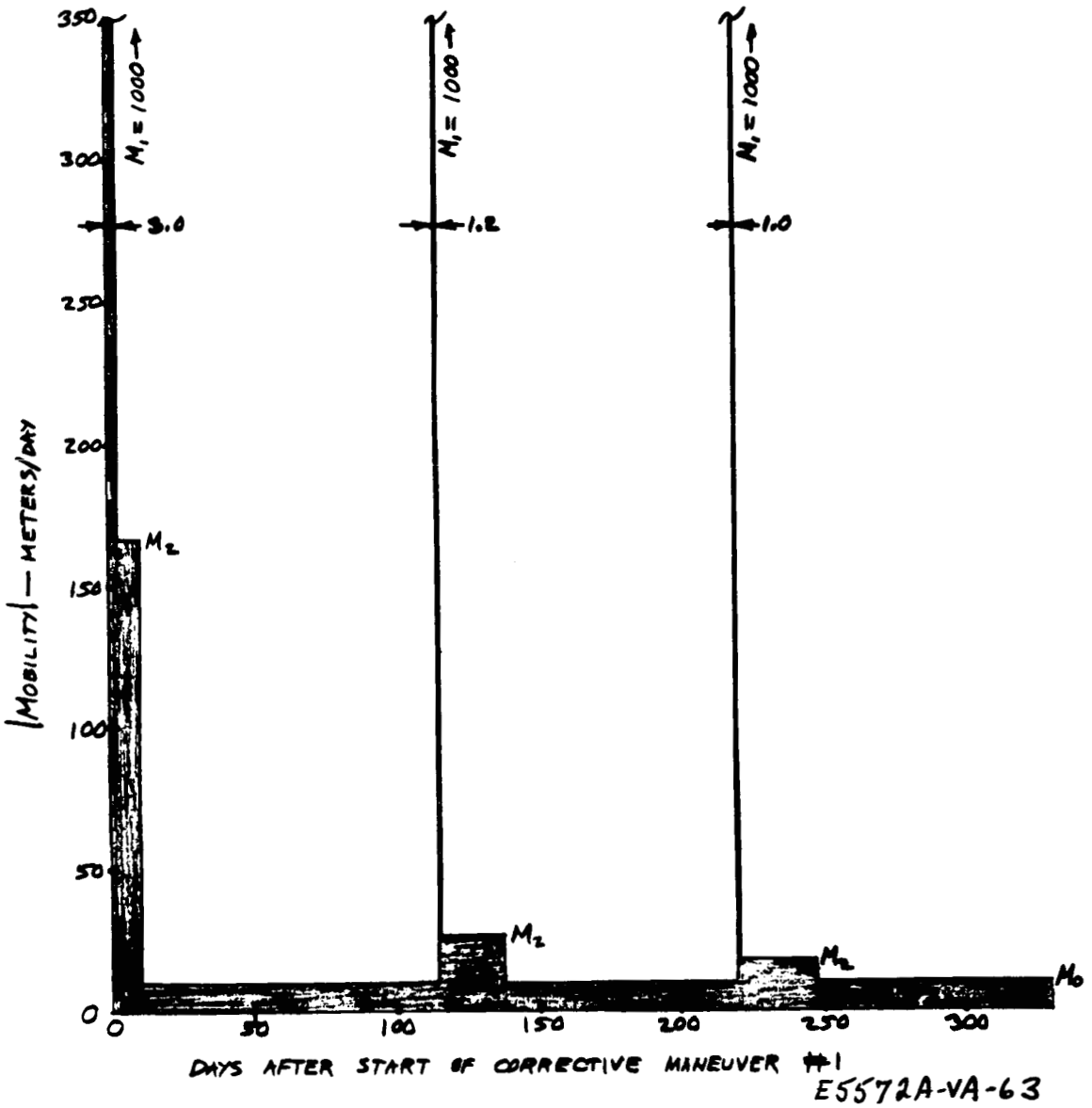

Figure 3-13. Mobility Plotted Over the Three Control Periods

3.4 COMPUTER PROGRAMS

3.4.1 Lifetime - 18

The Lifetime 18 program is essentially an orbital prediction program and was developed originally by the NASA Goddard Space Flight Center. It has the capability of predicting the variations of the five orbital elements which describe the plane of the orbit (semimajor axis, eccentricity, inclination, argument of perigee, and right ascension) but does not consider the position of the satellite within the plane of the orbit. Among the perturbing forces which can be considered by the program are those due to the second, third, and fourth spherical harmonics of the earth's gravitational field, the direct solar forces on a uniformly coated specular spherical satellite, the gravitational forces of both the sun and moon, and the atmospheric drag forces.

Due to the method of solution used in the program, it is extremely fast running for an orbital prediction program. For example, a complete 5-year case can be run in approximately 3 minutes of IBM 7094 MODII Computer time. The program uses a variation-of-parameters-type approach to the problem, but integrates over a much larger step size (1 day) than used in more standard orbital prediction programs. This is possible because the model on which the program is based uses an analytic integration of the perturbing forces over a complete orbit (thus eliminating secular terms) to provide expressions for the rates of change of the orbital elements per day. In this manner, the time consuming numerical integration within an orbit is eliminated, and the integration can proceed at a much larger step size.

The program has been modified extensively in several areas by Westinghouse Aerospace Division. The two prime areas of modification are in the earth shadow angle determination and in the atmospheric drag determination. The model used for the earth shadow angle calculation was redesigned to eliminate the sporadic occurrence of error conditions in the original model. The original model used for the atmospheric drag perturbation (Harris-Priester model), when used, increased the running time of the program by

a factor of approximately 30. This was due to the necessity of performing a numerical integration on the atmospheric drag perturbing forces within an orbit. Since this running time prohibits the study of any large number of cases, a simplified drag model based upon the Harris-Priester model was designed. This model is discussed in section IV of reference 4 and does not add appreciably to the running time of the program. Several additional modifications have been made to the program to calculate other quantities pertinent to the studies which have been made.

The program also has the capability of automatically plotting time histories of the orbital parameters. This plotting, in addition to the inclusion of the various perturbing forces and other program functions, is all made available to the user as options which can be specified with the data input to the program.

The most extensive use of the program has been in the area of studies pertaining to the manner in which the solar pressure perturbing forces affect the orbital eccentricity of a high area-to-mass ratio satellite. In these studies, the program has been used to calculate parametrically the maximum eccentricity reached by an orbit as a function of the launch conditions, that is, semimajor axis, eccentricity, inclination, right ascension, and argument of perigee. The most exhaustive studies have been performed on the variation with respect to launch semimajor axis and inclination, while the studies on the other parameters have been more restrictive.

In reference 4, the Lifetime 18 program is described in detail; block diagrams and flow charts are given for the main program and the pertinent subroutines; program listings are shown for the main program and the various subroutines; input and output specifications are given; and a glossary of program variables is supplied.

3.4.2 Lenticular Force, Torque, and Temperature Program

This program computes the forces, torques, and temperatures on a lenticular-shaped satellite due to radiation. The direct radiation effects of the sun and earth, solar reflections from the earth, and the reradiation of the satellite are taken into account. In the force model, emissions and reflections are completely diffuse, and absorptivity is constant with respect to the angle of incidence. Also, thermal lag and heat conduction, which are negligible, were ignored.

A table of forces and torques can be generated by the program for various satellite configurations, orientations, and altitudes. This table is used by other programs in determining satellite mobility and in the analysis of vehicle attitude control systems.

The computation model of the satellite is divided into N elemental surfaces. The total force, $d\bar{F}_i$, on each element is approximated by the force at the center of each element times its area, dA_i. The total force, $\bar{F}$, on the satellite is the vectorial sum of the area weighted element forces, that is:

$$\bar{F} = \sum_{i=1}^{N} d\bar{F}_i \, dA_i$$

Similarly, the total torque, $\bar{M}$, on the satellite is the vectorial sum of the crossproduct of the area weighted element forces and the moment arm, $\bar{R}_i$, to the element center:

$$\bar{M} = \sum_{i=1}^{N} \left(\bar{R}_i \times d\bar{F}_i \right) dA_i$$

The surface characteristics of emissivity and absorptivity of each of the quadrants are inputs to the program. Each quadrant of the satellite is divided into elemental surfaces in which the forces, torques, and temperatures are considered to be approximately constant. For all cases considered thus far, a division of four zones and three elements per zone, that is 12 elements per quadrant, was considered satisfactory. The element breakdown

was found to be inadequate for computing the form factors, thus each element is further subdivided into 16 subelements. The form factors between elements are computed by a process of averaging and summing the 16 subelements. The largest form factor from each element is further adjusted such that the sum of the form factors from that element is equal to one.

Three angles describe the orientation of the satellite with respect to the earth and sun. These angles are: (1) an orbit angle, γ; (2) a rotation about the radial axis (yaw), η; and (3) a rotation about the tangential axis (roll), ρ. The rotation about the radial axis is performed first, followed by the rotation about the tangential axis.

This program can write a table of forces and a table of torques on auxiliary output tapes. The force tape is an input to the mobility program (see paragraph 3.4.4). The table entries must be made for every 5 degrees of orbit angle from 180 to 360 and for every 5 degrees of yaw angle from 0 to 360. The values in this table are used by the mobility program to determine the forces in any orbit at that altitude. A more detailed description of the program is given in reference 4.

3.4.3 Sail Force Program

The sail force program was developed for the purpose of supplying a table of solar and thermal pressure forces on a plane-sail-only-type satellite to the mobility program (see paragraph 3.4.4). The perturbing forces considered by this program include those due to both direct solar and direct earth radiation, the forces due to earth reflected radiation, and those due to reradiation from the surface of the sail itself.

The capability of specifying the surface characteristics of the sail by input is included. The program then calculates the aforementioned forces at the various positions and orientations of the satellite in the reference orbit required by the mobility program. The reference orbit is defined as having the sun-line in the plane of the orbit. Forces are computed at 5-degree increments on the orbit angle from 180 to 360 degrees and at 5-degree

increments on yaw angle through a full 360-degree rotation. A variation of the pitch angle of the satellite is not required since a vertically oriented satellite is assumed. A separate magnetic tape containing these forces is automatically written by the program and can be used as direct input to the mobility program. For a more detailed description of this, the reader should refer to part III of reference 4.

3.4.4 Mobility Program

The mobility program is essentially an orbital prediction program and was developed for the specific purpose of efficiently calculating the orbital perturbations due to the solar and thermal pressure perturbing forces on a nonuniform satellite. The capability of including the perturbations due to the second spherical harmonic of the earth's potential field is also incorporated into the program.

In order to include the solar and thermal pressure perturbations, a precomputed table of forces, considering all possible positions and orientations of the satellite with respect to the sun, must be supplied to the program by means of a separate magnetic tape. Assuming a vertically oriented satellite (one axis locked on the earth), the program is designed to accept the forces as computed on a satellite in a reference orbit having the sun-line in the plane of the orbit. In this reference orbit (at any desired altitude), the forces must be computed for orbit angles from 180 to 360 degrees with respect to the sun-line and for all possible yaw angles at each orbit angle. Two separate programs have been developed to precompute these forces for an opaque lenticular shape and for a plane sail shape. These programs are described in paragraphs 3.4.2 and 3.4.3, respectively.

The method of solution used by the program is essentially the variation-of-parameters method with some simplifying modifications to increase the speed of the program. The program integrates the solar and thermal pressure perturbations by a trapezoidal rule type of numerical integration over

a complete orbit (to eliminate secular terms in the perturbations). The computed perturbations are then extrapolated over 1 day, and the computation proceeds for the next day. The orbital elements treated in this manner by the program are the semimajor axis, eccentricity, inclination, right ascension of the ascending node, argument of perigee, and mean anomaly. The perturbations due to the second spherical harmonic of the earth's gravitational field are calculated directly for each day and added to the solar and thermal pressure forces.

In addition to the calculation of the time variation of orbital elements for an actual satellite, the program has the optional capability of manufacturing and varying artificial orbital conditions such that the variation of the solar and thermal pressure perturbations (and, in particular, the mobility) can be studied over the full range of orbital conditions. Under this option, the program will vary the sun-line inclination to the orbital plane, i_s, and the angle, U_s, between the projection of the sun-line into the orbital plane and the perigee vector, can be varied through their full range of possible values in increments specified by input to the program. Perturbations are not accumulated under this option so that the instantaneous satellite perturbations are recorded as a function of the orbital conditions.

This program has been used extensively to study the mobility capabilities of various spherical, lenticular, and sail-shaped satellites. It has also been used as a check in determining the maximum eccentricity of the lenticular and sail-shaped satellites as compared to the spherical satellite. In this respect, it has proved to be very accurate. A comparison of results of the mobility program and the Lifetime 18 program, described in paragraph 3.4.1, show agreement with 3 percent for a period of 2 years. For more detailed descriptions of the mobility program, the reader should refer to part IV of reference 4.

3.4.5 Maneuver Time Program

The maneuver time program was developed in order to calculate the times required for a satellite to correct errors in both altitude and relative angular position of the satellite. A constant mobility is assumed for the satellite over the duration of the maneuver. It is further assumed that the correction will be accomplished by a two-stage process, that is, the satellite will initially be placed into either a decreasing or increasing energy mode and at some later predetermined time will be changed to the opposite mode. In this manner, both the altitude and relative angular position error can be simultaneously reduced to zero.

The program determines these maneuver times for the optimum correction maneuver. It can be seen that incrementing or decrementing the relative angular position correction by multiples of 360 degrees does not change the end conditions in that the same effective correction is made. In the course of computing the maneuver times, the multiple of 360 degrees which produces the optimum (smallest total time) maneuver is also determined. An additional check is made to determine the optimum maneuver with respect to the initial state of the satellite, that is, either increasing or decreasing energy mode. The program outputs the optimum correction procedures in addition to the time at which the energy mode change is required and the time at which the errors are reduced to zero. For additional details on the program and computational procedure, the reader should refer to part V of reference 4.

3.5 SKIN TEMPERATURE, MOBILITY TRADEOFF

3.5.1 Opaque Lens (Configuration A)

In order to determine a set of surface coatings for the opaque lens which would produce both feasible skin temperatures and a sufficient amount of mobility, a study has been made to determine the trends of both these quantities as functions of the coating pattern.

As a common starting point for the study, the coating configuration used in the Phase II study (reference 3) was examined. This configuration for a satellite weighing approximately 1200 pounds is known to be capable of producing about 125 degrees per month of mobility. Since previous studies have shown that mobility does not vary significantly as a function of the internal emissivity, an initial study was made to determine the optimum internal emissivity with respect to the skin temperatures on the lenticule.

The results of this study are shown in figure 3-14. The temperatures were calculated by means of a digital computer program based on a method described in Appendix C of the Phase II final report (reference 3). In these initial investigations, the effects of earth radiation on the satellite are neglected. The skin temperatures at various positions on the surface of the lenticule are given for the various configurations studied. The constant temperature surfaces are divided by planes intersecting the lenticular surface at equal distances from the plane of the rim.

As expected, the maximum temperature point occurs in the quadrant facing the sun with the lowest external emissivity. When the internal emissivity of that quadrant is low, the maximum temperature is seen to occur in the top segment of this quadrant while when the internal emissivity is high, the maximum temperature is seen to occur in the rim segment.

In general, it can be seen that the higher emissivity configurations distribute the energy more uniformly over the surface of the satellite, thus producing a more uniform temperature distribution. The results of this particular study indicate that a uniform internal emissivity of as high as possible a value will produce the most uniform temperature distribution and thus the lowest maximum temperature. For this reason, a uniform internal emissivity of 0.9 (highest practical internal emissivity which can be achieved by Goodyear) has been chosen.

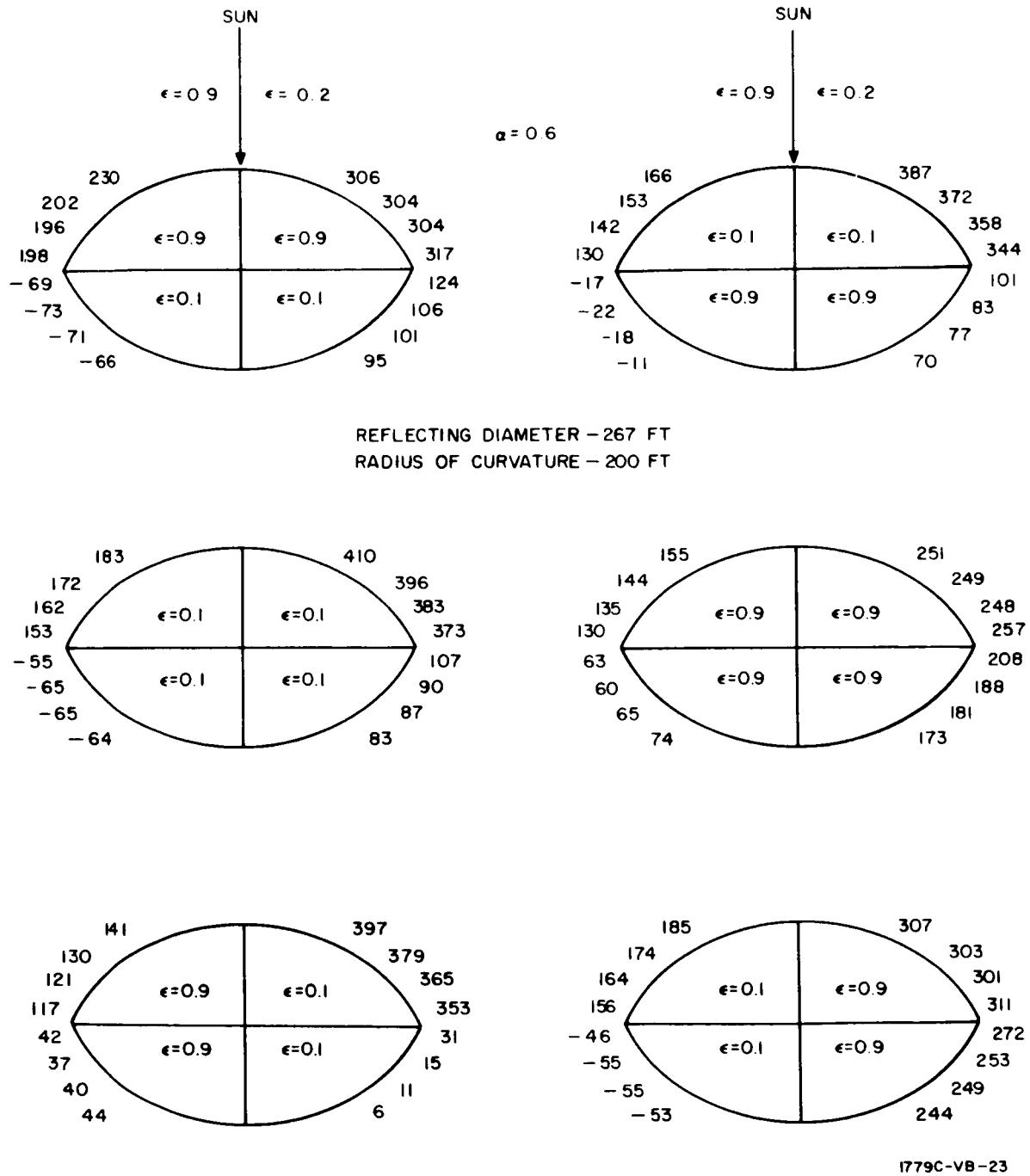

Figure 3-14. Internal Emissivity Study

In order to estimate the relative mobility associated with various configurations, a procedure used in estimating the relative mobility of a spherical satellite has been used. Since the absorptivity is assumed to be uniform over the surface, the mobility will be produced by a difference in the reradiation forces over the orbit. In the case of the spherical satellite, the difference in the tangential component of the reradiation forces when the axis of symmetry is aligned in opposite directions along the sun line has been found to be a very good indication of the relative mobility capabilities of various coating configurations. Since the lenticular shape under consideration is not too far removed from a sphere, it was believed, and in fact, has subsequently been shown, that the same quantity would be a good indication of the relative mobility capabilities of the lenticular configuration.

It can be shown that the reradiation force on a sphere when the axis of symmetry of the satellite is aligned with the sun line vector is:

$$F_R = \frac{-4\pi R^2}{3C}\left[\frac{\epsilon_1}{\epsilon_1+\epsilon_i}\left(\frac{C_s\alpha_s}{3}+\frac{\delta S}{2}\right)-\frac{\epsilon_2}{\epsilon_2+\epsilon_i}\frac{\delta S}{2}\right]$$

where δS is the product of the internal absorptivity and the radiation incident on the internal surface and can be determined by:

$$\delta S = \left[\frac{\frac{\epsilon_i}{\epsilon_1+\epsilon_i}}{\frac{\epsilon_1}{\epsilon_1+\epsilon_i}+\frac{\epsilon_2}{\epsilon_2+\epsilon_i}}\right]\frac{C_s\alpha_s}{2}$$

where ϵ_1 and ϵ_2 are the external emissivities of the sides facing toward and away from the sun, respectively; α_s is the solar absorptivity of the external surface; ϵ_i is the internal emissivity of the surface; C_S is the solar radiation density (440 Btu/hr ft^2); R is the radius of the sphere; and C is the speed of light.

The mobility of the satellite is then assumed to be directly proportional to the net difference in the reradiation force evaluated for opposite sides facing

the sun. Using the 125-degrees-per-month mobility of the configuration studied in Phase II as a base, the mobility of the various configurations has been estimated.

The distribution of skin temperatures for some of the configurations studied are shown in figures 3-15 through 3-18. In these figures, the effects of earth radiation are neglected. In general, it can be shown that the earth radiation will add approximately 20 degrees to both the maximum and minimum temperatures.

The configuration of figure 3-15 is that which was used in the Phase II final report. Figure 3-16 shows the effects of lowering the high emissivity to 0.8 and is seen not to affect the temperatures significantly. In figure 3-17 the lower emissivity is lowered to 0.1 and is seen to increase the temperatures significantly. In figure 3-18, the effects of reducing the absorptivity are shown to reduce the temperatures since less energy is absorbed by the satellite. Table 3-3 summarizes these results and also shows the estimated mobilities for each of these configurations.

At this point of the study, additional inputs were obtained from the Goodyear Aerospace Corporation with regard to the properties of the surface materials. The maximum allowable surface temperature was specified to be 250°F, and an external emissivity of 0.8 was specified as the highest value achievable.

Since none of the configurations fit the design criteria very closely, a new search was initiated to find the best combination of surface coatings. The previous studies indicated two directions for the search to take. The first was to maintain an external emissivity pattern of 0.8 and 0.2 while lowering the absorptivity until the temperature remained within the 250-degree limit. The second was to follow the same procedure using an external emissivity pattern of 0.8 and 0.1.

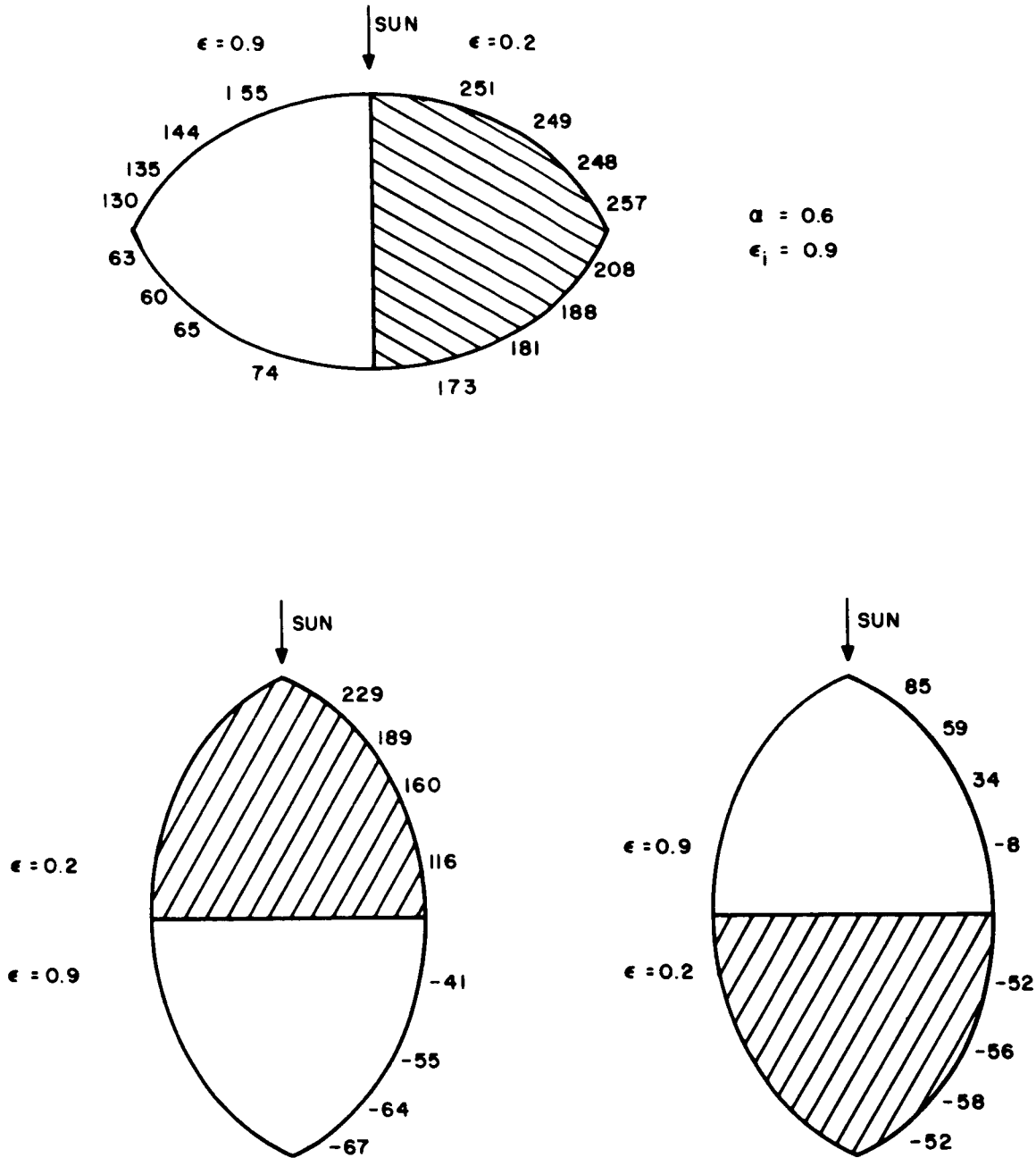

Figure 3-15. Skin Temperatures; 0.2 and 0.9 Emissivity and 0.6 Absorptivity

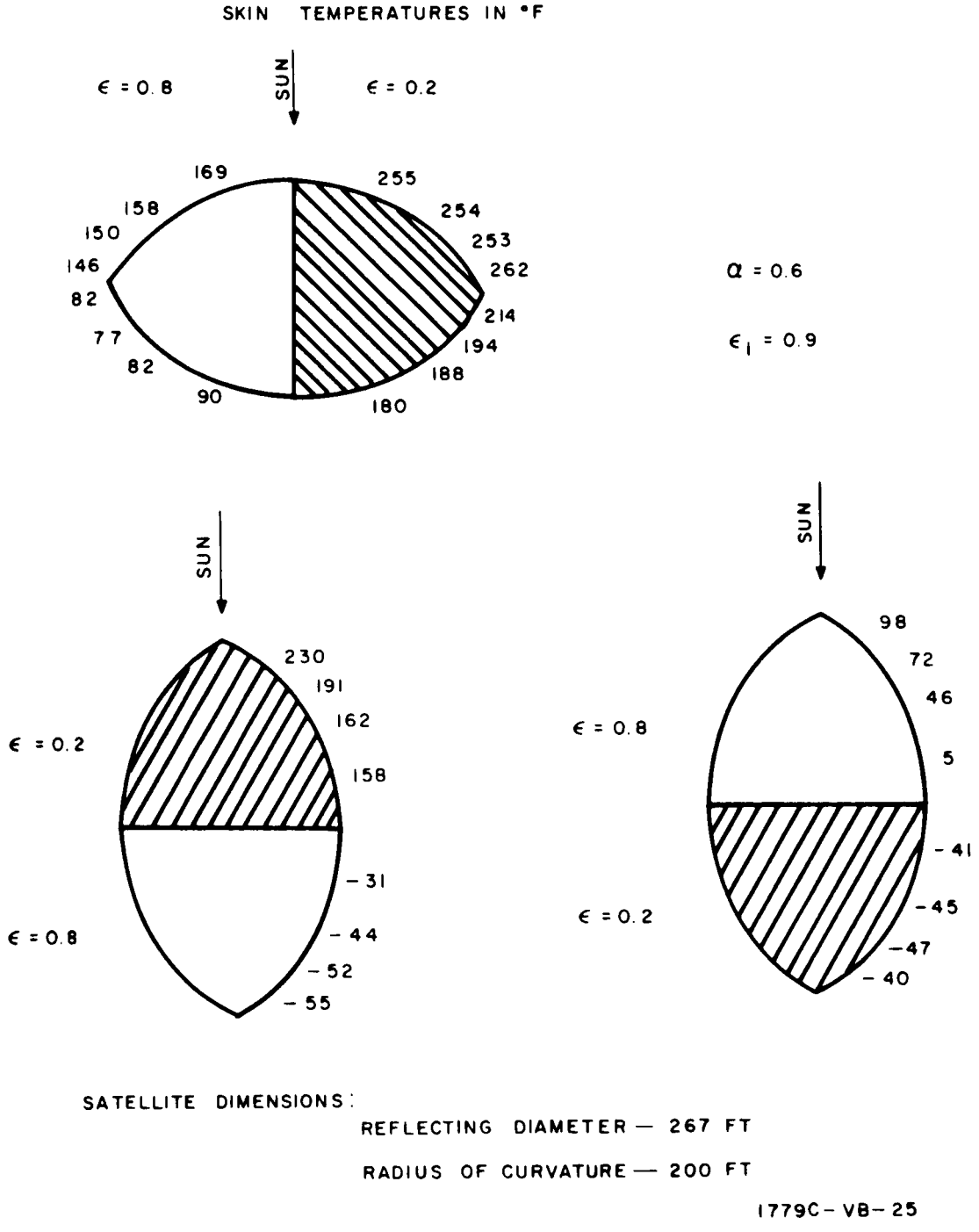

Figure 3-16. Skin Temperatures; 0.2 and 0.8 Emissivity and 0.6 Absorptivity

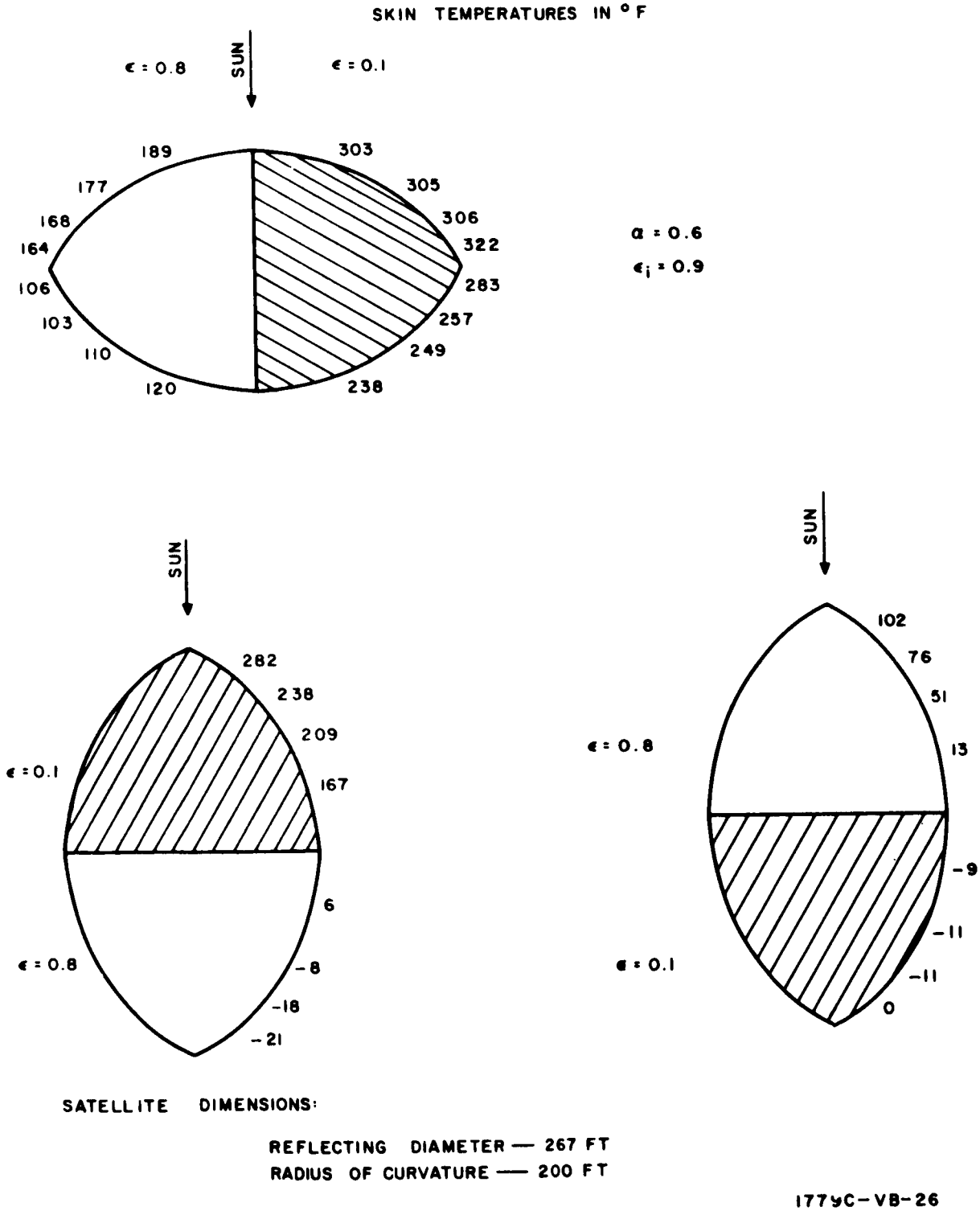

Figure 3-17. Skin Temperatures; 0.1 and 0.8 Emissivity and 0.6 Absorptivity

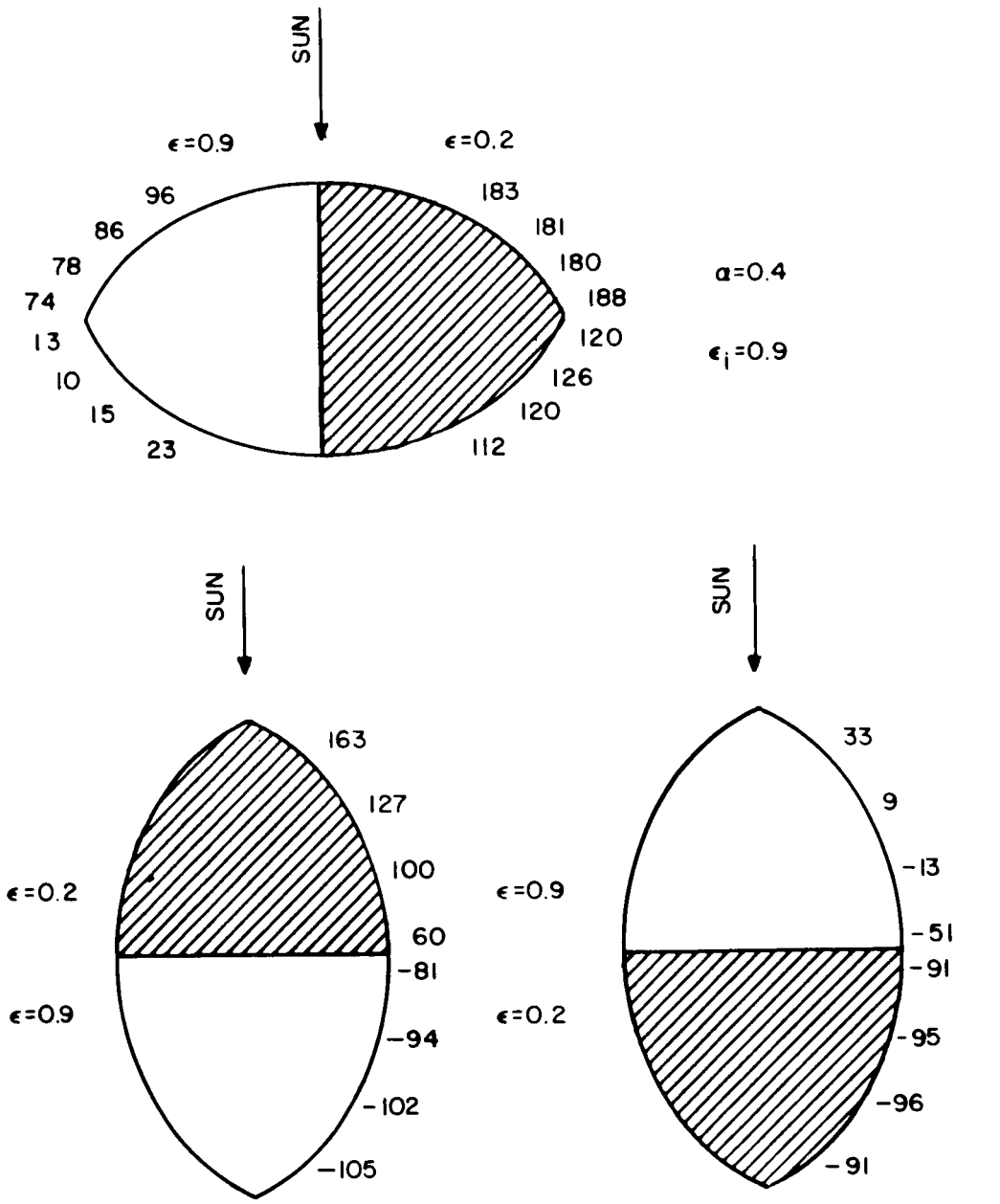

SATELLITE DIMENSIONS:
REFLECTING DIAMETER — 267 FT
RADIUS OF CURVATURE — 200 FT

1779C-VA-27

Figure 3-18. Skin Temperatures; 0.2 and 0.9 Emissivity and 0.4 Absorptivity

TABLE 3-3

TEMPERATURE, MOBILITY SUMMARY CHART

ϵ_1	ϵ_2	α	T_{max} (°F)	T_{min} (°F)	Mobility (deg/month)
0.9	0.2	0.6	257	-67	125
0.8	0.2	0.6	262	-55	119
0.8	0.1	0.6	322	-21	173
0.9	0.2	0.4	188	-105	83

The final skin temperatures of these two searches are shown in figures 3-19 and 3-20. The estimated mobility associated with the 0.8, 0.2 external emissivity pattern was 99 degrees per month while the other pattern produced 101 degrees per month. Thus, since the 0.8, 0.1 external emissivity pattern produced both slightly lower temperatures and slightly higher mobilities, it was selected as the pattern to be used for study in the current report.

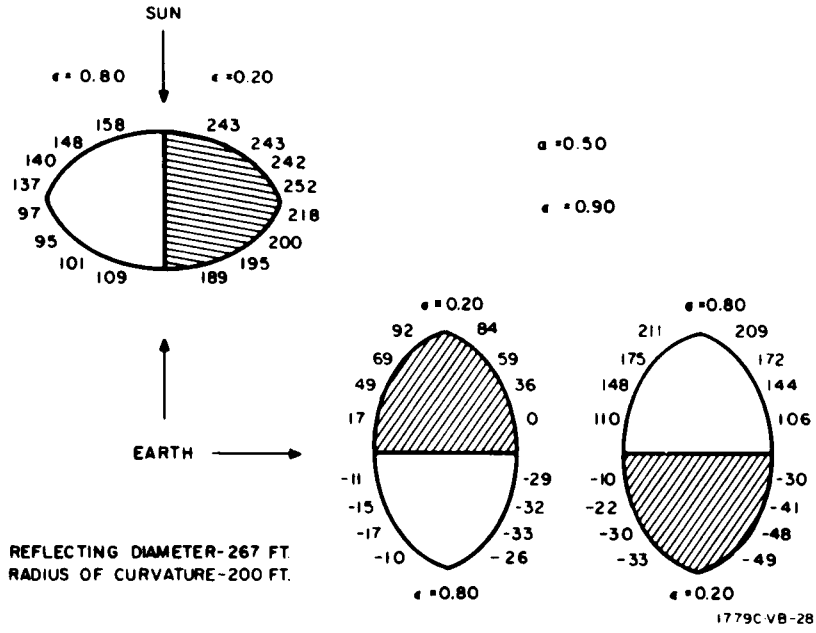

Figure 3-19. Skin Temperatures; 0.8 and 0.2 Emissivity and 0.5 Absorptivity

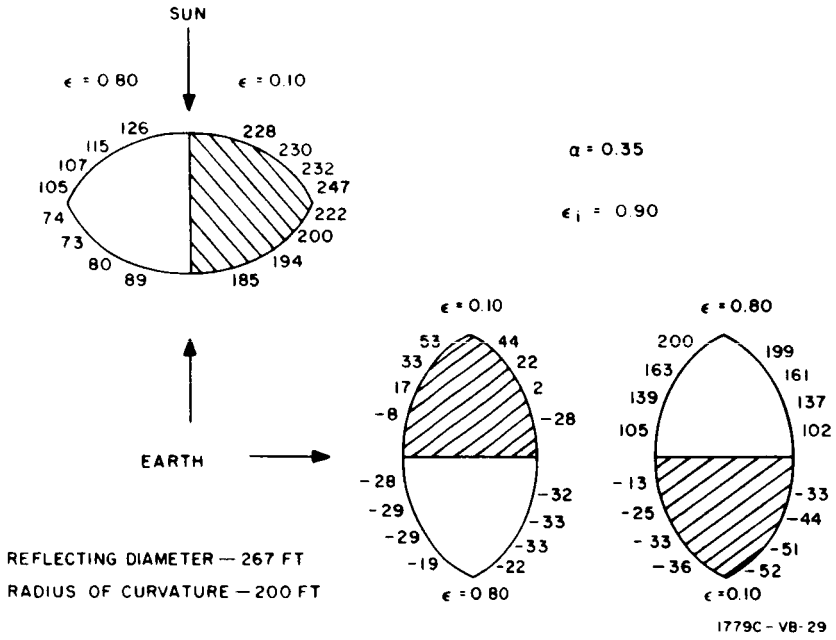

Figure 3-20. Skin Temperatures; 0.8 and 0.1 Emissivity and 0.35 Absorptivity

3.5.2 Sail Material (Configuration B)

In selecting a coating pattern for the sail material, the problem is similar to that encountered in selecting a pattern for the opaque lens. The pattern selected should both maintain a feasible temperature and produce as much mobility as possible.

In order to calculate the sail temperature, the balance of energy equation, which equates the energy absorbed by the sail to the energy emitted by the sail, can be written at the point where the plane of the sail is normal to the sun line vector as:

$$\alpha_i C_s = \sigma (\epsilon_1 + \epsilon_2) T^4$$

where:

- α_i - solar absorptivity of side facing the sun
- $\epsilon_1 \epsilon_2$ - emissivities of the two sides
- C_s - solar radiation density (440 Btu/hr ft^2)
- σ - Stefan-Boltzmann constant (1.73×10^{-9} Btu/hr ft^2 deg^4)
- T - surface temperature

Since the criteria as specified by Goodyear is that the surface temperature cannot exceed 250° Fahrenheit, it is sufficient to examine the point of maximum temperature. This is seen to occur when the side having the higher absorptivity is facing the sun under the normal condition described above. Thus, the maximum temperature can be expressed as:

$$T_m^4 = \frac{\alpha_m C_s}{\sigma (\epsilon_1 + \epsilon_2)}$$

From the analysis of Appendix VI of the Phase IV final report (reference 1) the mobility is seen to be directly proportional to the quantity:

$$\frac{\alpha_2 \epsilon_1 - \alpha_1 \epsilon_2}{\epsilon_1 + \epsilon_2}$$

For the coating configuration originally selected on the basis of the maximum mobility within the range of values of coating parameters specified by Goodyear (Appendix IV), a maximum temperature of 271°Fahrenheit was calculated. Since the later upper limit of 0.8 on the external emissivity is seen to both lower the temperature and increase the mobility, this was the next configuration considered. For this configuration, a temperature of 250° was calculated. Even though this temperature is within the safe limits, it must be remembered that the effects of earth radiation have not yet been considered. Although in normal operation the effects of earth radiation will be very small since the sail is aligned parallel to the earth's axis, a margin of safety of about 20° was sought to cope with any large attitude control errors which might be encountered in the detumbling phase.

As can be seen, there were two remaining possibilities for obtaining a further reduction in the maximum temperature. Either the higher absorptivity could be lowered or the lower emissivity could be raised. The effects of these two courses of action, along with the previous cases, are shown in table 3-4. In this table, the mobility of the original configuration is arbitrarily set to one, and the other mobilities are calculated relative to that case. For all cases, an absorptivity of 0.1 was used for side 1.

TABLE 3-4

SUMMARY CHART OF TEMPERATURE, MOBILITY STUDY

α_2	ϵ_1	ϵ_2	Relative Mobility	Maximum Temperature (°F)
0.9	0.7	0.1	1.000	271
0.9	0.8	0.1	1.018	250
0.9	0.8	0.2	0.904	232
0.8	0.8	0.1	0.904	230

Since there is little to choose between the last two cases with regards to either skin temperature or mobility, the configuration of the third case was chosen on a somewhat arbitrary basis as the configuration to be used in the final study of the sail mobility.

3.6 SATELLITE COVERAGE

3.6.1 Derivation

An infinite variety of satellite position arrangements can be conceived to provide world-wide communications coverage. Any analysis of the number of satellites required for full earth coverage must, of necessity, be limited to specific configurations. For the following discussion then, it is assumed that there are three orbit paths equally spaced about the equator, each having the same inclination. Each of these orbit paths contain N equally spaced satellites, all having the same semimajor axes (altitude). It is desired to find the smallest number of satellites which will provide 100-percent earth coverage continuously. Complete coverage is defined such that, at all times, every area on earth is in view of at least one satellite.

It is evident that three orbit paths having zero inclination could not cover the poles. It is also apparent that polar orbits are not desirable, since with polar orbits all uncovered, or open, areas are concentrated at low latitudes. Since little communication is desired in the polar regions, all possible open areas should be concentrated in these least populated polar areas. For this reason, the inclinations will generally be limited to the 30- to 60-degree values.

If it is assumed that one orbit path exists, and that this path contains an infinite number of satellites at a specific altitude, the earth would be completely covered by a band the width of which would be:

$\theta = 2\cos^{-1}\left(\frac{r}{r+h}\right)$ where r and h are the earth's radius and altitude, respectively. The only open portions exist at the poles of the orbit path, located at N (90 - i) degrees, 90 degrees W, and S(90 - i) degrees, 90 degrees E of the ascending node, where i is the inclination. The radius of the open areas would be (90 - θ) degrees. Now, if three such bands, the ascending nodes of which are spaced 120 degrees apart about the equator, are used, complete coverage will be obtained as long as these open areas

do not all overlap. For inclinations less than 45 degrees, these areas will be equally spaced around the earth's poles; so long as the boundaries of the open areas do not include the poles, complete coverage is obtained.

Reduction of the number of satellites per orbit (N) to a finite number puts scallops in the open area limit circle; the circle required to circumscribe the open areas now becomes the open area limit, since orbit time phasing can allow the scallops to coincide with each other, causing blackout. The limiting increase in the open-area radius is

$$R = 90 - (90 - \iota) - (90 - \theta) = -(90 - \iota - \theta)$$

A spherical triangle can be drawn to describe this limit.

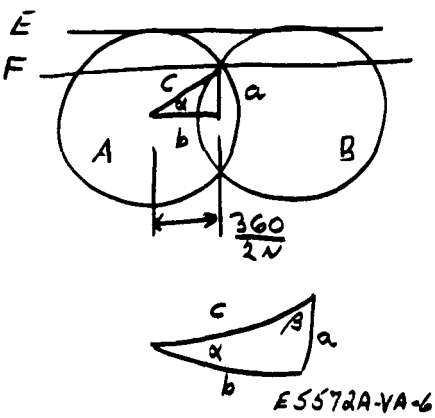

Circles A and B are fields of view of two adjacent satellites. Line E is the open area limit for N = ∞; F is the allowable open area limit for a finite N.

$$a = 90 - \iota = \theta - [90 - (90 - \iota) - (90 - \theta)]$$

$$b = 360^\circ / 2N_o$$

$$c = \cos^{-1} \frac{r}{r+h}$$

From spherical trigonometry:

$$b = \sin^{-1}\left(\tan a \cot\left[\sin^{-1}\left(\frac{\sin a}{\sin c}\right)\right]\right) = \frac{360^\circ}{2N_o} \qquad (3\text{-}61)$$

From this, N can be determined. For a randomly chosen altitude, N_o will not be an integer, and the nearest higher integer, N, must be used.

The allowable variation in angular spacing of the satellite will then be:

$$\frac{360}{2N_o} - \frac{360}{2N} = 180\left(\frac{N - N_o}{NN_o}\right) \qquad (3\text{-}62)$$

Note that the altitude can be adjusted such that $N_o = N$, so that no allowable error exists. If, then, the next higher value of N is used, the failure

of one satellite in each orbit can be compensated by respacing the remaining satellites.

It should be noted that if the relative positions (or phasing) of satellites in different orbit paths are synchronized, complete coverage could be obtained for fewer satellites per orbit, and/or lower altitudes. Even with unsynchronized orbits, outage would occur only when phasing caused three scallops to coincide. Further, if communications to the earth's polar region were not required further reduction in N and h could be affected; or, if small outage areas can be allowed for specific times, improvement could be made. Without specific allowances, the above procedure is a simple method for determining the requirements for full coverage.

Visualization of this problem is greatly simplified by the use of a 12- to 15-in. sphere upon which the open-area circles can be drawn. A 14-in. ball, sand blasted to provide a surface which would accept pencil markings, yet would be erasable, was used in conjunction with a protractor mounted on three legs to provide the various required patterns. Use of such an analog is greatly superior to any method employing the various map projections. Substituting $a = 90-i$ and $c = \cos^{-1} r/(r+h)$ and solving equation 3-61 for N_o yields:

$$N_o = \frac{180^\circ}{\sin^{-1}\left[\tan(90-i)\cot\left(\sin^{-1}\left[\frac{\sin(90-i)}{\sin\cos^{-1}\left(\frac{r}{r+h}\right)}\right]\right)\right]} \qquad (3\text{-}63)$$

Since r, h, and i are all independent parameters, various curves are easily obtained from this equation. Similar equations can be developed in the same manner for an increased number of orbit planes. Note that for inclinations exceeding 45 degrees, the same sort of answers would be applicable except that the open areas would tend to appear about the equator rather than about the poles; lower inclinations are thus desirable.

3.6.2 Sample Problem

Altitude 4000 nmi.

Inclination 40 degrees.

Three orbit paths.

Find the required number of sat/orb (N) and the allowable error A.

Assume N = ∞

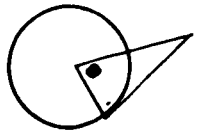

coverage: $\sin^{-1}\frac{344}{744} = 27.6°$

$\Theta = 90 - 27.6 = 62.4°$

One orbit path would cover a band 124.8 degrees wide around the world, leaving an open portion at each pole, of radius

$90 - 62.4 = 27.6°$

The poles will be located -90 degrees longitude, (90-40 degrees) = 50 degrees N latitude; and 90 degrees longitude, -(90 - 40) = 50 degrees S latitude from the ascending node. Locate these on the globe. This, for a 13.85-in. globe would require a radius of

$2r \sin\frac{\Theta}{2} = 13.65 \sin 13.8° = 3.44$ in.

Put these on the globe with the compass. The coverage will be complete, with N = ∞. The minimum required N will occur when open area limits cross the N and S poles exactly; since, at that point, an open can occur. The angle required is:

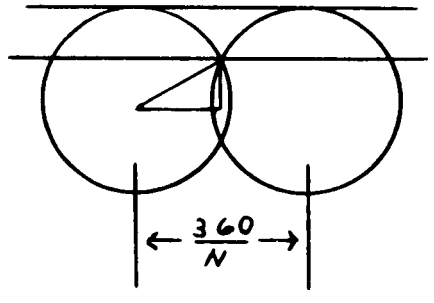

$90 - 50 - 27.6 = 12.4°$

A spherical triangle can be drawn:

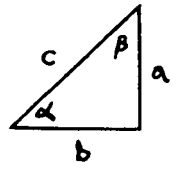

$a = 62.4 - 12.4 = 50° = 90 - i$

$c = 62.4°$

$$\sin \alpha = \frac{\sin a}{\sin c} = \frac{\sin 50}{\sin 62.4} = .865 \; ; \; \alpha = 60^\circ$$

$$\sin b = \tan a \cot \alpha = \tan 50 \cot 60 = .687$$

$$b = 43.5^\circ = \frac{360}{2N} \; ; \; N = 4.13$$

Use N=5 since an integer is required.

Note that a slight increase in altitude would allow the use of only four sat/orb. With five S/O, $\frac{360}{2N}$ = 36 degrees instead of 43.5 degrees previously determined. An error of ±6.75 degrees would still permit complete coverage.

It should be noted that an error in position much greater than 6.75 degrees can be allowed in one satellite if no error exists in other orbits. Even with considerable error in all orbits, opens will appear only occasionally because of intraorbit phasing. However, since small differences in orbit periods will allow slow phase shifts between orbits, opens will eventually occur if these units are exceeded.

A particular altitude exists for each given inclination for which there could exist no allowable error. For the sample shown, the altitude need only be decreased until 360/2N = 6 is 36 degrees

$$a = 50^\circ \; ; \; b = 36^\circ$$

$$\cot \alpha = \frac{\sin b}{\tan a} = \frac{\sin 36}{\tan 50} = .494^\circ \; ; \; \alpha = 63.7^\circ$$

$$\sin c = \frac{\sin a}{\sin \alpha} = \frac{\sin 50}{\sin 63.7} = .867 \; ; \; c = 60^\circ$$

$$\frac{r}{r+h} = .5 \; ; \; h = 3440 \text{ NM}$$

At this altitude, only five S/O are needed, with no allowable error; or six S/O could be used, with maximum allowable error. If six S/O were used, and a failure occurred, the remaining units could be repositioned to provide full coverage. Even with one satellite completely out of position (or

inoperable), opens would be of short duration, and would rarely occur. So many combinations of errors can occur that to tabulate each possibility would be tedious. The method used above, (so long as the inclinations are correct, the semimajor axes are equal, and the ellipticites are < 10 percent), will be certain to provide complete coverage. Further refinement can be readily made if careful specifications are made as to the coverage allowed. For instance, if coverage of the north and south polar areas is not required above a particular latitude or if outage areas of specific size are allowed for specific lengths of time, the number of satellites per orbit can be reduced considerably.

The concept of determining open areas and their limits is, after a little practice, much simpler to visualize than that of attempting to determine the positive coverage of a large number of satellites. The use of a sphere with bounded areas drawn on its surface is by far the best analog available for visualization of the coverage problem.

3. 6. 3 Synchronized Orbits

Thus far, no synchronization between orbits has been considered. However, since all satellites in all orbit planes will have the same semimajor axes, and since the orbit position control system is capable of controlling each satellite position accurately, the phase synchronization between the satellites of one orbit plane, and those of other orbit planes is quite feasible.

Open-area radii have thus far been set such that no combination of intra-orbit phasing can produce blackout. If the three orbits are phased such that equivalent satellites in each pass over the equator with angular separations of 360/3N, the maximum points of the open areas will never meet, so that increased coverage can be obtained. The amount of gain obtainable depends upon N, i, and h.

As an example, for i = 45, and N = 4,

$$\cot \alpha = \frac{\sin b}{\tan a} = \frac{\sin 45^\circ}{\tan 45^\circ} = .707; \quad \alpha = 54.7^\circ$$

$$\sin C = \frac{\sin a}{\sin \alpha} = \frac{\sin 45^\circ}{\sin 54.7^\circ} = .867 \; ; \; C = 60^\circ$$

$$\frac{r}{r+h} = \sin 30^\circ = .5$$

$h = 3440$ NM minimum required altitude

Now, if $b = \frac{360}{3N}$ = 30 degrees and c is 60 degrees:

$$\sin\beta = \frac{\sin b}{\sin c} = \frac{\sin 30}{\sin 60} = .577 \; ; \; \beta = 35.3$$

$$\sin a = \tan b \cot\beta = .817 \; ; \; a = 55^\circ$$

This indicates a reduction of 60 - 55 = 5 degrees in the radius of the open area circles, for synchronized orbits. This would allow a safety factor of $\pm \frac{1}{4}(\frac{360}{2N} - \frac{360}{3N}) = \pm 3.75$ degrees which could be allowed any satellite in any orbit, in any combination, without blackout.

3.7 DERIVATION OF AVERAGE AREA-TO-MASS RATIO FOR MAXIMUM ECCENTRICITY

In order that the maximum eccentricity data shown in paragraph 2.2.4.1 may be related to the configuration A and B satellites, equivalent spheres have been derived for the two configurations. The maximum eccentricity data are, of course, generated by means of the Lifetime 18 program. This requires that an equivalent uniformly coated specular sphere be derived for each of the configurations.

As an aid in the derivation and as a means of checking the results, the mobility program (which considers both the continuously varying projected area of the satellite and the nonuniform coating) has been run on several selected cases for each of the configurations. In order to show the accuracy of the mobility program for this purpose in comparison with the Lifetime 18 program, a force tape was generated using the characteristics of the Echo I satellite and considering the direct solar energy input only. This is, of

course, exactly the configuration considered by the Lifetime 18 program. The results of this test are shown in figure 3-21. This figure shows the time variation of eccentricity as calculated by the two programs for a particular orbit. As can be seen, the results compare almost exactly during the first year and at the end of the second year differ by only approximately 3 percent. Based upon this comparison, it is assumed that the mobility program can be used to check the results of the equivalent sphere derivations.

Also shown in figure 3-21 are the results of a mobility program run on the same satellite, but assuming a diffuse surface coating instead of specular. As can be seen, this causes a significantly higher level of eccentricity to be reached. The difference can be explained by the fact that the total solar pressure force on a uniform diffuse sphere follows the relationship:

$$F_s \propto \left(1 + \frac{4}{9} r\right)$$

where r is the reflectivity of the surface. In the case of a specular sphere, the reflected components of force cancel and the force is simply proportional to the incident energy. Since a surface reflectivity of 0.9 was used in the cases shown in figure 3-21, the factor of 1.4 between the diffuse and spherical results is thus explained. This phenomenom is used in the derivations shown below.

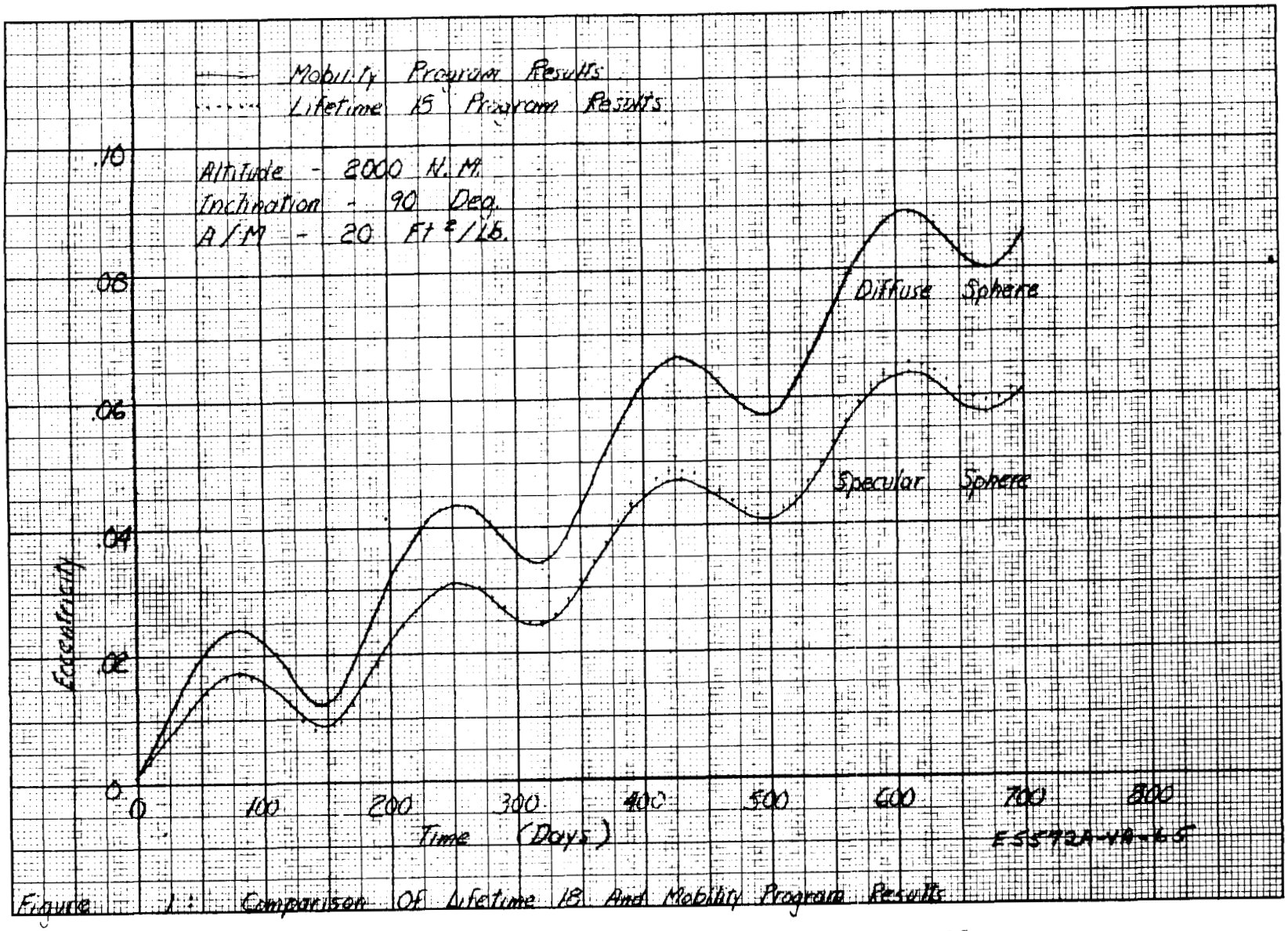

Figure 3-21. Comparison of Lifetime 18 and Mobility Program Results

3.7.1 Configuration A Opaque Lenticule Equivalent Sphere

It is shown that, in general, the solar pressure perturbation on a satellite is directly proportional to the projected area of the satellite to the sun and inversely proportional to the satellite mass. Therefore, the approach taken to deriving an equivalent sphere has been to calculate an average projected area of the satellite over all orbital conditions.

Consider the orbital geometry shown in figure 3-22. If the sun-line is in the plane of the orbit ($i_s = 0$), then the projected area of the satellite to the sun at an orbit angle of γ equal to 0 and 90 degrees is:

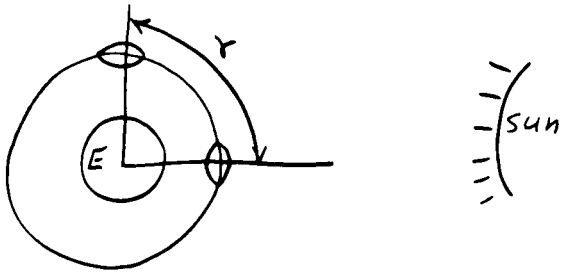

E5572A-VA-66

Figure 3-22. Orbital Geometry

$$A_L(\gamma = 0) = \frac{\pi D^2}{4}$$

$$A_L(\gamma = 90) = 2R^2 \sin^{-1}\left(\frac{D}{2R}\right) - DR\cos\left[\sin^{-1}\frac{D}{2R}\right]$$

where R is the radius of curvature of the lenticule and D is the diameter. Assuming that the area varies sinusoidally between these two points, that is:

$$A_L(\gamma) = \frac{A_L(\gamma=0) + A_L(\gamma=90)}{2} + \frac{A_L(\gamma=0) - A_L(\gamma=90)}{2}\cos 2\gamma$$

then the average projected area of the satellite over the orbit for i_s equal to zero is simply the average of the projected areas at these two points. Furthermore, it can be seen that when the sun-line is perpendicular to the orbital plane, the projected area over the orbit is constant and equal to the previously defined area at the point γ equal to 90 degrees. Thus:

$$A_L(i_s=0) = \frac{A_L(\gamma=0) + A_L(\gamma=90)}{2} \quad ; \quad A_L(i_s=90) = A_L(\gamma=90)$$

Again, assuming a sinusoidal variation as a function of i_s, the average projected area over the orbit as a function of i_s becomes:

$$A_L(i_s) = \frac{A_L(i_s=0) + A_L(i_s=90)}{2} + \frac{A_L(i_s=0) - A_L(i_s=90)}{2} \cos 2 i_s$$

It is also known that a force normal to the plane of the orbit does not contribute to the eccentricity perturbation. Thus, when averaging the projected area over all values of i_s, the projected areas must be weighed by a cosine of i_s term. Under this assumption, the average projected area is:

$$\bar{A}_L = \frac{\int_0^{\pi/2} A_L(i_s) \cos i_s \, d i_s}{\int_0^{\pi/2} \cos i_s \, d i_s}$$

and

$$\bar{A}_L = \frac{A_L(i_s=0) + A_L(i_s=90)}{2} + \frac{A_L(i_s=0) - A_L(i_s=90)}{6}$$

Then, including the diffuse reflection factor discussed above, the opaque lenticule has an equivalent uniform specular spherical area-to-mass ratio of:

$$\frac{A_L}{M} = \frac{\bar{A}_L \left(1 + \frac{4}{9} r\right)}{M}$$

where M is the mass of the satellite. This equivalent spherical area-to-mass ratio has been checked with selected computer comparison runs on both the mobility and Lifetime 18 programs. The results for a set of these runs are shown in figure 3-23. All data shown on this figure were obtained from the mobility program. The eccentricity variation for three different shaped satellites (R = 250', D = 333'; R = 150', D = 252') in the same orbit is shown.

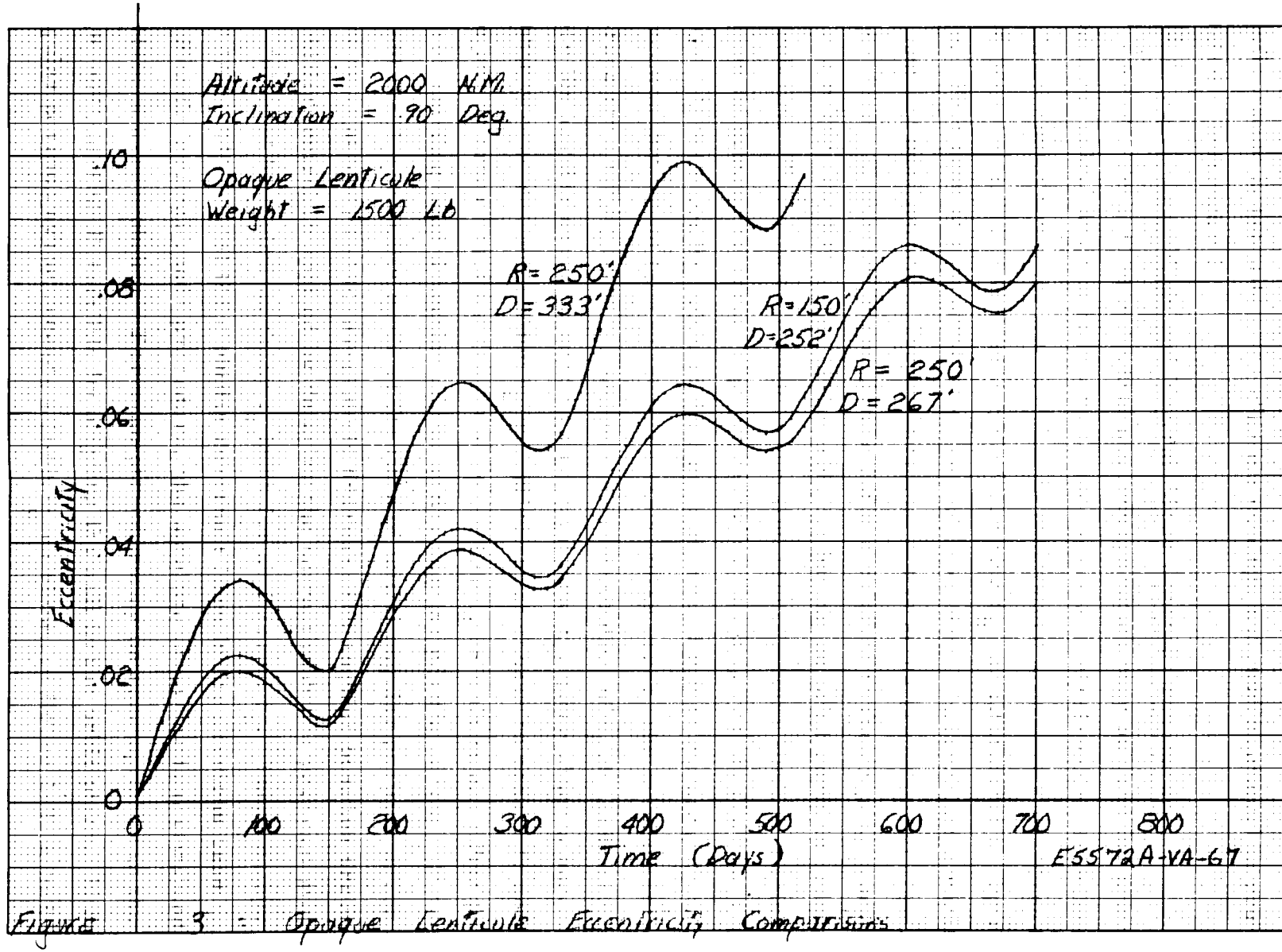

Figure 3 - Opaque Lenticule Eccentricity Comparisons

Figure 3-23. Opaque Lenticule Eccentricity Comparisons

The manner in which these results compare, on the equivalent sphere basis, to the Lifetime 18 results of figure 3-21 (same orbit) is summarized in table 3-5. In this table, the columns headed with prediction pertain to the predicted average projected area of the satellite ($\bar{A}_L$) and the predicted ratio of mobility program derived results to Lifetime 18 derived results. The ratio is predicted on the basis of the derived average area-to-mass ratio. The columns headed with actual results pertain to the ratio between the program results at the first, second, and third eccentricity peaks and the average of the three ratios. The eccentricity peaks were chosen as comparison points since the principal use of the average area-to-mass ratio will be to scale maximum eccentricity data. The final column in the table simply gives the percentage difference between the predicted ratio and the average actual ratio.

As can be seen, the actual ratios compare favorably with the predicted ratios at all eccentricity peaks for these three cases, and the maximum percentage difference is approximately 5 percent.

TABLE 3-5

COMPARISON OF PREDICTED TO ACTUAL ECCENTRICITIES

Case Identifier	Prediction		Actual Results				Percent Difference
	Average Area ($ft.^2$)	Ratio to LT 18	Ratio to LT 18 (1st peak)	Ratio to LT 18 (2nd peak)	Ratio to LT 18 (3rd peak)	Average Ratio to LT 18	
R = 150', D = 252' 90-degree inclination	32,800	1.41	1.32	1.36	1.33	1.34	5.1
R = 250', D = 267' 90-degree inclination	27,900	1.20	1.16	1.25	1.23	1.21	.8
R = 250', D = 333' 90-degree inclination	48,400	2.08	2.01	2.08	2.03	2.04	1.9
R = 250', D = 333' 45-degree inclination	48,400	2.08	2.02	2.10	-	2.06	1.0
R = 250', D = 333' 0-degree Inclination	48,400	2.08	1.94	1.94	-	1.94	6.0
One ft^2 Sail 0-degree Inclination	0.590	0.885	0.885	0.99	-	0.922	4.1
One ft^2 Sail 45-degree Inclination	0.570	0.855	0.755	0.85	-	0.80	6.7
One ft^2 Sail 90-degree Inclination	0.515	0.772	0.62	0.865	0.81	0.76	1.6

Shown in figures 3-24, 3-25, and 3-26 are both mobility program and Lifetime 18 program results for the larger lenticule (R = 250', D = 333') at three different orbit inclinations. Again these results are summarized in table 3-5. It can be seen that these results also compare favorably with the predicted results. It is important to note that there is no readily discernible variation of the ratio of actual to predicted as a function of orbital inclination. Therefore, the scaling factor has been made independent of inclination. The scaling factors are also independent of altitude since the solar pressure perturbing forces are independent of altitude.

3.7.2 Configuration B Wire Mesh Lenticule With Sail

For the configuration B satellite (wire mesh lenticule with sail), the wire mesh lenticule is assumed to act in the same manner as the opaque lenticule but at a reduced area. It is further assumed that one cap of the wire mesh lenticule covers 5 percent of the total area when in the orientation defined by γ equal to 0 in figure 3-22. It is also assumed that the percentage of radiation intercepted by the side facing away from the sun will follow an x (1 - x) relationship where x is the percentage intercepted by the side facing the sun. By definition, the x at γ equal to 0 is 0.05. When γ is equal to 90 degrees, the wire mesh will be effectively closer together and the x can be redefined as a function of the projected area ratio:

$$x(\gamma = 90) = \frac{.05\, A_L(\gamma = 0)}{A_L(\gamma = 90)}$$

Then, the projected area of the wire mesh lenticule at these two points is:

$$A_M(\gamma = 0) = [.05 + .05(1 - .05)]\, A_L(\gamma = 0)$$

$$A_M(\gamma = 90) = [x(\gamma = 90) + x(\gamma = 90)(1 - x(\gamma = 90))]\, A_L(\gamma = 90)$$

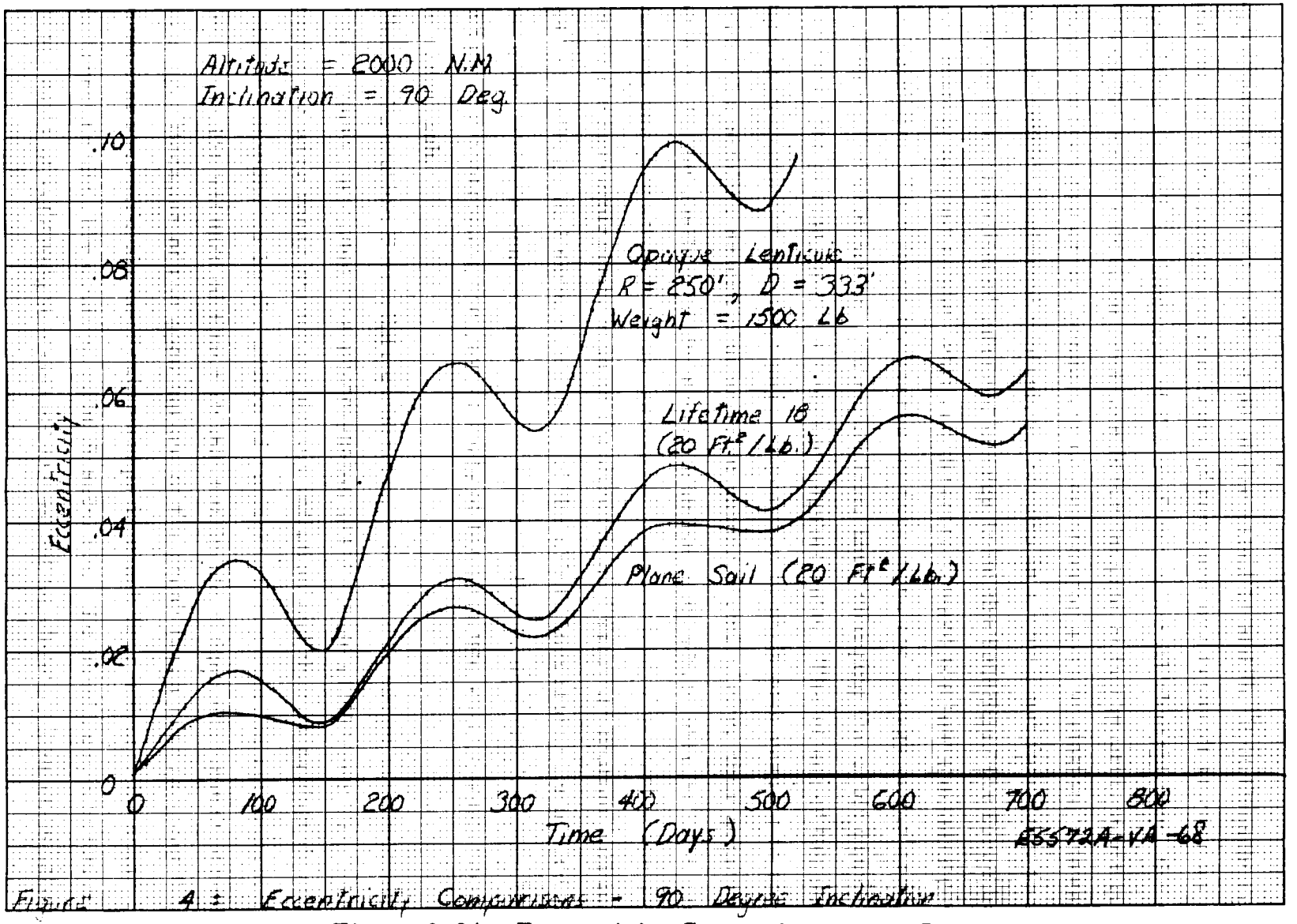

Figure 3-24. Eccentricity Comparisons - 90-Degree Inclination

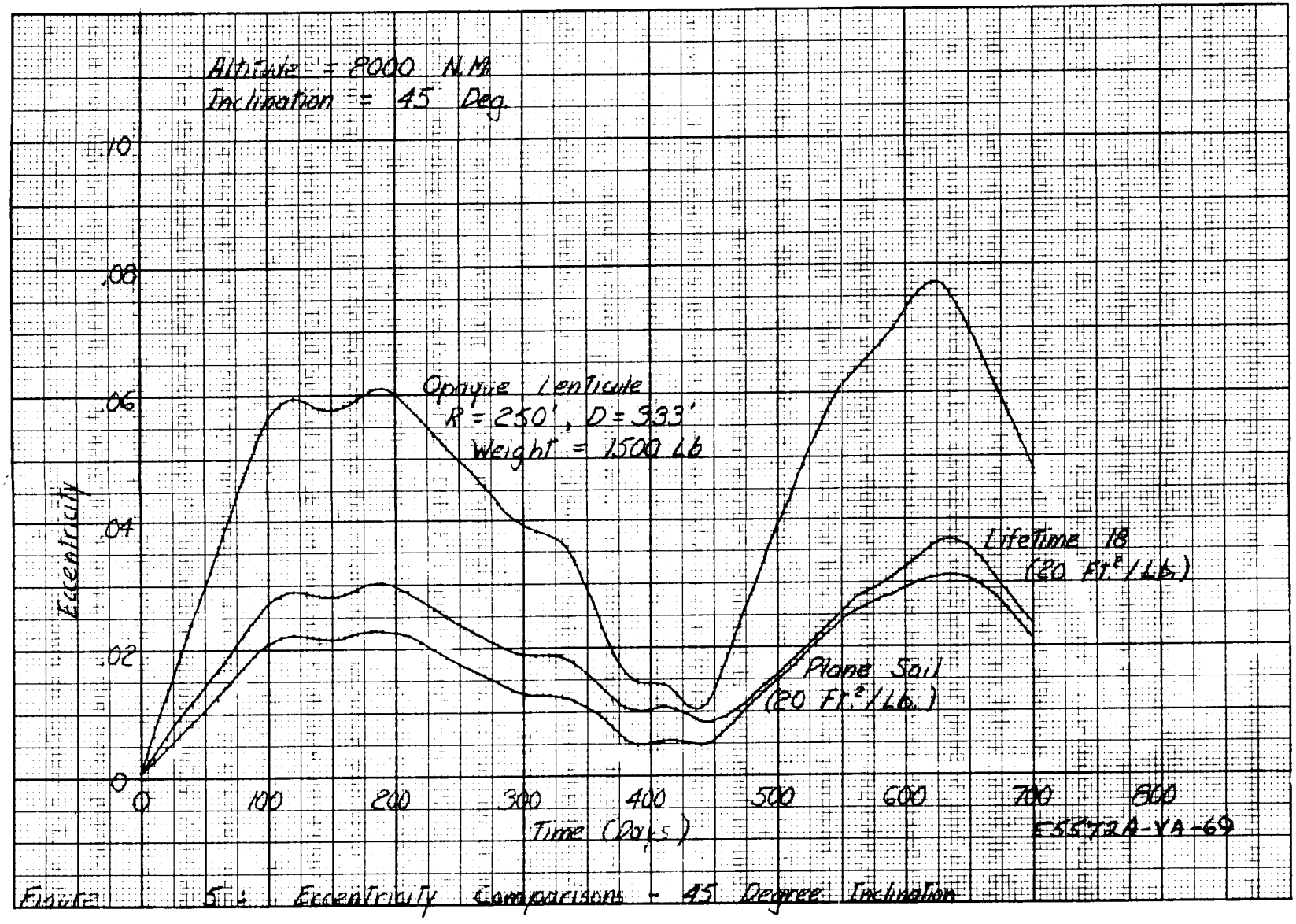

Figure 3-25. Eccentricity Comparisons - 45-Degree Inclination

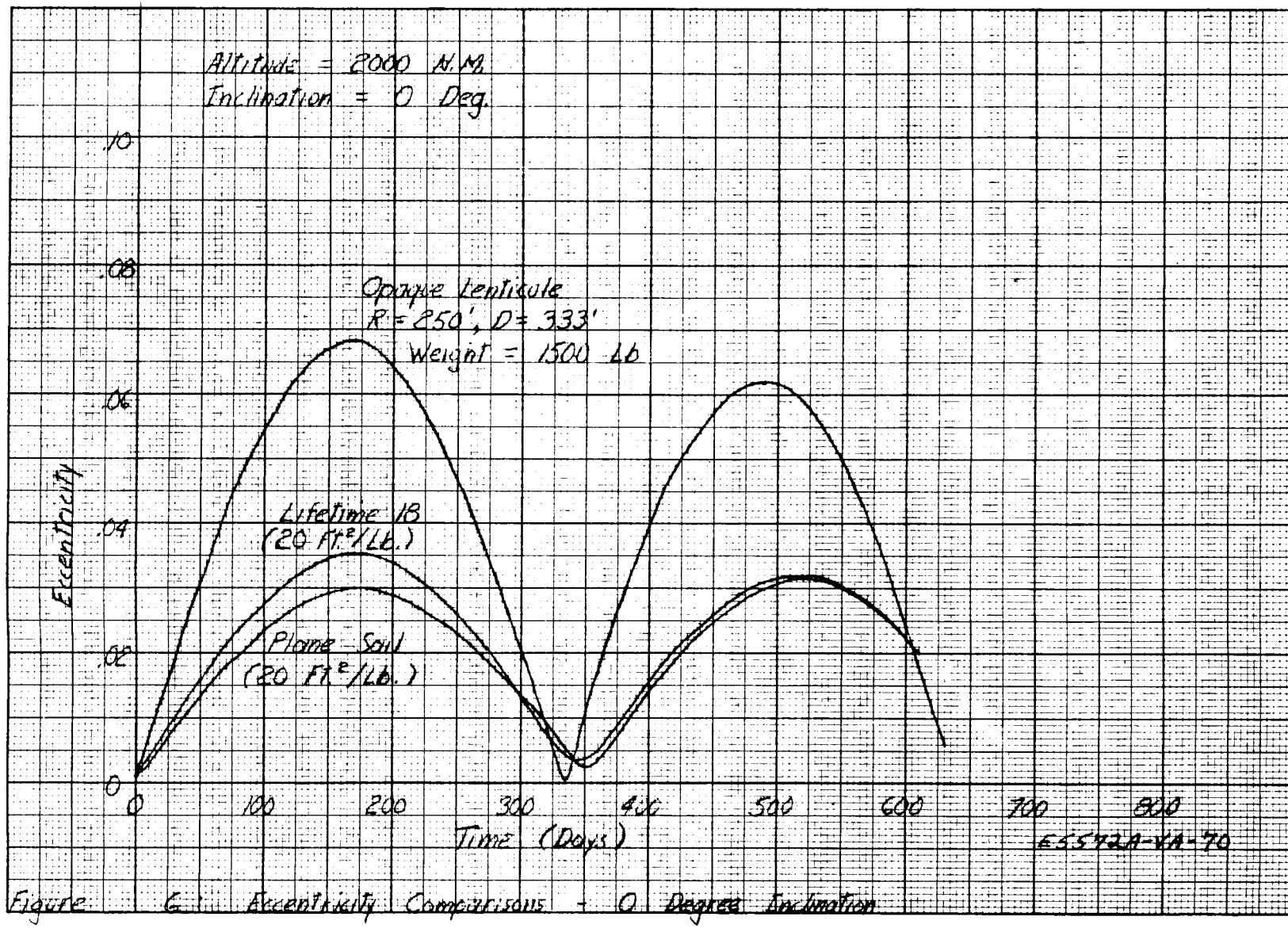

Figure 6: Eccentricity Comparisons - 0 Degree Inclination

Figure 3-26. Eccentricity Comparisons - 0-Degree Inclination

From this point, the derivation is equivalent to that of the opaque lenticule and the average area of the wire mesh lenticule is:

$$\overline{A}_M = \frac{A_M(i_s=0) + A_M(i_s=90)}{2} + \frac{A_M(i_s=0) - A_M(i_s=90)}{6}$$

The plane sail surface is assumed to be oriented as in the fixed compensation method of control (sail angle of 22.5 degrees). Thus, when the sunline is in the plane of the orbit, the projected area at the points γ equal to 0 and 90 is:

$$A_s(\gamma=0) = 0; \quad A_s(\gamma=90) = A\cos 22.5^\circ = .928\ A$$

It can also be seen that the projected area around the orbit will vary essentially as a sine function of γ and is:

$$A_s(\gamma) = .928\ A \sin\gamma$$

Thus, the average projected area over the orbit is simply:

$$A_s(i_s=0) = .928\ A\left(\frac{2}{\pi}\right) = .590\ A$$

where A is the surface area of the sail. The projected area when the sunline is perpendicular to the orbital plane is:

$$A_s(i_s=90) = A \sin 22.5^\circ = .383\ A$$

Again, assuming a sinusoidal variation between these points, the average area over the orbit as a function of i_s is:

$$A_s(i_s) = A_s(i_s=90) + [A_s(i_s=0) - A_s(i_s=90)]\cos i_s$$

For any orbital inclination, a reasonably good approximation of the average projected area can be obtained by averaging those areas from i_s equal 0 to the orbital inclination or:

$$\bar{A}_s = A_s(i_s = 90) + \frac{[A_s(i_s = 0) - A_s(i_s = 90)]}{\epsilon} \sin i$$

where i is the orbital inclination expressed in radians. In addition to this, the contribution of the reflected solar energy to the force must be considered. In the case of a plane surface, the reflected component is proportional to (1 + r) where r is the reflectivity. Thus, the average area-to-mass ratio of the configuration B satellite is:

$$\frac{A_B}{M} = \frac{\bar{A}_M + \bar{A}_s (1 + \hat{r})}{M}$$

where $\hat{r}$ is the average reflectivity of the two sides of the sail. The equivalent spherical area-to-mass ratio for the sail alone has been checked with selected computer comparison runs on both the mobility and Lifetime 18 programs. These results are shown as a part of figures 3-24, 3-25, and 3-26. These results are also summarized in table 3-5. It can be seen that these predictions are, in general, not as accurate as for the opaque lenticule. The manner in which the actual ratios vary from peak to peak indicates that the sail eccentricity is not as predictable as that of the opaque lenticule. However, the percentage difference is still well within acceptable limits.

3.8 PHYSICAL CAUSES OF ORBITAL RESONANCE

The reason for expecting a point of maximum eccentricity for low inclination orbits is illustrated in figure 3-27. If the circular orbit shown by the solid circle is used as a starting point, then initially solar pressure will add energy to the orbit in the vicinity of the point P. This will tend to create an apogee at a point 180 degrees away. Similarly, solar pressure will subtract energy from the orbit in the region of the orbit opposite the point, P, thus tending to create a perigee near the point P. If both the orbit and the sun were to remain stationary in inertial space, it can be seen that the eccentricity of the orbit would keep increasing indefinitely until the satellite fell into the earth's atmosphere.

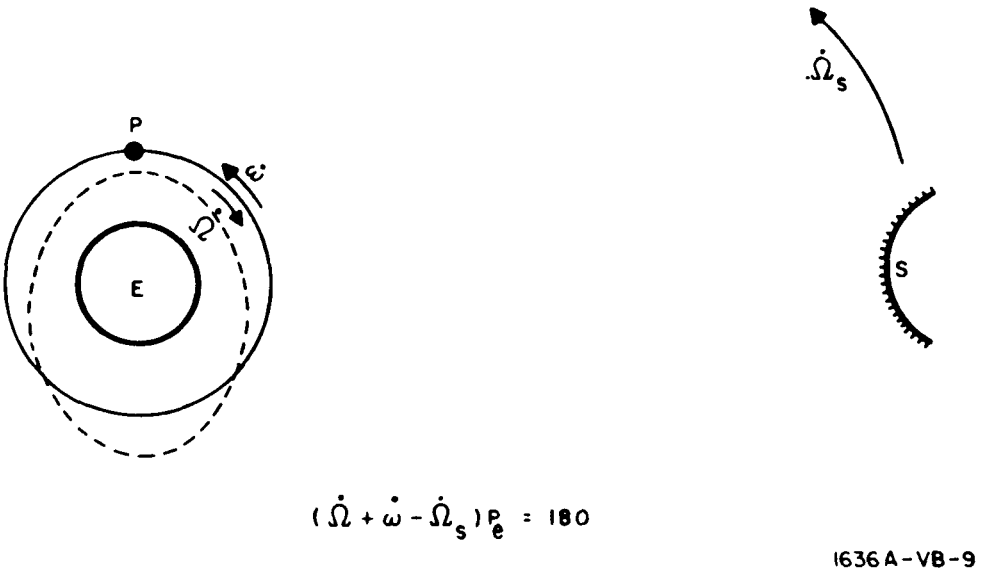

Figure 3-27. Maximum Eccentricity Philosophy

However, the point of the perigee moves with relation to the sun-line due to three separate considerations. First, the precession of the right ascension causes the perigee to move at a rate, $\dot{\Omega}$, with respect to the sun-line. The motion of the argument of the perigee also causes the perigee to move at a rate $\dot{\omega}$ with respect to the sun-line and the apparent motion of the sun causes the sun-line to move at a rate $\dot{\Omega}_s$, with respect to the perigee. When the combination of these three motions has caused the perigee to move 90 degrees with respect to the sun-line, the solar pressure force will begin subtracting energy in the vicinity of the perigee and adding energy in the vicinity of the apogee, thus causing the eccentricity of the orbit to decrease. Thus, the period of the eccentricity is defined in the following manner.

$$(\dot{\Omega} + \dot{\omega} - \dot{\Omega}_s) P_e = 180$$

where P_e is the period of the eccentricity and all the angular rotations are defined as positive clockwise.

It can be seen that the period of oscillation, P_e, becomes infinite when the following condition is satisfied:

$$\dot{\Omega} + \dot{\omega} - \dot{\Omega}_s = 0$$

For this situation, the argument of the perigee effectively remains stationary in inertial space with respect to the sun-line, and the eccentricity keeps increasing indefinitely. This condition is seen to correspond to resonance condition No. 1 listed in paragraph 2.2.4.1 and is known to be a very stable resonance for low inclination orbits.

A different type of condition causes a resonance to occur at high inclinations. This resonance is caused by a stair-stepping effect on the eccentricity illustrated in figure 3-28. Consider the situation where a satellite is started in a circular orbit and the sun-line lies in the plane of the orbit as shown in the figure. Then, if the direction of motion is indicated by $\dot{u}$, the solar pressure forces will tend to create a perigee at the point, P. The perigee will move in the direction shown by $\dot{\omega}$, and the effective motion of the sun-line is indicated by the combination of the apparent motion of the sun and the precession of the right ascension, $\dot{\Omega}$. Then, for the resonant condition:

$$|\dot{\omega}| = |\dot{\Omega}_s - \dot{\Omega}|$$

The solar pressure forces will add energy in the region of the perigee and subtract energy in the region of the apogee during the first 90 degrees of rotation; but, at the same time that the perigee passes the 90-degree point, the sun-line also passes the most normal point to the orbit; and the solar pressure forces are reversed in sign. Thus, energy is again being added in the region of the perigee and being subtracted in the region of the apogee causing the eccentricity to continue to increase. A typical plot of eccentricity for this condition is shown in the figure. The eccentricity continues to build up indefinitely except for a leveling off at 90 and 270 degrees from the original point where the sun-line is most nearly normal to the plane of the orbit.

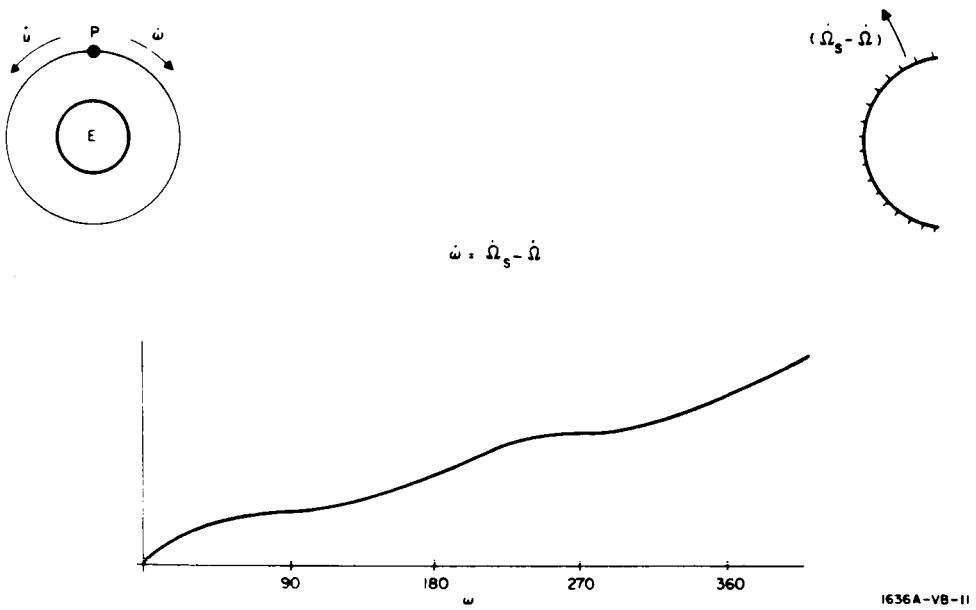

Figure 3-28. Stair - Step Resonance

This condition is seen to correspond to resonance conditions No. 3 and No. 4 listed in paragraph 2.2.4.1, and in the form of No. 3, is known to be a stable resonance for high inclination orbits.

REFERENCES

1. "Feasibility and Parametric Design Study of the Application of A Station-Keeping System to Passive Communication Satellites, Phase IV - Final Report," Prepared for NASA(LRC) Under Contract NAs1-3131, Westinghouse Defense and Space Center, Aerospace Division, Baltimore, Maryland, January 1965.

2. "Feasibility Study and Preliminary Design of Gravity-Gradient-Stabilized Lenticular Test Satellite," GER-11502, Prepared for NASA(LRC) Under Contract NAs 1-3114, Goodyear Aerospace Corporation, June 1964.

3. "Feasibility and Parametric Design Study of the Application of A Station-Keeping System to Passive Communications Satellites, Phase II - Final Report," Prepared for NASA(LRC) Under Contract NAs 1-3131, Westinghouse Defense and Space Center, Aerospace Division, Baltimore, June 1964.

4. "Digital Computer Programs Used for Orbit Position Control Study of Advanced Lenticular Passive Communications Satellites," Final Report, Prepared Under Contract NAs 1-5194, October 1965.